NEW INSIGHTS IN SKELETAL MUSCLE CHANNELOPATHIES - A RAPIDLY EXPANDING FIELD

EDITED BY: Lorenzo Maggi, Emma Matthews and Jean-François Desaphy
PUBLISHED IN: Frontiers in Neurology

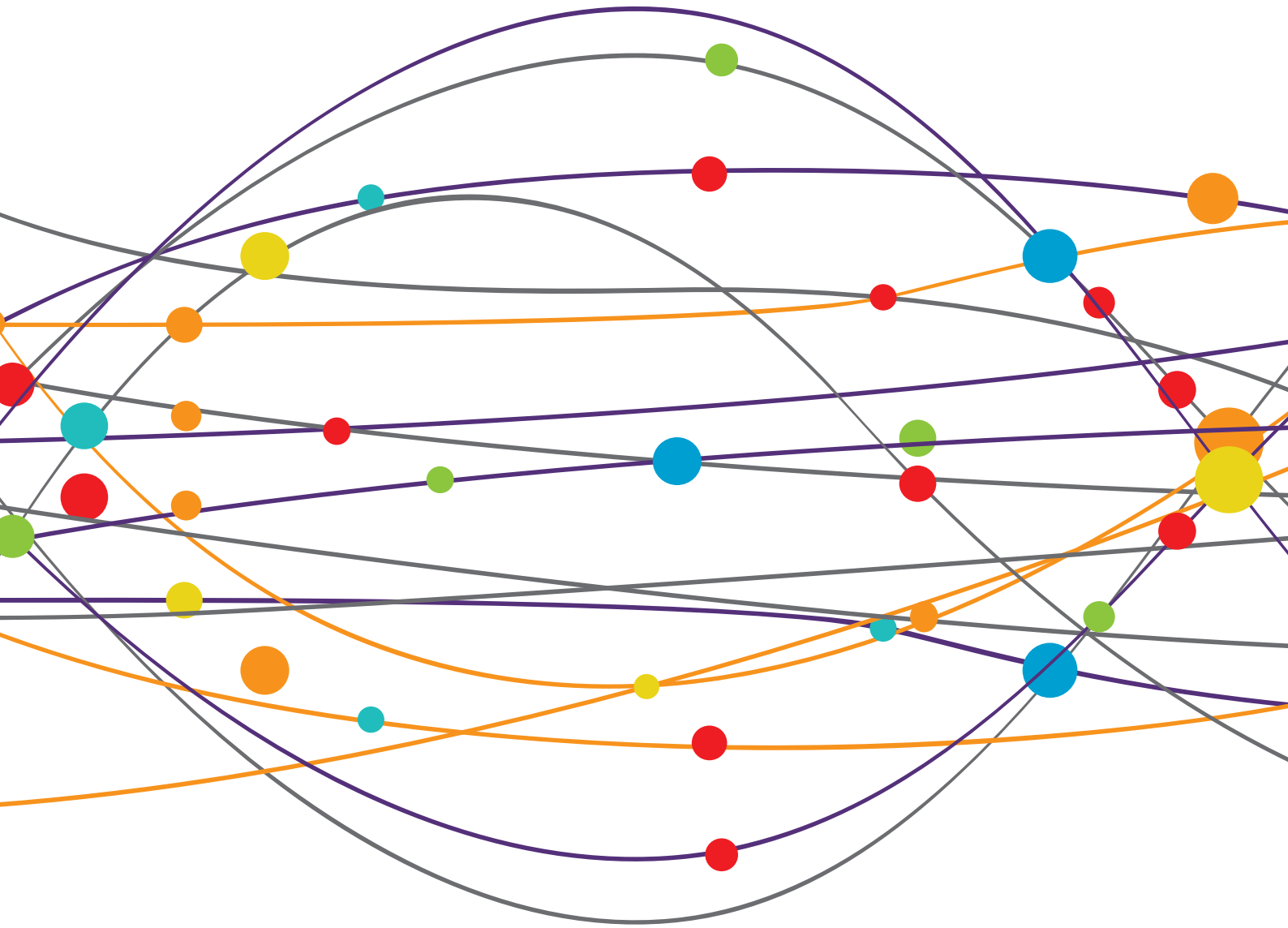

frontiers Research Topics

frontiers

Frontiers eBook Copyright Statement

The copyright in the text of individual articles in this eBook is the property of their respective authors or their respective institutions or funders. The copyright in graphics and images within each article may be subject to copyright of other parties. In both cases this is subject to a license granted to Frontiers.

The compilation of articles constituting this eBook is the property of Frontiers.

Each article within this eBook, and the eBook itself, are published under the most recent version of the Creative Commons CC-BY licence. The version current at the date of publication of this eBook is CC-BY 4.0. If the CC-BY licence is updated, the licence granted by Frontiers is automatically updated to the new version.

When exercising any right under the CC-BY licence, Frontiers must be attributed as the original publisher of the article or eBook, as applicable.

Authors have the responsibility of ensuring that any graphics or other materials which are the property of others may be included in the CC-BY licence, but this should be checked before relying on the CC-BY licence to reproduce those materials. Any copyright notices relating to those materials must be complied with.

Copyright and source acknowledgement notices may not be removed and must be displayed in any copy, derivative work or partial copy which includes the elements in question.

All copyright, and all rights therein, are protected by national and international copyright laws. The above represents a summary only. For further information please read Frontiers' Conditions for Website Use and Copyright Statement, and the applicable CC-BY licence.

ISSN 1664-8714
ISBN 978-2-88966-451-1
DOI 10.3389/978-2-88966-451-1

About Frontiers

Frontiers is more than just an open-access publisher of scholarly articles: it is a pioneering approach to the world of academia, radically improving the way scholarly research is managed. The grand vision of Frontiers is a world where all people have an equal opportunity to seek, share and generate knowledge. Frontiers provides immediate and permanent online open access to all its publications, but this alone is not enough to realize our grand goals.

Frontiers Journal Series

The Frontiers Journal Series is a multi-tier and interdisciplinary set of open-access, online journals, promising a paradigm shift from the current review, selection and dissemination processes in academic publishing. All Frontiers journals are driven by researchers for researchers; therefore, they constitute a service to the scholarly community. At the same time, the Frontiers Journal Series operates on a revolutionary invention, the tiered publishing system, initially addressing specific communities of scholars, and gradually climbing up to broader public understanding, thus serving the interests of the lay society, too.

Dedication to Quality

Each Frontiers article is a landmark of the highest quality, thanks to genuinely collaborative interactions between authors and review editors, who include some of the world's best academicians. Research must be certified by peers before entering a stream of knowledge that may eventually reach the public - and shape society; therefore, Frontiers only applies the most rigorous and unbiased reviews.
Frontiers revolutionizes research publishing by freely delivering the most outstanding research, evaluated with no bias from both the academic and social point of view. By applying the most advanced information technologies, Frontiers is catapulting scholarly publishing into a new generation.

What are Frontiers Research Topics?

Frontiers Research Topics are very popular trademarks of the Frontiers Journals Series: they are collections of at least ten articles, all centered on a particular subject. With their unique mix of varied contributions from Original Research to Review Articles, Frontiers Research Topics unify the most influential researchers, the latest key findings and historical advances in a hot research area! Find out more on how to host your own Frontiers Research Topic or contribute to one as an author by contacting the Frontiers Editorial Office: frontiersin.org/about/contact

NEW INSIGHTS IN SKELETAL MUSCLE CHANNELOPATHIES - A RAPIDLY EXPANDING FIELD

Topic Editors:
Lorenzo Maggi, Fondazione IRCCS Istituto Neurologio Carlo Besta, Italy
Emma Matthews, University College London, United Kingdom
Jean-François Desaphy, University of Bari Aldo Moro, Italy

Jean-François Desaphy is a co-inventor, with no personal financial interest, of a European patent assigned to a pharmaceutical company regarding the use of a company drug in myotonic syndromes.

Citation: Maggi, L., Matthews, E., Desaphy, J.-F., eds. (2021). New Insights in Skeletal Muscle Channelopathies - A Rapidly Expanding Field. Lausanne: Frontiers Media SA. doi: 10.3389/978-2-88966-451-1

Table of Contents

frontiers in Neurology

EDITORIAL
published: 17 December 2020
doi: 10.3389/fneur.2020.626772

Editorial: New Insights in Skeletal Muscle Channelopathies - A Rapidly Expanding Field

Lorenzo Maggi[1]*, *Emma Matthews*[2,3] and *Jean-François Desaphy*[4]

[1] Neuroimmunology and Neuromuscular Diseases, Fondazione Istituto di Ricovero e Cura a Carattere Scientifico (IRCCS) Istituto Neurologico Carlo Besta, Milan, Italy, [2] The Atkinson-Morley Neuromuscular Centre, St George's University Hospitals NHS Foundation Trust, London, United Kingdom, [3] Department of Neuromuscular Diseases, Queen Square Institute of Neurology, UCL, London, United Kingdom, [4] Department of Biomedical Sciences and Human Oncology, School of Medicine, University of Bari Aldo Moro, Policlinico, Bari, Italy

Keywords: SCN4A gene, CLCN1 gene, CACNA1S, myotonia, periodic paralysis, channelopathies

Editorial on the Research Topic

New Insights in Skeletal Muscle Channelopathies - A Rapidly Expanding Field

Skeletal muscle channelopathies (SMCs) are a heterogeneous group of rare genetic neuromuscular diseases resulting in long–term disabilities, posing a significant burden to patients, their families and National Health Care Services. SMCs are caused by mutations in genes encoding skeletal muscle ion channels that control muscle excitability, such as CLCN1, SCN4A, CACNA1S, and KCNJ2. The resultant effect of mutations on muscle excitability is to cause either episodic muscle weakness or myotonia. Based on these predominant clinical feature, SMCs are typically classified as non-dystrophic myotonias (NDMs) or periodic paralyzes (PPs). Given the episodic nature of clinical symptoms diagnosis can be challenging and requires a high degree of clinical suspicion. To date, only symptomatic treatments to reduce myotonia or frequency of paralytic attacks are available and there are no disease-modifying therapies. Although numerous drugs are proposed, data on their efficacy in SMCs consists mostly of case series, open-label and single-blind, controlled trials. The ability to perform randomized controlled trials to generate evidence based treatment approaches has been limited in part by disease rarity and the challenges of recruitment, although a few randomized controlled trials have recently been performed. Mexiletine is now generally considered the gold-standard treatment for NDM, following a phase 2 international randomized, placebo-controlled, crossover clinical trial and a series of N-of-1 trials of mexiletine vs. placebo. Mexiletine however, has reported side effects, mainly gastrointestinal, in a significant proportion of patients. Additionally, 10–30% of patients have a suboptimal or no response. In the periodic paralyzes carbonic anhydrase inhibitors have traditionally been used as the treatment of choice and a recent RCT confirmed the efficacy of dichlorphenamide in hypokalaemic PP. Treatment options are expanding however, and newer drugs have recently been reported as effective in SMC treatment, including flecainide, lamotrigine, and ranolazine. Recently, many achievements have increased complexity in the SMCs field, including the recognition of new phenotypes caused by mutations in *SCN4A* and *CACNA1S* genes, such as severe neonatal episodic laryngospasms, severe fetal hypokinesia, congenital myopathy, rhabdomyolysis, myalgia and exercise intolerance, congenital myasthenic syndrome, and sudden infant death syndrome. Conversely, new genes associated with PP (often with additional clinical features) have been reported, e.g., *ATP1A2*, *KCNJ5*, *RYR1*, *mATP6*, and *mATP8*. In addition, guidelines on clinical presentation and management of NDMs have been recently published by a panel of international experts (1).

Clinical studies reported in this Frontiers in Neurology special issue provide an up to date review of current knowledge of SMCs clinical phenotypes and management. They also highlight ongoing

OPEN ACCESS

Edited and reviewed by:
Giovanni Meola,
University of Milan, Italy

***Correspondence:**
Lorenzo Maggi
lorenzo.maggi@istituto-besta.it

Specialty section:
This article was submitted to Neuromuscular Diseases, a section of the journal Frontiers in Neurology

Received: *06 November 2020*
Accepted: *20 November 2020*
Published: *17 December 2020*

Citation:
Maggi L, Matthews E and Desaphy J-F (2020) Editorial: New Insights in Skeletal Muscle Channelopathies - A Rapidly Expanding Field. Front. Neurol. 11:626772. doi: 10.3389/fneur.2020.626772

gaps in our knowledge e.g., clinically useful predictors of disease progression, and response to therapy, a lack of disease modifying therapies, inadequate randomized controlled trial evidence for many symptomatic treatments and the role of genotype specific drug efficacy in clinical practice.

Studies on specific patient populations are needed to better clarify SMCs genotype-phenotype correlations and disease epidemiology and to aid in the clinical interpretation of diagnostic genetic testing. In this regard, Orsini et al. described a cohort of patients with congenital myotonia caused by mutations in *CLCN1* gene, originating from a specific region in southern Italy, with a common set of mutations different from those reported in Italian patients in other regions. Maggi et al. reported clinical and molecular features of a large cohort of patients with *SCN4A* gene mutations, clinically ranging from PP to NDM and to neonatal disease, further supporting these phenotypes represent a continuum in the clinical spectrum. Further studies are warranted to investigate genetic and non-genetic modifiers of the phenotype.

Laboratory investigations of ion channelopathies are fundamental. First, they assist in confirming whether a new mutation is disease causing, especially in the case of a new or unusual clinical phenotype. Shi et al. described the effect of a sodium channel mutation associated with normokalemic periodic paralysis, while Elia et al. reported a new phenotype characterized by myopathy and joint and skeletal anomalies secondary to a severe myotonia. Functional studies shed light on the molecular mechanisms linking the genotype to the clinical phenotype. Altamura et al. described a ClC-1 chloride channel mutation linked to recessive myotonia congenita, which likely induces a protein misfolding resulting in non-functional channels. The molecular defects induced by ClC-1 channel mutations are reviewed by Jeng et al., showing a complexity of pathomechanisms in myotonia congenita. In this context, important hints can also be provided for by more physiological studies; For instance, the study by Leermakers et al. suggests that the ClC-1 channel may be regulated by ATP and operate as a sensor of skeletal muscle metabolic state, limiting muscle excitability when energy status is low. Regarding sodium channel myotonia, studies of Elia et al. and Pagliarani et al. highlighted the correlation between sodium channel functional defect and severity of the clinical phenotype. Yet, although many studies on the genotype/phenotype relationship have been already published, a number of issues are still unresolved, as reviewed by Morales and Pusch for myotonic syndromes. Importantly, such studies may help identifying possible treatment targets.

The treatment of SCMs remains largely focused on symptomatic improvement. Although RCT data is lacking for many therapies used in clinical practice significant data has been generated for the efficacy and safety of mexiletine in the short-term. Modoni et al. contribute to evidence that this efficacy is maintained in the long-term of clinical practice and provide further re-assurance of minimal cardiac side effects occurring in the SMCs. Meyer et al. illustrate that symptoms of weakness and pain are also prevalent in the NDMs and remind us that when considering the holistic treatment of patients these should not be ignored. It is clear that available therapies are not effective for or tolerated by all patients and newer targeted and disease modifying approaches are needed but Meyer et al. also provide data that morbidity may be impacted by an under-utilization of available anti-myotonics.

SMCs research is now moving toward the proposed interdisciplinary approach, possibly the only promising strategy to find efficient new treatments and a cure for these diseases. We are confident that this Frontiers in Neurology issue may represent a milestone in the field to make clear where we are and provide new paths.

AUTHOR CONTRIBUTIONS

LM, EM, and J-FD contributed to the Editorial. All authors contributed to the article and approved the submitted version.

REFERENCES

1. Stunnenberg BC, LoRusso S, Arnold D, Barohn RJ, Cannon SC, Fontaine B, et al. Guidelines on clinical presentation and management of nondystrophic myotonias. *Muscle Nerve.* (2020) 62:430–44. doi: 10.1002/mus.26887

Conflict of Interest: The authors declare that the research was conducted in the absence of any commercial or financial relationships that could be construed as a potential conflict of interest.

Copyright © 2020 Maggi, Matthews and Desaphy. This is an open-access article distributed under the terms of the Creative Commons Attribution License (CC BY). The use, distribution or reproduction in other forums is permitted, provided the original author(s) and the copyright owner(s) are credited and that the original publication in this journal is cited, in accordance with accepted academic practice. No use, distribution or reproduction is permitted which does not comply with these terms.

frontiers in Neurology

CASE REPORT
published: 25 October 2019
doi: 10.3389/fneur.2019.01138

SCN4A p.R675Q Mutation Leading to Normokalemic Periodic Paralysis: A Family Report and Literature Review

Jiejing Shi[1], Qianqian Qu[1], Haiyan Liu[1], Wenhao Cui[1], Yan Zhang[1], Haidong Lv[1] and Zuneng Lu[2]**

[1] Department of Neurology, Jiaozuo People's Hospital of Henan Province, Jiaozuo, China, [2] Department of Neurology, Renmin Hospital of Wuhan University, Wuhan, China

Objective: To investigate the clinical features, skeletal muscle imaging, and muscle pathological characteristics of normokalemic periodic paralysis (NormoKPP) caused by mutation of SCN4A gene p.R675Q.

Methods: The clinical data, skeletal muscle imaging, pathological data, and gene test results of a family with NormoKPP were collected in detail in October 2018. The previous literature was reviewed and used for comparative analysis.

Results: The proband was a 28-year-old male with paroxysmal weakness of both lower limbs for 14 years. Limb weakness was mainly manifested in the proximal extremities of both lower limbs, which occurred two to three times a year. The muscle weakness of each attack lasted for 1–2 weeks and gradually recovered. The blood potassium levels were normal. The abnormal signals of the posterior thigh muscle group and the medial calf muscle group could be seen on the magnetic resonance imaging (MRI) of the skeletal muscle, and the target-fiber could be seen in some muscle fibers in muscle pathology. The father of the proband and his brother had the same symptoms. In the same family, 10 people received genetic testing. The results showed that five had a mutation of SCN4A gene p.R675Q. The mutation gene came from the father of the proband.

Conclusion: NormoKPP is a clinically rare form of sodium ion channel disease. The clinical manifestations, skeletal muscle imaging, and pathological changes are different from the common hypokalemic periodic paralysis. SCN4A gene detection is an important means for the diagnosis of NormoKPP.

Keywords: normokalemic periodic paralysis, SCN4A mutation, muscle imaging, muscle biopsy, pedigree

OPEN ACCESS

Edited by:
Lorenzo Maggi,
Neurological Institute Foundation Carlo Besta, Italy

Reviewed by:
Antonio Di Muzio,
Università degli Studi G. d'Annunzio Chieti e Pescara, Italy
Carmelo Rodolico,
University of Messina, Italy

****Correspondence:***
Haidong Lv
hnlhd666@163.com
Zuneng Lu
lzn196480@126.com

Specialty section:
This article was submitted to Neuromuscular Diseases, a section of the journal Frontiers in Neurology

Received: *17 July 2019*
Accepted: *10 October 2019*
Published: *25 October 2019*

Citation:
Shi J, Qu Q, Liu H, Cui W, Zhang Y, Lv H and Lu Z (2019) SCN4A p.R675Q Mutation Leading to Normokalemic Periodic Paralysis: A Family Report and Literature Review. Front. Neurol. 10:1138. doi: 10.3389/fneur.2019.01138

INTRODUCTION

Periodic paralysis (PP) is an ion channel disease characterized by recurrent muscle weakness caused by mutations in the skeletal muscle ion channel gene. According to the level of potassium in the blood, it can be divided into hypokalemic, normokalemic, and hyperkalemic periodic paralysis (1). Among them, normokalemic periodic paralysis (NormoKPP) is the rarest subtype of PP. NomoKPP is an autosomal dominant hereditary disease. At present, there are more than 20 kinds of sodium channel alpha subunit SCN4A gene mutations reported, including R675G, R675Q, R675H, R675W, R1129Q, T704M, and M1592V. However, these mutations have also been reported to cause

hypokalemic periodic paralysis and hyperkalemic periodic paralysis. The NormoKPP caused by the p.R675Q mutation of the skeletal muscle SCN4A gene has not been reported. In this study, the clinical features, muscle magnetic resonance imaging (MRI), and muscle pathology of a family case of NormoKPP was confirmed by genetic testing. We also conducted a thorough literature review.

MATERIALS AND METHODS

Clinical Features

The proband was a 28-year-old male truck driver. The main complaint was "paroxysmal weakness of both lower limbs for 14 years, recurrence in February" in October 2018. About 14 years ago, the patient sweated after taking two tablets of Analgin orally because of a cold. In the morning, he developed limb weakness, with both lower limbs as the most important. He could not get out of bed or turn over. After about 1 week, the symptoms gradually improved and returned to normal. The effect of "low potassium" treatment in local hospitals is poor. Afterwards, the onset of muscle weakness lasted for 1–2 weeks, two to three times a year, and occurred mostly in the morning during summer. In most cases, it is still feasible to walk, but it is laborious to go up the stairs and some even cannot walk in serious cases. The blood potassium test was normal many times during the attack, and the symptoms of oral potassium chloride solution did not improve significantly. After a cold 2 months ago, limb weakness occurred again, mainly in the lower limbs; both upper limbs could be raised above the head, squatting and standing was difficult, and his ability to walk was weakened. The blood potassium was normal when measured at the local hospital. After 1 week, the proximal muscle strength of both lower extremities basically returned to normal, but the distal muscle strength of the left lower extremity did not completely return to normal. The symptoms of limb weakness still fluctuated in the past month. After walking for 100 m, the calves became sour and weak. So far, muscle strength has not completely recovered. He came to our hospital for treatment. He has a past of physical fitness. His father began to suffer from paroxysmal limb weakness in his teens, mostly in the morning with squatting and standing difficulties and walking weakness. It lasted for about a week, three to five times a year, and there had been no attack in nearly 10 years. His elder brother had intermittent weakness of both lower limbs since he was 16 years old, mainly in the calves, and he had difficulties standing on his tiptoes. He had an average attack of about two times a year. He had been tested for blood potassium in local hospitals many times. A total of four siblings, two sisters, and their mothers, were in good health and had no similar medical history. Physical examination: cranial nerve (–); normal limb muscle tension; upper limb muscle strength grade 5; lower limb proximal muscle strength grade 4; distal muscle strength grade 4+; tendon reflex of upper extremities (+); tendon reflex of lower extremities had disappeared; bilateral pathological signs (–); bilateral depth and shallow sensation were normal; extremities had no muscle atrophy and hypertrophy; there was no muscle tenderness.

METHODS

Neuroelectrophysiology

Motor conduction velocity (MCV), sensory conduction velocity (SCV), and Concentric circular needle electromyography (EMG) were measured using the Japanese photoelectric MEB-9200K myoelectric evoked potential meter. Bilateral tibialis anterior, quadriceps femoris, gastrocnemius, and biceps brachii were selected for electromyography. The conduction velocity of the bilateral common peroneal nerve, tibial nerve, superficial peroneal nerve, and sural nerve was measured. There was parallel detection of F wave and H-reflex in both lower limbs.

Muscle MRI

Axial scanning of the lower limbs of the patient was performed using a GE 1.0T nuclear magnetic resonance machine. The scanning sequences included T1WI, T2WI, and STIR.

Muscle Pathology

The proband was given an open biopsy under local anesthesia, and the left gastrocnemius muscle was selected as the biopsy muscle. Muscle specimens were fixed by liquid nitrogen, frozen in sections, subjected to tissue HE, MGT, ORO, PAS, ATPase, and NADH staining, and observed under a light microscope.

Genetic Testing

With the informed consent of the proband and his family members, genetic testing was performed on the proband and 10 families. Genomic DNA was extracted from 4 ml venous blood for screening of single gene genetic diseases of whole genome exons, which were detected by Jin Jun Inspection Center.

RESULTS

Neuroelectrophysiology

SCV: The sensory nerves of both lower limbs were normal. MCV: The motor nerves of both lower limbs were normal. F wave: The F-waves of nerves detected in both lower limbs were normal. H-reflex: The H-reflex amplitude of the examined nerves in the left lower limb was lower than that in the opposite side, and the right side was normal. EMG: The muscles of the upper and lower limbs were normal. However, the patient failed to perform a long exercise test (2).

Laboratory Examination

CK 380 μ/L, CKMB 26 μ/L, LDH 185 μ/L, LAC 2.31 mmol/L, ALT 27 μ/L, AST 23 μ/L, K^+ 4.31 mmol/L, $Ca2^+$ 2.34 mmol/L, Na^+ 142 mmol/L, and CL^- 105 mmol/L.

MRI Scan

The muscle groups of bilateral gluteus maximus, bilateral gluteus medius, bilateral adductor maximus, and bilateral sartorius, the medial head of left gastrocnemius and the posterior leg showed diffuse increase signals and present reduction of muscle volume (**Figure 1**).

Muscle Pathology

The left gastrocnemius muscle biopsy was performed with the consent of the patient (**Figure 2**).

Genetic Testing

After obtaining the consent of the probands and their families, 10 pedestrians were tested for the probands and their families. The results showed that there was a heterozygous mutation in the patient-related gene SCN4A: c.2024 4 > A (guanine > adenine), which led to the change of amino acid p.R675Q. Family validation results showed that the heterozygous mutation results came from the father, and there were the same heterozygous mutations at this locus in his brother, his son, and his daughter (**Figure 3**). There were no mutations in the genes of her mother, her son, her eldest sister's son, her second sister's daughter, and her brother's daughter. Other relatives did not receive genetic testing (**Figure 4**).

DISCUSSION

NormoKPP is a rare type of PP. Patients often develop symptoms around the age of 10, which is characterized by paroxysmal muscle weakness, without changes in serum potassium concentration. Each attack of limb weakness lasts for a relatively long time, usually several days to weeks, before returning to normal. Most of the symptoms are alleviated in adulthood while a few can be left with persistent muscle weakness and muscle atrophy (1). In this family, all three patients had onset in adolescence, limb weakness mainly involved both lower limbs, and both proximal and distal muscles were involved. After the

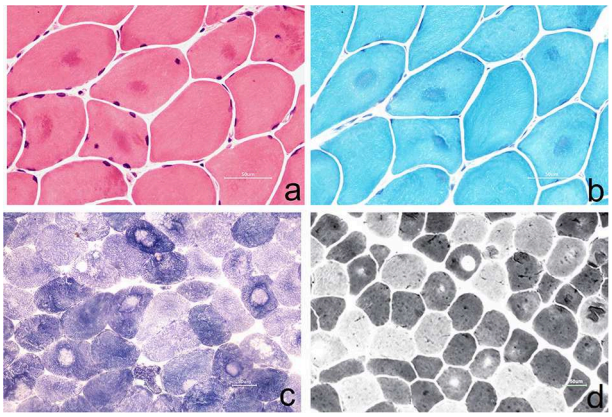

FIGURE 2 | (a) Muscle fibers vary slightly in size, with round-like changes. Some of them show eosinophilic deep-stained areas in the center of muscle fibers (HE staining, ×400); **(b)** some muscle fibers were dyed dark blue in the center of the by MGT staining, and no typical RRF were observed (MGT staining, ×400); **(c)** the arrangement of myofibrils in some muscle fibers was disordered, and the absence of activity in the center of muscle fibers resulted in target-fiber (NADH staining ×200); **(d)** the distribution of type I and type II muscle fibers was basically normal, and the phenomenon of target-fiber appeared mostly in type II muscle fibers (ATPase staining ×200).

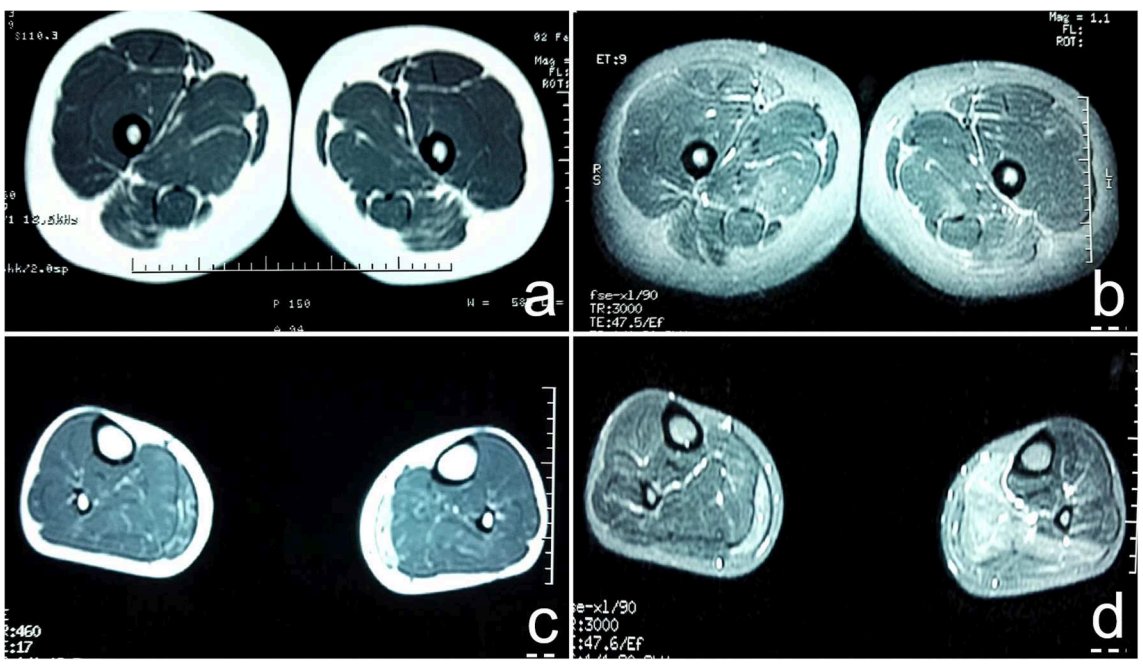

FIGURE 1 | (a) T1WI sequence showed diffuse increase in signal intensity of bilateral gluteus maximus, gluteus medius, adductor maximus, and sartorius muscles; **(b)** T2W1 with fat suppression showed multiple high signal intensity in strips and lines in bilateral gluteus maximus, gluteus medius, adductor maximus, and sartorius muscles; **(c)** T1WI showed diffuse increase in signal intensity of medial head of bilateral gastrocnemius, present reduction of muscle volume. The medial head of the lateral gastrocnemius was obvious; **(d)** T2W1 with fat suppression showed that the signal intensity of the medial head of the right gastrocnemius and the posterior leg muscle group increased unevenly, especially the medial head of the left gastrocnemius.

attack, the clinical symptoms recovered slowly, and the muscle weakness symptoms lasted for a long time. In most cases, the symptoms gradually recovered after 1–2 weeks. Both the proband and his brother had a history of distal limb weakness lasting for more than 4 weeks, which has not been reported in previous literature (3–9).

There are different degrees of high signal on fat-suppressed T2WI. The most vulnerable muscles are the soleus, anterior, lateral head of gastrocnemius, and medial head of gastrocnemius (10). However, there are few studies on skeletal muscle imaging in patients with NormoKPP, and the literature is limited. In this case, the patient's leg MRI showed a diffuse increase in the bilateral gluteus maximus, gluteus medius, adductor magnus, and sartorius in the STIR sequence, which is suggestive of muscle edema. The STIR and T2WI sequence showed diffuse and uneven increase of signal intensity in the medial head of the right gastrocnemius and the posterior calve muscle group, significant in the medial head of left gastrocnemius, suggesting muscle edema and partial fatization. In T1WI, there were multiple cases of linear high signal intensity in the above muscles, diffuse increase of signal intensity in the medial head of left gastrocnemius, and present reduction of muscle volume; the medial head of the bilateral gastrocnemius was obvious, suggesting that the muscles of the lower limbs of the patient were replaced by fat and had mild muscle atrophy. This has not been reported in the literature.

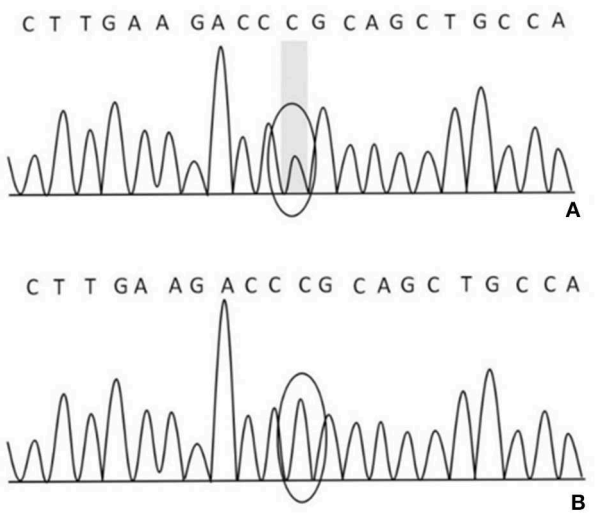

FIGURE 3 | (A) There was a heterozygous mutation c.2024 4>A in the proband, his father, brother, son, and daughter on chr17-62034874; **(B)** there was no mutation in his mother, son, the eldest sister's son, the second sister's daughter, and his brother's daughter on chr17-62034874.

Muscle biopsy in NormoKPP patients is also less reported (3–9). It has been reported that pathological findings include the enlargement of the sarcoplasmic reticulum, an increase of mitochondria, accumulation of myotubes, and focal myofibrillar necrosis in persistent limb weakness (11). In this case, a muscle biopsy showed that the muscle fibers were slightly different in size with round-like changes. In the center of some muscle fibers, eosinophilic deep-stained areas were seen, and no obvious infiltration of denatured and necrotic muscle fibers and inflammatory cells was observed. In nicotinamide adenine dinucleotidehydrogen (NADH) staining, the arrangement of myofibrils in some muscle fibers was disordered, and the absence of activity in the center of the muscle fibers resulted in target-fiber, which was seldom reported in previous literature. The modified Gomoritrichrome (MGT) staining showed that some muscle fibers were dyed dark blue in the center, consistent with the NADH staining, and no typical tubular aggregation and ragged red fibers (RRF) were observed. ATPase staining showed that the distribution of type I and II muscle fibers was basically normal, and the phenomenon of target-fiber appeared mostly

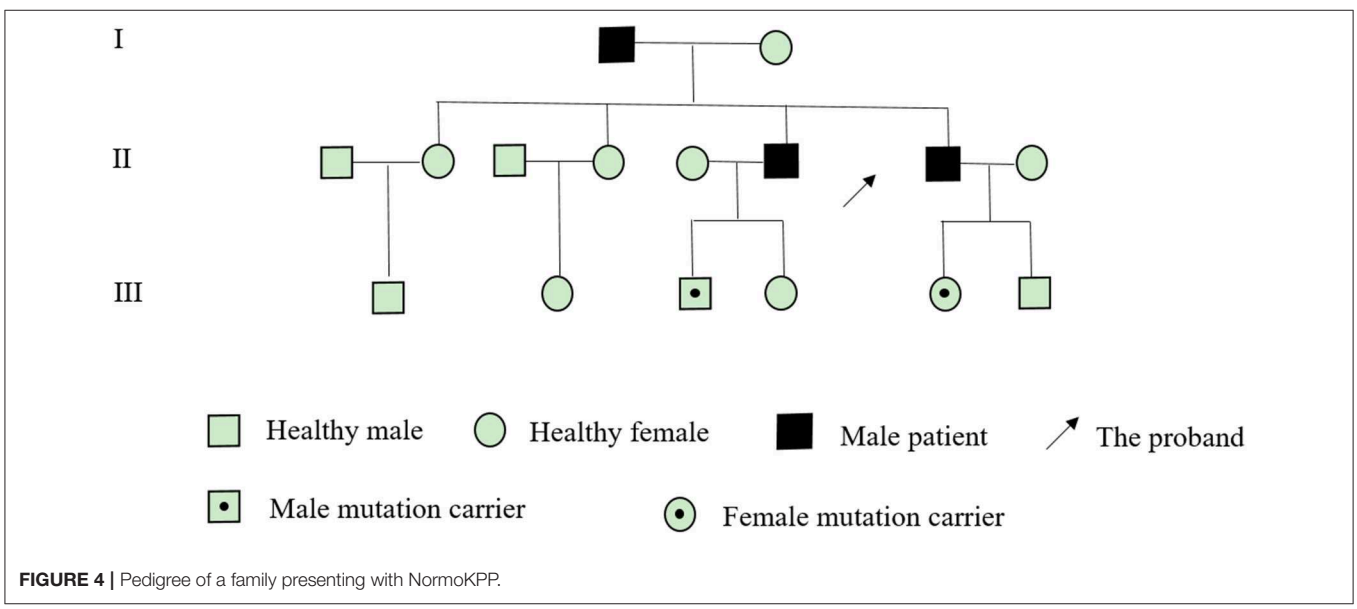

FIGURE 4 | Pedigree of a family presenting with NormoKPP.

in type II muscle fibers. However, the pathological changes mentioned above are rarely reported in the previous literature.

The SCN4A gene is located on the 17q23-25 chromosome (11), and its mutation can lead to various types of periodic paralysis. R675Q mutation is located in the DIIS4 region of the sodium channel. This mutation may increase the continuous current of the sodium channel, change the voltage-dependent activation process, lead to abnormal depolarization of resting potential, slow down the inactivation process, thus affecting the normal function of sodium channel, and lead to disease (11). The genetic testing results of this family suggest that the mutation of R675Q in the SCN4A gene comes from the father, and the brother also carries the gene. Compared with the previously reported cases of NormoKPP, the familial NormoKPP caused by the mutation of p.R675Q in the SCN4A gene has not been reported (7, 8, 12). The clinical features of such patients were long duration of muscle weakness symptoms and slow recovery of muscle strength. However, with the increase of age, the number of seizures gradually decreased or terminated. Skeletal muscle MRI is characterized by abnormal signals of the posterior thigh muscles and the medial calf muscles. Muscle pathology showed that some of the muscle fibers have a target-fiber phenomenon.

It has been reported that most of the gene mutations of NormoKPP are common to HyperKPP (13, 14). Therefore, in clinical practice, we should make a comprehensive analysis based on clinical characteristics and biochemical detection, combined with skeletal muscle imaging and pathological changes and genetic testing results to determine the final clinical diagnosis. But, why the same gene mutation of SCN4A causes PP of different types of serum potassium levels still needs further study.

ETHICS STATEMENT

The studies involving human participants were reviewed and approved by the ethics committee of the Jiaozuo People's Hospital of Henan Province, Henan, China. The patients/participants provided their written informed consent to participate in this study.

AUTHOR CONTRIBUTIONS

JS was responsible for writing papers. QQ and HLi are responsible for data collection. WC was responsible for making important revisions to papers. YZ was responsible for data analysis. HLv and ZL are responsible for providing overall ideas.

REFERENCES

1. Fontaine B. Periodic paralysis. *Adv Genet*. (2008) 63:3–23. doi: 10.1016/S0065-2660(08)01001-8
2. Fournier E, Tabti N. Clinical electrophysiology of muscle diseases and episodic muscle disorders. *Handb Clin Neurol*. (2019) 161:269–80. doi: 10.1016/B978-0-444-64142-7.00053-9
3. Wei CJ, Wang D, Wang S, Jiao H, Hong DJ, Pu LH, et al. Clinical and molecular genetic analysis of a family with normokalemic periodic paralysis. *Chin J Pediatr*. (2013) 51:47–51. doi: 10.3760/cma.j.issn.0578-1310.2013.01.009
4. Vicart S, Sternberg D, Fournier E, Ochsner F, Laforet P, Kuntzer T, et al. New mutations of SCN4A cause a potassium sensitive normokalemic periodic paralysis. *Neurology*. (2004) 63:2120–7. doi: 10.1212/01.WNL.0000145768.09934.EC
5. Song YW, Kim SJ, Heo TH, Kim MH, Kim JB. Normokalemic periodic paralysis is not a distinct disease. *Muscle Nerve*. (2012) 46:914–6. doi: 10.1002/mus.23441
6. Fu C, Wang Z, Wang L, Li J, Sang Q, Chen J, et al. Familial normokalemic periodic paralysis associated with mutation in the SCN4A p.M1592V. *Front Neurol*. (2018) 9:430. doi: 10.3389/fneur.2018.00430
7. Liu XL, Huang XJ, Luan XH, Zhou HY, Wang T, Wang JY, et al. Mutations of SCN4A gene cause different diseases: 2 case reports and literature review. *Channels*. (2015) 9:82–7. doi: 10.1080/19336950.2015.1012945
8. Wu L, Zhang B, Kang Y, Wu W. Enhanced slow inactivation of the human skeletal muscle sodium channel causing normokalemic periodic paralysis. *Cell Mol Neurobiol*. (2014) 34:707–14. doi: 10.1007/s10571-014-0052-y
9. Hong D, Luan X, Chen B, Zheng R, Zhang W, Wang Z, et al. Both hypokalaemic and normokalaemic periodic paralysis in different members of a single family with novel R1129Q mutation in SCN4A gene. *J Neurol Neurosurg Psychiatry*. (2010) 81:703–4. doi: 10.1136/jnnp.2009.177451
10. Jia BX, Yang Q, Wang H, Guo XH. The genetic and skeletal muscle imaging characteristics of hypokalaemic periodic paralysis patients. *Chin J Neuroimmunol Neurol*. (2014) 21:36–40. doi: 10.3969/j.issn.1006-2963.2014.01.010
11. Vicart S, Sternberg D, Fontaine B, Meola G. Human skeletal muscle sodium channelopathyies. *Neurol Sci*. (2005) 26:194–202. doi: 10.1007/s10072-005-0461-x
12. Wu L, Wu W, Yan G, Wang X, Liu J. The construction and preliminary investigation of the cell model of a novel mutation R675Q in the SCN4A gene identified in a chinese family with normokalemic periodic paralysis. *Chin J Med Genet*. (2008) 25:629–32. doi: 10.3321/j.issn:1003-9406.2008.06.004
13. Chinnery PF, Walls YJ, Hanna MG, Bates D, Fawcett PR. Normokalemic periodic paralysis revisited: does it exist? *Ann Neurol*. (2002) 52:251–2. doi: 10.1002/ana.10257
14. Guo XH, Wu WP, Zhu K, Wang HB, Si YL, Mao YL, et al. Genetic study on the relationship between normokalemic periodic paralysis and hyperkalemic periodic paralysis. *Chin J Neurol*. (2003) 36:428–432. doi: 10.3760/j.issn:1006-7876.2003.06.009

Conflict of Interest: The authors declare that the research was conducted in the absence of any commercial or financial relationships that could be construed as a potential conflict of interest.

Copyright © 2019 Shi, Qu, Liu, Cui, Zhang, Lv and Lu. This is an open-access article distributed under the terms of the Creative Commons Attribution License (CC BY). The use, distribution or reproduction in other forums is permitted, provided the original author(s) and the copyright owner(s) are credited and that the original publication in this journal is cited, in accordance with accepted academic practice. No use, distribution or reproduction is permitted which does not comply with these terms.

frontiers in Neurology

REVIEW
published: 17 January 2020
doi: 10.3389/fneur.2019.01404

An Up-to-Date Overview of the Complexity of Genotype-Phenotype Relationships in Myotonic Channelopathies

Fernando Morales[1*†] *and Michael Pusch*[2*†]

[1] *Instituto de Investigaciones en Salud, Universidad de Costa, San José, Costa Rica,* [2] *Istituto di Biofisica, CNR, Genova, Italy*

OPEN ACCESS

Edited by:
Emma Matthews, Institute of Neurology, Faculty of Brain Sciences, University College London, United Kingdom

Reviewed by:
Pia Bernasconi, Fondazione Neurologico "Carlo Besta", Italy
Doreen Fialho, University College London Hospitals NHS Foundation Trust, United Kingdom

***Correspondence:**
Fernando Morales
fernando.moralesmontero@ucr.ac.cr
Michael Pusch
pusch@ge.ibf.cnr.it

[†] *These authors have contributed equally to this work*

Specialty section:
This article was submitted to Neuromuscular Diseases, a section of the journal Frontiers in Neurology

Received: *24 October 2019*
Accepted: *23 December 2019*
Published: *17 January 2020*

Citation:
Morales F and Pusch M (2020) An Up-to-Date Overview of the Complexity of Genotype-Phenotype Relationships in Myotonic Channelopathies. Front. Neurol. 10:1404. doi: 10.3389/fneur.2019.01404

Myotonic disorders are inherited neuromuscular diseases divided into dystrophic myotonias and non-dystrophic myotonias (NDM). The latter is a group of dominant or recessive diseases caused by mutations in genes encoding ion channels that participate in the generation and control of the skeletal muscle action potential. Their altered function causes hyperexcitability of the muscle membrane, thereby triggering myotonia, the main sign in NDM. Mutations in the genes encoding voltage-gated Cl^- and Na^+ channels (respectively, *CLCN1* and *SCN4A*) produce a wide spectrum of phenotypes, which differ in age of onset, affected muscles, severity of myotonia, degree of hypertrophy, and muscle weakness, disease progression, among others. More than 200 *CLCN1* and 65 *SCN4A* mutations have been identified and described, but just about half of them have been functionally characterized, an approach that is likely extremely helpful to contribute to improving the so-far rather poor clinical correlations present in NDM. The observed poor correlations may be due to: (1) the wide spectrum of symptoms and overlapping phenotypes present in both groups (Cl^- and Na^+ myotonic channelopathies) and (2) both genes present high genotypic variability. On the one hand, several mutations cause a unique and reproducible phenotype in most patients. On the other hand, some mutations can have different inheritance pattern and clinical phenotypes in different families. Conversely, different mutations can be translated into very similar phenotypes. For these reasons, the genotype-phenotype relationships in myotonic channelopathies are considered complex. Although the molecular bases for the clinical variability present in myotonic channelopathies remain obscure, several hypotheses have been put forward to explain the variability, which include: (a) differential allelic expression; (b) trans-acting genetic modifiers; (c) epigenetic, hormonal, or environmental factors; and (d) dominance with low penetrance. Improvements in clinical tests, the recognition of the different phenotypes that result from particular mutations and the understanding of how a mutation affects the structure and function of the ion channel, together with genetic screening, is expected to improve clinical correlation in NDMs.

Keywords: myotonia, channelopathies, clinical and genetic variability, clinical correlations, functional analyses

NEUROMUSCULAR DISEASES

Neuromuscular diseases are a clinically, genetically, and biochemically heterogeneous group of more than 80 different entities (https://www.mda.org/disease/list), some of which share clinical and dystrophic features (1, 2). The main tissue affected (some diseases are multisystemic) in these diseases is the skeletal muscle, which is the organ in charge of locomotion and other body movements, and contributes to metabolic energy in multicellular organisms. Malfunction of this organ due to structural, physiological, or biochemical changes, often caused by specific genetic mutations, can lead to progressive muscle weakness/wasting with detrimental health consequences (3). Clinical features, such as disease severity, progression, age of onset of symptoms, and prognosis are highly variable (2). Hereditary neuromuscular diseases have been classified into several groups depending on the group of muscles targeted by specific gene mutations. However, clinically different phenotypes have been found in various patients with different mutations in the same gene, and even in separate patients carrying identical mutations (4, 5). The respective genes encode structural proteins, enzymes, ion channels, some of them causing muscular dystrophies (1–3). Muscular dystrophies, which can be inherited as dominant or recessive diseases, include limb girdle muscular dystrophies, congenital muscular dystrophies, dystrophinopathies, facioscapulohumeral muscular dystrophy, Emery–Dreifuss muscular dystrophies, and myotonic dystrophies. This review will focus on a group of disease that have been classified within the group of myotonic conditions, more specifically, the myotonic channelopathies.

MYOTONIC DISEASES

Electrical properties of the skeletal muscle fiber membrane (in a wide variety of different organisms) are characterized by a high resting membrane permeability for Cl^- ions. These Cl^- ions are transported by Cl^- ion channels belonging to the CLC family, which includes Cl^- ion channels and Cl^-/H^+ exchangers that are found in all phyla from bacteria to mammals (6–8). The ClC-1 channel is specifically present in skeletal muscle where it accounts for the chloride conductance, G_{Cl}, which amounts to ∼80% of the resting membrane conductance in resting muscles (9–15). Due to this high conductance and because the equilibrium potential of Cl^- is close to the muscle resting membrane potential, ClC-1 conducts membrane currents that inhibit muscle excitability (6). The effective Cl^- homeostasis is central in the generation and propagation of the action potential in muscle fibers.

Indeed, it is believed that the prominent role of G_{Cl} in action potential repolarization and membrane potential stabilization is related to the large cell size and the peculiar t-tubular system of skeletal muscle. If repolarization were mediated exclusively by K^+ channels (as in most neurons), the extracellular K^+ concentration in the restricted t-tubular space would rise significantly, leading to depolarization and eventual inactivation of Na^+ channels (15). In fact, the "myotonic runs" of repeated action potential firing are partially caused by K^+ accumulation (15). Importantly, a still open question is whether ClC-1 channels are actually preferentially located in the t-tubular membrane or in the surface sarcolemma (16–19).

It is well-known that excitation-contraction coupling, triggered by the nerve-impulse induced muscle action potential, is orchestrated by multiple factors (mainly ion channels) that lead to the release of Ca^{2+} from the sarcoplasmic reticulum. However, changes in the electrical properties of an excitable muscle, that can occur by both acquired or inherited bases, are well-recognized causes of muscle malfunction in humans (20). Reduction in muscle excitability may be the major cause of muscle weakness leading to fatigue (21), while hyperexcitability may lead to a sustained bursts of discharges that cause involuntary after-contractions, a phenomenon known as myotonia, the classical and leading sign of several hereditary diseases of skeletal muscle (20, 22). Therefore, myotonia is a clinical sign of skeletal muscle that results from an increased excitability of the muscle fiber membrane such that a single nerve stimulus triggers a burst of repetitive action potentials causing a delay in the temporal course of muscle relaxation (23). In patients, this condition can be detected as both electrical and clinical myotonia (24, 25). Electrical myotonia is detected on electromyographic (EMG) tests as repetitive muscle fiber potential discharges, with waxing and waning frequency and amplitude with a firing rate between 20 and 80 Hz, while clinical myotonia is physically demonstrated by slowed muscle relaxation during repetitive hand grip, eye closure, or after tapping various muscles, such as the finger extensors (26).

Symptomatically, patients experience myotonia as stiffness at the beginning of motion, better exemplified during initial attempts at relaxation of hand grip (grip myotonia) and following percussion of the muscle located in the bases of the thumb (percussion myotonia) (27). Myotonia can ameliorate with repeated movements, a phenomenon known as warm-up, but also, it can get worse with activity and become paradoxical (28, 29).

Diseases associated with this sign are collectively termed myotonias and according to other clinical features (progressive muscle wasting and weakness, dystrophic changes), they are classified as: (1) dystrophic myotonias (DM) and (2) non-dystrophic myotonias (NDM). Myotonic dystrophy type 1 (DM1) and type 2 (DM2), caused by the expansion of unstable microsatellites, belong to the first group, and are beyond the scope of this review. A group of five diseases, collectively called myotonic channelopathies, caused by mutations in voltage-gated Na^+ and Cl^- channel genes, belong to the second group (30). This review is focused on the latter group of diseases.

NON-DYSTROPHIC MYOTONIAS

Dominantly or recessively inherited disorders caused by ion channel dysfunction include myotonia congenita (MC) (Thomsen's disease and Becker type myotonia), paramyotonia congenita (PC), hyperkalemic periodic paralysis (hyperPP) with myotonia and the sodium channel myotonias (SCM). These diseases show distinctive clinical features that allow separating them from the myotonic dystrophies. They are divided into

two groups: the chloride and the sodium channelopathies. The first group, called myotonia congenita (MC), is subdivided in Thomsen's disease and the Becker generalized myotonia. The other group of three diseases listed above belong to the sodium channelopathies (24, 25, 30–32).

PHENOTYPE OF MYOTONIC CHANNELOPATHIES

Chloride Channelopathies

For precise control of muscle contraction by nerve activity, in normal conditions, a single nerve action potential triggers only a single muscle action potential. This is to a large extent guaranteed by the large G_{Cl} that aids in repolarizing the action potential and, once repolarized, continues to stabilize the membrane potential, preventing thereby the insurgence of a train of action potentials (33). Reduction of the Cl^- conductance in the skeletal muscle causes myotonia congenita (MC), the most common ion channel disease (34). The first description of this pathology dates back to the late nineteenth century, when Danish physician Asmus Julius Thomas Thomsen described it for himself and for some of his family members, with an autosomal dominant inheritance pattern (35). The dominant form of MC was called Thomsen's disease (DMC) after that (36). Almost a century after that first description, German professor Peter Emil Becker described a MC variant with autosomal recessive inheritance pattern, a variant that was called recessive generalized myotonia or Becker myotonia (RMC) (37). MC is electrophysiologically characterized by presenting increased excitability of the muscular fiber, which is due to repetitive action potentials of the muscle membranes; this is reflected in clinical myotonia, muscular stiffness (that is worse after rest) and hypertrophy (38, 39). Myotonia in MC is clinically highly variable, ranging from myotonic discharges only detectable on the EMG test to disabling muscle stiffness at an early age (5). The leg muscles are commonly affected and handgrip myotonia is detected in about ¾ of patients (22). Almost every skeletal muscle in the body might show muscular stiffness, but it is ameliorated by exercise (warm-up phenomenon). The clinical picture depends on whether the disease is inherited as autosomal dominant or autosomal recessive. RMC is more common (in most countries) and severe than DMC (5, 24, 25, 40–42). In DMC, age of onset is usually at birth or very early in infancy. The child might show unusually defined muscles in the extremities, delayed relaxation of the eyelids after forceful closure following sneezing or during crying, and hypertrophy is rare in childhood but common in adulthood (31, 43). Severity varies from mild to moderate, there is no progression of the symptoms, and patients can experience a normal life (43). In RMC, age of onset is usually later than in DMC (25, 43), but it has been also reported that age of onset could be earlier in RMC (44). Myotonia is generalized with moderate to pronounced hypertrophy, where many patients use to have a body-builder appearance due to hypertrophy triggered by the involuntary after-contractions (20, 43). Myotonia is more severe in the recessive variant and usually, typical transient muscular weakness (lasting from seconds to as long as 30 min) is also observed (10, 45), which may lead to recurrent falls (31, 34). Muscle strength is normal in this variant but the disease slowly progresses in some patients (34, 46).

Sodium Channelopathies

The upstroke of the action potential is mediated by opening of voltage-gated Nav1.4 sodium channels that generate an inward Na^+ current that renders the cells positive inside (depolarization) (31). Malfunction of these channels cause several human hereditary diseases of the skeletal muscle. Diseases belonging to this group are: paramyotonia congenita (PC), hyperkalemic periodic paralysis (HyperPP) with myotonia and the sodium channel myotonias (SCM). Similar to MC, these diseases are characterized by increased muscle membrane excitability that leads to repetitive action potentials; however, the underlying physiological defect is different compared with the chloride channelopathies (24, 47). Symptoms in sodium channelopathies are episodic and vary from patient to patient and also from time to time on each affected individual (47). Clinical myotonia, affecting hands, face, upper and lower extremities is generalized, going from absent to very severe, depending on the disease, and usually gets worse with exercise; while electrical myotonia may be diffusely present in all muscle and in some cases, may worsen due to cold exposure, which may also induce weakness in some patients, and clinical myotonia. The length of the attack is very variable, lasting from minutes up to 7 days. Muscle hypertrophy is not as common as in the chloride channelopathies, but it is present in variable degrees in some patients. Age of onset of the disease is usually in the first decade and it might progress later in life in some patients (25, 27, 48–50).

PC was first described by Eulenburg (51). Age of onset of first symptoms is at birth or during the first decade of live, affecting mainly the muscles from neck, face and upper limbs. As indicated by its name, PC shows paradoxical myotonia, which gets worse with repeated movements and/or cold exposure. PC show variable weakness, which becomes evident after myotonic stiffness attacks, the major symptom in PC (20, 47). PC patients may experience HyperPP weakness-like phenotype after pronounce cooling or vigorous exercise (20).

In HyperPP, age of onset of the first symptoms (recurrent episodes of weakness as the main symptom) is during childhood. Symptoms are triggered by ingestion of K^+-rich food, rest after vigorous exercise, and other environmental factors (47, 52–54). The episodes of weakness vary from minutes to several hours, with normal weakness between attacks. Patients affected with HyperPP frequently have myotonia (symptomatically in 12.5% or by EMG in 50% of patients), which can be from mild to moderate, particularly with the onset of a weakness attack. Some patients develop paramyotonia, highlighting the extensive clinical overlapping between these two conditions (20, 47, 53, 55).

SCM is less well-defined with onset of first symptoms from childhood, as in acetazolamide-responsive myotonia, to adolescence, as in myotonia fluctuans (47). Myotonia can be present from mild (in myotonia fluctuans) to severe (in myotonia permanens affecting swallowing and breathing); no periodic paralysis has been observed in SCM patients, while there are

some patients that have shown potassium-aggravated myotonia (K^+-sensitive myotonia) (20).

GENETICS AND MUTATION IN MYOTONIC CHANNELOPATHIES

Chloride Channelopathies

As mentioned above, MC is the most common hereditary ion channel disorder in humans, showing a prevalence between 1:23,000 and 1:50,000 for the recessive form (Becker Myotonia), while the dominant form (Thomsen's disease) is a bit less common in most countries (40, 42, 56). Both conditions are caused by mutations in the chloride voltage-gated channel 1 (*CLCN1*) gene (10, 57–59), which is located in chromosome 7q35 and encodes the voltage-gate chloride channel (ClC-1), belonging to the CLC family of chloride channels (60, 61). Although the pathogenesis of MC is not fully understood, it is well-known that mutations in *CLCN1* produce a reduction of the Cl^- conductance that leads to membrane hyperexcitability, triggering repetitive action potentials (24, 25, 31). The channel conducts chloride ions over the entire physiological voltage ranges and is the major mediator of chloride conductance in skeletal muscle (13, 14, 31, 62, 63). Two subunits of the channel are required to come together to form the functional channel, and thus, work as double-barreled homodimers (64–66). The *CLCN1* gene has 23 exons, with more than 200 different mutations described in this disease (4, 41, 43, 67, 68) (http://www.hgmd.cf.ac.uk/ac/index.php). Mutations are found through the entire gene sequence, being present in the N-terminal, transmembrane, and C-terminal domains of ClC-1. Different types of mutations have been found in the *CLCN1* gene, including nonsense, splice-site, missense, frameshift (insertion/deletions), and deletion/duplication mutations, with exon eight becoming a hot spot for DMC (20, 41, 67, 69–71). The recessive inheritance is conceptually explained by a loss-of-function effect caused by the mutations without significantly impacting on the formation or function of dimeric ClC-1 channels. On the other hand, the dominant inheritance is explained by a dominant-negative effect of mutated subunits on heteromeric mutant/WT channels. Most of the 200 different mutations identified and described behave as recessive, with the majority of the patients being compound heterozygous (carriers of two different recessive mutations). Only about 27 mutations have been associated with DMC, while about other 59 mutations have an unclear inheritance pattern, are sporadic or have been also shown to display a recessive inheritance pattern (http://www.hgmd.cf.ac.uk/ac/index.php). Therefore, a clear distinction between dominant and recessive mutations is not always possible (5, 39, 41, 43, 72–74). Thus, far, there is no other clinical phenotype associated with mutations in the *CLCN1* gene.

Sodium Channelopathies

Na^+ channelopathies are not as common as Cl^- channelopathies, showing a combined prevalence of about 1:100,000 (42). These disorders are caused by mutations in the sodium voltage-gated channel alpha subunit 4 (*SCN4A*) gene, which is located in chromosome 17q23 and encodes the voltage-gated sodium channel (Nav1.4) of skeletal muscle (75–77). They are a heterogeneous group of autosomal dominant disorders with high penetrance (20, 55). Mutations in *SCN4A* cause disruption of fast inactivation of the channel, which can be incomplete or slowed (78–80), leading to repetitive action potentials (myotonic runs) and consequent intracellular sodium accumulation that depolarizes muscle cells and can lead to inactivation of the Na^+ channels (25, 31, 32, 47). Depending if depolarization is mild or not, myotonia or paralysis might appear, respectively (81). Nav1.4 is a channel formed by a single unit of Nav1.4 protein, which contains four repeated domains (DI-DIV), each one consisting of six transmembrane segments (S1–S6). The loops between S5–S6 segments from the four domains come together to form the ion-conducting pore, acting as a selective filter. Meanwhile, the S4 segment of each domain is in charge of sensing the voltage changes (31, 32, 47). The *SCN4A* gene has 24 exons, with about 83 different mutations described in the gene, but only about 65 of them have been associated with myotonia (40, 82–86) (http://www.hgmd.cf.ac.uk/ac/index.php). All *SCN4A* mutations correspond to missense mutations, with the single exception of a deletion/insertion mutation located in the splice site in intron 21 (87, 88). All *SCN4A* myotonia mutations studied produce a gain-of-function effect of Nav1.4, resulting in defects of channel inactivation or enhancement of activation, which explain the dominant inheritance pattern of the diseases (20, 82). Mutations have been located through the entire gene sequence, but depending on the disease, they tend to group differentially. For instance, mutations associated with HyperPP with myotonia are generally located in the inner regions of the transmembrane segments or in the intracellular interlinking loops in repeat domains DII and DIV of the channel, eliciting a persisting inward sodium current, which impairs repolarization and increases membrane excitability (82, 89). In PC, mutations have been found throughout the gene, with exon 24 appearing to be a hot spot (90), but their impairment of fast inactivation is less notorious than the one associated with HyperPP (81). Regarding SCM, although mutations have been found throughout the gene, there are more likely located in the N terminus of the channel, in repeat domain D1, particularly in the inactivation gate (82). Interestingly, in recent papers, the authors describe several *SCN4A* mutations, previously reported in unrelated myotonia-positive families, new or *de novo* mutations, that contribute to apnea during the physiological stress of seizures, severe respiratory failure or associated with paradoxical vocal fold motion (PVFM) (91–93). Neonatal laryngospasm and unusual distribution of myotonia and other NDM signs have also been reported in several NDM patients, who have been shown to carry different *SCN4A* mutations, such as G1306E, I693T, A799S, N1297K, and T1313M (although not all patients that carry these mutations show childhood or neonatal respiratory problems) (78, 94–99). This expands the spectrum of phenotypes associated with mutations in the *SCN4A* gene. In addition to myotonic diseases associated with *SCN4A* mutations, other diseases, that are beyond the scope of this review, also present mutations in this gene, such as: hyperkalemic periodic paralysis without myotonia (HyperPP), hypokalemic periodic paralysis (HyppoPP), normokalemic periodic paralysis (NormoPP), and

congenital myasthenic syndrome (CMS) (20, 82). Recently, it has also been suggested that a subset of cases with sudden infant death syndrome (SIDS) might be due to *SCN4A* mutations, as one report (and the only one thus far) has found novel or very rare functionally disruptive *SCN4A* genetic variants associated with SIDS, although the authors indicate that new studies in other populations are required to confirm their finding (100).

COMPLEX GENOTYPE-PHENOTYPE RELATIONSHIPS IN MYOTONIC CHANNELOPATHIES

In order to provide accurate prognostic information to the patients and families affected with a hereditary disease, it is essential to have appropriated genotype-phenotype relationships. In the case of the non-dystrophic myotonias, this has been extremely difficult mainly due to two factors: (1) the wide spectrum of symptoms and overlapping phenotypes present in both groups (Cl^- and Na^+ myotonic channelopathies) (24, 25, 47), and (2) both genes, *CLCN1* and *SCN4A*, present high genotypic variability, with more than 200 or 65 different mutations already described, respectively (http://www.hgmd.cf.ac.uk/ac/index.php) (23, 43). Although many mutations cause a unique and reproducible phenotype in all patients, some *SCN4A* and *CLCN1* mutations cause similar phenotypes. Most worryingly, for several mutations, very different clinical phenotypes have been found in different carriers of the same mutation (23, 25, 47, 101), severely compromising the genotype-phenotype correlation in NDM. Another important limitation for the improvement of genotype-phenotype correlations has been the lack of a sufficient number of individuals carrying each mutation (23), in particular in the case of novel mutations [such as the very recent study that described seven novel *CLCN1* mutations (68)], which makes the situation even more complex, not without mentioning all those cases that show myotonia or a myotonia-like phenotype but in which the mutation has not been found. It is worth mentioning though, that correlation of mutations with the clinical phenotype gives insights into the pathophysiology of human channelopathies, and although some correlation exists between specific mutations and the associated clinical manifestations, this is vague (47).

The poor correlations are most evident in Cl^- channelopathies, where the same mutation can be inherited as dominant or recessive with different clinical manifestations, for example, F167L (39, 67, 68, 102, 103), A313T (67, 104), or W433R (44) (see **Table 1**). By recording and analyzing the ion currents of heterologously expressed mutant channels in different *in vitro* expression systems (*Xenopus* oocytes or HEK cells), much progress has been made in understanding how specific mutations affect the function of a particular ion channel, in providing insights onto the mechanism for the inheritance pattern, but also in the role that the voltage-gated ion channels play in excitable tissues (20, 25, 105). These analyses have contributed to improve to some extent, the clinical correlations through a better understanding of the channel dysfunction and its associated clinical picture. Nevertheless, of the more than 200 or 65 different Cl^- and Na^+ mutations, only about 80 and 30 different mutations, respectively, have been functionally characterized (http://www.hgmd.cf.ac.uk/ac/index.php). However, these functional analyses have contributed to understand in a better way the recessive or dominant behavior of different *CLCN1* mutation than the overlapping phenotypes and clinical variability shown by some specific mutation (39, 67, 102, 103). For instance, in general, it has been reported that several recessively inherited *CLCN1* mutations show biophysical defects like reduced open probability, reduced single-channel conductance, or biochemical instability, in a manner that does impinge in a significant manner on the formation or function of heteromeric mutants/WT channels (13, 106, 107). A simple example are early stop codon mutations which do not result in the expression of ClC-1 subunits (108). In this regard, it has to be remembered that to provoke myotonia, G_{Cl} has to be lowered below roughly 30% (109–112). On the other hand, several dominantly inherited *CLCN1* mutations have been shown to exert *in vitro* a dominant negative effect in co-expression with WT (39, 58, 64, 107, 113, 114). In many cases the dominant negative effect is mediated by a shift of the open probability of the "common gate" to more positive voltages (107, 113, 114). These properties provide a rational to explain the dominant inheritance. However, this does not explain the clinical variability observed in both RMC and DMC. Interestingly, there is a group of 12 *CLCN1* mutations (see **Table 2**) in which the functional *in vitro* analyses have not been able to demonstrate differences with the WT channel, suggesting the presence of additional factors in skeletal muscle fibers, not present in oocytes/HEK cells, that are involved in the disease. Such factors could be related, for example, to subcellular targeting, a still open question for ClC-1 (18, 19). For these mutations, a powerful experimental approach would be the generation and analysis of knock-in mice carrying the myotonia-related *CLCN1* mutations, since myotonic mice are an established model for chloride channel myotonia (13, 115). Such knock-in mice could provide important information that cannot be obtained in heterologous expression systems. Additionally, patient derived induced pluripotent stem cells (iPSCs), combined with suitable myogenic differentiation (116), or the use of CRISPR/Cas approaches in order to correct (genome editing) specific mutations (followed by evaluating the off-target activities of CRISPR/Cas systems), might provide future avenues of studying the impact or correction of ion-channel mutations. However, in particular for *CLCN1*, these approaches are complicated by the fact that *CLCN1* expression (*in vivo*) requires fully differentiated and innervated muscle fibers (117). Importantly, many of these approaches also apply for the study of sodium channel mutations (see below).

Clinical correlations in sodium channel myotonic disorders are not as complex as the chloride channel myotonic disorders. As with MC, functional analyses in Na^+ myotonic channelopathies have contributed to the understanding of the pathophysiological mechanism and improvement of clinical correlation, which are more accurate in this case. These analyses have been able to provide that Na^+ channel mutations have four major effects on Nav1.4 function: (1) enhanced activation;

TABLE 1 | *CLCN1* mutations behaving as dominant/recessive.

Mutation	Inheritance	Phenotype	Functional effects in heterologous expression systems (references of functional evidence)	References of genetic evidence
c.501C>G, p.F167L	Recessive	Generalized Myotonia (compound heterozygous)	From very small shift of po to not different from WT (103, 118)	(39, 102)
	Dominant	Thomsen's like phenotype		(67, 103)
c.689G>A, p.G230E	Recessive	Generalized Myotonia (compound heterozygous)	Dominant negative effect, dramatic change in ion selectivity (58, 114)	(38)
	Dominant	Thomsen's disease		(104, 119)
c.803C>T, p.T268M	Recessive	Generalized Myotonia (compound heterozygous)	Changed po of the common gate (120)	(121)
	Dominant	Thomsen's disease		(119)
c.920T>C, p.F307S	Recessive	Generalized Myotonia (compound heterozygous)	Dominant negative effect, shifted the voltage dependence of po to positive potentials (74)	(122)
	Dominant	Thomsen's disease		(74)
c.937G>A, p.A313T	Recessive	Generalized Myotonia (compound heterozygous)	Drastically shifted the voltage dependence of po to positive potentials (74)	(104)
	Dominant	Thomsen's disease		
c.950G>A, p.R317Q	Recessive	Generalized Myotonia (compound heterozygous)	Shifted gating to positive potentials (113)	(62)
	Dominant	Thomsen's disease		(39)
c.1013G>A, p.R338Q	Recessive	Generalized Myotonia (compound heterozygous)	Shifted the voltage dependence of po to positive potentials (118)	(102)
	Dominant	Thomsen's disease		(38)
c.1297T>C, p.W433R	Recessive	Generalized Myotonia (compound heterozygous)	Not determined	(44)
	Dominant	Thomsen's disease		
c.1478C>A, p.A493E	Recessive	Generalized Myotonia (compound heterozygous and homozygous)	Unavailable	(123)
	Dominant	Thomsen's disease		(123)
c.1592C>T, p.A531V	Recessive	Generalized Myotonia (compound heterozygous)	Not determined	(5, 124)
	Dominant	Thomsen's disease		(5)
c.1667T>A, p.I556N	Recessive	Generalized Myotonia (homozygous)	Shifted the voltage dependence of po to positive potentials with minimal dominant negative effect (74)	(104)
	Dominant	Thomsen's disease (incomplete dominance)		
c.1936A>G, p.M646V	Recessive	Generalized Myotonia (compound heterozygous)	Unavailable	(123)
	Dominant	Thomsen's disease		(123)
c.2680C>T, p.R894X	Recessive	Generalized Myotonia (compound heterozygous)	Large reduction, but not complete abolition of chloride currents, and weak dominant effects (39)	(39, 121)
	Dominant	Thomsen's disease		(39, 102)

(2) impaired slow inactivation; (3) impaired fast inactivation; and (4) accelerated recovery from fast inactivation. But, as with the *CLCN1* mutations, while these effects explain the dominant behavior of the mutations (dominant gain-of-function effect), they contribute little to the explanation of the clinical variability seen in this group of NDM. Nevertheless, it is well-accepted that: (1) a large fraction of persistent current and an incomplete slow inactivation of the channel may cause a strong long-lasting depolarization, providing the bases for weakness in HyperPP; (2) a slowing of fast inactivation and an incomplete closure of the channel may explain the paradoxical myotonia characteristic of PC; and (3) an increased persistent fraction and/or slowing of fast inactivation might explain the slight depolarization that causes myotonia in affected patients with SCM [reviewed in (47)]. But this does not explain the clinical variation observed in different patients, or even the overlapping symptoms seen with MC. In the case of *SCN4A* mutations, to the best of our knowledge, there have not been reported mutations that, functionally, behave as the WT channel.

Interestingly, there have been few patients carrying a *SCN4A* mutation who have been shown to carry a second mutation in *CLCN1* (see **Table 3**). These patients have shown an exacerbated or atypical Na^+ channel disease phenotype, suggesting that both mutation may act synergistically to influence the clinical and neurophysiological phenotype observed in those patients (130). For many years, it was common practice to screen just one among *CLCN1* or *SCN4A* genes, based on the presumptive clinical phenotype. It is thus likely that a significant group of the first (or even some of recent cases) NMDs cases (with atypical/unclear phenotype, unclear inheritance pattern or dual inheritance-dominant or recessive) with molecular diagnosis, carry a second mutation in any of this ion channel genes, and, maybe even in other loci. Based on this and suggested by many authors, the recommendation is that in those NDM cases with atypical phenotypes or inheritance pattern, both *CLCN1* and *SCN4A* genes are screened. However, thanks to new technologies and price reduction, it might now be possible to carry out deep sequencing, such as whole genome sequencing or gene-targeted sequencing (by next generation sequencing-NGS), in these patients. These new approaches not only would allow to properly screen these genes and genotype NDM patients, but also, could contribute to identify gene modifiers that might be involved in modulating their phenotypes. In fact, very recently it was published the first report using whole genome sequencing for screening the *CLCN1* gene in RMC patients (131). These

TABLE 2 | *CLCN1* mutations behaving similar to ClC-1 WT in *in vitro* expression systems.

Mutation	Phenotype	Functional analysis result	Heterologous expression system	References
c.209C>T, p.S70L	Compatible with RMC	Macroscopic current amplitudes and current slopes comparable to WT	HEK293 cells	(125)
c.244A>G, p.T82A	Compatible with RMC	No effect on chloride currents, very similar to WT	tsA201 cells	(126)
c.313C>T, p.R105C	Compatible with RMC	Chloride currents similar to WT	HEK293 cells, *Xenopus* oocytes	(103, 106)
c.352T>G, p.W118G	Myotonia positive patients	Currents amplitudes similar to WT	HEK293 cells	(127)
c.449A>G, p.Y150C	Compatible with RMC	Currents indistinguishable from WT	*Xenopus* oocytes	(107)
c.501C>G, p.F167L	Compatible with RMC or DMC	Currents very similar to WT	HEK293 cells, *Xenopus* oocytes	(103, 106)
c.782A>G, p.Y261C	Compatible with RMC	Currents indistinguishable from WT	*Xenopus* oocytes	(107)
c.979G>A, p.V327I	Compatible with RMC	Currents very similar to WT	*Xenopus* oocytes	(61)
c.1357C>T, p.R453W	Compatible with RMC	No effect on chloride currents, very similar to WT	tsA201 cells	(126)
c.1412C>T, p.S471F	Myotonia positive patients	Electrophysiological parameters similar to WT	*Xenopus* oocytes	(128)
c.1883T>C, p.L628P	Compatible with RMC	Currents very similar to WT	tsA201 cells	(129)
c.2533G>A, p.G845S	Myotonia positive patients	Currents indistinguishable from WT ClC-1	tsA201 cells	(108)

RMC, recessive myotonia congenita; DMC, dominant myotonia congenita; WT, wild type; NDM, non-dystrophic myotonia.

TABLE 3 | Simultaneous mutations in *CLCN1* and *SCN4A* in NDM patients showing an atypical phenotype.

Mutations	Phenotype	Heterologous expression system/functional data	References
SCN4A c.3917G>A, p.G1306E *CLCN1* c.1453A>G, p.M485V	Patient 1. Myotonic discharges with type II electrophysiology pattern. PC-like phenotype. Some signs of MC	ND	(132)
SCN4A c.4010G>C, p.R1337P *CLCN1* c.803C>T, p.T268M	Patient 2. Myotonic discharges with type II electrophysiology pattern. PC-like phenotype. Some signs of MC		
SCN4A c.2079T>G, p.I693M *CLCN1* c.2926C>T, p.Arg976X	Patient 3. Myotonic discharges with type III electrophysiology pattern. SCM-like phenotype. Some signs of MC		
SCN4A c.3870C>A, p.F1290L *CLCN1* c.2848 G>A, p.E950K	Myotonic discharges with type III electrophysiology pattern. SCM-like phenotype with periodic paralysis	HEK293 cells/*SCN4A* = enhanced activation-*CLCN1* = ND	(133)
SCN4A c.3890A>G, p.N1297S *CLCN1* c.501C>G, p.F167L	Mild NDM phenotype. SCM-like phenotype	HEK293 cells/*SCN4A* = impairment of fast and slow inactivation-*CLCN1* = ND	(134)
SCN4A c.665G>A, p.R222Q *CLCN1* c.1650G>A p.T550T	Patient with severe myotonia and without fulminant paralytic episodes	HEK293 cells/*SCN4A* = enhanced activation-*CLCN1* = ND	(135)

MC, myotonia congenita; PC, paramyotonia congenita; SCM, sodium channel myotonias; NDM, non-dystrophic myotonia; ND, not determined.

new approaches could be very useful to screen those patients with atypical phenotypes and those in which the effect of the identified mutation does not differ from the wild-type channel (see below).

The molecular bases for the clinical variability present in myotonic channelopathies remain obscure. Yet, a deeper understanding is needed to improve genotype-phenotype correlations. Several hypotheses have been put forward to explain the clinical variability, which include: (a) differential allelic expression; (b) *trans*-acting genetic modifiers; (c) epigenetic, hormonal or environmental factors; and (d) dominance with low penetrance (20, 47, 136–138). These putatively acting (alone or in combination) mechanisms might contribute to explain why the same mutation causes different degrees of channel dysfunction in different patients (74), and therefore elicit a modulation in the NDM phenotype. Importantly, to the best of our knowledge, none of these possibilities has been established experimentally in NMD patients or are under current investigation.

The above considerations suggest that it is not only important to study as many individuals or mutations as possible, but also to try to obtain functional data for all mutations. In addition, deeper insight is expected from bioinformatics and structural approaches combined with information on nearby mutations, aided by the recently obtained 3D structure of the ClC-1 protein (139, 140). The results of these studies, in addition to explaining in a better way the different symptoms associated with particular mutations, would contribute to improving clinical correlations. Improvements in clinical tests, the recognition of the different phenotypes that result from particular mutations and the understanding of how a mutation affects the structure and function of the ion channel, together with genetic screening, is expected to improve clinical correlation in NDMs, which could ultimately be translated into better clinical management and to a better quality of life of affected patients and their families.

Finally, a solid knowledge of functional defects caused by specific mutations might help in the development of selective drugs targeted at a correction of such effects. For example,

gating modifier drugs could be developed to invert the shift of the voltage-dependence of some dominant *CLCN1* mutations. Several small molecule compounds are indeed known to interfere with the open probability of ClC-1 channels, suggesting the principal feasibility of such an approach (141, 142). In particular, derivatives of clofibric acid have been shown to shift the voltage-dependence of ClC-1 and the related ClC-0 to more positive voltages (141–143). The development of novel molecules that specifically bind to and stabilize the open state of the channel could be aided by the recent determination of the structure of ClC-1 (139, 140). Another possible line of intervention regards patients with mutations that lead to protein folding defects. Such defects might be treated with small molecules that act as "correctors." Such an approach is already in clinical use in other diseases, such as cystic fibrosis (144). Since correctors are assumed to stabilize the folded state of the channel, it might be tempting to start the search of correctors using ClC-1 inhibitors, like 9-anthrazene carboxylic acid (9AC) (143). However, all known ClC-1 inhibitors are of rather low affinity and quite unspecific (8). Therefore, such correctors are likely only to be discovered using high-throughput screening, as done for the most common CFTR mutation causing cystic fibrosis (118). Indeed, generic correctors, such as 4-phenylbutyrate, miglustat, and sildenafil have proven unsuccessful for cystic fibrosis (118).

For preparing this review, we (both authors) have used our personal historical literature database of publications regarding *CLCN1* and *SCN4A* related myotonia, as well as PubMed searches using the keywords "myotonia AND (CLCN1/CLC-1, SCN4A/Nav1.4, apnea, laryngospasm)."

AUTHOR CONTRIBUTIONS

All authors listed have made a substantial, direct and intellectual contribution to the work, and approved it for publication.

FUNDING

MP was supported by a grant from the Fondazione AIRC per la Ricerca sul Cancro (grant # IG 21558) and the Italian Research Ministry (PRIN 20174TB8KW). FM was supported by the Universidad de Costa Rica.

REFERENCES

1. Emery AE. The muscular dystrophies. *Lancet.* (2002) 359:687–95. doi: 10.1016/S0140-6736(02)07815-7
2. Mercuri E, Muntoni F. Muscular dystrophies. *Lancet.* (2013) 381:845–60. doi: 10.1016/S0140-6736(12)61897-2
3. Rahimov F, Kunkel LM. The cell biology of disease: cellular and molecular mechanisms underlying muscular dystrophy. *J Cell Biol.* (2013) 201:499–510. doi: 10.1083/jcb.201212142
4. Colding-Jorgensen E. Phenotypic variability in myotonia congenita. *Muscle Nerve.* (2005) 32:19–34. doi: 10.1002/mus.20295
5. Sun C, Tranebjaerg L, Torbergsen T, Holmgren G, Van Ghelue M. Spectrum of CLCN1 mutations in patients with myotonia congenita in Northern Scandinavia. *Eur J Hum Genet.* (2001) 9:903–9. doi: 10.1038/sj.ejhg.5200736
6. Pedersen TH, Riisager A, de Paoli FV, Chen TY, Nielsen OB. Role of physiological ClC-1 Cl- ion channel regulation for the excitability and function of working skeletal muscle. *J Gen Physiol.* (2016) 147:291–308. doi: 10.1085/jgp.201611582
7. Stauber T, Weinert S, Jentsch TJ. Cell biology and physiology of CLC chloride channels and transporters. *Compr Physiol.* (2012) 2:1701–44. doi: 10.1002/cphy.c110038
8. Jentsch TJ, Pusch M. CLC chloride channels and transporters: structure, function, physiology, and disease. *Physiol Rev.* (2018) 98:1493–590. doi: 10.1152/physrev.00047.2017
9. Jentsch TJ, Steinmeyer K, Schwarz G. Primary structure of Torpedo marmorata chloride channel isolated by expression cloning in *Xenopus* oocytes. *Nature.* (1990) 348:510–4. doi: 10.1038/348510a0
10. Koch MC, Steinmeyer K, Lorenz C, Ricker K, Wolf F, Otto M, et al. The skeletal muscle chloride channel in dominant and recessive human myotonia. *Science.* (1992) 257:797–800. doi: 10.1126/science.1379744
11. Miller C. ClC chloride channels viewed through a transporter lens. *Nature.* (2006) 440:484–9. doi: 10.1038/nature04713
12. Bryant SH, Morales-Aguilera A. Chloride conductance in normal and myotonic muscle fibres and the action of monocarboxylic aromatic acids. *J Physiol.* (1971) 219:367–83. doi: 10.1113/jphysiol.1971.sp009667
13. Steinmeyer K, Klocke R, Ortland C, Gronemeier M, Jockusch H, Grunder S, et al. Inactivation of muscle chloride channel by transposon insertion in myotonic mice. *Nature.* (1991) 354:304–8. doi: 10.1038/354304a0
14. Steinmeyer K, Ortland C, Jentsch TJ. Primary structure and functional expression of a developmentally regulated skeletal muscle chloride channel. *Nature.* (1991) 354:301–4. doi: 10.1038/354301a0
15. Bretag AH. Muscle chloride channels. *Physiol Rev.* (1987) 67:618–724. doi: 10.1152/physrev.1987.67.2.618
16. Lamb GD, Murphy RM, Stephenson DG. On the localization of ClC-1 in skeletal muscle fibers. *J Gen Physiol.* (2011) 137:327–9. doi: 10.1085/jgp.201010580
17. Zifarelli G, Pusch M. Relaxing messages from the sarcolemma. *J Gen Physiol.* (2010) 136:593–6. doi: 10.1085/jgp.201010567
18. DiFranco M, Herrera A, Vergara JL. Chloride currents from the transverse tubular system in adult mammalian skeletal muscle fibers. *J Gen Physiol.* (2011) 137:21–41. doi: 10.1085/jgp.201010496
19. Lueck JD, Rossi AE, Thornton CA, Campbell KP, Dirksen RT. Sarcolemmal-restricted localization of functional ClC-1 channels in mouse skeletal muscle. *J Gen Physiol.* (2010) 136:597–613. doi: 10.1085/jgp.201010526
20. Cannon SC. Channelopathies of skeletal muscle excitability. *Compr Physiol.* (2015) 5:761–90. doi: 10.1002/cphy.c140062
21. Kent-Braun JA, Fitts RH, Christie A. Skeletal muscle fatigue. *Compr Physiol.* (2012) 2:997–1044. doi: 10.1002/cphy.c110029
22. Trivedi JR, Bundy B, Statland J, Salajegheh M, Rayan DR, Venance SL, et al. Non-dystrophic myotonia: prospective study of objective and patient reported outcomes. *Brain.* (2013) 136(Pt 7):2189–200. doi: 10.1093/brain/awt133
23. Matthews E, Fialho D, Tan SV, Venance SL, Cannon SC, Sternberg D, et al. The non-dystrophic myotonias: molecular pathogenesis, diagnosis and treatment. *Brain.* (2010) 133(Pt 1):9–22. doi: 10.1093/brain/awp294
24. Heatwole CR, Moxley RT III. The nondystrophic myotonias. *Neurotherapeutics.* (2007) 4:238–51. doi: 10.1016/j.nurt.2007.01.012
25. Platt D, Griggs R. Skeletal muscle channelopathies: new insights into the periodic paralyses and nondystrophic myotonias. *Curr Opin Neurol.* (2009) 22:524–31. doi: 10.1097/WCO.0b013e32832efa8f
26. AANEM. American Association of Electrodiagnostic Medicine glossary of terms in electrodiagnostic medicine. *Muscle Nerve Suppl.* (2001) 10:S1–50.
27. Hudson AJ, Ebers GC, Bulman DE. The skeletal muscle sodium and chloride channel diseases. *Brain.* (1995) 118(Pt 2):547–63. doi: 10.1093/brain/118.2.547
28. Ricker K, Hertel G, Langscheid K, Stodieck G. Myotonia not aggravated by cooling. Force and relaxation of the adductor pollicis in normal subjects and in myotonia as compared to paramyotonia. *J Neurol.* (1977) 216:9–20. doi: 10.1007/BF00312810
29. Streib EW. AAEE minimonograph #27: differential diagnosis of myotonic syndromes. *Muscle Nerve.* (1987) 10:603–15. doi: 10.1002/mus.880100704

30. Morales F, Cuenca P. Aspectos geneticos y moleculares de las enfermedades miotonicas. *Rev Neurol.* (2004) 38:668–74. doi: 10.33588/rn.3807.2003483
31. Jurkat-Rott K, Lerche H, Lehmann-Horn F. Skeletal muscle channelopathies. *J Neurol.* (2002) 249:1493–502. doi: 10.1007/s00415-002-0871-5
32. Lehmann-Horn F, Jurkat-Rott K, Rudel R. Periodic paralysis: understanding channelopathies. *Curr Neurol Neurosci Rep.* (2002) 2:61–9. doi: 10.1007/s11910-002-0055-9
33. Goodman BE. Channels active in the excitability of nerves and skeletal muscles across the neuromuscular junction: basic function and pathophysiology. *Adv Physiol Educ.* (2008) 32:127–35. doi: 10.1152/advan.00091.2007
34. Imbrici P, Altamura C, Pessia M, Mantegazza R, Desaphy JF, Camerino DC. ClC-1 chloride channels: state-of-the-art research and future challenges. *Front Cell Neurosci.* (2015) 9:156. doi: 10.3389/fncel.2015.00156
35. Thomsen J. Tonische Krampfe in willkurlich beweglichen Muskeln in Folge von ererbter psychischer Disposition (Ataxia muscularis?). *Arch Psychiatr Nervenkr.* (1876) 6:702–18.
36. Westphal C. Demonstration zweier Falle von Thomsen'scher Krankheit. *Berl Klin Wschr.* (1883) 20:153.
37. Becker PE. Zur Genetik der Myotonien. In: Kuhn E, editor. *Progressive Muskeldystrophie–Myotonie–Myasthenie*. Berlin: Springer Verlag (1966). p. 247–55.
38. Zhang J, George AL Jr, Griggs RC, Fouad GT, Roberts J, Kwiecinski H, et al. Mutations in the human skeletal muscle chloride channel gene (CLCN1) associated with dominant and recessive myotonia congenita. *Neurology.* (1996) 47:993–8. doi: 10.1212/WNL.47.4.993
39. Meyer-Kleine C, Steinmeyer K, Ricker K, Jentsch TJ, Koch MC. Spectrum of mutations in the major human skeletal muscle chloride channel gene (CLCN1) leading to myotonia. *Am J Hum Genet.* (1995) 57:1325–34.
40. Lehmann-Horn F, Jurkat-Rott K. Voltage-gated ion channels and hereditary disease. *Physiol Rev.* (1999) 79:1317–72. doi: 10.1152/physrev.1999.79.4.1317
41. Pusch M. Myotonia caused by mutations in the muscle chloride channel gene CLCN1. *Hum Mutat.* (2002) 19:423–34. doi: 10.1002/humu.10063
42. Horga A, Raja Rayan DL, Matthews E, Sud R, Fialho D, Durran SC, et al. Prevalence study of genetically defined skeletal muscle channelopathies in England. *Neurology.* (2013) 80:1472–5. doi: 10.1212/WNL.0b013e31828cf8d0
43. Lossin C, George AL Jr. Myotonia congenita. *Adv Genet.* (2008) 63:25–55. doi: 10.1016/S0065-2660(08)01002-X
44. Dupre N, Chrestian N, Bouchard JP, Rossignol E, Brunet D, Sternberg D, et al. Clinical, electrophysiologic, and genetic study of non-dystrophic myotonia in French-Canadians. *Neuromuscul Disord.* (2009) 19:330–4. doi: 10.1016/j.nmd.2008.01.007
45. Koch MC, Ricker K, Otto M, Wolf F, Zoll B, Lorenz C, et al. Evidence for genetic homogeneity in autosomal recessive generalised myotonia (Becker). *J Med Genet.* (1993) 30:914–7. doi: 10.1136/jmg.30.11.914
46. Mankodi A. Myotonic disorders. *Neurol India.* (2008) 56:298–304. doi: 10.4103/0028-3886.43448
47. Vicart S, Sternberg D, Fontaine B, Meola G. Human skeletal muscle sodium channelopathies. *Neurol Sci.* (2005) 26:194–202. doi: 10.1007/s10072-005-0461-x
48. Fournier E, Arzel M, Sternberg D, Vicart S, Laforet P, Eymard B, et al. Electromyography guides toward subgroups of mutations in muscle channelopathies. *Ann Neurol.* (2004) 56:650–61. doi: 10.1002/ana.20241
49. Ptacek LJ, Tawil R, Griggs RC, Meola G, McManis P, Barohn RJ, et al. Sodium channel mutations in acetazolamide-responsive myotonia congenita, paramyotonia congenita, and hyperkalemic periodic paralysis. *Neurology.* (1994) 44:1500–3. doi: 10.1212/WNL.44.8.1500
50. Sansone VA. The Dystrophic and Nondystrophic Myotonias. *Continuum (Minneap Minn).* (2016) 22:1889–915. doi: 10.1212/CON.0000000000000414
51. Von Eulenburg A. Über eine familiäre durch 6 Generationen verfolgbare Form kongenitaler Paramyotonie. *Neurol Zentralbl.* (1986) 5:265–72.
52. Jurkat-Rott K, Lehmann-Horn F. Genotype-phenotype correlation and therapeutic rationale in hyperkalemic periodic paralysis. *Neurotherapeutics.* (2007) 4:216–24. doi: 10.1016/j.nurt.2007.02.001
53. Weber F, Jurkat-Rott K, Lehmann-Horn F. Hyperkalemic periodic paralysis. In: Adam MP, Ardinger HH, Pagon RA, Wallace SE, Bean LJH, Stephens K, et al., editors. *GeneReviews®*. Seattle, WA (1993). Available online at: https://www.ncbi.nlm.nih.gov/books/NBK1496
54. Charles G, Zheng C, Lehmann-Horn F, Jurkat-Rott K, Levitt J. Characterization of hyperkalemic periodic paralysis: a survey of genetically diagnosed individuals. *J Neurol.* (2013) 260:2606–13. doi: 10.1007/s00415-013-7025-9
55. Cannon SC. Sodium Channelopathies of Skeletal Muscle. *Handb Exp Pharmacol.* (2018) 246:309–30. doi: 10.1007/164_2017_52
56. Becker PE. *Myotonia Congenita and Syndromes Associated with Myotonia*. Sttutgart: Thieme (1977).
57. George AL Jr, Crackower MA, Abdalla JA, Hudson AJ, Ebers GC. Molecular basis of Thomsen's disease (autosomal dominant myotonia congenita). *Nat Genet.* (1993) 3:305–10. doi: 10.1038/ng0493-305
58. Steinmeyer K, Lorenz C, Pusch M, Koch MC, Jentsch TJ. Multimeric structure of ClC-1 chloride channel revealed by mutations in dominant myotonia congenita (Thomsen). *Embo J.* (1994) 13:737–43. doi: 10.1002/j.1460-2075.1994.tb06315.x
59. Abdalla JA, Casley WL, Cousin HK, Hudson AJ, Murphy EG, Cornelis FC, et al. Linkage of Thomsen disease to the T-cell-receptor beta (TCRB) locus on chromosome 7q35. *Am J Hum Genet.* (1992) 51:579–84.
60. Grunnet M, Jespersen T, Colding-Jorgensen E, Schwartz M, Klaerke DA, Vissing J, et al. Characterization of two new dominant ClC-1 channel mutations associated with myotonia. *Muscle Nerve.* (2003) 28:722–32. doi: 10.1002/mus.10501
61. Lorenz C, Meyer-Kleine C, Steinmeyer K, Koch MC, Jentsch TJ. Genomic organization of the human muscle chloride channel CIC-1 and analysis of novel mutations leading to Becker-type myotonia. *Hum Mol Genet.* (1994) 3:941–6. doi: 10.1093/hmg/3.6.941
62. Esteban J, Neumeyer AM, McKenna-Yasek D, Brown RH. Identification of two mutations and a polymorphism in the chloride channel CLCN-1 in patients with Becker's generalized myotonia. *Neurogenetics.* (1998) 1:185–8. doi: 10.1007/s100480050027
63. Zhang J, Sanguinetti MC, Kwiecinski H, Ptacek LJ. Mechanism of inverted activation of ClC-1 channels caused by a novel myotonia congenita mutation. *J Biol Chem.* (2000) 275:2999–3005. doi: 10.1074/jbc.275.4.2999
64. Saviane C, Conti F, Pusch M. The muscle chloride channel ClC-1 has a double-barreled appearance that is differentially affected in dominant and recessive myotonia. *J Gen Physiol.* (1999) 113:457–68. doi: 10.1085/jgp.113.3.457
65. Middleton RE, Pheasant DJ, Miller C. Homodimeric architecture of a ClC-type chloride ion channel. *Nature.* (1996) 383:337–40. doi: 10.1038/383337a0
66. Ludewig U, Pusch M, Jentsch TJ. Two physically distinct pores in the dimeric ClC-0 chloride channel. *Nature.* (1996) 383:340–3. doi: 10.1038/383340a0
67. Fialho D, Schorge S, Pucovska U, Davies NP, Labrum R, Haworth A, et al. Chloride channel myotonia: exon 8 hot-spot for dominant-negative interactions. *Brain.* (2007) 130(Pt 12):3265–74. doi: 10.1093/brain/awm248
68. Milla CP, De Castro CP, Gomez-Gonzalez C, Martinez-Montero P, Pascual Pascual SI, Molano Mateos J. Myotonia congenita: mutation spectrum of CLCN1 in Spanish patients. *J Genet.* (2019) 98:71. doi: 10.1007/s12041-019-1115-0
69. Raja Rayan DL, Haworth A, Sud R, Matthews E, Fialho D, Burge J, et al. A new explanation for recessive myotonia congenita: exon deletions and duplications in CLCN1. *Neurology.* (2012) 78:1953–8. doi: 10.1212/WNL.0b013e318259e19c
70. Tang CY, Chen TY. Physiology and pathophysiology of CLC-1: mechanisms of a chloride channel disease, myotonia. *J Biomed Biotechnol.* (2011) 2011:685328. doi: 10.1155/2011/685328
71. de Diego C, Gamez J, Plassart-Schiess E, Lasa A, Del Rio E, Cervera C, et al. Novel mutations in the muscle chloride channel CLCN1 gene causing myotonia congenita in Spanish families. *J Neurol.* (1999) 246:825–9. doi: 10.1007/s004150050462
72. Koty PP, Pegoraro E, Hobson G, Marks HG, Turel A, Flagler D, et al. Myotonia and the muscle chloride channel: dominant mutations show variable penetrance and founder effect. *Neurology.* (1996) 47:963–8. doi: 10.1212/WNL.47.4.963
73. Brugnoni R, Kapetis D, Imbrici P, Pessia M, Canioni E, Colleoni L, et al. A large cohort of myotonia congenita probands: novel mutations and a high-frequency mutation region in exons 4 and 5 of the CLCN1 gene. *J Hum Genet.* (2013) 58:581–7. doi: 10.1038/jhg.2013.58
74. Kubisch C, Schmidt-Rose T, Fontaine B, Bretag AH, Jentsch TJ. ClC-1 chloride channel mutations in myotonia congenita: variable penetrance of

mutations shifting the voltage dependence. *Hum Mol Genet.* (1998) 7:1753–60. doi: 10.1093/hmg/7.11.1753
75. Koch MC, Ricker K, Otto M, Grimm T, Hoffman EP, Rudel R, et al. Confirmation of linkage of hyperkalaemic periodic paralysis to chromosome 17. *J Med Genet.* (1991) 28:583–6. doi: 10.1136/jmg.28.9.583
76. Ptacek LJ, George AL Jr, Barchi RL, Griggs RC, Riggs JE, Robertson M. Identification of a mutation in the gene causing hyperkalemic periodic paralysis. *Cell.* (1991) 67:1021–7. doi: 10.1016/0092-8674(91)90374-8
77. Ptacek LJ, Trimmer JS, Agnew WS, Roberts JW, Petajan JH, Leppert M. Paramyotonia congenita and hyperkalemic periodic paralysis map to the same sodium-channel gene locus. *Am J Hum Genet.* (1991) 49:851–4.
78. Lerche H, Heine R, Pika U, George AL Jr, Mitrovic N, Browatzki M, et al. Human sodium channel myotonia: slowed channel inactivation due to substitutions for a glycine within the III-IV linker. *J Physiol.* (1993) 470:13–22. doi: 10.1113/jphysiol.1993.sp019843
79. Chahine M, George AL Jr, Zhou M, Ji S, Sun W, Barchi RL, et al. Sodium channel mutations in paramyotonia congenita uncouple inactivation from activation. *Neuron.* (1994) 12:281–94. doi: 10.1016/0896-6273(94)90271-2
80. Lehmann-Horn F, Rudel R, Ricker K. Membrane defects in paramyotonia congenita (Eulenburg). *Muscle Nerve.* (1987) 10:633–41. doi: 10.1002/mus.880100709
81. Hanna MG. Genetic neurological channelopathies. *Nat Clin Pract Neurol.* (2006) 2:252–63. doi: 10.1038/ncpneuro0178
82. Jurkat-Rott K, Holzherr B, Fauler M, Lehmann-Horn F. Sodium channelopathies of skeletal muscle result from gain or loss of function. *Pflugers Arch.* (2010) 460:239–48. doi: 10.1007/s00424-010-0814-4
83. Jurkat-Rott K, Lehmann-Horn F. Muscle channelopathies and critical points in functional and genetic studies. *J Clin Invest.* (2005) 115:2000–9. doi: 10.1172/JCI25525
84. Cannon SC. Pathomechanisms in channelopathies of skeletal muscle and brain. *Annu Rev Neurosci.* (2006) 29:387–415. doi: 10.1146/annurev.neuro.29.051605.112815
85. Fialho D, Hanna MG. Periodic paralysis. *Handb Clin Neurol.* (2007) 86:77–106. doi: 10.1016/S0072-9752(07)86004-0
86. Huang W, Liu M, Yan SF, Yan N. Structure-based assessment of disease-related mutations in human voltage-gated sodium channels. *Protein Cell.* (2017) 8:401–38. doi: 10.1007/s13238-017-0372-z
87. Kubota T, Roca X, Kimura T, Kokunai Y, Nishino I, Sakoda S, et al. A mutation in a rare type of intron in a sodium-channel gene results in aberrant splicing and causes myotonia. *Hum Mutat.* (2011) 32:773–82. doi: 10.1002/humu.21501
88. Stenson PD, Ball EV, Mort M, Phillips AD, Shiel JA, Thomas NS, et al. Human gene mutation database (HGMD): 2003 update. *Hum Mutat.* (2003) 21:577–81. doi: 10.1002/humu.10212
89. Lehmann-Horn F, Kuther G, Ricker K, Grafe P, Ballanyi K, Rudel R. Adynamia episodica hereditaria with myotonia: a non-inactivating sodium current and the effect of extracellular pH. *Muscle Nerve.* (1987) 10:363–74. doi: 10.1002/mus.880100414
90. Davies NP, Eunson LH, Gregory RP, Mills KR, Morrison PJ, Hanna MG. Clinical, electrophysiological, and molecular genetic studies in a new family with paramyotonia congenita. *J Neurol Neurosurg Psychiatry.* (2000) 68:504–7. doi: 10.1136/jnnp.68.4.504
91. Turkdogan D, Matthews E, Usluer S, Gundogdu A, Uluc K, Mannikko R, et al. Possible role of SCN4A skeletal muscle mutation in apnea during seizure. *Epilepsia Open.* (2019) 4:498–503. doi: 10.1002/epi4.12347
92. Pechmann A, Eckenweiler M, Schorling D, Stavropoulou D, Lochmuller H, Kirschner J. *De novo* variant in SCN4A causes neonatal sodium channel myotonia with general muscle stiffness and respiratory failure. *Neuromuscul Disord.* (2019) 29:907–9. doi: 10.1016/j.nmd.2019.09.001
93. Purkey MR, Valika T. A unique presentation and etiology of neonatal paradoxical vocal fold motion. *Int J Pediatr Otorhinolaryngol.* (2019) 125:199–200. doi: 10.1016/j.ijporl.2019.07.011
94. Lehmann-Horn F, D'Amico A, Bertini E, Lomonaco M, Merlini L, Nelson KR, et al. Myotonia permanens with Nav1.4-G1306E displays varied phenotypes during course of life. *Acta Myol.* (2017) 36:125–34.
95. Caietta E, Milh M, Sternberg D, Lepine A, Boulay C, McGonigal A, et al. Diagnosis and outcome of SCN4A-related severe neonatal episodic laryngospasm (SNEL): 2 new cases. *Pediatrics.* (2013) 132:e784–7. doi: 10.1542/peds.2012-3065
96. Singh RR, Tan SV, Hanna MG, Robb SA, Clarke A, Jungbluth H. Mutations in SCN4A: a rare but treatable cause of recurrent life-threatening laryngospasm. *Pediatrics.* (2014) 134:e1447–50. doi: 10.1542/peds.2013-3727
97. Gay S, Dupuis D, Faivre L, Masurel-Paulet A, Labenne M, Colombani M, et al. Severe neonatal non-dystrophic myotonia secondary to a novel mutation of the voltage-gated sodium channel (SCN4A) gene. *Am J Med Genet A.* (2008) 146A:380–3. doi: 10.1002/ajmg.a.32141
98. Matthews E, Guet A, Mayer M, Vicart S, Pemble S, Sternberg D, et al. Neonatal hypotonia can be a sodium channelopathy: recognition of a new phenotype. *Neurology.* (2008) 71:1740–2. doi: 10.1212/01.wnl.0000335269.21550.0e
99. Lion-Francois L, Mignot C, Vicart S, Manel V, Sternberg D, Landrieu P, et al. Severe neonatal episodic laryngospasm due to *de novo* SCN4A mutations: a new treatable disorder. *Neurology.* (2010) 75:641–5. doi: 10.1212/WNL.0b013e3181ed9e96
100. Mannikko R, Wong L, Tester DJ, Thor MG, Sud R, Kullmann DM, et al. Dysfunction of NaV1.4, a skeletal muscle voltage-gated sodium channel, in sudden infant death syndrome: a case-control study. *Lancet.* (2018) 391:1483–92. doi: 10.1016/S0140-6736(18)30021-7
101. Lee SC, Kim HS, Park YE, Choi YC, Park KH, Kim DS. Clinical diversity of SCN4A-mutation-associated skeletal muscle sodium channelopathy. *J Clin Neurol.* (2009) 5:186–91. doi: 10.3988/jcn.2009.5.4.186
102. George AL Jr, Sloan-Brown K, Fenichel GM, Mitchell GA, Spiegel R, Pascuzzi RM. Nonsense and missense mutations of the muscle chloride channel gene in patients with myotonia congenita. *Hum Mol Genet.* (1994) 3:2071–2.
103. Vindas-Smith R, Fiore M, Vasquez M, Cuenca P, Del Valle G, Lagostena L, et al. Identification and functional characterization of CLCN1 mutations found in nondystrophic myotonia patients. *Hum Mutat.* (2016) 37:74–83. doi: 10.1002/humu.22916
104. Plassart-Schiess E, Gervais A, Eymard B, Lagueny A, Pouget J, Warter JM, et al. Novel muscle chloride channel (CLCN1) mutations in myotonia congenita with various modes of inheritance including incomplete dominance and penetrance. *Neurology.* (1998) 50:1176–9. doi: 10.1212/WNL.50.4.1176
105. Planells-Cases R, Jentsch TJ. Chloride channelopathies. *Biochim Biophys Acta.* (2009) 1792:173–89. doi: 10.1016/j.bbadis.2009.02.002
106. Desaphy JF, Gramegna G, Altamura C, Dinardo MM, Imbrici P, George AL Jr, et al. Functional characterization of ClC-1 mutations from patients affected by recessive myotonia congenita presenting with different clinical phenotypes. *Exp Neurol.* (2013) 248:530–40. doi: 10.1016/j.expneurol.2013.07.018
107. Wollnik B, Kubisch C, Steinmeyer K, Pusch M. Identification of functionally important regions of the muscular chloride channel CIC-1 by analysis of recessive and dominant myotonic mutations. *Hum Mol Genet.* (1997) 6:805–11. doi: 10.1093/hmg/6.5.805
108. Ulzi G, Lecchi M, Sansone V, Redaelli E, Corti E, Saccomanno D, et al. Myotonia congenita: novel mutations in CLCN1 gene and functional characterizations in Italian patients. *J Neurol Sci.* (2012) 318:65–71. doi: 10.1016/j.jns.2012.03.024
109. Barchi RL. Myotonia. An evaluation of the chloride hypothesis. *Arch Neurol.* (1975) 32:175–80. doi: 10.1001/archneur.1975.00490450055007
110. Kwiecinski H, Lehmann-Horn F, Rudel R. Drug-induced myotonia in human intercostal muscle. *Muscle Nerve.* (1988) 11:576–81. doi: 10.1002/mus.880110609
111. Adrian RH, Marshall MW. Action potentials reconstructed in normal and myotonic muscle fibres. *J Physiol.* (1976) 258:125–43. doi: 10.1113/jphysiol.1976.sp011410
112. Furman RE, Barchi RL. The pathophysiology of myotonia produced by aromatic carboxylic acids. *Ann Neurol.* (1978) 4:357–65. doi: 10.1002/ana.410040411
113. Pusch M, Steinmeyer K, Koch MC, Jentsch TJ. Mutations in dominant human myotonia congenita drastically alter the voltage dependence of the CIC-1 chloride channel. *Neuron.* (1995) 15:1455–63. doi: 10.1016/0896-6273(95)90023-3

114. Fahlke C, Beck CL, George AL Jr. A mutation in autosomal dominant myotonia congenita affects pore properties of the muscle chloride channel. *Proc Natl Acad Sci USA.* (1997) 94:2729–34. doi: 10.1073/pnas.94.6.2729
115. Reininghaus J, Fuchtbauer EM, Bertram K, Jockusch H. The myotonic mouse mutant ADR: physiological and histochemical properties of muscle. *Muscle Nerve.* (1988) 11:433–9. doi: 10.1002/mus.880110504
116. Jiwlawat N, Lynch E, Jeffrey J, Van Dyke JM, Suzuki M. Current progress and challenges for skeletal muscle differentiation from human pluripotent stem cells using transgene-free approaches. *Stem Cells Int.* (2018) 2018:6241681. doi: 10.1155/2018/6241681
117. Klocke R, Steinmeyer K, Jentsch TJ, Jockusch H. Role of innervation, excitability, and myogenic factors in the expression of the muscular chloride channel ClC-1. A study on normal and myotonic muscle. *J Biol Chem.* (1994) 269:27635–9.
118. Zhang J, Bendahhou S, Sanguinetti MC, Ptacek LJ. Functional consequences of chloride channel gene (CLCN1) mutations causing myotonia congenita. *Neurology.* (2000) 54:937–42. doi: 10.1212/WNL.54.4.937
119. Brugnoni R, Galantini S, Confalonieri P, Balestrini MR, Cornelio F, Mantegazza R. Identification of three novel mutations in the major human skeletal muscle chloride channel gene (CLCN1), causing myotonia congenita. *Hum Mutat.* (1999) 14:447. doi: 10.1002/(SICI)1098-1004(199911)14:5<447::AID-HUMU13>3.0.CO;2-Z
120. Duffield M, Rychkov G, Bretag A, Roberts M. Involvement of helices at the dimer interface in ClC-1 common gating. *J Gen Physiol.* (2003) 121:149–61. doi: 10.1085/jgp.20028741
121. Deymeer F, Cakirkaya S, Serdaroglu P, Schleithoff L, Lehmann-Horn F, Rudel R, et al. Transient weakness and compound muscle action potential decrement in myotonia congenita. *Muscle Nerve.* (1998) 21:1334–7. doi: 10.1002/(SICI)1097-4598(199810)21:10<1334::AID-MUS16>3.0.CO;2-1
122. Colding-Jorgensen E, Dun OM, Schwartz M, Vissing J. Decrement of compound muscle action potential is related to mutation type in myotonia congenita. *Muscle Nerve.* (2003) 27:449–55. doi: 10.1002/mus.10347
123. Ivanova EA, Dadali EL, Fedotov VP, Kurbatov SA, Rudenskaia GE, Proskokova TN, et al. The spectrum of CLCN1 gene mutations in patients with nondystrophic Thomsen's and Becker's myotonias. *Genetika.* (2012) 48:1113–23. doi: 10.1134/S1022795412090049
124. Papponen H, Toppinen T, Baumann P, Myllyla V, Leisti J, Kuivaniemi H, et al. Founder mutations and the high prevalence of myotonia congenita in northern Finland. *Neurology.* (1999) 53:297–302. doi: 10.1212/WNL.53.2.297
125. Ronstedt K, Sternberg D, Detro-Dassen S, Gramkow T, Begemann B, Becher T, et al. Impaired surface membrane insertion of homo- and heterodimeric human muscle chloride channels carrying amino-terminal myotonia-causing mutations. *Sci Rep.* (2015) 5:15382. doi: 10.1038/srep15382
126. Portaro S, Altamura C, Licata N, Camerino GM, Imbrici P, Musumeci O, et al. Clinical, molecular, and functional characterization of CLCN1 mutations in three families with recessive myotonia congenita. *Neuromolecular Med.* (2015) 17:285–96. doi: 10.1007/s12017-015-8356-8
127. Raheem O, Penttila S, Suominen T, Kaakinen M, Burge J, Haworth A, et al. New immunohistochemical method for improved myotonia and chloride channel mutation diagnostics. *Neurology.* (2012) 79:2194–200. doi: 10.1212/WNL.0b013e31827595e2
128. Lin MJ, You TH, Pan H, Hsiao KM. Functional characterization of CLCN1 mutations in Taiwanese patients with myotonia congenita via heterologous expression. *Biochem Biophys Res Commun.* (2006) 351:1043–7. doi: 10.1016/j.bbrc.2006.10.158
129. Imbrici P, Maggi L, Mangiatordi GF, Dinardo MM, Altamura C, Brugnoni R, et al. ClC-1 mutations in myotonia congenita patients: insights into molecular gating mechanisms and genotype-phenotype correlation. *J Physiol.* (2015) 593:4181–99. doi: 10.1113/JP270358
130. Skov M, Riisager A, Fraser JA, Nielsen OB, Pedersen TH. Extracellular magnesium and calcium reduce myotonia in ClC-1 inhibited rat muscle. *Neuromuscul Disord.* (2013) 23:489–502. doi: 10.1016/j.nmd.2013.03.009
131. Wei Z, Huaxing M, Xiaomei W, Juan W, Xueli C, Jing Z, et al. Identification of two novel compound heterozygous CLCN1 mutations associated with autosomal recessive myotonia congenita. *Neurol Res.* (2019) 41:1069–74. doi: 10.1080/01616412.2019.1672392
132. Furby A, Vicart S, Camdessanche JP, Fournier E, Chabrier S, Lagrue E, et al. Heterozygous CLCN1 mutations can modulate phenotype in sodium channel myotonia. *Neuromuscul Disord.* (2014) 24:953–9. doi: 10.1016/j.nmd.2014.06.439
133. Kato H, Kokunai Y, Dalle C, Kubota T, Madokoro Y, Yuasa H, et al. A case of non-dystrophic myotonia with concomitant mutations in the SCN4A and CLCN1 genes. *J Neurol Sci.* (2016) 369:254–8. doi: 10.1016/j.jns.2016.08.030
134. Maggi L, Ravaglia S, Farinato A, Brugnoni R, Altamura C, Imbrici P, et al. Coexistence of CLCN1 and SCN4A mutations in one family suffering from myotonia. *Neurogenetics.* (2017) 18:219–25. doi: 10.1007/s10048-017-0525-5
135. Thor MG, Vivekanandam V, Sampedro-Castaneda M, Tan SV, Suetterlin K, Sud R, et al. Myotonia in a patient with a mutation in an S4 arginine residue associated with hypokalaemic periodic paralysis and a concomitant synonymous CLCN1 mutation. *Sci Rep.* (2019) 9:17560. doi: 10.1038/s41598-019-54041-0
136. Duno M, Colding-Jorgensen E, Grunnet M, Jespersen T, Vissing J, Schwartz M. Difference in allelic expression of the CLCN1 gene and the possible influence on the myotonia congenita phenotype. *Eur J Hum Genet.* (2004) 12:738–43. doi: 10.1038/sj.ejhg.5201218
137. Modoni A, D'Amico A, Dallapiccola B, Mereu ML, Merlini L, Pagliarani S, et al. Low-rate repetitive nerve stimulation protocol in an Italian cohort of patients affected by recessive myotonia congenita. *J Clin Neurophysiol.* (2011) 28:39–44. doi: 10.1097/WNP.0b013e31820510d7
138. Suetterlin K, Mannikko R, Hanna MG. Muscle channelopathies: recent advances in genetics, pathophysiology and therapy. *Curr Opin Neurol.* (2014) 27:583–90. doi: 10.1097/WCO.0000000000000127
139. Park E, MacKinnon R. Structure of the CLC-1 chloride channel from Homo sapiens. *Elife.* (2018) 7:e36629. doi: 10.7554/eLife.36629
140. Wang K, Preisler SS, Zhang L, Cui Y, Missel JW, Gronberg C, et al. Structure of the human ClC-1 chloride channel. *PLoS Biol.* (2019) 17:e3000218. doi: 10.1371/journal.pbio.3000218
141. Estevez R, Schroeder BC, Accardi A, Jentsch TJ, Pusch M. Conservation of chloride channel structure revealed by an inhibitor binding site in ClC-1. *Neuron.* (2003) 38:47–59. doi: 10.1016/S0896-6273(03)00168-5
142. Liantonio A, Accardi A, Carbonara G, Fracchiolla G, Loiodice F, Tortorella P, et al. Molecular requisites for drug binding to muscle CLC-1 and renal CLC-K channel revealed by the use of phenoxy-alkyl derivatives of 2-(p-chlorophenoxy)propionic acid. *Mol Pharmacol.* (2002) 62:265–71. doi: 10.1124/mol.62.2.265
143. Pusch M, Accardi A, Liantonio A, Guida P, Traverso S, Camerino DC, et al. Mechanisms of block of muscle type CLC chloride channels (Review). *Mol Membr Biol.* (2002) 19:285–92. doi: 10.1080/09687680210166938
144. De Boeck K, Davies JC. Where are we with transformational therapies for patients with cystic fibrosis? *Curr Opin Pharmacol.* (2017) 34:70–5. doi: 10.1016/j.coph.2017.09.005

Conflict of Interest: The authors declare that the research was conducted in the absence of any commercial or financial relationships that could be construed as a potential conflict of interest.

The reviewer DF and handling editor declared their shared affiliation at the time of the review.

Copyright © 2020 Morales and Pusch. This is an open-access article distributed under the terms of the Creative Commons Attribution License (CC BY). The use, distribution or reproduction in other forums is permitted, provided the original author(s) and the copyright owner(s) are credited and that the original publication in this journal is cited, in accordance with accepted academic practice. No use, distribution or reproduction is permitted which does not comply with these terms.

frontiers in Neurology

ORIGINAL RESEARCH
published: 06 February 2020
doi: 10.3389/fneur.2020.00063

CLCN1 Molecular Characterization in 19 South-Italian Patients With Dominant and Recessive Type of Myotonia Congenita

*Chiara Orsini†, Roberta Petillo†, Paola D'Ambrosio†, Manuela Ergoli, Esther Picillo, Marianna Scutifero, Luigia Passamano, Alessandro De Luca‡ and Luisa Politano**

Cardiomiology and Medical Genetics, Department of Experimental Medicine, University of Campania "Luigi Vanvitelli", Naples, Italy

OPEN ACCESS

Edited by:
Emma Matthews, University College London, United Kingdom

Reviewed by:
Fiore Manganelli, University of Naples Federico II, Italy
Paola Sandroni, Mayo Clinic, United States

***Correspondence:**
Luisa Politano
luisa.politano@unicampania.it; poli3295@gmail.com

†These authors have contributed equally to the work

‡Present address:
Alessandro De Luca, UOS di Diagnosi Genetica Molecolare, Fondazione IRCCS Casa Sollievo della Sofferenza, San Giovanni Rotondo, Italy

Specialty section:
This article was submitted to Neuromuscular Diseases, a section of the journal Frontiers in Neurology

Received: *25 September 2019*
Accepted: *17 January 2020*
Published: *06 February 2020*

Citation:
Orsini C, Petillo R, D'Ambrosio P, Ergoli M, Picillo E, Scutifero M, Passamano L, De Luca A and Politano L (2020) CLCN1 Molecular Characterization in 19 South-Italian Patients With Dominant and Recessive Type of Myotonia Congenita. Front. Neurol. 11:63. doi: 10.3389/fneur.2020.00063

Myotonia congenita is a genetic disease characterized by impaired muscle relaxation after forceful contraction (myotonia). It is caused by mutations in the *CLCN1* gene, encoding the voltage-gated chloride channel of skeletal muscle, ClC-1. According to the pattern of inheritance, two distinct clinical forms have been described, Thomsen disease, inherited as an autosomal dominant trait and Becker disease inherited as an autosomal recessive trait. We report genetic and clinical data concerning 19 patients—13 familial and six isolated cases—all but one originating from the Campania Region, in southern Italy. Twelve patients (63.2%) present Becker type myotonia and 7 (36.8%) Thomsen type. Sex ratio M:F in Becker type is 6:6, while in Thomsen myotonia 4:3. The age of onset of the disease ranged from 2 to 15 years in Becker patients, and from 4 to 20 years in Thomsen. Overall 18 mutations were identified, 10 located in the coding part of the gene (exons 1, 3, 4, 5, 7, 8, 13, 15, 21, 22), and four in the intron part (introns 1, 2, 10, 18). All the exon mutations but two were missense mutations. Some of them, such as *c.2551G > A, c.817G > A* and *c.86A > C* recurred more frequently. About 70% of mutations was inherited with an autosomal recessive pattern, two (c.86A and *c.817G>A*) with both mechanisms. Three novel mutations were identified, never described in the literature: p.Gly276Ser, p.Phe486Ser, and p.Gln812*, associated with Becker phenotype. Furthermore, we identified three *CLCN1* mutations—c.86A>C + c.2551G > A, c.313C > T + c.501C > G and 899G > A + c.2284+5C > T, two of them inherited *in cis* on the same allele, in three unrelated families. The concomitant occurrence of both clinical pictures—Thomsen and Becker—was observed in one family. Intra-familial phenotypic variability was observed in two families, one with Becker phenotype, and one with Thomsen disease. In the latter an incomplete penetrance was hypothesized.

Keywords: *CLCN1* mutations, myotonia congenita, Becker myotonia, Thomsen myotonia, southern Italy

INTRODUCTION

Myotonia congenita is a genetic disease characterized by impaired muscle relaxation after forceful contraction (myotonia). The term "myotonia" indicates the main characteristic of this pathology, i.e., the presence of the so-called *myotonic phenomenon*, usually defined as "the delay in muscle relaxation after a prolonged contraction" (1, 2). The diseases characterized by the presence of

the "myotonia" can be subdivided into two large groups (3): Myotonic Dystrophies (DM), characterized by the *presence* of progressive muscular atrophy and weakness, and multi-systemic involvement and Non-dystrophic myotonias (NDM), characterized by the *absence* of progressive muscle atrophy and weakness, and multi-systemic involvement. The latter include the so-called *Muscular Channelopathies,* due to mutations in genes that code for proteins in the channels of sodium, chlorine, calcium, and potassium, some of which may be responsible for both myotonic and periodic paralysis.

Myotonia congenita is the most common muscle channelopathy. First described by Thomsen in 1876 as an autosomal dominant disease (4), a monograph on the pathology was published in 1907 by Sergio Pansini, a medical doctor at the University of Naples. The recessive form was described by PE Becker in 1963 (5). Their prevalence is estimated in 1: 100,000 live births, with onset in both childhood and adulthood (2). Depending on whether the mutation is present on both alleles or only on one of them, the clinical pictures of Becker's myotonia (BM, AR), or Thomsen myotonia (TM, AD), are observed. Both diseases are characterized by muscle stiffness, warm-up or heating (movement improves with repetition), trigger events (cold, stress, and exercise). Pregnancy and menstruation can worsen the symptoms. Usually patients with Becker's myotonia present a more severe clinical picture (1).

Myotonia congenita is due to mutations in the *CLCN1* gene (ClC-1 chlorine channel), located on the long arm of chromosome 7, in position 7q34. *CLCN1* (OMIM # 118425) consists of 23 exons and has a transcript of 3,093 nucleotides. ClC-1 protein, consisting of 988 amino acids, represents the main voltage-dependent chloride channel in skeletal muscle cells and stabilizes the resting potential of the membrane (6). When the Cl^- ion conductance falls below 40%, an accumulation of K^+ ions in the T tubules occurs, with consequent depolarization of the cell membrane and appearance of myotonia (7). More than 275 variants, causative of myotonia congenita, have been identified; about 95% of them are point mutations, while 1–5% deletions or duplications (8). Most of these mutations cause Becker myotonia, while only about 20 pathogenetic variants have so far been associated with Thomsen myotonia. At least 12 mutations can cause both pathologies for different pathogenetic mechanisms, as variants with dominant-negative effect, reduced penetrance, incomplete dominance, aplotypic background, differences in helix expression or, more simply, inability of current techniques to identify the second pathogenic variant (2). In a simplified way, mutations located at the fast gates level are recessive phenotype mutations, whereas mutations located at the slow gates level are dominant phenotype mutations (9). Recessive mutations may affect the structure of the ClC-1 protein, alter its transport, or disable the formation of dimers (10, 11); on the contrary dominant mutations have a dominant negative effect on dimerization (10). The diagnosis is based on clinical data, serum creatine kinase (CK) levels, usually normal or only slightly increased between 3 and 4 times the upper reference limit, presence of myotonic discharges on the EMG, and genetic analysis.

The current therapy is based on the use of drugs such as Mexiletine (12), Phenytoin, Carbamazepine and Acetazolamide (13, 14). However, studies in progress are evaluating new-

TABLE 1 | Clinical data of MC patients.

Patient ID	Current age in Y	Gender	Age of onset in years	Transient weakness	Muscle pain/ stiffness	Hypertrophy	Cold effect	Warm Up phenomenon	EMG myotonic	Clinical course	Phenotype	Therapy
N1	69	M	6	Yes	No	Yes	Worse	Yes	Yes	Stable	Thomsen	None
N2	42	F	13	No	No	No	Worse	Yes	Yes	Stable	Thomsen	None\Mex not effective
N3	25	F	6	Yes	No	Yes	Worse	Yes	Yes	Worse	Becker	Mex, effective
N4	28	M	9	Yes	No	Yes	Worse	Yes	Yes	Worse	Becker	Mex, effective
N5	78	F	20	No	Yes	No	No	Yes	Yes	Stable	Thomsen	Mex, effective
N6	36	M	20	No	Yes	No	No	Yes	Yes	Stable	Thomsen	Mex, effective
N7	24	M	4	Yes	No	Yes	Worse	Yes		Stable	Becker	Mex, effective
N8	30	F	5	Yes	No	Yes	Worse	Yes		Stable	Becker	Mex, effective
N9	19	F	asymptomatic								Becker	None
N10	17	M	2	No	No	Yes	Worse	Yes	Yes	Stable	Becker	Mex, effective
N11	70	M	asymptomatic								Thomsen	None
N12	47	M	6	Yes	Yes	Yes	Worse	Yes		Stable	Thomsen	None
N13	27	M	15	Yes	No	Yes	Worse	Yes		Stable	Becker	Mex, effective
N14	53	M	14	Yes	No	Yes	No	Yes		Worse	Becker	Mex, effective
N15	32	M	12	Yes	No	Yes	Worse	Yes		Stable	Becker	Mex, effective
N16	33	F	7	Yes	No	Yes	No	Yes		Worse	Becker	Mex, effective
N17	39	F	10	No	No	Yes	Worse	Yes		Stable	Thomsen	None
N18	17	F	5	No	Yes	Yes	No	Yes		Worse	Becker	None
N19	42	F	4	Yes	Yes	Yes	Worse	Yes		Stable	Becker	None

generation molecules (13, 15), and "gating" or "traffic" corrector drugs through the so-called *pharmacological chaperones* (16, 17). We report genetic and clinical data concerning 19 patients—13 familial and 6 isolated cases—all but one originating from the Campania Region, in southern Italy.

METHODS

Clinical Diagnosis

We investigated 19 patients—13 of them from 7 families—with clinically defined Myotonia congenita. All patients were referred to our clinics due to variable increases of creatine kinase (CK) or grades of muscle stiffness. At the time of the first examination, information about family history, age of onset of symptoms, current therapy was collected. All patients underwent skeletal muscle and cardiological evaluation, spirometry, routine hematochemistry, and muscle enzymes. EMG was available in 6/19 patients.

Genetic Diagnosis

Genomic DNA was extracted from peripheral blood, collected in EDTA-containing tubes, by standard procedures. Written informed consent for DNA storage and use for genetic analysis and research purposes was obtained from all patients (parents or tutors for patients under age) and relatives, as required by the Ethical Committee of the University of Campania "Luigi Vanvitelli" in accordance with the Declaration of Helsinki. The genetic analysis was performed at the C.S.S.

Mendel Institute of Rome, Italy, through the direct sequencing of *CLCN1* gene and Sanger sequencing. The evaluation of the pathogenic variants was made through the ANNOVAR and Alamut® Software Suite (Interactive Biosoftware). Variants not described in the literature were analyzed by using dedicated softwares, such as Mutation tester, Polyphen2, Provean, M-CAP.

RESULTS

Clinical Diagnosis

Clinical data for MC patients are shown in **Table 1**. Out of 19 patients, 13 are familial with more than one individual affected, while six are isolated cases. Of the latter, one (N17) exhibits a *de novo* mutation not found in her parents. The other five patients (N14-N16, N18-N19) show homozygous or compound heterozygous mutations, whose inheritance was confirmed in their parents.

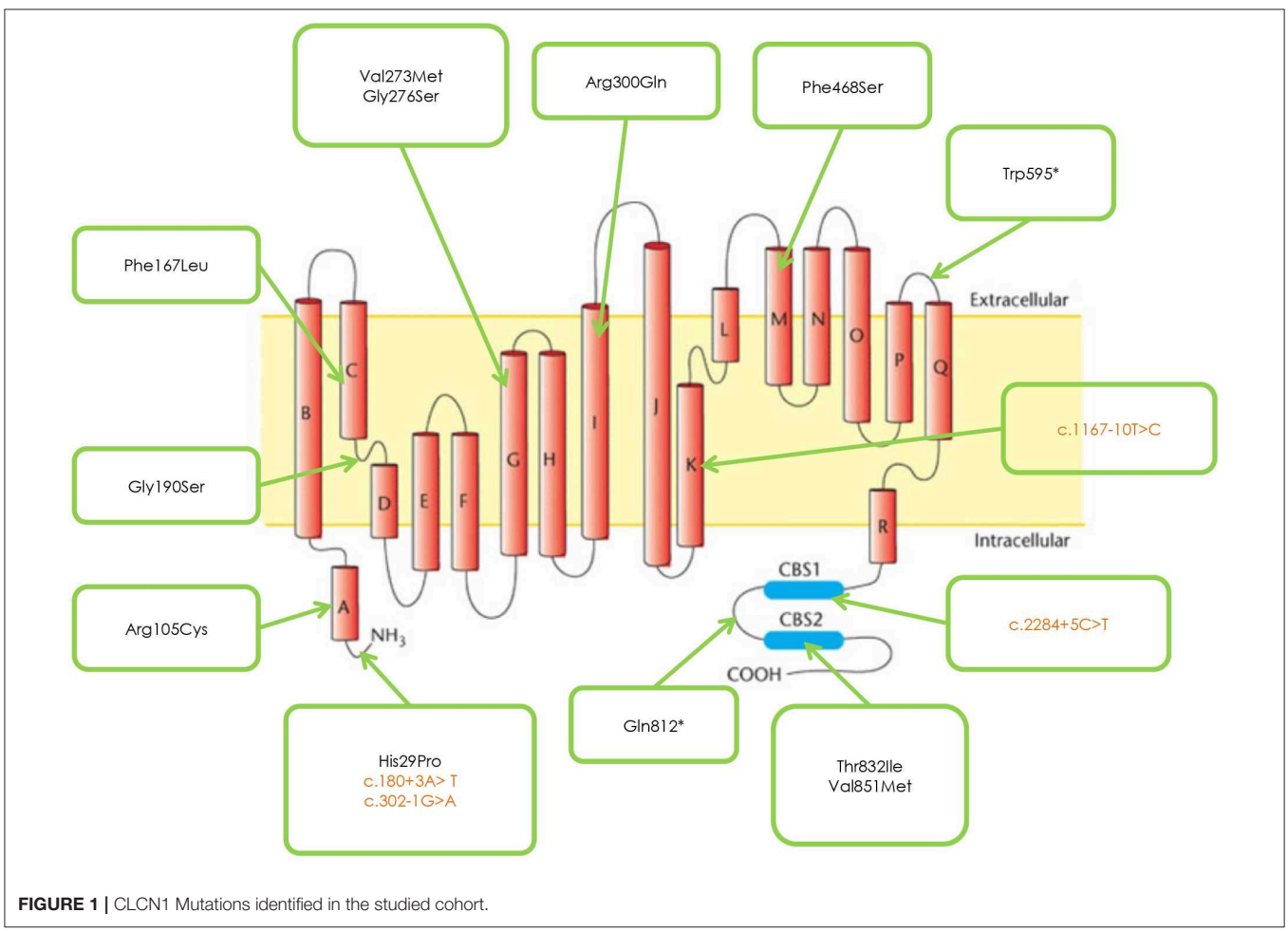

FIGURE 1 | CLCN1 Mutations identified in the studied cohort.

Twelve patients (63.2%) present Becker type myotonia and seven (36.8%) Thomsen type. Sex ratio M:F in Becker type is 6:6, while in Thomsen myotonia 4:3. The age of onset of the disease ranged from 2 to 15 years in Patients with BM, and from 4 to 20 years in patients with TM. Two patients, one with Thomsen type (N11) and the other with Becker type (N9) are asymptomatic, while their relatives present the typical symptoms of the disease. The warm up phenomenon was present in 100% of patients; transient weakness, referred by 63.1% of all patients, predominates in BM patients (75%) compared with TM patients (26.3%). Muscle pain was present in 42.8% of patients with TM, but in only 16.6% of BM patients. Muscle hypertrophy and cold effect predominates in BM patients (75%) compared to TM patients (50%). The warm up phenomenon is a constant feature in both TM and BM. EMG, available in six patients—three TM and three BM—showed the typical myotonic discharges.

Muscle biopsy—performed on 5/19 patients, two Thomsen and three Becker—showed a normal histological picture in 2, aspecific alterations in 2 and absence of 2B fibers in 1 patient.

Genetic Analysis

Figure 1 and **Table 2** shows the mutations identified in our patients. Out of 18 identified mutations, 14 are located in the coding part of the gene (exons 1, 3, 4, 5, 7, 8, 13, 15, 21, 22) and 4 in the intron part (introns 1, 2, 10, 18). All the exonic mutations but two are missense mutations. Some of them such as p. His29Pro, p.Phe167Leu, p.Val273Met, and p.Val851Met, occur with a relative higher frequency.

About 70% of mutations are inherited with an AR pattern, the mutation p.Val851Met with an AD pattern, two—p.His29Pro and p.Val273Met – with both mechanisms.

Patients sharing the protein variation p.Gly190Ser have a more severe phenotype than patients with the mutations p. Phe167Leu or Arg105Cys.

Three novel mutations were identified, never described in the literature p. Gly276Ser, Phe486Ser, and p.Gln812*, associated with Becker phenotype, two in homozygosis and one in compound heterozygosity. The neuromyological examination of these three patients revealed in the first case (mutation p. Gly276Ser) a slowly progressive Becker phenotype with onset at the age of 16, associated with muscle stiffness, transient weakness cold-aggravated, hand and jaw myotonia; in the second patient (mutation p.Phe486Ser), the onset was earlier, at the age of 7, and the clinical course more severe; in the third patient (mutation p. Gln812*), the onset was in childhood, but the disease's course was mild and, at the current age of 42, the patient reports to be stable.

In three unrelated families (N1; N5; N11) two *CLCN1* mutations, inherited in cis on the same allele were identified, in particular $c.86A > C + c.2551G > A$, (patients N1-N2), $c.313C > T + 501C > G$ (patients N11-N12), and $c.899G > A + c.2284{+}5C > T$ (patient N5).

TABLE 2 | Genetic data of MC patients.

Patient ID	Current age in years	Gender	Inheritance	Relationship	Exon/Intron position	DNA change	Protein
N1	69	M	AD	Father of N2	ex 1 + ex 22/int 10	c. 86A > C + c.2551G > A in cis/c.1167-10T > C	p. His29Pro + p. Val851Met in cis /?
N2	42	F	AD	Daughter of N1	ex 1 + ex 22/int 10	c. 86A > C + c.2551G > A in cis/c.1167-10T > C	p. His29Pro + p. Val851Met in cis /?
N3	25	F	AR	Niece of N1 and sister of N4	ex 4/int. 10	c.501C > G/c. 1167-10T > C	p.Phe167Leu/?
N4	28	M	AR	Nephew of N1 and brother of N3	ex 4/int. 10	c.501C > G/c. 1167-10T > C	p.Phe167Leu/?
N5	78	F	AD	Mother of N6	ex 7/ex 8 + int 18	c. 817G > A/c.899G > A + c.2284+5C > T in cis	p.Val273Met/p.Arg300Gln + ?
N6	36	M	AD	Son of N5	ex 7	c.817G > A heterozygous	p.Val273Met
N7	24	M	AR	Brother of N8	ex 15	c.1785G > A homozygous	p.Trp595*
N8	30	F	AR	Sister of N7	ex 15	c.1785G > A homozygous	p.Trp595*
N9	19	F	AR	Sister of N10	int 2/ex 5	c.302-1G > A/c.568-569GG > TC	?/p. Gly190Ser
N10	17	M	AR	Brother of N9	int 2/ex 5	c.302-1G > A/c.568-569GG > TC	?/p. Gly190Ser
N11	70	M	AD	Father of N12	ex 3 + ex 4	c.313C > T + c.501C > G in cis	p.Arg105Cys + p.Phe167Leu in cis
N12	47	M	AD	Son of N11	ex 3 + ex 4	c.313C > T + c.501C > G in cis	p.Arg105Cys + p.Phe167Leu in cis
N13	27	M	AR	2 siblings affected	int 2/ex 7	c.302-1G > A/c.826G > A	?/p.Gly276Ser
N14	53	M	AR		ex 7	c.817G > A homozygous	p.Val273Met
N15	32	M	AR		int 1/ex 21	c.180+3A > T/c.2495C > T	p.THr832Ile
N16	33	F	AR		ex 13	c.1403T > C homozygous	p. Phe468Ser
N17	39	F	AD	*De novo* mutation	ex 22	c.2551G > A heterozygous	p. Val851Met
N18	17	F	AR		ex 1 /ex 7	c.86A > C/c.817G > A	p.His29Pro/p.Val273Met
N19	42	F	AR		ex 21	c.2423C > T homozygous	p.Gln812*

**indicates stop codon point mutation.*

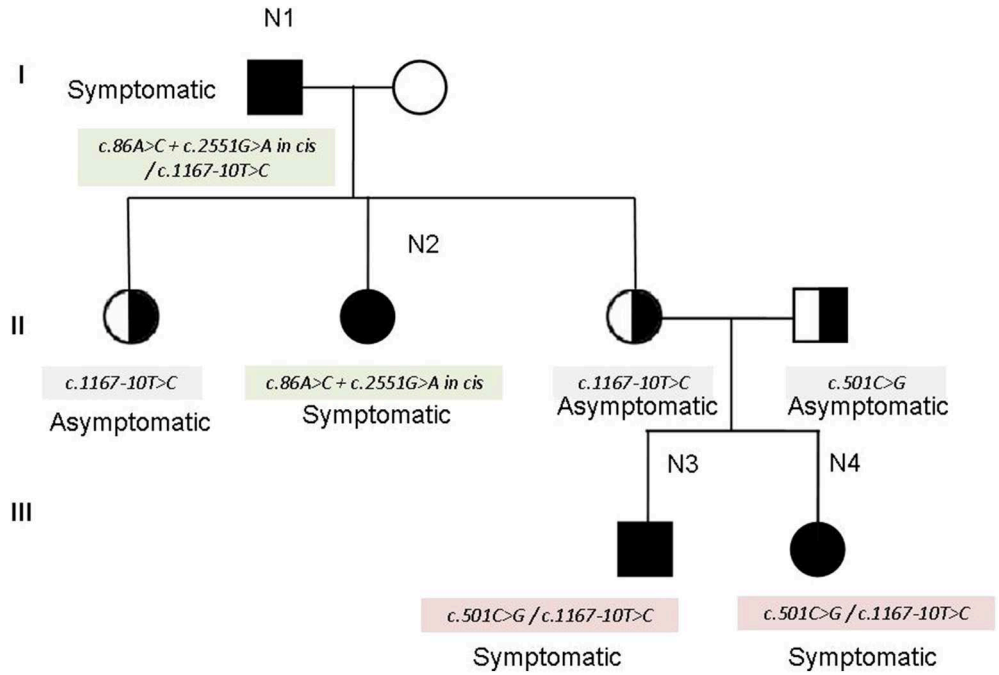

FIGURE 2 | Family tree of individuals N1–N4.

The family N1–N4 (see family tree in **Figure 2**) deserves particular comment. The father (N1 in the tables) and one of the three daughters (N2 in the tables) show the cis mutation *c.86A > C + c. 2551G > A* (pathogenetic) on one allele, and the mutation c. *1167-10T> C* on the other allele. The other two daughters inherited the mutation *c. 1167-10T > C* and are clinically unaffected. However, one of the two unaffected daughters had—quite unexpectedly—two children (individuals N3 and N4 in the tables) showing the characteristic symptoms of myotonia since their childhood. The genetic analysis in this part of the family revealed that her husband—unaffected—was a carrier of the mutation *c.501C > G* in the CLCN1gene, found in combination with *c. 1167-10T > C* in N3 and N4. Therefore, the combination of the mutations *c. 1167-10T > C* and *c.501C > G* may explain the affected phenotype observed in N3 and N4 (see the family tree). In fact, the mutation *c.501C > G* has been already described as affecting or probably affecting function in both compound heterozygosity and in homozygosity (14).

Four mutations found in our cohort of patients, in particular p. Arg105Cys, p.Gly190Ser, p.Thr832Ile, and p.Val851Met were electrophysiologically studied by the group of prof. F. Desaphy and their characteristics published by Altamura et al. (6).

An intra-familial phenotypic variability was observed in two families (patients N9-N10 and N11-N12), one with Thomsen and the other with Becker myotonia. An incomplete penetrance was hypothesized in the Thomsen family, as the father at the age of 70 is still asymptomatic while the son presents symptoms since the age of 6.

Eleven patients were on mexiletine, with an improvement of symptoms; in one patient the drug was ineffective; seven refused therapy. An improvement in muscle symptoms was reported by two patients undergoing steroid therapy for intercurrent diseases.

DISCUSSION

Mutations in *CLCN1* are widely distributed along the entire gene sequence (12). Unlike the report by Brugnoni et al. (14), who described in a cohort of 106 Italian patients a higher frequency of mutations in exons 4 and 5 of the *CLCN1* gene, mutations in these exons were only seen in 3 of our families.

The mutation p. Gly190Ser, found in both Thomsen and Becker phenotypes, causes a more severe clinical presentation in the latter, compared with mutations p. Phe167Leu or p. Arg105Cys, as demonstrated through the electrophysiological studies by Desaphy et al. (18) and Egushi et al. (14).

The neuromyological examination of the three patients carrying the novel mutations p.Gly276Ser, p.Phe468Ser, and p. Gln812* revealed a different clinical presentation, with a more severe course of the disease associated to the mutation p. Phe486Ser. We report the first case of documented concomitant occurrence of Thomsen and Becker clinical pictures in the same family.

In conclusion, our data, describe a set of *CLCN1* mutations in the population of Southern Italy different from those previously indicated (19–21) in the Italian cohort of MC patients. Furthermore, they report three novel mutations that widen the spectrum of mutations characterizing the clinical picture of these patients.

DATA AVAILABILITY STATEMENT

The raw data supporting the conclusions of this article will be made available by the authors, without undue reservation, to any qualified researcher.

ETHICS STATEMENT

The studies involving human participants were reviewed and approved by Ethical Committee of University of Campania. Written informed consent for DNA storage and use for genetic analysis and research purposes was obtained from all patients (parents or tutors for patients under age) and relatives, as required by the Ethical Committee of the University of Campania Luigi Vanvitelli, in accordance with the Declaration of Helsinki. Written informed consent for participation was not required for this study in accordance with the national legislation and the institutional requirements.

AUTHOR CONTRIBUTIONS

LPo conceived and designed the study and drafted the manuscript with input from the co-authors. RP, PD'A, CO, LPa, and MS performed the clinical diagnosis and follow-up of patients. ME and EP prepared DNA samples for the analysis. AD performed the molecular analysis of the patients, at the CSS Mendel Institute in Rome. All authors approved the final version of the manuscript.

REFERENCES

1. Cherian A, Baheti NN, Kuruvilla A. Muscle channelopathies and electrophysiological approach. *Ann Indian Acad Neurol.* (2008) 11:20–7. doi: 10.4103/0972-2327.40221
2. Dunø M, Colding-Jørgensen E.Myotonia Congenita. In: Adam MP, Ardinger HH, Pagon RA, Wallace SE, Bean LJH, Stephens K, Amemiya A, editors. GeneReviews® [Internet]. Seattle, WA: University of Washington (2005).
3. Hahn C, Salajegheh MK. Myotonic disorders: a review article. *Iran J Neurol.* (2016) 15:46–53.
4. Chand A, Chhuttani PN. Myotonia congenita (Thomsen's disease). *Ind Med Gaz.* (1945) 80:350.
5. Becker PE. On the genetics of myotonias (A Preliminary Survey)]. *Internist (Berl).* (1963) 4:384–92.
6. Altamura C, Lucchiari S, Sahbani D, Ulzi G, Comi GP, D'Ambrosio P, et al. The analysis of myotonia congenita mutations discloses functional clusters of amino acids within the CBS2 domain and the C-terminal peptide of the ClC-1 channel. *Hum Mutat.* (2018) 39:1273–83.doi: 10.1002/humu.23581
7. Zhang J, Bendahhou S, Sanguinetti MC, Ptácek LJ. Functional consequences of chloride channel gene (CLCN1) mutations causing myotonia congenita. *Neurology.* (2000) 54:937–42. doi: 10.1212/wnl.54.4.937
8. Raja Rayan DL, Haworth A, Sud R, Matthews E, Fialho D, Burge J, et al. A new explanation for recessive myotonia congenita: exon deletions and duplications in CLCN1. *Neurology.* (2012) 78:1953–8. doi: 10.1212/WNL.0b013e318259e19c
9. Imbrici P, Altamura C, Pessia M, Mantegazza R, Desaphy JF, Camerino DC. ClC-1 chloride channels: state-of-the-art research and future challenges. *Front Cell Neurosci.* (2015) 9:156. doi: 10.3389/fncel.2015.00156
10. Fialho D, Schorge S, Pucovska U, Davies NP, Labrum R, Haworth A, et al. Chloride channel myotonia: exon 8 hot-spot for dominant-negative interactions. *Brain.* (2007) 130(Pt 12):3265–74. doi: 10.1093/brain/awm248
11. Papponen H, Nissinen M, Kaisto T, Myllylä VV, Myllylä R, Metsikkö K. F413C and A531V but not R894X myotonia congenita mutations cause defective endoplasmic reticulum export of the muscle-specific chloride channel CLC-1. *MuscleNerve.* (2008) 37:317-25. doi: 10.1002/mus.20922
12. Statland JM, Bundy BN, Wang Y, Rayan DR, Trivedi JR, Sansone VA, et al. Mexiletine for symptoms and signs of myotonia in nondystrophic myotonia: a randomized controlled trial. *JAMA.* (2012) 308:1357–65. doi: 10.1001/jama.2012.12607
13. Markhorst JM, Stunnenberg BC, Ginjaar IB, Drost G, Erasmus CE, Sie LT. Clinical experience with long-term acetazolamide treatment in children with nondystrophic myotonias: a three-case report. *Pediatr Neurol.* (2014) 51:537–41. doi: 10.1016/j.pediatrneurol.2014.05.027
14. Eguchi H, Tsujino A, Kaibara M, Hayashi H, Shirabe S, Taniyama K, et al. Acetazolamide acts directly on the human skeletal muscle chloride channel. *Muscle Nerve.* (2006) 34:292–7. doi: 10.1002/mus.20585
15. Novak KR, Norman J, Mitchell JR, Pinter MJ, Rich MM. Sodium channel slow inactivation as a therapeutic target for myotonia congenita. *Ann Neurol.* (2015) 77:320–32. doi: 10.1002/ana.24331
16. Trivedi JR, Cannon SC, Griggs RC. Nondystrophic myotonia: challenges and future directions. *Exp Neurol.* (2014) 253:28–30. doi: 10.1016/j.expneurol.2013.12.005
17. Imbrici P, Liantonio A, Camerino GM, De Bellis M, Camerino C, Mele A, et al. Therapeutic approaches to genetic ion channelopathies and perspectives in drug discovery. *Front Pharmacol.* (2016) 7:121. doi: 10.3389/fphar.2016.00121
18. Desaphy JF, Gramegna G, Altamura C, Dinardo MM, Imbrici P, George AL Jr, et al. Functional characterization of ClC-1 mutations from patients affected by recessive myotonia congenita presenting with different clinical phenotypes. *Exp Neurol.* (2013) 248:530–40. doi: 10.1016/j.expneurol.2013.07.018
19. Brugnoni R, Kapetis D, Imbrici P, Pessia M, Canioni E, Colleoni L, et al. A large cohort of myotonia congenital probands: novel mutations and a high-frequency mutation region in exons 4 and 5 of the CLCN1 gene. *J Hum Genet.* (2013) 58:581–7. doi: 10.1038/jhg.2013.58
20. Portaro S, Altamura C, Licata N, Camerino GM, Imbrici P, Musumeci O, et al. Clinical, molecular, and functional characterization of CLCN1 mutations in three families with recessive myotonia congenita. *Neuromol Med.* (2015) 17:285–96. doi: 10.1007/s12017-015-8356-8
21. Meola G, Cardani R. Myotonic dystrophies: an update on clinical aspects, genetic, pathology, and molecular pathomechanisms. *Biochim Biophys Acta.* (2015) 1852:594–606. doi: 10.1016/j.bbadis.2014.05.019

Conflict of Interest: The authors declare that the research was conducted in the absence of any commercial or financial relationships that could be construed as a potential conflict of interest.

Copyright © 2020 Orsini, Petillo, D'Ambrosio, Ergoli, Picillo, Scutifero, Passamano, De Luca and Politano. This is an open-access article distributed under the terms of the Creative Commons Attribution License (CC BY). The use, distribution or reproduction in other forums is permitted, provided the original author(s) and the copyright owner(s) are credited and that the original publication in this journal is cited, in accordance with accepted academic practice. No use, distribution or reproduction is permitted which does not comply with these terms.

frontiers in Neurology

REVIEW
published: 11 February 2020
doi: 10.3389/fneur.2020.00076

Defective Gating and Proteostasis of Human ClC-1 Chloride Channel: Molecular Pathophysiology of Myotonia Congenita

Chung-Jiuan Jeng[1,2], *Ssu-Ju Fu*[1,3], *Chia-Ying You*[3], *Yi-Jheng Peng*[3], *Cheng-Tsung Hsiao*[3,4], *Tsung-Yu Chen*[5] and *Chih-Yung Tang*[3,6*]

[1] Institute of Anatomy and Cell Biology, School of Medicine, National Yang-Ming University, Taipei, Taiwan, [2] Brain Research Center, National Yang-Ming University, Taipei, Taiwan, [3] Department of Physiology, College of Medicine, National Taiwan University, Taipei, Taiwan, [4] Department of Neurology, Taipei Veterans General Hospital, Taipei, Taiwan, [5] Center for Neuroscience, University of California, Davis, Davis, CA, United States, [6] College of Medicine, Graduate Institute of Brain and Mind Sciences, National Taiwan University, Taipei, Taiwan

The voltage-dependent ClC-1 chloride channel, whose open probability increases with membrane potential depolarization, belongs to the superfamily of CLC channels/transporters. ClC-1 is almost exclusively expressed in skeletal muscles and is essential for stabilizing the excitability of muscle membranes. Elucidation of the molecular structures of human ClC-1 and several CLC homologs provides important insight to the gating and ion permeation mechanisms of this chloride channel. Mutations in the human *CLCN1* gene, which encodes the ClC-1 channel, are associated with a hereditary skeletal muscle disease, myotonia congenita. Most disease-causing *CLCN1* mutations lead to loss-of-function phenotypes in the ClC-1 channel and thus increase membrane excitability in skeletal muscles, consequently manifesting as delayed relaxations following voluntary muscle contractions in myotonic subjects. The inheritance pattern of myotonia congenita can be autosomal dominant (Thomsen type) or recessive (Becker type). To date over 200 myotonia-associated ClC-1 mutations have been identified, which are scattered throughout the entire protein sequence. The dominant inheritance pattern of some myotonia mutations may be explained by a dominant-negative effect on ClC-1 channel gating. For many other myotonia mutations, however, no clear relationship can be established between the inheritance pattern and the location of the mutation in the ClC-1 protein. Emerging evidence indicates that the effects of some mutations may entail impaired ClC-1 protein homeostasis (proteostasis). Proteostasis of membrane proteins comprises of biogenesis at the endoplasmic reticulum (ER), trafficking to the surface membrane, and protein turn-over at the plasma membrane. Maintenance of proteostasis requires the coordination of a wide variety of different molecular chaperones and protein quality control factors. A number of regulatory molecules have recently been shown to contribute to post-translational modifications of ClC-1 and play critical roles in the ER quality control, membrane trafficking, and peripheral quality control of this

OPEN ACCESS

Edited by:
Jean-François Desaphy, University of Bari Aldo Moro, Italy

Reviewed by:
Christoph Fahlke, Julich Research Centre, Germany
Raùl Estévez, University of Barcelona, Spain

***Correspondence:**
Chih-Yung Tang
tang@ntu.edu.tw

Specialty section:
This article was submitted to Neuromuscular Diseases, a section of the journal Frontiers in Neurology

Received: *06 December 2019*
Accepted: *22 January 2020*
Published: *11 February 2020*

Citation:
Jeng C-J, Fu S-J, You C-Y, Peng Y-J, Hsiao C-T, Chen T-Y and Tang C-Y (2020) Defective Gating and Proteostasis of Human ClC-1 Chloride Channel: Molecular Pathophysiology of Myotonia Congenita. Front. Neurol. 11:76. doi: 10.3389/fneur.2020.00076

chloride channel. Further illumination of the mechanisms of ClC-1 proteostasis network will enhance our understanding of the molecular pathophysiology of myotonia congenita, and may also bring to light novel therapeutic targets for skeletal muscle dysfunction caused by myotonia and other pathological conditions.

Keywords: skeletal muscle, genetic disease, mutation, channelopathy, protein quality control, protein degradation, membrane trafficking, proteostasis network

INTRODUCTION

Myotonia is characterized as delayed muscle relaxation following voluntary or induced (e.g., electrical or mechanical stimulations) contraction, indicating hyperexcitability in the plasma membrane of skeletal muscle fibers. In myotonia associated with muscle dystrophies (myotonic dystrophy), trinucleotide and tetranucleotide repeat mutations in the *DMPK* and *ZNF9*/*CNBP* genes, respectively, lead to progressive dysfunction in multiple systems including the heart, brain, eye, and skeletal muscle (1–3). Non-dystrophic myotonias, in contrast, result from mutations in the genes encoding muscle ion channels, leading to electrical hyperexcitation and excessive contraction of skeletal muscles (4–7).

Disease arising from ion channel disorders is commonly known as channelopathy. One of the channelopathies associated with non-dystrophic myotonia concerns a chloride (Cl^-) channel critical for the function of skeletal muscles, the voltage-dependent ClC-1 Cl^- channel. Mutations in the human *CLCN1* gene lead to involuntary muscle contractions caused by anomalous sarcolemmal action potentials, clinically known as myotonia congenita (8–11). The worldwide prevalence rate of myotonia congenita is estimated to be 1:100,000, with a higher prevalence (about 1:10,000) in northern Scandinavia (12–14). To date, over 200 distinct mutations in the human ClC-1 protein have been linked to myotonia congenita (9, 15). This review aims to provide an up-to-date overview of the mechanisms of disease-related disruption of ClC-1 channel function. Specifically, we will address the significance of impaired ClC-1 protein stability and trafficking in the molecular pathophysiology of myotonia congenita.

STRUCTURE AND FUNCTION OF THE CLC-1 CHANNEL

The ClC-1 protein is a member of the CLC channel/transporter superfamily. The mammalian CLC family consists of nine members, with four (ClC-1, ClC-2, ClC-Ka, ClC-Kb) Cl^- channels predominantly residing in the plasma membrane, and the rest (ClC-3, ClC-4, ClC-5, ClC-6, ClC-7) Cl^-/H^+ antiporters (counter transporters) mostly located in intracellular organelles (16–20). The structural detail of the CLC channels/transporters is made available by latest breakthroughs in obtaining the crystal or cryogenic electron microscopy (cryo-EM) structures of various CLC proteins, including bacterial ClC-ec1, thermophilic algal CmClC, bovine ClC-K, and most recently human ClC-1 (21–26). Together they provide important insight to the gating and ion permeation mechanisms of the ClC-1 channel.

The human ClC-1 channel is a transmembrane protein consisting of 988 amino acids (a.a.; with an apparent molecular weight of about 120 kDa), generally divided into the amino (N)-terminal transmembrane portion (up to about 590 a.a.) and the carboxyl (C)-terminal cytoplasmic portion (**Figure 1A**). The transmembrane portion of the human ClC-1 protein is composed of 18 α-helices (helices A–R), with 17 (helices B–R) membrane-associated. Most of these helices are not perpendicular to the plasma membrane, but rather notably tilted. Interestingly, many of these helices fail to span the entire width of the lipid membrane. Furthermore, the cytoplasmic C-terminal portion also contains two tandem helical regions, the cystathionine β-synthase (CBS) domains (CBS1 and CBS2), which fold into an ATP-binding site (27).

Both functional and structural analyses support the notion that, like the other members of the CLC protein family, a functional ClC-1 channel comprises of a homodimeric structure [**Figure 1B**; (21–26, 28–32)]. The H, I, P, and Q helices in each ClC-1 subunit constitute the subunit interface between the two protomers (the dimer interface) (**Figure 1C**). Moreover, within each subunit of the ClC-1 homodimer, there is a separate ion-conducting pore (mainly formed by residues located at helices D, F, N, and R) known as the protopore. In other words, the ion-conducting pore of ClC-1 is entirely contained within each subunit of the dimer, and a functional ClC-1 channel thus harbors two protopores.

Consistent with the functional properties originally inferred from single-channel recordings of its fish homolog (the *Torpedo* ClC-0 channel), the opening of ClC-1 channel entails three different conductance levels that correspond to the opening of two independent ion-conducting pores, a phenomenon coined the "double-barreled" single-channel behavior (16, 28–33). This notion is further supported by cryo-EM analyses showing the presence of two protopores in a human ClC-1 homodimer (24, 25). As in all CLC channels, the opening and closing (gating) of the two protopores in ClC-1 is controlled by two distinct mechanisms (16, 20): (i) the "fast-gate" that controls the opening and closing of each protopore independently from the partner fast-gate, and (ii) the "common-gate" that controls the two protopores simultaneously. Thus, activation of the ClC-1 ion-conducting pathway requires the opening of both the common-gate and the fast-gate.

The opening kinetics of the ClC-1 fast-gate accelerates significantly in response to membrane depolarization (33–35). This gating mechanism is fast enough to counteract the

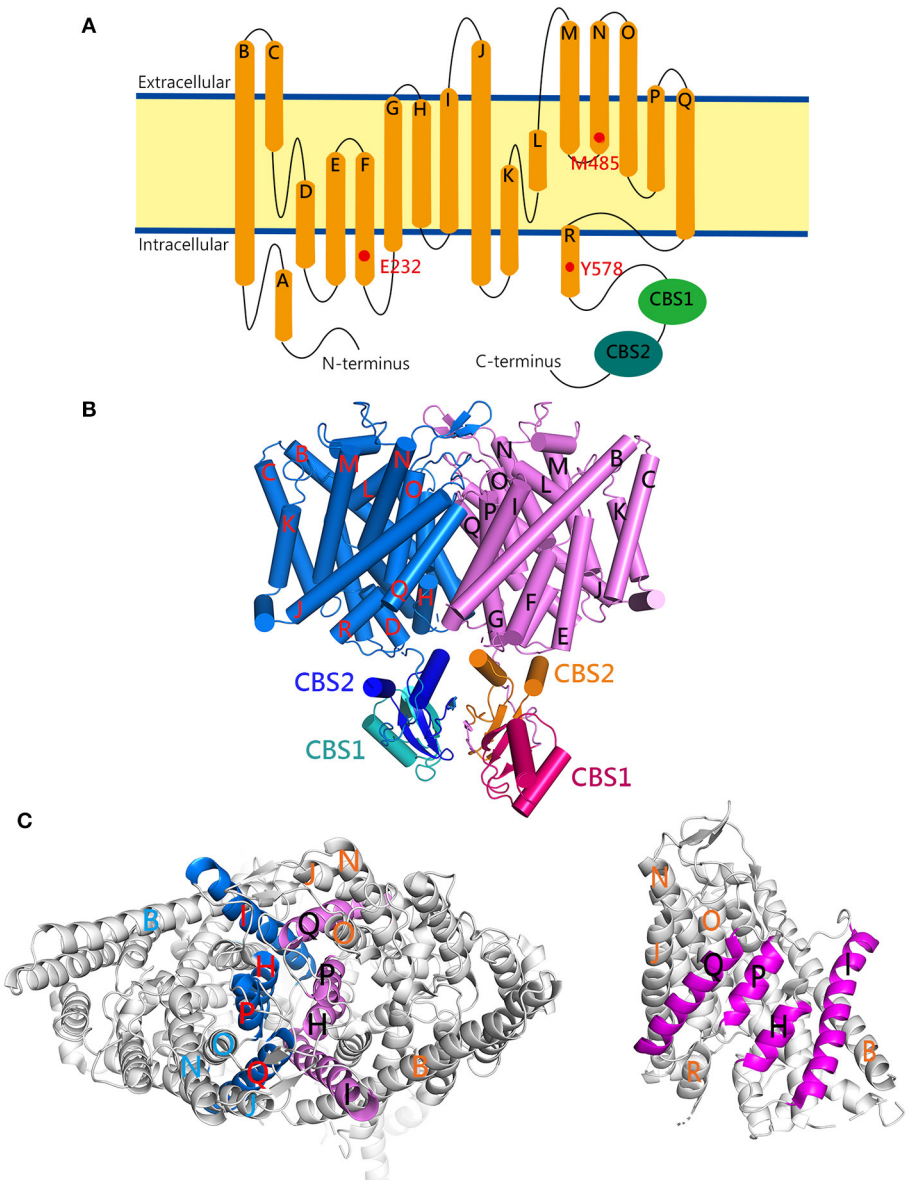

FIGURE 1 | The cryo-EM structure of the human ClC-1 channel. **(A)** Membrane topology of the ClC-1 subunit. The α-helices (A–R) are represented as cylinders. The locations of three pore-lining residues (E232, M485, Y578) and two cystathionine β-synthase (CBS) domains (CBS1, CBS2) are indicated. **(B)** Lateral view of the ClC-1 dimer (PDB code: 6QVC; presented using Pymol). The α-helices are shown as cylinders. The transmembrane portions of the two subunits in the dimer are colored in blue and magenta, respectively. Also highlighted are the CBS domains in the cytoplasmic carboxyl-terminal portion of each subunit. **(C)** The dimer interface of ClC-1. The interface-forming helices (H, I, P, Q) are drawn as colored ribbons. (Left) The ClC-1 dimer is viewed from the extracellular side. (Right) The ClC-1 subunit is viewed from the dimer interface of the opposing subunit.

depolarization conferred by voltage-gated sodium (Na^+) channels during an action potential, and is thus important for regulating skeletal muscle contraction. Besides the control by membrane potential, the fast-gate is also subject to modulation by Cl^- and H^+ (30, 33–36). Similar to voltage-gated cation channels, the open probability (P_o) of ClC-1 fast-gating is higher at more depolarized membrane potentials. Unlike voltage-gated cation channels, however, the ClC-1 protein does not seem to contain any transmembrane segment serving as the "voltage sensor." Rather, like ClC-0, the voltage-dependent activation of the fast-gate of ClC-1 may also arise from the coupling of Cl^- transport with the gating process (34, 37, 38). This gating-permeation coupling mechanism is supported by two findings: reducing the extracellular Cl^- concentration shifts the steady-state voltage dependence of P_o (P_o-V curve) of ClC-1 fast-gating toward a more depolarized membrane potential, and extracellular Cl^- raises the P_o by increasing the opening rate of the ClC-1 fast-gate (33–35). Together, these observations can be

explained by a Cl^--gating model in which the binding of Cl^- to the protopore opens the ClC-1 fast-gate, and Cl^- crossing the membrane electric field provides the fundamental mechanism for the observed voltage dependence (16). Importantly, the glutamate-232 residue (E232), located at the beginning of helix F of human ClC-1 (**Figure 1A**), may protrude its negatively-charged side-chain into the Cl^--permeation pathway, and serve as the gate that controls each individual protopore (16, 23–25, 39–41). Other notable pore-lining residues in the human ClC-1 include methionine 485 (M485; located at helix N) and tyrosine 578 (Y578; located at helix R) (**Figure 1A**). The former is located at the narrowest constriction at the extracellular opening of the pore and may serve as a hydrophobic barrier, while the latter constitutes a Cl^--binding site at the intracellular opening of the pore and forms part of the selectivity filter (24, 25).

The opening rate and P_o of the ClC-1 common-gate (also known as the slow-gate) are voltage-dependent as well, both becoming higher at more depolarized membrane potentials (33, 35, 42). Nevertheless, the detailed mechanism of the common-gating remains obscure (20). Formation of heterodimeric CLC channels comprising ClC-0 and ClC-1 or ClC-2 concatemers results in the loss of the ClC-0 common-gating, but without detectably affecting single channel conductance of individual ClC-0, ClC-1, and ClC-2 protopores (32). Interestingly, dissociation of the common-gating was observed in heterodimeric ClC-1-ClC-2 concatemers (43). Moreover, mutations of several residues located at or close to the dimer interface lead to significant alterations of the ClC-1 common-gating (42, 44–46). Together these results suggest that the mechanism of the common-gating entails the relative motion of the two channel subunits (i.e., inter-subunit interactions). In ClC-0, the common-gating may additionally involve the movement of the C-terminal cytoplasmic domain (47). Consistent with this idea, nucleotides (such as ATP) binding to the C-terminal cytoplasmic CBS domains seems to preclude the opening of the ClC-1 common-gate (27, 48–50). This may involve interactions between the CBS2 domain and the intracellular loop connecting helices D and E (24). Finally, the pore-lining E232 and Y578 have also been implicated in the ClC-1 common-gating (51).

Despite the presence of low-level expression in some other tissues, the ClC-1 channel is virtually exclusively expressed in skeletal muscles (52, 53). While multiple types of Cl^- channels exist in skeletal muscles, the ClC-1 channel is the most abundant (54–56). In most adult mammalian cells, the extracellular Cl^- concentration is significantly higher than its intracellular counterpart, leading to a negative Cl^- equilibrium potential (57). The physiological significance of the ClC-1 channel is further highlighted by the finding that Cl^- channel conductance may contribute up to 80% of the resting membrane conductance of skeletal muscle (58–60), and that Cl^- conductance is essential for preventing excessive firing of muscle action potentials (61). In addition to the sarcolemma, a significant Cl^- conductance is also present in the transverse-tubule system of skeletal muscle (59, 62–64). Although the precise subcellular localization pattern of ClC-1 in skeletal muscles remains contentious (56, 65–70), it is likely that ClC-1 is important for maintaining an effective Cl^- homeostasis system in both the sarcolemma and the transverse-tubule system. Taken together, activation of the ClC-1 channel is crucial for ensuring electrical stability of skeletal muscles by resetting membrane excitability after firing an action potential.

Several lines of evidence suggest that regulation of skeletal muscle fatigue involves alteration of ClC-1 channel activation (62, 71–74). During exercise, intensive firing of action potentials associated with active muscle contractions may result in extracellular accumulation of potassium (K^+) ions, which in turn would depolarize muscle membrane potential and thereby induce slow inactivation of voltage-gated Na^+ channels. Given that a sufficient inward Na^+ current is required for adequate firing of action potentials, the reduction of the amount of active voltage-gated Na^+ channels could disrupt the efficiency of excitation-contraction coupling in skeletal muscles and consequently lead to muscle fatigue. Furthermore, intensive exercise may cause muscle acidosis (74–76) as well as elevate intracellular calcium (Ca^{2+}) concentration that activates protein kinase C (PKC). Interestingly, both intracellular acidosis and PKC activation are known to inhibit ClC-1 channel activation (49, 77–79). This down-regulation of skeletal muscle membrane Cl^- conductance, as well as the ensuing reduction in the membrane input conductance, effectively counteracts the effect of K^+-induced slow inactivation of Na^+ channels, restoring muscle excitability and preventing muscle fatigue. On the other hand, in fast-twitch muscle fibers during prolonged muscle activities, the intracellular ATP level appears to be notably lowered (74, 80), which in turn reduces ATP inhibition of ClC-1 common-gating. This enhanced opening of the ClC-1 channel is expected to decrease muscle excitability and may serve to safeguard the cellular integrity of fast-twitch muscle fibers during metabolic stress (73).

MYOTONIA-ASSOCIATED ABERRANT GATING OF HUMAN CLC-1 CHANNEL

Consistent with its physiological role as the cardinal Cl^- channel in skeletal muscles, hereditary defects in the gene encoding the ClC-1 channel result in prominently reduced membrane Cl^- conductance, and thus significant muscle hyperexcitability (i.e., myotonia) in animals such as goats, mice, and dogs (52, 58, 61, 81–86). Over 200 mutations in the human skeletal muscle ClC-1 gene (*CLCN1*) on chromosome 7 have been linked to myotonia congenita, which can be inherited in an autosomal recessive (Becker type) or autosomal dominant (Thomsen type) manner (8–11, 15, 87, 88). In general, the recessive Becker myotonia is clinically more severe than the dominant Thomsen form. Disease-causing *CLCN1* mutations comprise of missense, non-sense, splice-site, and frameshift mutations. The majority of *CLCN1* mutations are associated with recessive inheritance, with about 20 or less causing dominant myotonia congenita. Furthermore, about 10 mutations seem to display either a recessive or a dominant pattern (dual inheritance pattern). Myotonia-causing mutations are scattered over the entire human ClC-1 protein, including the cytosolic N- and C-terminal regions and the transmembrane domains. Overall, it is impossible to predict the inheritance

pattern of *CLCN1* mutations based on mutation type or mutation location.

Myotonia congenita is one of the first proven human channelopathies. A significant number of disease-causing *CLCN1* mutations manifest as loss-of-function phenotypes in the gating/permeation of the ClC-1 channel, including the absence of discernible Cl^- currents (non-functional), significant shifts in the P_o-V curve of fast- and/or common-gating to depolarized potentials (positive shift), and an inverted voltage-dependence in activation (hyperpolarization-activated) (10, 45, 88–93). Haploinsufficiency imparted by each loss-of-function mutant allele may therefore explain the recessive inheritance pattern of myotonia congenita. Nonetheless, since many non-functional ClC-1 mutants on only one allele fail to induce myotonia in animal models (81, 82), whether haploinsufficiency contributes to dominant inheritance remains an open question. Instead it has been suggested that dominant myotonia may be due to dominant-negative effects of the mutant subunit on the wild-type (WT) counterpart in heterozygous patients (38, 94, 95). In line with this idea, many ClC-1 mutant proteins associated with recessive myotonia (e.g., truncation mutants) do not seem to exert significant dominant-negative effects, which may be attributed to their inability to associate with the WT subunit (10).

A working hypothesis on the mechanism of the dominant-negative effect of disease-causing *CLCN1* mutations is that the inheritance pattern of a mutation is decided by its functional effect on ClC-1 channel gating; mutations that impinge on the common-gating result in dominant myotonia, whereas those only changing the gating of individual protopores lead to a recessive inheritance pattern (30, 38, 95). With the exception of truncation mutations very close to the C-terminus of the human ClC-1 channel, almost all dominant mutations are missense mutations, most of which instigate significant positive-shift of the P_o-V curve such that activation of the mutant channels becomes insufficient to sustain effective membrane repolarization in skeletal muscles. In other words, in the heterodimeric ClC-1 channel formed by a WT subunit and a mutant subunit associated with dominant myotonia, the common-gate controlling both protopores may be profoundly influenced by the disease-causing mutation in the mutant subunit, thereby producing a dominant-negative effect. Consistent with this notion, many mutations causing dominant myotonia notably affect the common-gating of human ClC-1 (10, 24, 42, 44, 45, 87, 88, 96). In contrast, a recessive myotonia mutation involves a missense mutation at the pore-lining M485 (M485V) that drastically changes the voltage-dependent gating and the single-channel conductance of homodimeric mutant CLC-1 channels; upon co-expression with the WT subunit, however, the M485V mutant fails to detectably affect the gating or conductance properties of heterodimeric ClC-1 channels (94).

It is important to address the fact that many disease-associated *CLCN1* mutations do yield functional Cl^- channels with normal gating function. For example, the biophysical properties of several recessive ClC-1 mutant channels are either only slightly different or virtually indistinguishable from those of WT channels (10, 97, 98). Likewise, some dominant ClC-1 mutants do not seem to show detectable gating defects (99–101), indicating that the foregoing hypothesis on dominant-negative mechanism is not applicable to these mutants. The association of certain *CLCN1* mutations with a dual inheritance pattern further highlights the inadequacy of the gating hypothesis (10, 95, 102, 103). Together these examples clearly demonstrate that mechanisms beyond aberrant channel gating also contribute to the molecular pathophysiology of myotonia congenita.

MYOTONIA-ASSOCIATED DISRUPTION OF HUMAN CLC-1 PROTEOSTASIS

Since the skeletal muscle Cl^- conductance is predominantly determined by the total number of functional membrane ClC-1 channels, myotonia congenita-associated loss-of-function mutations might involve anomalous gating/permeation in individual ClC-1 channels or reduced ClC-1 protein abundance at the plasma membrane. Direct evidence supporting the latter hypothesis was first demonstrated for three disease-causing mutations located at the distal C-terminal region (A885P, R894X, and P932L): Upon heterologous expression in *Xenopus* oocytes, they all manifested significantly decreased ClC-1 protein expression at the surface membrane (104). Immunohistochemical examinations of muscle tissues from human patients carrying the R849X mutation further confirmed a dramatic loss of human ClC-1 staining in the sarcolemma (105). Importantly, despite the presence of a notable reduction in whole-cell Cl^- current amplitude, only A885P, but not R894X and P932L, is associated with a positive shift of the steady-state voltage-dependent activation property [**Table 1**; (35, 84, 104)]. Therefore, the myotonia-causing loss of muscle ClC-1 conductance in the patients can be mainly attributed to reduced surface expression of the mutant channel proteins.

Protein abundance is determined by the cellular maintenance of protein homeostasis (proteostasis), which controls the concentration, conformation, interaction, and subcellular localization of individual proteins (112, 113). The biological mechanisms governing proteostasis entail translational and post-translational regulations. For membrane proteins, post-translational regulation of cell surface protein density comprises of (i) protein quality control at the endoplasmic reticulum (ER quality control) (**Figure 2A**), (ii) trafficking to the surface membrane (membrane trafficking) (**Figure 2B**), and (iii) protein turn-over at the plasma membrane (peripheral quality control) [**Figure 2C**; (114, 115)].

Like other membrane proteins, the biogenesis of ion channels begins at the ER. After the initial translocation of a newly synthesized polypeptide into the ER membrane, channel protein folding is assisted co-translationally and post-translationally by multiple molecular chaperones and cochaperones through a series of substrate bindings and releases (116, 117). Membrane protein folding and assembly are closely monitored by the ER quality control system, composed of chaperones and associated factors, to ensure that only properly folded proteins are allowed to exit the ER [**Figure 2A**; (118, 119)]. Moreover, the ER quality control system recognizes and targets incorrectly folded or assembled proteins for ER-associated

TABLE 1 | Gating and proteostasis properties of myotonia-causing mutant ClC-1 channels associated with reduced surface protein expression.

Amino acid change	Inheritance	*Po*-V curve	Proteostasis defect	References
Q43R	R	Like WT	Impaired membrane trafficking	(98)
Y137D	R	Like WT	Reduced total protein level, impaired membrane trafficking	(98)
Q160H	R	Like WT	Reduced total protein level, impaired membrane trafficking	(98)
Q412P	R	Like WT	n.d.	(97)
F413C	R	Positive shift	Impaired membrane trafficking	(100, 105, 106)
A493E	D/R	Non-functional	Reduced total protein level	(107)
A531V	R	Like WT	Enhanced ERAD, impaired membrane trafficking, defective stability at the plasma membrane	(106, 108–111)
A885P	D*	Positive shift	n.d.	(84, 104)
R894X	D/R	Negative shift	Reduced total protein level	(35, 104–106)
P932L	D/R	Like WT	n.d.	(99, 104)

D, dominant; D, dominant myotonic goat; ERAD, endoplasmic reticulum-associated degradation; n.d., mechanism not determined; P_o-V, the steady-state voltage dependence of channel open probability; R, recessive; WT, wild-type.*

degradation (ERAD), which involves retrotranslocation of ubiquitinated, misfolded membrane proteins into the cytoplasm, followed with degradation by ubiquitin-proteasome machinery (120, 121). After exiting the ER, properly folded membrane proteins are packaged into ER-derived transport vesicles and then delivered to the Golgi apparatus, wherein proteins are subject to further maturation and glycosylation. Significantly, membrane proteins are also subject to a rigorous quality control at the Golgi (114, 115, 122). In general, during this membrane trafficking process, transport vesicles are progressively transferred through the ER-Golgi intermediate compartment, the *cis*-Golgi network, the Golgi stack (*cis*-, *medial*-, and *trans*-Golgi compartments), and finally to the *trans*-Golgi network, from which mature proteins are shipped to the plasma membrane [**Figure 2B**; (123–126)]. Emerging evidence further indicates that at the plasma membrane, misfolded membrane proteins escaped from the ER/Golgi quality control or generated in post-ER compartments are recognized by the molecular chaperones/cochaperones of the peripheral quality control system. (114, 127–129). The peripheral quality control system then removes the improperly folded proteins by ubiquitin modification, endocytosis, and subsequent trafficking to the lysosome for protein degradation (**Figure 2C**).

A significant number of different human disorders have been associated with proteostasis impairment that entails chronic expression of misfolded, mutant proteins with defective stability (130–132). For mutant membrane proteins with proteostasis deficiencies, the underlying molecular pathophysiological mechanisms may involve enhanced ERAD, impaired membrane trafficking, and/or defective stability at the plasma membrane (114, 125, 133, 134). Some of the well characterized proteostasis deficiencies concern the mutant Cl^- channels and K^+ channels causing cystic fibrosis and long-QT syndrome, respectively (135, 136). In the case of the aforementioned myotonia congenita-associated human ClC-1 mutants A885P, R894X, and P932L, their defective surface protein density appears to arise from reduced total protein levels and/or impaired membrane trafficking (104). The precise mechanism underlying their proteostasis impairment, however, remains elusive.

To date, at least 10 myotonia-related ClC-1 mutants have been shown to display reduced protein expression at the plasma membrane (**Table 1**). Most of these mutations belong to recessive myotonia, with some others involving dominant or dual inheritance patterns. The locations of the mutations scatter over cytoplasmic N- and C-terminal regions, as well as transmembrane domains (**Figure 3**). Apart from proteostasis impairment, these ClC-1 mutants also show aberrant channel gating function (**Figure 3** and **Table 1**). Given that the majority of previous studies of disease-causing mutations focus on functional characterizations without thorough biochemical analyses, it is conceivable that a significant fraction of the other known ClC-1 mutant channels with loss-of-function phenotypes may also be associated with defective proteostasis.

As far as proteostasis mechanisms are concerned, the most comprehensive analyses were performed for the A531V mutant (located at helix O), a recessively inherited mutation found prevalently in northern Finland and Scandinavia (12, 13). Despite an overall Po-V curve indistinguishable from that of the WT, the A531V mutant is associated with substantially reduced whole-cell current density (108, 109). Upon over-expression in both muscles and non-muscle cell lines, the A531V mutant exhibits significantly reduced protein levels that can be attributed to enhanced protein degradation (106, 108). Further studies show that the nature of this excessively reduced protein expression involves both proteasomal and lysosomal degradation, suggesting that the A531V mutant is associated with enhanced ERAD, as well as defective protein stability at the plasma membrane (108, 110, 111). Moreover, immunofluorescence analyses reveal a notable ER-retention pattern, indicating that the proteostasis defect of the A531V mutant also entails impaired membrane trafficking (106, 108). Together, these observations are consistent with the idea that the

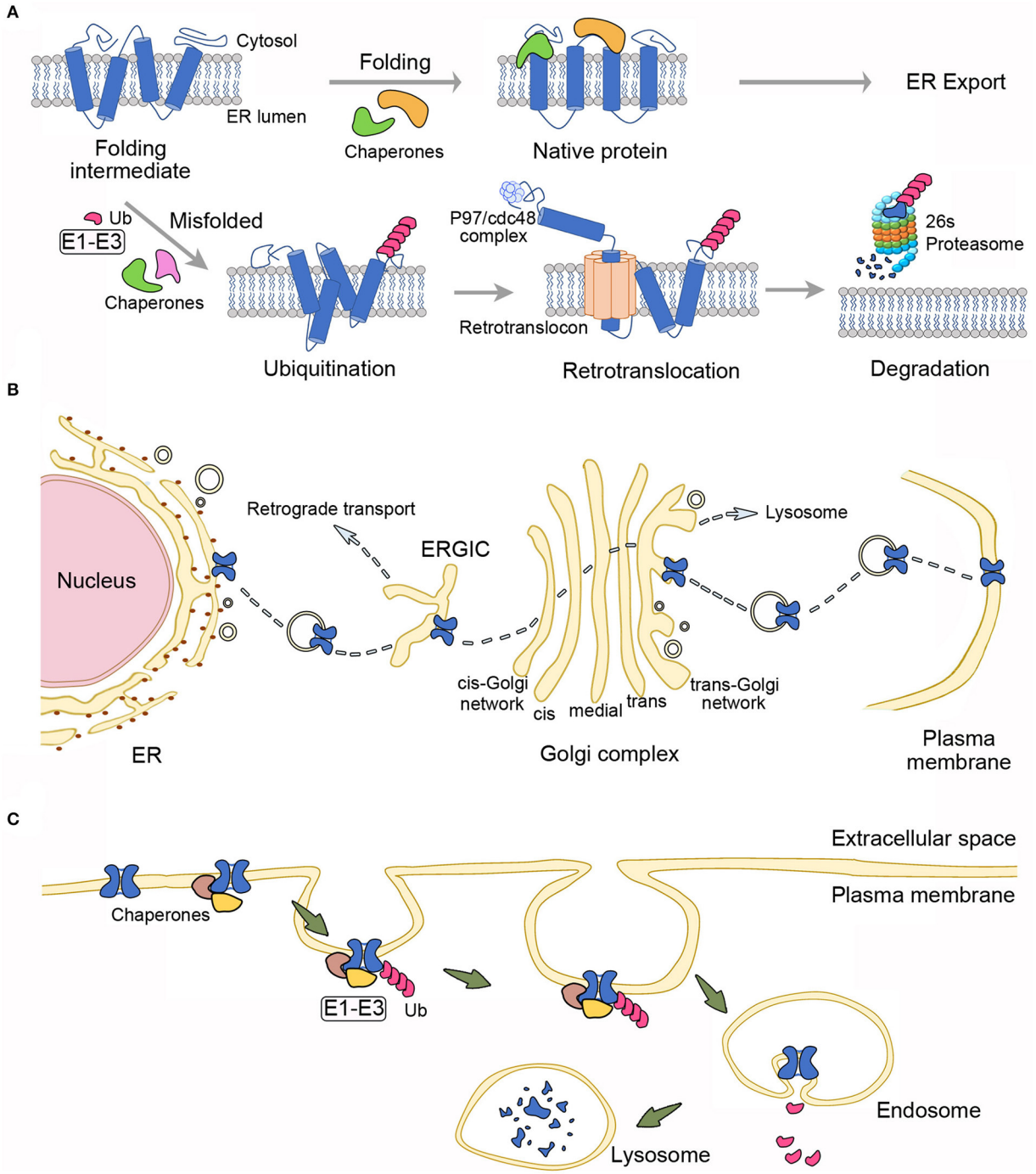

FIGURE 2 | Proteostasis mechanisms governing the surface expression of membrane proteins. **(A)** Endoplasmic reticulum (ER) quality control. Protein folding at the ER is assisted by multiple molecular chaperones and cochaperones. Proteins with native folding conformation may pass the ER quality control system and are allowed to exit the ER. Chaperones/cochaperones also recognize misfolded proteins, which are subject to covalent linkage with ubiquitin (Ub) via the concerted action of three types of ubiquitination enzymes (E1–E3). The ER-associated degradation system will further target ubiquitinated proteins for retrotranslocation into the cytoplasm through the channel-like, ER membrane-localized retrotranslocon, as well as with the facilitation by the ATPase p97/Cdc48 complex. Retrotranslocated proteins are then destined for degradation by the 26S proteasome. **(B)** Membrane trafficking. Immature, native membrane proteins from the ER are packaged into transport vesicles and transferred through the ER-Golgi intermediate compartment (ERGIC) and the Golgi complex, wherein they go through further post-translational modifications. Mature proteins are eventually ushered to the plasma membrane. Misfolded proteins that escape the ER quality control system and reach the Golgi complex may still be recognized by the Golgi quality control system, followed by retrograde transport back to the ER, or antegrade transport to the lysosome. **(C)** Peripheral quality control. Molecular chaperones/cochaperones at the plasma membrane may recognize membrane proteins with conformational defects and recruit enzymes (E1–E3) for ubiquitination of the misfolded proteins, which in turn are targeted for endocytosis and lysosomal degradation.

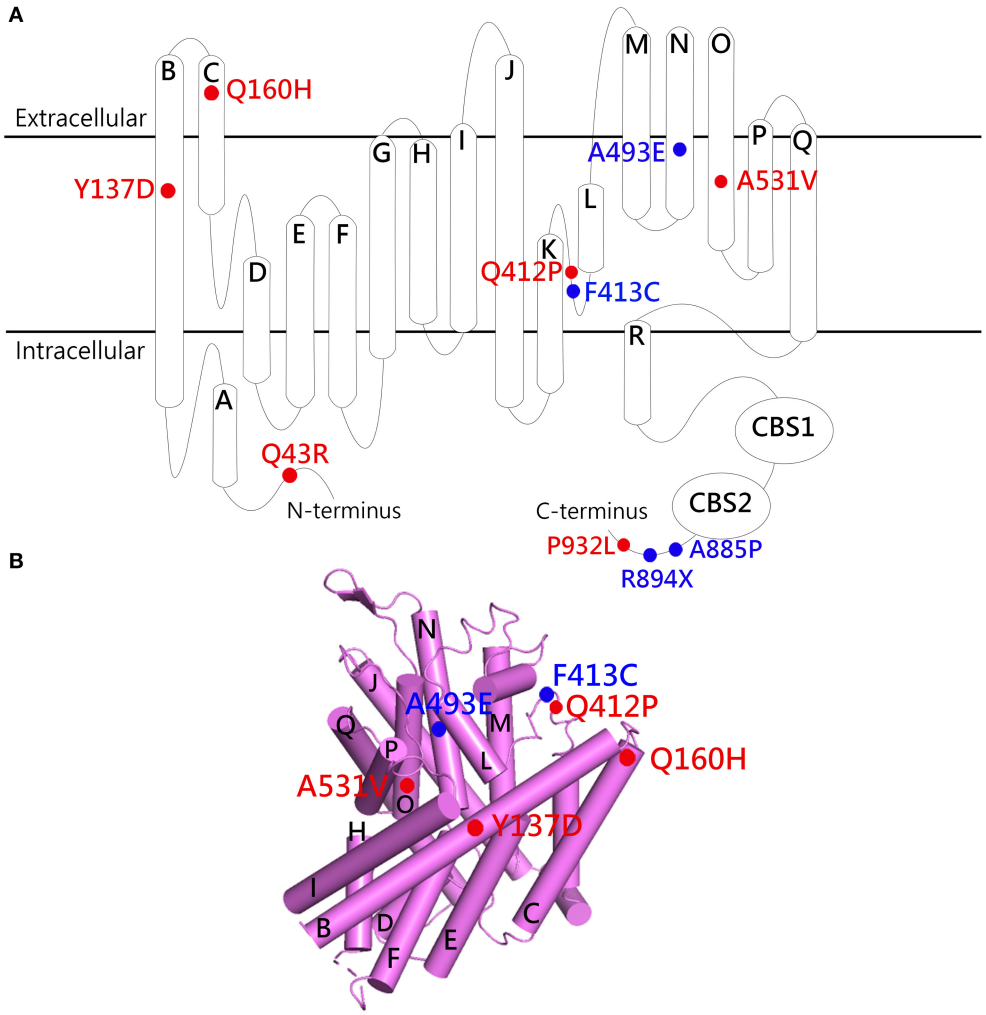

FIGURE 3 | Structural localization of myotonia congenita-associated ClC-1 mutations with defective proteostasis. **(A)** Membrane topology of the ClC-1 subunit. **(B)** Lateral view of the transmembrane portion of the human ClC-1 cryo-EM structure (PDB code: 6QVC; presented using Pymol). The α-helices are shown as cylinders. Red labels, mutants with gating properties similar to those of WT; blue labels, mutants with altered gating properties. See **Table 1** for more details.

A531V mutant contains a serious folding anomaly that renders most of the mutant proteins undesirable for the quality control systems at the ER, Golgi, and plasma membrane, shifting ClC-1 proteostasis toward the degradation pathway.

Nonetheless, it remains unclear why a conservative alanine-to-valine mutation at residue 531 in the transmembrane helix O results in such a dramatic impairment in human ClC-1 proteostasis, and how the mutation subtly disrupts the structure of ClC-1 without notably affecting its biophysical properties. One possibility is that the misfolded ClC-1 mutant protein is predominantly misrouted in its proteostasis pathway, reducing the likelihood of correct folding; for the small fraction of mutant proteins passing the quality control system, the native protein conformation may be reasonably safeguarded, sparing the gating function of the channel. Another plausible idea is that the mutation may introduce an ER-retention signal or disrupt or an ER-export signal. Some of the known ER-retention or ER-export signal sequences in other ion channels and membrane proteins include RXR, KKXX, and VXXSL (137–140), none of which is present in residues 511–551 of the ClC-1 WT or the A531V mutant. Moreover, all known ER-retention/export signals are located in the intracellular region, whereas A531 is at the transmembrane helix O, adjacent to the dimer interface helices P and Q (**Figure 3**).

Although the evidence is as of yet not available, it is likely that some myotonia congenita-related ClC-1 mutations may result in aberrant membrane targeting/subcellular localization in skeletal muscles. One major limitation to better understanding of this critical question is that proteostasis pathways as well as subcellular localization patterns of ClC-1 channels *in situ* remain elusive. As discussed above in the "Structure and Function" section, it is still controversial whether the ClC-1

channel is located at the sarcolemma and/or the transverse-tubule system of skeletal muscles. Although biophysical and pharmacological studies support the presence of ClC-1-like Cl^- channel conductance in the transverse-tubules of rat skeletal muscles (62, 63, 72), immunohistochemical characterizations of muscle cryosections suggest that, in WT mice, the ClC-1 immunoreactivity is primarily found in the sarcolemmal membrane but not in the transverse-tubules of skeletal muscles (66). A similar sarcolemma-restricted immunohistochemical staining pattern is also observed in skeletal muscles of the arrested development of righting response (ADR) mouse (65, 141), a commonly used mouse model for recessive myotonia (82, 142). Nevertheless, the prominent sarcolemmal localization of ClC-1 in skeletal muscles seems to disappear immediately after the myofibers are isolated and maintained in cell culture conditions, suggesting that the subcellular localization of ClC-1 is tightly regulated by the physiological conditions within skeletal muscles (65). The mechanism underlying the foregoing discrepancy between physiological and immunological localizations of ClC-1 in skeletal muscles remains to be determined. This discrepancy may reflect the presence of certain ClC-1 splice variants in the transverse-tubule system that lack the proper epitopes for the antibodies used in the immunohistochemical studies (143), or the disruption of antibody-epitope interaction by endogenous ClC-1-binding proteins under certain physiological conditions.

PROTEOSTASIS NETWORK OF HUMAN CLC-1 CHANNEL

As mentioned above, most of the newly synthesized, myotonia-causing A531V mutant proteins are incapable of passing the scrutiny of the cellular protein triage system and hence are subject to excessive proteasomal and lysosomal degradations. Even though application of the proteasome inhibitor MG132 effectively rescues the total protein level of the mutant ClC-1 channel, most of the MG132-rescued A531V proteins fail to be delivered to the plasma membrane (108). Accordingly, MG132 treatment does not rescue the reduced functional current of the mutant channel (108). Similarly, blocking the endosomal-lysosomal degradation system leads to a notable enhancement of A531V protein level, but fails to discernibly increase the whole-cell current density of the mutant channel (108). Together these results indicate that the defective surface protein density and the functional expression of the A531V mutant cannot be fixed by simply suppressing the degradation pathway. Rather, we must correct the impaired proteostasis of the mutant ClC-1 channel.

At the cellular level, proteostasis is maintained by over 2,000 macromolecules comprising chaperones/cochaperones, folding enzymes, and degradation and trafficking components, collectively known as the proteostasis network (130, 144). Until recently, the proteostasis network of human ClC-1 was virtually unknown. Nor was it clear how the ER and peripheral quality control systems recognize and mediate the degradation of disease-associated mutant ClC-1 proteins such as A531V.

In ERAD, which involves modification of misfolded proteins by the ubiquitin-proteasome system (**Figure 2A**), protein ubiquitination is mediated by a concerted action of multiple cytosolic and/or ER-resident enzymes, and may take place while transmembrane proteins are still located at the ER (128, 129, 145, 146). One of the key enzymes mediating protein ubiquitination is E3 ubiquitin ligase, which catalyzes the covalent linkage of ubiquitin to a substrate protein (145, 147). In higher eukaryotes, there are over 1000 distinct E3 ligases, divided into two major families: the homologous to E6-AP C-terminus (HECT) family and the really interesting new gene (RING) family (129, 148, 149). To date, over 20 HECT proteins and more than 600 RING proteins are known to express in human cells. We have demonstrated that polyubiquitination and degradation of human ClC-1 channel are catalyzed by two subtypes of the cullin (CUL)-RING E3 ubiquitin ligase complex, CUL4A/B-damage-specific DNA binding protein 1 (DDB1)-cereblon (CRBN) (110). CUL4A and 4B serve as scaffold proteins, facilitating the transfer of ubiquitin from the E2 ubiquitin-conjugating enzyme to a substrate protein, DDB1 is the adapter protein linking CUL4A/B and the substrate receptor, and CRBN works as the substrate receptor protein that directly recruits ClC-1 (150–152). This is the first direct evidence indicating that the CUL4 E3 ubiquitin ligase promotes degradation of ion channels. Incidentally, CUL E3 ligase activity is known to play an essential role in skeletal muscle homeostasis, myoblast differentiation, and myogenic differentiation of skeletal muscle stem cells (153, 154).

A cardinal process during protein biogenesis at the ER is the conformation surveillance of nascent polypeptides by chaperones and cochaperones that facilitate protein folding and thus minimize degradation/aggregation of non-native-state proteins (118, 155, 156). Moreover, for misfolded proteins that lose their stable conformations, chaperones/cochaperones assist them to the proteolytic pathway. We have also identified some of the key macromolecules participating in the protein quality control of human ClC-1 at the ER, including the interconnected molecular chaperones heat shock cognate protein 70 (Hsc70) and heat shock protein 90β (Hsp90β), and the cochaperones FK506-binding protein 8 (FKBP8 or FKBP38), activator of Hsp90 ATPase homolog 1 (Aha1), and Hsp70/Hsp90 organizing protein (HOP) (111). Hsc70 and Hsp90β are the constitutively active isoforms of Hsp70 and Hsp90, respectively, and both have been shown to take part in the ER quality control (155). FKBP8, Aha1, and HOP are well-established cochaperones for Hsp70 and Hsp90. The ER-resident membrane-anchored immunophilin FKBP8 may serve as a potential peptidyl-prolyl *cis-trans* isomerase, and the cytosolic proteins Aha1 and HOP regulate the ATPase activity of Hsp90 as well as the interaction of Hsp70 and Hsp90 (155, 157–159). All of the identified chaperones and cochaperones facilitate ClC-1 protein expression, and FKBP8 displays additional effect on promoting protein stability and membrane trafficking. Interestingly, we also noticed that Hsp90β and FKBP8 co-exist in the same protein complex with the E3 ligase scaffold protein CUL4, and appear to contribute to the regulation of CUL4 protein stability as well.

Figure 4 outlines our current model on the proteostasis network of human ClC-1 channel. Hsc70 and HOP may facilitate the early protein biogenesis process of ClC-1, followed by a concerted action by Aha1, Hsp90β, and FKBP8 (the Hsp90β cycle) to further promote ClC-1 folding. Hsp90β and FKBP8

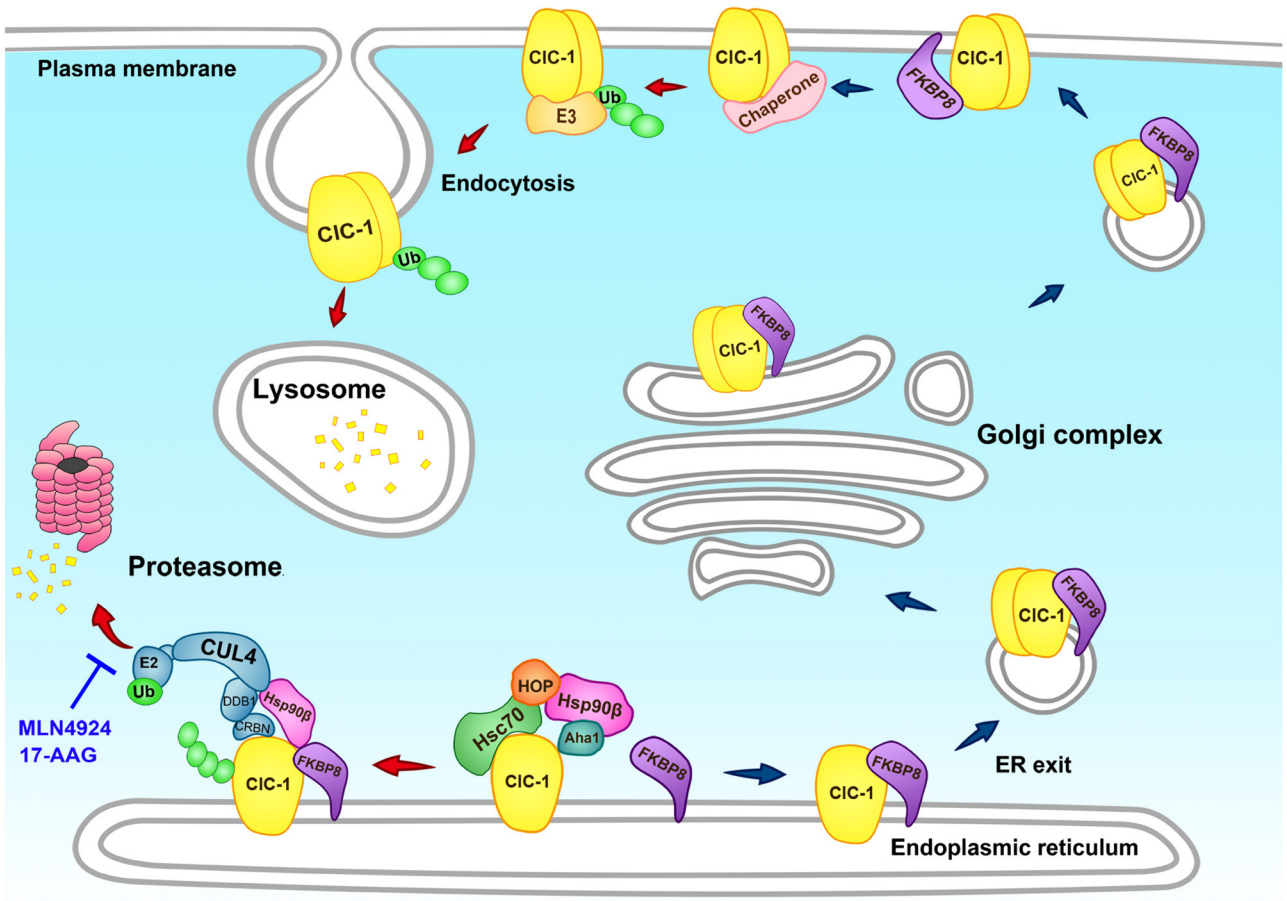

FIGURE 4 | Schematic model of the proteostasis network of the human ClC-1 channel. The endoplasmic reticulum (ER) quality control system of the CLC-1 protein comprises of the constitutively expressed molecular chaperones Hsc70 and Hsp90β, as well as the cochaperones HOP, Aha1, and FKBP8. Hsc70 and HOP assist the early stage of ClC-1 folding, whereas Aha1, Hsp90β, and FKBP8 promote the late stage of ClC-1 folding. ER-associated degradation of ClC-1 is mediated by the CUL4-DDB1-CRBN E3 ubiquitin ligase complex that catalyzes the transfer of ubiquitin (Ub) from the E2 ubiquitin-conjugating enzyme (E2) for covalent linkage to ClC-1. Ubiquitinated ClC-1 is targeted for eventual degradation by the proteasome. Hsp90β and FKBP8 may additionally regulate ER-associated degradation of ClC-1 by modulating the protein stability of CRBN, the substrate receptor of the CUL4-DDB1-CRBN ligase complex. Proteasomal degradation of ClC-1 can be effectively attenuated by the cullin E3 ligase blocker MLN4924 and the Hsp90 inhibitor 17-AAG. Moreover, FKBP8 is essential for ER exit and membrane trafficking of ClC-1. At the plasma membrane, FKBP8 further promotes surface ClC-1 protein stability. Other chaperones/cochaperones may also contribute to the peripheral quality control system of ClC-1. Misfolded ClC-1 is subject to ubiquitination by the as yet unknown E3 ubiquitin ligase (E3), followed by endocytosis and lysosomal degradation.

may also regulate the degradation of misfolded ClC-1 by the CUL4-DDB1-CRBN E3 ligase complex. We propose that, in the ER quality control, Hsp90β may serve as a molecular hub assisting the interaction of ClC-1 with Aha1, FKBP8, and CUL4, and therefore dynamically couple the ClC-1 protein folding and degradation pathways.

Our recent biochemical analyses suggest that, outside the ER, FKBP8 co-localizes with ClC-1 at both the Golgi complex and the plasma membrane; moreover, at the cell surface, FKBP8 enhances membrane ClC-1 protein level and promotes surface ClC-1 stability (160). Therefore, as depicted in **Figure 4**, we further propose that FKBP8 contributes to the ER export, membrane trafficking, and peripheral quality control of the human ClC-1 channel. It is an open question whether the rest of the chaperones/cochaperones implicated in ClC-1 ER quality control also play a role in the proteostasis of this Cl^- channel at the cell surface. In addition, the molecular nature of the E3 ligase catalyzing cell surface ClC-1 ubiquitination and the ensuing endosomal-lysosomal degradation mechanism is still unclear.

CLINICAL SIGNIFICANCE

Current treatment for myotonia congenita primarily involves reduction of muscle tone by suppressing action potential firing in skeletal muscles. The medications prescribed for treating non-dystrophic myotonia include the anti-arrhythmic agent

mexiletine and the anti-epileptic agent lamotrigine (161–163). Both drugs effectively block voltage-gated Na^+ channels and repetitive action potential firing in a use-dependent manner (164–167). At present, there is no treatment specifically designed to correct defective gating or proteostasis of disease-causing mutant ClC-1 channels.

In direct contrast to the aforementioned lack of effect of proteasomal/lysosomal inhibitors on enhancing functional current (108), suppression of CUL4A/B E3 ligase and promotion of chaperone/cochaperone activities significantly enhance the surface protein level and whole-cell current density of the myotonia-causing A531V mutant (110, 111). The results thus suggest that direct manipulation of the proteostasis network effectively corrects the impaired biogenesis of misfolded ClC-1 protein. Importantly, we identified two emerging small-molecule anti-cancer agents that may ameliorate defective proteostasis of ClC-1: MLN4924 and 17-allylamino-17-demethoxygeldanamycin (17-AAG) [**Figure 4**; (110, 111)]. MLN4924, which inhibits cullin E3 ubiquitin ligase activity by blocking the conjugation of the ubiquitin-like molecule NEDD8 to the cullin scaffold protein (168, 169), is currently undergoing clinical trials in cancer patients (170–173). The molecule 17-AAG, which suppresses the ATPase activity of Hsp90 by blocking ATP binding to the chaperone (174, 175), is also being tested in various clinical trials as an anti-cancer agent (174–176).

For human diseases caused by proteostasis impairment, it is essential to identify or develop novel biological and chemical therapeutics aiming at optimizing protein conformation and enhancing proteostasis capacity (130, 177, 178). For example, the Hsp90 inhibitor 17-AAG may serve as a potential pharmacological chaperone (pharmacochaperone) for modifying impaired proteostasis network of neurodegenerative diseases such as motor neuron degeneration and spinocerebellar ataxia (131, 179, 180). Therefore, our demonstration that 17-AAG improves the defective proteostasis of A531V raises a possibility that 17-AAG and other small-molecule pharmacochaperones could be clinically applied in the future to correct the protein folding defect of myotonia-causing ClC-1 mutant proteins.

The clinical implication of correcting defective ClC-1 proteostasis with pharmacological proteostasis network modifiers is actually beyond the scope of myotonia congenita, as ClC-1 dysfunction has been identified in other pathological conditions associated with anomalous skeletal muscle function. In myotonic dystrophy type 1 and 2 (DM1 and DM2), for example, mutations in the *DMPK* and *ZNF9*/*CNBP* genes, respectively, disrupt the alternative splicing of the *CLCN1* gene, creating a secondary reduction in sarcolemmal ClC-1 protein expression and current density (181–184). Correction of ClC-1 splicing with an antisense-induced exon skipping technique appears to eliminate the myotonia phenotype in a mouse model of DM1 (185). Interestingly, several studies further indicate the presence of significant co-segregation of DM2 with myotonia congenita-causing ClC-1 mutations such as F413C and R894X, both associated with defective ClC-1 proteostasis [**Figure 3** and **Table 1**; (186, 187)]. Similar to the pathological mechanism of myotonic dystrophy, emerging evidence suggests that Huntington disease also involves aberrant mRNA splicing of the *CLCN1* gene, thereby manifesting as hyperexcitability of skeletal muscles (188, 189). Moreover, statins, among the most effective agents in treating dyslipidemia, are associated with a significant incidence of myotoxicity (manifesting as symptoms such as muscle weakness, muscle pain, muscle stiffness, and muscle cramps), and may instigate considerably reduced ClC-1 protein expression and Cl^- conductance in skeletal muscles (190–193). Significantly, despite the possibility that statins may cause notable Ca^{2+} release from mitochondria and sarcoplasmic reticulum, statin-induced down-regulation of ClC-1 expression in skeletal muscles cannot be explained by reduced *CLCN1* transcription or enhanced PKC-mediated inhibition of ClC-1 channel activation (191, 192), suggesting the potential presence of a statin-induced disruption of ClC-1 proteostasis. Therefore, future development of specific and effective ClC-1 proteostasis modifiers may shed light on new therapeutic strategies for ameliorating the foregoing debilitating muscle symptoms.

Another issue of clinical relevancy concerns CRBN, the ClC-1-binding substrate receptor protein of the CUL4 E3 ligase complex. CRBN is known to be the binding target of thalidomide and lenalidomide (194–196), both immunomodulatory drugs used for the treatment of multiple myeloma (197, 198). Common side effects of thalidomide and lenalidomide treatments include muscle weakness and muscle cramps (197, 199), suggesting the presence of drug-induced hyperexcitability in skeletal muscles. Importantly, both thalidomide and lenalidomide suppress CUL4-DDB1-mediated ubiquitination and degradation of CRBN, thereby effectively promoting the degradation of some substrate proteins for the CUL4-DDB1-CRBN E3 ubiquitin ligase complex (200, 201). Given our previous demonstration that CUL4-DDB1-CRBN mediates ERAD of human ClC-1 channel and that over-expression of CRBN significantly suppresses ClC-1 protein level (110), it is possible that thalidomide/lenalidomide-induced muscle cramps observed in myeloma patients is in part attributable to enhanced degradation of human ClC-1 channel in skeletal muscles. In light of our proof-of-concept evidence that the small-molecule CUL4 inhibitor MLN4924 can effectively promote surface expression and current density of ClC-1 (110), relief from thalidomide/lenalidomide-induced side effects in skeletal muscles may be achievable in the future by developing muscle-specific, MLN4924-like CUL4-DDB1-CRBN E3 ligase modulators.

As elaborated in the "Structure and Function" section, depending on muscle fiber types, regulation of skeletal muscle fatigue may involve reduced and enhanced activation of ClC-1 channel through PKC activation and ATP diminishment, respectively. A recent study on the effect of exercise training on skeletal muscles in human subjects further suggests that ClC-1 protein abundance is higher in the fast-twitch than in the slow-twitch muscle fibers, and that, compared to recreationally active individuals, trained cyclists are associated with lower ClC-1 protein abundance (202). These observations imply that low ClC-1 abundance enhances muscle excitability and contractility and is beneficial for exercise performance. Although the role of transcriptional regulation of ClC-1 expression in skeletal muscles is well documented (20), it remains an open question whether cellular maintenance of proteostasis may also

contribute to developmental and physiological controls of ClC-1 protein abundance. Most importantly, the foregoing results appear to suggest an intriguing ClC-1 proteostasis adaptation mechanism that accommodates the differential physiological roles of fast- and slow-twitch fibers, and improves muscle contraction efficiency in response to exercise training. It is therefore imperative to understand the detailed proteostasis network of ClC-1 for elucidating the physiology of muscle training and the pathophysiology of muscle disorders.

CONCLUSION

Myotonia congenita is a ClC-1 channelopathy that involves skeletal muscle hyperexcitability due to a significant loss of muscle Cl^- conductance. Comprehensive genetic analyses have identified over 200 mutations in the human *CLCN1* gene associated with this hereditary disease. Biophysical investigations in the last three decades have revealed the mechanistic roles of aberrant gating and permeation properties in various myotonia-causing ClC-1 mutants. Determination of the cryo-EM structure of human ClC-1 provides further insight to the structural-functional mechanisms underlying dominant and recessive forms of myotonia congenita. Overwhelming evidence, however, indicates that aberrant channel gating and permeation *per se* are insufficient to explain the molecular pathophysiology of myotonia congenita, which can also result from abnormal biochemical and cell biological properties of ClC-1. Therefore, the field is in need of advanced understanding of theses aspects such as *in vivo* subcellular localization patterns and post-translational regulations. Another crucial task concerns the illumination of specific proteostasis mechanisms governing the biogenesis, trafficking, and quality control of WT and misfolded mutant ClC-1 proteins. Detailed elucidation of the ClC-1 proteostasis network may hold great promise for identifying ClC-1-specific abnormalities that may serve as targets for novel pharmacological interventions of myotonia congenita, as well as other pathological conditions causing skeletal muscle dysfunctions.

AUTHOR CONTRIBUTIONS

S-JF, C-YY, Y-JP, and C-TH: preparation and revision of table and figures. C-JJ, T-YC, and C-YT: writing and revision of manuscript.

FUNDING

This work was supported by research grants from Ministry of Science and Technology, Taiwan to C-JJ (108-2320-B-010-039-MY3) and C-YT (108-2320-B-002-033-MY3), and from National Institutes of Health, USA (R01GM065447) to T-YC.

REFERENCES

1. Meola G, Cardani R. Myotonic dystrophies: an update on clinical aspects, genetic, pathology, and molecular pathomechanisms. *Biochim Biophys Acta.* (2015) 1852:594–606. doi: 10.1016/j.bbadis.2014.05.019
2. Udd B, Krahe R. The myotonic dystrophies: molecular, clinical, and therapeutic challenges. *Lancet Neurol.* (2012) 11:891–905. doi: 10.1016/S1474-4422(12)70204-1
3. Wenninger S, Montagnese F, Schoser B. Core clinical phenotypes in myotonic dystrophies. *Front Neurol.* (2018) 9:303. doi: 10.3389/fneur.2018.00303
4. Raja Rayan DL, Hanna MG. Skeletal muscle channelopathies: nondystrophic myotonias and periodic paralysis. *Curr Opin Neurol.* (2010) 23:466–76. doi: 10.1097/WCO.0b013e32833cc97e
5. Cannon SC. Pathomechanisms in channelopathies of skeletal muscle and brain. *Annu Rev Neurosci.* (2006) 29:387–415. doi: 10.1146/annurev.neuro.29.051605.112815
6. Suetterlin K, Mannikko R, Hanna MG. Muscle channelopathies: recent advances in genetics, pathophysiology and therapy. *Curr Opin Neurol.* (2014) 27:583–90. doi: 10.1097/WCO.0000000000000127
7. Kullmann DM. Neurological channelopathies. *Annu Rev Neurosci.* (2010) 33:151–72. doi: 10.1146/annurev-neuro-060909-153122
8. Koch MC, Steinmeyer K, Lorenz C, Ricker K, Wolf F, Otto M, et al. The skeletal muscle chloride channel in dominant and recessive human myotonia. *Science.* (1992) 257:797–800. doi: 10.1126/science.1379744
9. Lossin C, George AL Jr. Myotonia congenita. *Adv Genet.* (2008) 63:25–55. doi: 10.1016/S0065-2660(08)01002-X
10. Pusch M. Myotonia caused by mutations in the muscle chloride channel gene CLCN1. *Hum Mutat.* (2002) 19:423–34. doi: 10.1002/humu.10063
11. Jurkat-Rott K, Lerche H, Lehmann-Horn F. Skeletal muscle channelopathies. *J Neurol.* (2002) 249:1493–502. doi: 10.1007/s00415-002-0871-5
12. Papponen H, Toppinen T, Baumann P, Myllyla V, Leisti J, Kuivaniemi H, et al. Founder mutations and the high prevalence of myotonia congenita in northern Finland. *Neurology.* (1999) 53:297–302. doi: 10.1212/WNL.53.2.297
13. Sun C, Tranebjaerg L, Torbergsen T, Holmgren G, Van Ghelue M. Spectrum of CLCN1 mutations in patients with myotonia congenita in Northern Scandinavia. *Eur J Hum Genet.* (2001) 9:903–9. doi: 10.1038/sj.ejhg.5200736
14. Emery AE. Population frequencies of inherited neuromuscular diseases–a world survey. *Neuromuscul Disord.* (1991) 1:19–29. doi: 10.1016/0960-8966(91)90039-U
15. Portaro S, Altamura C, Licata N, Camerino GM, Imbrici P, Musumeci O, et al. Clinical, molecular, and functional characterization of CLCN1 mutations in three families with recessive myotonia congenita. *Neuromolecular Med.* (2015) 17:285–96. doi: 10.1007/s12017-015-8356-8
16. Chen TY. Structure and function of clc channels. *Annu Rev Physiol.* (2005) 67:809–39. doi: 10.1146/annurev.physiol.67.032003.153012
17. Jentsch TJ, Poet M, Fuhrmann JC, Zdebik AA. Physiological functions of CLC Cl- channels gleaned from human genetic disease and mouse models. *Annu Rev Physiol.* (2005) 67:779–807. doi: 10.1146/annurev.physiol.67.032003.153245
18. Picollo A, Pusch M. Chloride/proton antiporter activity of mammalian CLC proteins ClC-4 and ClC-5. *Nature.* (2005) 436:420–3. doi: 10.1038/nature03720
19. Scheel O, Zdebik AA, Lourdel S, Jentsch TJ. Voltage-dependent electrogenic chloride/proton exchange by endosomal CLC proteins. *Nature.* (2005) 436:424–7. doi: 10.1038/nature03860
20. Jentsch TJ, Pusch M. CLC chloride channels and transporters: structure, function, physiology, and disease. *Physiol Rev.* (2018) 98:1493–590. doi: 10.1152/physrev.00047.2017
21. Feng L, Campbell EB, Hsiung Y, MacKinnon R. Structure of a eukaryotic CLC transporter defines an intermediate state in the transport cycle. *Science.* (2010) 330:635–41. doi: 10.1126/science.1195230

22. Dutzler R, Campbell EB, Cadene M, Chait BT, MacKinnon R. X-ray structure of a ClC chloride channel at 3.0 A reveals the molecular basis of anion selectivity. *Nature.* (2002) 415:287–94. doi: 10.1038/415287a
23. Dutzler R, Campbell EB, MacKinnon R. Gating the selectivity filter in ClC chloride channels. *Science.* (2003) 300:108–12. doi: 10.1126/science.1082708
24. Wang K, Preisler SS, Zhang L, Cui Y, Missel JW, Gronberg C, et al. Structure of the human ClC-1 chloride channel. *PLoS Biol.* (2019) 17:e3000218. doi: 10.1371/journal.pbio.3000218
25. Park E, MacKinnon R. Structure of the CLC-1 chloride channel from Homo sapiens. *Elife.* (2018) 7:e36629. doi: 10.7554/eLife.36629
26. Park E, Campbell EB, MacKinnon R. Structure of a CLC chloride ion channel by cryo-electron microscopy. *Nature.* (2017) 541:500–5. doi: 10.1038/nature20812
27. Tseng PY, Yu WP, Liu HY, Zhang XD, Zou X, Chen TY. Binding of ATP to the CBS domains in the C-terminal region of CLC-1. *J Gen Physiol.* (2011) 137:357–68. doi: 10.1085/jgp.201010495
28. Miller C. Open-state substructure of single chloride channels from Torpedo electroplax. *Philos Trans R Soc Lond B Biol Sci.* (1982) 299:401–11. doi: 10.1098/rstb.1982.0140
29. Miller C, White MM. Dimeric structure of single chloride channels from Torpedo electroplax. *Proc Natl Acad Sci USA.* (1984) 81:2772–5. doi: 10.1073/pnas.81.9.2772
30. Saviane C, Conti F, Pusch M. The muscle chloride channel ClC-1 has a double-barreled appearance that is differentially affected in dominant and recessive myotonia. *J Gen Physiol.* (1999) 113:457–68. doi: 10.1085/jgp.113.3.457
31. Fahlke C, Knittle T, Gurnett CA, Campbell KP, George AL Jr. Subunit stoichiometry of human muscle chloride channels. *J Gen Physiol.* (1997) 109:93–104. doi: 10.1085/jgp.109.1.93
32. Weinreich F, Jentsch TJ. Pores formed by single subunits in mixed dimers of different CLC chloride channels. *J Biol Chem.* (2001) 276:2347–53. doi: 10.1074/jbc.M005733200
33. Accardi A, Pusch M. Fast and slow gating relaxations in the muscle chloride channel CLC-1. *J Gen Physiol.* (2000) 116:433–44. doi: 10.1085/jgp.116.3.433
34. Rychkov GY, Pusch M, Astill DS, Roberts ML, Jentsch TJ, Bretag AH. Concentration and pH dependence of skeletal muscle chloride channel ClC-1. *J Physiol.* (1996) 497(Pt 2):423–35. doi: 10.1113/jphysiol.1996.sp021778
35. Hebeisen S, Fahlke C. Carboxy-terminal truncations modify the outer pore vestibule of muscle chloride channels. *Biophys J.* (2005) 89:1710–20. doi: 10.1529/biophysj.104.056093
36. Chen MF, Chen TY. Different fast-gate regulation by external Cl(-) and H(+) of the muscle-type ClC chloride channels. *J Gen Physiol.* (2001) 118:23–32. doi: 10.1085/jgp.118.1.23
37. Chen TY, Miller C. Nonequilibrium gating and voltage dependence of the ClC-0 Cl- channel. *J Gen Physiol.* (1996) 108:237–50. doi: 10.1085/jgp.108.4.237
38. Pusch M, Steinmeyer K, Koch MC, Jentsch TJ. Mutations in dominant human myotonia congenita drastically alter the voltage dependence of the CIC-1 chloride channel. *Neuron.* (1995) 15:1455–63. doi: 10.1016/0896-6273(95)90023-3
39. Dutzler R. The structural basis of ClC chloride channel function. *Trends Neurosci.* (2004) 27:315–20. doi: 10.1016/j.tins.2004.04.001
40. Dutzler R. Structural basis for ion conduction and gating in ClC chloride channels. *FEBS Lett.* (2004) 564:229–33. doi: 10.1016/S0014-5793(04)00210-8
41. Chen TY. Coupling gating with ion permeation in ClC channels. *Sci STKE.* (2003) 2003:pe23. doi: 10.1126/stke.2003.188.pe23
42. Duffield M, Rychkov G, Bretag A, Roberts M. Involvement of helices at the dimer interface in ClC-1 common gating. *J Gen Physiol.* (2003) 121:149–61. doi: 10.1085/jgp.20028741
43. Stolting G, Fischer M, Fahlke C. ClC-1 and ClC-2 form hetero-dimeric channels with novel protopore functions. *Pflugers Arch.* (2014) 466:2191–204. doi: 10.1007/s00424-014-1490-6
44. Accardi A, Ferrera L, Pusch M. Drastic reduction of the slow gate of human muscle chloride channel (ClC-1) by mutation C277S. *J Physiol.* (2001) 534:745–52. doi: 10.1111/j.1469-7793.2001.00745.x
45. Weinberger S, Wojciechowski D, Sternberg D, Lehmann-Horn F, Jurkat-Rott K, Becher T, et al. Disease-causing mutations C277R and C277Y modify gating of human ClC-1 chloride channels in myotonia congenita. *J Physiol.* (2012) 590:3449–64. doi: 10.1113/jphysiol.2012.232785
46. Cederholm JM, Rychkov GY, Bagley CJ, Bretag AH. Inter-subunit communication and fast gate integrity are important for common gating in hClC-1. *Int J Biochem Cell Biol.* (2010) 42:1182–8. doi: 10.1016/j.biocel.2010.04.004
47. Bykova EA, Zhang XD, Chen TY, Zheng J. Large movement in the C terminus of CLC-0 chloride channel during slow gating. *Nat Struct Mol Biol.* (2006) 13:1115–9. doi: 10.1038/nsmb1176
48. Zhang XD, Tseng PY, Chen TY. ATP inhibition of CLC-1 is controlled by oxidation and reduction. *J Gen Physiol.* (2008) 132:421–8. doi: 10.1085/jgp.200810023
49. Tseng PY, Bennetts B, Chen TY. Cytoplasmic ATP inhibition of CLC-1 is enhanced by low pH. *J Gen Physiol.* (2007) 130:217–21. doi: 10.1085/jgp.200709817
50. Bennetts B, Yu Y, Chen TY, Parker MW. Intracellular beta-nicotinamide adenine dinucleotide inhibits the skeletal muscle ClC-1 chloride channel. *J Biol Chem.* (2012) 287:25808–20. doi: 10.1074/jbc.M111.327551
51. Bennetts B, Parker MW. Molecular determinants of common gating of a ClC chloride channel. *Nat Commun.* (2013) 4:2507. doi: 10.1038/ncomms3507
52. Steinmeyer K, Ortland C, Jentsch TJ. Primary structure and functional expression of a developmentally regulated skeletal muscle chloride channel. *Nature.* (1991) 354:301–4. doi: 10.1038/354301a0
53. Zhang XD, Morishima S, Ando-Akatsuka Y, Takahashi N, Nabekura T, Inoue H, et al. Expression of novel isoforms of the CIC-1 chloride channel in astrocytic glial cells *in vitro*. *Glia.* (2004) 47:46–57. doi: 10.1002/glia.20024
54. Jentsch TJ, Maritzen T, Zdebik AA. Chloride channel diseases resulting from impaired transepithelial transport or vesicular function. *J Clin Invest.* (2005) 115:2039–46. doi: 10.1172/JCI25470
55. Jentsch TJ, Stein V, Weinreich F, Zdebik AA. Molecular structure and physiological function of chloride channels. *Physiol Rev.* (2002) 82:503–68. doi: 10.1152/physrev.00029.2001
56. Pedersen TH, Riisager A, de Paoli FV, Chen TY, Nielsen OB. Role of physiological ClC-1 Cl- ion channel regulation for the excitability and function of working skeletal muscle. *J Gen Physiol.* (2016) 147:291–308. doi: 10.1085/jgp.201611582
57. Tang CY, Chen TY. Physiology and pathophysiology of CLC-1: mechanisms of a chloride channel disease, myotonia. *J Biomed Biotechnol.* (2011) 2011:685328. doi: 10.1155/2011/685328
58. Bryant SH, Morales-Aguilera A. Chloride conductance in normal and myotonic muscle fibres and the action of monocarboxylic aromatic acids. *J Physiol.* (1971) 219:367–83. doi: 10.1113/jphysiol.1971.sp009667
59. Dulhunty AF. Distribution of potassium and chloride permeability over the surface and T-tubule membranes of mammalian skeletal muscle. *J Membr Biol.* (1979) 45:293–310. doi: 10.1007/BF01869290
60. Bretag AH. Muscle chloride channels. *Physiol Rev.* (1987) 67:618–724. doi: 10.1152/physrev.1987.67.2.618
61. Adrian RH, Bryant SH. On the repetitive discharge in myotonic muscle fibres. *J Physiol.* (1974) 240:505–15. doi: 10.1113/jphysiol.1974.sp010620
62. Dutka TL, Murphy RM, Stephenson DG, Lamb GD. Chloride conductance in the transverse tubular system of rat skeletal muscle fibres: importance in excitation-contraction coupling and fatigue. *J Physiol.* (2008) 586:875–87. doi: 10.1113/jphysiol.2007.144667
63. Coonan JR, Lamb GD. Effect of transverse-tubular chloride conductance on excitability in skinned skeletal muscle fibres of rat and toad. *J Physiol.* (1998) 509(Pt 2):551–64. doi: 10.1111/j.1469-7793.1998.551bn.x
64. Palade PT, Barchi RL. Characteristics of the chloride conductance in muscle fibers of the rat diaphragm. *J Gen Physiol.* (1977) 69:325–42. doi: 10.1085/jgp.69.3.325
65. Papponen H, Kaisto T, Myllyla VV, Myllyla R, Metsikko K. Regulated sarcolemmal localization of the muscle-specific ClC-1 chloride channel. *Exp Neurol.* (2005) 191:163–73. doi: 10.1016/j.expneurol.2004.07.018
66. Lueck JD, Rossi AE, Thornton CA, Campbell KP, Dirksen RT. Sarcolemmal-restricted localization of functional ClC-1 channels in mouse skeletal muscle. *J Gen Physiol.* (2010) 136:597–613. doi: 10.1085/jgp.201010526
67. Zifarelli G, Pusch M. Relaxing messages from the sarcolemma. *J Gen Physiol.* (2010) 136:593–6. doi: 10.1085/jgp.201010567

68. Lamb GD, Murphy RM, Stephenson DG. On the localization of ClC-1 in skeletal muscle fibers. *J Gen Physiol.* (2011) 137:327–9; author reply 331–3. doi: 10.1085/jgp.201010580
69. Fahlke C. Chloride channels take center stage in a muscular drama. *J Gen Physiol.* (2011) 137:17–9. doi: 10.1085/jgp.201010574
70. DiFranco M, Herrera A, Vergara JL. Chloride currents from the transverse tubular system in adult mammalian skeletal muscle fibers. *J Gen Physiol.* (2011) 137:21–41. doi: 10.1085/jgp.201010496
71. Cairns SP, Lindinger MI. Do multiple ionic interactions contribute to skeletal muscle fatigue? *J Physiol.* (2008) 586:4039–54. doi: 10.1113/jphysiol.2008.155424
72. Pedersen TH, Nielsen OB, Lamb GD, Stephenson DG. Intracellular acidosis enhances the excitability of working muscle. *Science.* (2004) 305:1144–7. doi: 10.1126/science.1101141
73. Baekgaard Nielsen O, de Paoli FV, Riisager A, Pedersen TH. Chloride channels take center stage in acute regulation of excitability in skeletal muscle: implications for fatigue. *Physiology.* (2017) 32:425–34. doi: 10.1152/physiol.00006.2015
74. Allen DG, Lamb GD, Westerblad H. Skeletal muscle fatigue: cellular mechanisms. *Physiol Rev.* (2008) 88:287–332. doi: 10.1152/physrev.00015.2007
75. Roos A, Boron WF. Intracellular pH transients in rat diaphragm muscle measured with DMO. *Am J Physiol.* (1978) 235:C49–54. doi: 10.1152/ajpcell.1978.235.1.C49
76. Wilson JR, McCully KK, Mancini DM, Boden B, Chance B. Relationship of muscular fatigue to pH and diprotonated Pi in humans: a 31P-NMR study. *J Appl Physiol.* (1988) 64:2333–9. doi: 10.1152/jappl.1988.64.6.2333
77. Riisager A, de Paoli FV, Yu WP, Pedersen TH, Chen TY, Nielsen OB. Protein kinase C-dependent regulation of ClC-1 channels in active human muscle and its effect on fast and slow gating. *J Physiol.* (2016) 594:3391–406. doi: 10.1113/JP271556
78. Bennetts B, Parker MW, Cromer BA. Inhibition of skeletal muscle ClC-1 chloride channels by low intracellular pH and ATP. *J Biol Chem.* (2007) 282:32780–91. doi: 10.1074/jbc.M703259200
79. Rosenbohm A, Rudel R, Fahlke C. Regulation of the human skeletal muscle chloride channel hClC-1 by protein kinase C. *J Physiol.* (1999) 514(Pt 3):677–85. doi: 10.1111/j.1469-7793.1999.677ad.x
80. Karatzaferi C, de Haan A, Ferguson RA, van Mechelen W, Sargeant AJ. Phosphocreatine and ATP content in human single muscle fibres before and after maximum dynamic exercise. *Pflugers Arch.* (2001) 442:467–74. doi: 10.1007/s004240100552
81. Gronemeier M, Condie A, Prosser J, Steinmeyer K, Jentsch TJ, Jockusch H. Nonsense and missense mutations in the muscular chloride channel gene Clc-1 of myotonic mice. *J Biol Chem.* (1994) 269:5963–7.
82. Steinmeyer K, Klocke R, Ortland C, Gronemeier M, Jockusch H, Grunder S, Jentsch TJ. Inactivation of muscle chloride channel by transposon insertion in myotonic mice. *Nature.* (1991) 354:304–8. doi: 10.1038/354304a0
83. Rhodes TH, Vite CH, Giger U, Patterson DF, Fahlke C, George AL Jr. A missense mutation in canine C1C-1 causes recessive myotonia congenita in the dog. *FEBS Lett.* (1999) 456:54–8. doi: 10.1016/S0014-5793(99)00926-6
84. Beck CL, Fahlke C, George AL Jr. Molecular basis for decreased muscle chloride conductance in the myotonic goat. *Proc Natl Acad Sci USA.* (1996) 93:11248–52. doi: 10.1073/pnas.93.20.11248
85. Adrian RH, Marshall MW. Action potentials reconstructed in normal and myotonic muscle fibres. *J Physiol.* (1976) 258:125–43. doi: 10.1113/jphysiol.1976.sp011410
86. Lipicky RJ, Bryant SH. Sodium, potassium, and chloride fluxes in intercostal muscle from normal goats and goats with hereditary myotonia. *J Gen Physiol.* (1966) 50:89–111. doi: 10.1085/jgp.50.1.89
87. Colding-Jorgensen E. Phenotypic variability in myotonia congenita. *Muscle Nerve.* (2005) 32:19–34. doi: 10.1002/mus.20295
88. Fialho D, Schorge S, Pucovska U, Davies NP, Labrum R, Haworth A, et al. Chloride channel myotonia: exon 8 hot-spot for dominant-negative interactions. *Brain.* (2007) 130:3265–74. doi: 10.1093/brain/awm248
89. Fahlke C, Rudel R, Mitrovic N, Zhou M, George AL Jr. An aspartic acid residue important for voltage-dependent gating of human muscle chloride channels. *Neuron.* (1995) 15:463–72. doi: 10.1016/0896-6273(95)90050-0
90. Zhang J, Sanguinetti MC, Kwiecinski H, Ptacek LJ. Mechanism of inverted activation of ClC-1 channels caused by a novel myotonia congenita mutation. *J Biol Chem.* (2000) 275:2999–3005. doi: 10.1074/jbc.275.4.2999
91. Ryan A, Rudel R, Kuchenbecker M, Fahlke C. A novel alteration of muscle chloride channel gating in myotonia levior. *J Physiol.* (2002) 545:345–54. doi: 10.1113/jphysiol.2002.027037
92. Ha K, Kim SY, Hong C, Myeong J, Shin JH, Kim DS, et al. Electrophysiological characteristics of six mutations in hClC-1 of Korean patients with myotonia congenita. *Mol Cells.* (2014) 37:202–12. doi: 10.14348/molcells.2014.2267
93. Imbrici P, Altamura C, Pessia M, Mantegazza R, Desaphy JF, Camerino DC. ClC-1 chloride channels: state-of-the-art research and future challenges. *Front Cell Neurosci.* (2015) 9:156. doi: 10.3389/fncel.2015.00156
94. Wollnik B, Kubisch C, Steinmeyer K, Pusch M. Identification of functionally important regions of the muscular chloride channel CIC-1 by analysis of recessive and dominant myotonic mutations. *Hum Mol Genet.* (1997) 6:805–11. doi: 10.1093/hmg/6.5.805
95. Kubisch C, Schmidt-Rose T, Fontaine B, Bretag AH, Jentsch TJ. ClC-1 chloride channel mutations in myotonia congenita: variable penetrance of mutations shifting the voltage dependence. *Hum Mol Genet.* (1998) 7:1753–60. doi: 10.1093/hmg/7.11.1753
96. Skalova D, Zidkova J, Vohanka S, Mazanec R, Musova Z, Vondracek P, et al. CLCN1 mutations in Czech patients with myotonia congenita, *in silico* analysis of novel and known mutations in the human dimeric skeletal muscle chloride channel. *PLoS ONE.* (2013) 8:e82549. doi: 10.1371/journal.pone.0082549
97. Vindas-Smith R, Fiore M, Vasquez M, Cuenca P, Del Valle G, Lagostena L, et al. Identification and functional characterization of CLCN1 mutations found in nondystrophic myotonia patients. *Hum Mutat.* (2016) 37:74–83. doi: 10.1002/humu.22916
98. Ronstedt K, Sternberg D, Detro-Dassen S, Gramkow T, Begemann B, Becher T, et al. Impaired surface membrane insertion of homo- and heterodimeric human muscle chloride channels carrying amino-terminal myotonia-causing mutations. *Sci Rep.* (2015) 5:15382. doi: 10.1038/srep15382
99. Simpson BJ, Height TA, Rychkov GY, Nowak KJ, Laing NG, Hughes BP, et al. Characterization of three myotonia-associated mutations of the CLCN1 chloride channel gene via heterologous expression. *Hum Mutat.* (2004) 24:185. doi: 10.1002/humu.9260
100. Zhang J, Bendahhou S, Sanguinetti MC, Ptacek LJ. Functional consequences of chloride channel gene (CLCN1) mutations causing myotonia congenita. *Neurology.* (2000) 54:937–42. doi: 10.1212/WNL.54.4.937
101. Wu FF, Ryan A, Devaney J, Warnstedt M, Korade-Mirnics Z, Poser B, et al. Novel CLCN1 mutations with unique clinical and electrophysiological consequences. *Brain.* (2002) 125:2392–407. doi: 10.1093/brain/awf246
102. George AL Jr, Sloan-Brown K, Fenichel GM, Mitchell GA, Spiegel R, Pascuzzi RM. Nonsense and missense mutations of the muscle chloride channel gene in patients with myotonia congenita. *Hum Mol Genet.* (1994) 3:2071–2.
103. Meyer-Kleine C, Steinmeyer K, Ricker K, Jentsch TJ, Koch MC. Spectrum of mutations in the major human skeletal muscle chloride channel gene (CLCN1) leading to myotonia. *Am J Hum Genet.* (1995) 57:1325–34.
104. Macias MJ, Teijido O, Zifarelli G, Martin P, Ramirez-Espain X, Zorzano A, et al. Myotonia-related mutations in the distal C-terminus of ClC-1 and ClC-0 chloride channels affect the structure of a poly-proline helix. *Biochem J.* (2007) 403:79–87. doi: 10.1042/BJ20061230
105. Raheem O, Penttila S, Suominen T, Kaakinen M, Burge J, Haworth A, et al. New immunohistochemical method for improved myotonia and chloride channel mutation diagnostics. *Neurology.* (2012) 79:2194–200. doi: 10.1212/WNL.0b013e31827595e2
106. Papponen H, Nissinen M, Kaisto T, Myllyla VV, Myllyla R, Metsikko K. F413C and A531V but not R894X myotonia congenita mutations cause defective endoplasmic reticulum export of the muscle-specific chloride channel CLC-1. *Muscle Nerve.* (2008) 37:317–25. doi: 10.1002/mus.20922
107. Gaitan-Penas H, Armand-Ugon M, Macaya A, Estevez R. CLCN1 Myotonia congenita mutation with a variable pattern of inheritance suggests a novel mechanism of dominant myotonia. *Muscle Nerve.* (2018) 58:157–60. doi: 10.1002/mus.26098

108. Lee TT, Zhang XD, Chuang CC, Chen JJ, Chen YA, Chen SC, et al. Myotonia congenita mutation enhances the degradation of human CLC-1 chloride channels. *PLoS ONE.* (2013) 8:e55930. doi: 10.1371/journal.pone.0055930
109. Desaphy JF, Gramegna G, Altamura C, Dinardo MM, Imbrici P, George AL Jr, et al. Functional characterization of ClC-1 mutations from patients affected by recessive myotonia congenita presenting with different clinical phenotypes. *Exp Neurol.* (2013) 248:530–40. doi: 10.1016/j.expneurol.2013.07.018
110. Chen YA, Peng YJ, Hu MC, Huang JJ, Chien YC, Wu JT, et al. The Cullin 4A/B-DDB1-Cereblon E3 ubiquitin ligase complex mediates the degradation of CLC-1 chloride channels. *Sci Rep.* (2015) 5:10667. doi: 10.1038/srep10667
111. Peng YJ, Huang JJ, Wu HH, Hsieh HY, Wu CY, Chen SC, et al. Regulation of CLC-1 chloride channel biosynthesis by FKBP8 and Hsp90β. *Sci Rep.* (2016) 6:32444. doi: 10.1038/srep32444
112. Sala AJ, Bott LC, Morimoto RI. Shaping proteostasis at the cellular, tissue, and organismal level. *J Cell Biol.* (2017) 216:1231–41. doi: 10.1083/jcb.201612111
113. Balch WE, Morimoto RI, Dillin A, Kelly JW. Adapting proteostasis for disease intervention. *Science.* (2008) 319:916–9. doi: 10.1126/science.1141448
114. Apaja PM, Lukacs GL. Protein homeostasis at the plasma membrane. *Physiology.* (2014) 29:265–77. doi: 10.1152/physiol.00058.2013
115. Arvan P, Zhao X, Ramos-Castaneda J, Chang A. Secretory pathway quality control operating in Golgi, plasmalemmal, and endosomal systems. *Traffic.* (2002) 3:771–80. doi: 10.1034/j.1600-0854.2002.31102.x
116. Saibil H. Chaperone machines for protein folding, unfolding and disaggregation. *Nat Rev Mol Cell Biol.* (2013) 14:630–42. doi: 10.1038/nrm3658
117. Braakman I, Hebert DN. Protein folding in the endoplasmic reticulum. *Cold Spring Harb Perspect Biol.* (2013) 5:a013201. doi: 10.1101/cshperspect.a013201
118. Hebert DN, Molinari M. In and out of the ER: protein folding, quality control, degradation, and related human diseases. *Physiol Rev.* (2007) 87:1377–408. doi: 10.1152/physrev.00050.2006
119. Araki K, Nagata K. Protein folding and quality control in the ER. *Cold Spring Harb Perspect Biol.* (2011) 3:a007526. doi: 10.1101/cshperspect.a007526
120. Ruggiano A, Foresti O, Carvalho P. Quality control: ER-associated degradation: protein quality control and beyond. *J Cell Biol.* (2014) 204:869–79. doi: 10.1083/jcb.201312042
121. Preston GM, Brodsky JL. The evolving role of ubiquitin modification in endoplasmic reticulum-associated degradation. *Biochem J.* (2017) 474:445–69. doi: 10.1042/BCJ20160582
122. Sun Z, Brodsky JL. Protein quality control in the secretory pathway. *J Cell Biol.* (2019) 218:3171–87. doi: 10.1083/jcb.201906047
123. Derby MC, Gleeson PA. New insights into membrane trafficking and protein sorting. *Int Rev Cytol.* (2007) 261:47–116. doi: 10.1016/S0074-7696(07)61002-X
124. Chia PZ, Gleeson PA. Membrane tethering. *F1000Prime Rep.* (2014) 6:74. doi: 10.12703/P6-74
125. Cobbold C, Monaco AP, Sivaprasadarao A, Ponnambalam S. Aberrant trafficking of transmembrane proteins in human disease. *Trends Cell Biol.* (2003) 13:639–47. doi: 10.1016/j.tcb.2003.10.008
126. Gomez-Navarro N, Miller E. Protein sorting at the ER-Golgi interface. *J Cell Biol.* (2016) 215:769–78. doi: 10.1083/jcb.201610031
127. Babst M. Quality control: quality control at the plasma membrane: one mechanism does not fit all. *J Cell Biol.* (2014) 205:11–20. doi: 10.1083/jcb.201310113
128. Foot N, Henshall T, Kumar S. Ubiquitination and the regulation of membrane proteins. *Physiol Rev.* (2017) 97:253–81. doi: 10.1152/physrev.00012.2016
129. MacGurn JA, Hsu PC, Emr SD. Ubiquitin and membrane protein turnover: from cradle to grave. *Annu Rev Biochem.* (2012) 81:231–59. doi: 10.1146/annurev-biochem-060210-093619
130. Powers ET, Morimoto RI, Dillin A, Kelly JW, Balch WE. Biological and chemical approaches to diseases of proteostasis deficiency. *Annu Rev Biochem.* (2009) 78:959–91. doi: 10.1146/annurev.biochem.052308.114844
131. Labbadia J, Morimoto RI. The biology of proteostasis in aging and disease. *Annu Rev Biochem.* (2015) 84:435–64. doi: 10.1146/annurev-biochem-060614-033955
132. Hipp MS, Park SH, Hartl FU. Proteostasis impairment in protein-misfolding and -aggregation diseases. *Trends Cell Biol.* (2014) 24:506–14. doi: 10.1016/j.tcb.2014.05.003
133. Guerriero CJ, Brodsky JL. The delicate balance between secreted protein folding and endoplasmic reticulum-associated degradation in human physiology. *Physiol Rev.* (2012) 92:537–76. doi: 10.1152/physrev.00027.2011
134. Okiyoneda T, Apaja PM, Lukacs GL. Protein quality control at the plasma membrane. *Curr Opin Cell Biol.* (2011) 23:483–91. doi: 10.1016/j.ceb.2011.04.012
135. Lukacs GL, Verkman AS. CFTR: folding, misfolding and correcting the DeltaF508 conformational defect. *Trends Mol Med.* (2012) 18:81–91. doi: 10.1016/j.molmed.2011.10.003
136. Foo B, Williamson B, Young JC, Lukacs G, Shrier A. hERG quality control and the long QT syndrome. *J Physiol.* (2016) 594:2469–81. doi: 10.1113/JP270531
137. Ma D, Jan LY. ER transport signals and trafficking of potassium channels and receptors. *Curr Opin Neurobiol.* (2002) 12:287–92. doi: 10.1016/S0959-4388(02)00319-7
138. Vandenberghe W, Bredt DS. Early events in glutamate receptor trafficking. *Curr Opin Cell Biol.* (2004) 16:134–9. doi: 10.1016/j.ceb.2004.01.003
139. Nufer O, Guldbrandsen S, Degen M, Kappeler F, Paccaud JP, Tani K, et al. Role of cytoplasmic C-terminal amino acids of membrane proteins in ER export. *J Cell Sci.* (2002) 115:619–28.
140. Wang X, Matteson J, An Y, Moyer B, Yoo JS, Bannykh S, et al. COPII-dependent export of cystic fibrosis transmembrane conductance regulator from the ER uses a di-acidic exit code. *J Cell Biol.* (2004) 167:65–74. doi: 10.1083/jcb.200401035
141. Gurnett CA, Kahl SD, Anderson RD, Campbell KP. Absence of the skeletal muscle sarcolemma chloride channel ClC-1 in myotonic mice. *J Biol Chem.* (1995) 270:9035–8. doi: 10.1074/jbc.270.16.9035
142. Klocke R, Steinmeyer K, Jentsch TJ, Jockusch H. Role of innervation, excitability, and myogenic factors in the expression of the muscular chloride channel ClC-1. A study on normal and myotonic muscle. *J Biol Chem.* (1994) 269:27635–9.
143. Aromataris EC, Rychkov GY. ClC-1 chloride channel: matching its properties to a role in skeletal muscle. *Clin Exp Pharmacol Physiol.* (2006) 33:1118–23. doi: 10.1111/j.1440-1681.2006.04502.x
144. Hutt DM, Balch WE. Expanding proteostasis by membrane trafficking networks. *Cold Spring Harb Perspect Biol.* (2013) 5:a013383. doi: 10.1101/cshperspect.a013383.
145. Glickman MH, Ciechanover A. The ubiquitin-proteasome proteolytic pathway: destruction for the sake of construction. *Physiol Rev.* (2002) 82:373–428. doi: 10.1152/physrev.00027.2001
146. Kleiger G, Mayor T. Perilous journey: a tour of the ubiquitin-proteasome system. *Trends Cell Biol.* (2014) 24:352–9. doi: 10.1016/j.tcb.2013.12.003
147. Abriel H, Staub O. Ubiquitylation of ion channels. *Physiology.* (2005) 20:398–407. doi: 10.1152/physiol.00033.2005
148. Deshaies RJ, Joazeiro CA. RING domain E3 ubiquitin ligases. *Annu Rev Biochem.* (2009) 78:399–434. doi: 10.1146/annurev.biochem.78.101807.093809
149. Rotin D, Kumar S. Physiological functions of the HECT family of ubiquitin ligases. *Nat Rev Mol Cell Biol.* (2009) 10:398–409. doi: 10.1038/nrm2690
150. Jackson S, Xiong Y. CRL4s: the CUL4-RING E3 ubiquitin ligases. *Trends Biochem Sci.* (2009) 34:562–70. doi: 10.1016/j.tibs.2009.07.002
151. Petroski MD, Deshaies RJ. Function and regulation of cullin-RING ubiquitin ligases. *Nat Rev Mol Cell Biol.* (2005) 6:9–20. doi: 10.1038/nrm1547
152. Hannah J, Zhou P. Distinct and overlapping functions of the cullin E3 ligase scaffolding proteins CUL4A and CUL4B. *Gene.* (2015) 573:33–45. doi: 10.1016/j.gene.2015.08.064
153. Blondelle J, Shapiro P, Domenighetti AA, Lange S. Cullin E3 ligase activity is required for myoblast differentiation. *J Mol Biol.* (2017) 429:1045–66. doi: 10.1016/j.jmb.2017.02.012
154. Gupta VA, Beggs AH. Kelch proteins: emerging roles in skeletal muscle development and diseases. *Skelet Muscle.* (2014) 4:11. doi: 10.1186/2044-5040-4-11

155. Kim YE, Hipp MS, Bracher A, Hayer-Hartl M, Hartl FU. Molecular chaperone functions in protein folding and proteostasis. *Annu Rev Biochem.* (2013) 82:323–55. doi: 10.1146/annurev-biochem-060208-092442
156. Houck SA, Cyr DM. Mechanisms for quality control of misfolded transmembrane proteins. *Biochim Biophys Acta.* (2011) 1818:1108–14. doi: 10.1016/j.bbamem.2011.11.007
157. Taipale M, Jarosz DF, Lindquist S. HSP90 at the hub of protein homeostasis: emerging mechanistic insights. *Nat Rev Mol Cell Biol.* (2010) 11:515–28. doi: 10.1038/nrm2918
158. Shirane M, Nakayama KI. Inherent calcineurin inhibitor FKBP38 targets Bcl-2 to mitochondria and inhibits apoptosis. *Nat Cell Biol.* (2003) 5:28–37. doi: 10.1038/ncb894
159. Okamoto T, Nishimura Y, Ichimura T, Suzuki K, Miyamura T, Suzuki T, et al. Hepatitis C virus RNA replication is regulated by FKBP8 and Hsp90. *EMBO J.* (2006) 25:5015–25. doi: 10.1038/sj.emboj.7601367
160. Peng YJ, Lee YC, Fu SJ, Chien YC, Liao YF, Chen TY, et al. FKBP8 Enhances protein stability of the CLC-1 chloride channel at the plasma membrane. *Int J Mol Sci.* (2018) 19:E3783. doi: 10.3390/ijms19123783
161. Andersen G, Hedermann G, Witting N, Duno M, Andersen H, Vissing J. The antimyotonic effect of lamotrigine in non-dystrophic myotonias: a double-blind randomized study. *Brain.* (2017) 140:2295–305. doi: 10.1093/brain/awx192
162. Stunnenberg BC, Raaphorst J, Groenewoud HM, Statland JM, Griggs RC, Woertman W, et al. Effect of Mexiletine on Muscle Stiffness in Patients With Nondystrophic myotonia evaluated using aggregated N-of-1 trials. *JAMA.* (2018) 320:2344–53. doi: 10.1001/jama.2018.18020
163. Statland JM, Bundy BN, Wang Y, Rayan DR, Trivedi JR, Sansone VA, et al. Mexiletine for symptoms and signs of myotonia in nondystrophic myotonia: a randomized controlled trial. *JAMA.* (2012) 308:1357–65. doi: 10.1001/jama.2012.12607
164. Zhao J, Dupre N, Puymirat J, Chahine M. Biophysical characterization of M1476I, a sodium channel founder mutation associated with cold-induced myotonia in French Canadians. *J Physiol.* (2012) 590:2629–44. doi: 10.1113/jphysiol.2011.223461
165. Wang GK, Russell C, Wang SY. Mexiletine block of wild-type and inactivation-deficient human skeletal muscle hNav1.4 Na^+ channels. *J Physiol.* (2004) 554:621–33. doi: 10.1113/jphysiol.2003.054973
166. Kuo CC, Lu L. Characterization of lamotrigine inhibition of Na^+ channels in rat hippocampal neurones. *Br J Pharmacol.* (1997) 121:1231–8. doi: 10.1038/sj.bjp.0701221
167. Xie X, Lancaster B, Peakman T, Garthwaite J. Interaction of the antiepileptic drug lamotrigine with recombinant rat brain type IIA Na^+ channels and with native Na^+ channels in rat hippocampal neurones. *Pflugers Arch.* (1995) 430:437–46. doi: 10.1007/BF00373920
168. Brownell JE, Sintchak MD, Gavin JM, Liao H, Bruzzese FJ, Bump NJ, et al. Substrate-assisted inhibition of ubiquitin-like protein-activating enzymes: the NEDD8 E1 inhibitor MLN4924 forms a NEDD8-AMP mimetic *in situ*. *Mol Cell.* (2010) 37:102–11. doi: 10.1016/j.molcel.2009.12.024
169. Soucy TA, Smith PG, Milhollen MA, Berger AJ, Gavin JM, Adhikari S, et al. An inhibitor of NEDD8-activating enzyme as a new approach to treat cancer. *Nature.* (2009) 458:732–6. doi: 10.1038/nature07884
170. Bulatov E, Ciulli A. Targeting Cullin-RING E3 ubiquitin ligases for drug discovery: structure, assembly and small-molecule modulation. *Biochem J.* (2015) 467:365–86. doi: 10.1042/BJ20141450
171. McMillin DW, Jacobs HM, Delmore JE, Buon L, Hunter ZR, Monrose V, et al. Molecular and cellular effects of NEDD8-activating enzyme inhibition in myeloma. *Mol Cancer Ther.* (2012) 11:942–51. doi: 10.1158/1535-7163.MCT-11-0563
172. Tanaka T, Nakatani T, Kamitani T. Inhibition of NEDD8-conjugation pathway by novel molecules: potential approaches to anticancer therapy. *Mol Oncol.* (2012) 6:267–75. doi: 10.1016/j.molonc.2012.01.003
173. Soucy TA, Dick LR, Smith PG, Milhollen MA, Brownell JE. The NEDD8 conjugation pathway and its relevance in cancer biology and therapy. *Genes Cancer.* (2010) 1:708–16. doi: 10.1177/1947601910382898
174. Powers MV, Workman P. Targeting of multiple signalling pathways by heat shock protein 90 molecular chaperone inhibitors. *Endocr Relat Cancer.* (2006) 13(Suppl. 1):S125–35. doi: 10.1677/erc.1.01324
175. Chiosis G, Rodina A, Moulick K. Emerging Hsp90 inhibitors: from discovery to clinic. *Anticancer Agents Med Chem.* (2006) 6:1–8. doi: 10.2174/187152006774755483
176. Pillai RN, Ramalingam SS. Heat shock protein 90 inhibitors in non-small-cell lung cancer. *Curr Opin Oncol.* (2014) 26:159–64. doi: 10.1097/CCO.0000000000000047
177. Lindquist SL, Kelly JW. Chemical and biological approaches for adapting proteostasis to ameliorate protein misfolding and aggregation diseases: progress and prognosis. *Cold Spring Harb Perspect Biol.* (2011) 3:a004507. doi: 10.1101/cshperspect.a004507
178. Tao YX, Conn PM. Pharmacoperones as novel therapeutics for diverse protein conformational diseases. *Physiol Rev.* (2018) 98:697–725. doi: 10.1152/physrev.00029.2016
179. Waza M, Adachi H, Katsuno M, Minamiyama M, Sang C, Tanaka F, et al. 17-AAG, an Hsp90 inhibitor, ameliorates polyglutamine-mediated motor neuron degeneration. *Nat Med.* (2005) 11:1088–95. doi: 10.1038/nm1298
180. Fujikake N, Nagai Y, Popiel HA, Okamoto Y, Yamaguchi M, Toda T. Heat shock transcription factor 1-activating compounds suppress polyglutamine-induced neurodegeneration through induction of multiple molecular chaperones. *J Biol Chem.* (2008) 283:26188–97. doi: 10.1074/jbc.M710521200
181. Lueck JD, Mankodi A, Swanson MS, Thornton CA, Dirksen RT. Muscle chloride channel dysfunction in two mouse models of myotonic dystrophy. *J Gen Physiol.* (2007) 129:79–94. doi: 10.1085/jgp.200609635
182. Charlet BN, Savkur RS, Singh G, Philips AV, Grice EA, Cooper TA. Loss of the muscle-specific chloride channel in type 1 myotonic dystrophy due to misregulated alternative splicing. *Mol Cell.* (2002) 10:45–53. doi: 10.1016/S1097-2765(02)00572-5
183. Cho DH, Tapscott SJ. Myotonic dystrophy: emerging mechanisms for DM1 and DM2. *Biochim Biophys Acta.* (2007) 1772:195–204. doi: 10.1016/j.bbadis.2006.05.013
184. Ursu SF, Alekov A, Mao NH, Jurkat-Rott K. ClC1 chloride channel in myotonic dystrophy type 2 and ClC1 splicing *in vitro*. *Acta Myol.* (2012) 31:144–53.
185. Wheeler TM, Lueck JD, Swanson MS, Dirksen RT, Thornton CA. Correction of ClC-1 splicing eliminates chloride channelopathy and myotonia in mouse models of myotonic dystrophy. *J Clin Invest.* (2007) 117:3952–7. doi: 10.1172/JCI33355
186. Cardani R, Giagnacovo M, Botta A, Rinaldi F, Morgante A, Udd B, et al. Co-segregation of DM2 with a recessive CLCN1 mutation in juvenile onset of myotonic dystrophy type 2. *J Neurol.* (2012) 259:2090–9. doi: 10.1007/s00415-012-6462-1
187. Suominen T, Schoser B, Raheem O, Auvinen S, Walter M, Krahe R, et al. High frequency of co-segregating CLCN1 mutations among myotonic dystrophy type 2 patients from Finland and Germany. *J Neurol.* (2008) 255:1731–6. doi: 10.1007/s00415-008-0010-z
188. Miranda DR, Wong M, Romer SH, McKee C, Garza-Vasquez G, Medina AC, et al. Progressive Cl- channel defects reveal disrupted skeletal muscle maturation in R6/2 Huntington's mice. *J Gen Physiol.* (2017) 149:55–74. doi: 10.1085/jgp.201611603
189. Waters CW, Varuzhanyan G, Talmadge RJ, Voss AA. Huntington disease skeletal muscle is hyperexcitable owing to chloride and potassium channel dysfunction. *Proc Natl Acad Sci USA.* (2013) 110:9160–5. doi: 10.1073/pnas.1220068110
190. du Souich P, Roederer G, Dufour R. Myotoxicity of statins: mechanism of action. *Pharmacol Ther.* (2017) 175:1–16. doi: 10.1016/j.pharmthera.2017.02.029
191. Camerino GM, Musumeci O, Conte E, Musaraj K, Fonzino A, Barca E, et al. Risk of myopathy in patients in therapy with statins: identification of biological markers in a pilot study. *Front Pharmacol.* (2017) 8:500. doi: 10.3389/fphar.2017.00500
192. Camerino GM, Bouche M, De Bellis M, Cannone M, Liantonio A, Musaraj K, et al. Protein kinase C theta (PKCtheta) modulates the ClC-1 chloride channel activity and skeletal muscle phenotype: a biophysical and gene expression study in mouse models lacking the PKCtheta. *Pflugers Arch.* (2014) 466:2215–28. doi: 10.1007/s00424-014-1495-1
193. Pierno S, Camerino GM, Cippone V, Rolland JF, Desaphy JF, De Luca A, et al. Statins and fenofibrate affect skeletal muscle chloride conductance in

rats by differently impairing ClC-1 channel regulation and expression. *Br J Pharmacol.* (2009) 156:1206–15. doi: 10.1111/j.1476-5381.2008.00079.x
194. Ito T, Ando H, Suzuki T, Ogura T, Hotta K, Imamura Y, et al. Identification of a primary target of thalidomide teratogenicity. *Science.* (2010) 327:1345–50. doi: 10.1126/science.1177319
195. Kronke J, Udeshi ND, Narla A, Grauman P, Hurst SN, McConkey M, et al. Lenalidomide causes selective degradation of IKZF1 and IKZF3 in multiple myeloma cells. *Science.* (2014) 343:301–5. doi: 10.1126/science.1244851
196. Lu G, Middleton RE, Sun H, Naniong M, Ott CJ, Mitsiades CS, et al. The myeloma drug lenalidomide promotes the cereblon-dependent destruction of Ikaros proteins. *Science.* (2014) 343:305–9. doi: 10.1126/science.1244917
197. Holstein SA, McCarthy PL. Immunomodulatory drugs in multiple myeloma: mechanisms of action and clinical experience. *Drugs.* (2017) 77:505–20. doi: 10.1007/s40265-017-0689-1
198. Kortum KM, Zhu YX, Shi CX, Jedlowski P, Stewart AK. Cereblon binding molecules in multiple myeloma. *Blood Rev.* (2015) 29:329–34. doi: 10.1016/j.blre.2015.03.003
199. Reece D, Kouroukis CT, Leblanc R, Sebag M, Song K, Ashkenas J. Practical approaches to the use of lenalidomide in multiple myeloma: a canadian consensus. *Adv Hematol.* (2012) 2012:621958. doi: 10.1155/2012/621958
200. Liu Y, Huang X, He X, Zhou Y, Jiang X, Chen-Kiang S, et al. A novel effect of thalidomide and its analogs: suppression of cereblon ubiquitination enhances ubiquitin ligase function. *FASEB J.* (2015) 29:4829–39. doi: 10.1096/fj.15-274050
201. Fischer ES, Bohm K, Lydeard JR, Yang H, Stadler MB, Cavadini S, et al. Structure of the DDB1-CRBN E3 ubiquitin ligase in complex with thalidomide. *Nature.* (2014) 512:49–53. doi: 10.1038/nature 13527
202. Thomassen M, Hostrup M, Murphy RM, Cromer BA, Skovgaard C, Gunnarsson TP, et al. Abundance of ClC-1 chloride channel in human skeletal muscle: fiber type specific differences and effect of training. *J Appl Physiol.* (2018) 125:470–8. doi: 10.1152/japplphysiol.01042.2017

Conflict of Interest: The authors declare that the research was conducted in the absence of any commercial or financial relationships that could be construed as a potential conflict of interest.

Copyright © 2020 Jeng, Fu, You, Peng, Hsiao, Chen and Tang. This is an open-access article distributed under the terms of the Creative Commons Attribution License (CC BY). The use, distribution or reproduction in other forums is permitted, provided the original author(s) and the copyright owner(s) are credited and that the original publication in this journal is cited, in accordance with accepted academic practice. No use, distribution or reproduction is permitted which does not comply with these terms.

frontiers in Neurology

ORIGINAL RESEARCH
published: 13 February 2020
doi: 10.3389/fneur.2020.00077

Myotonic Myopathy With Secondary Joint and Skeletal Anomalies From the c.2386C>G, p.L796V Mutation in *SCN4A*

Nathaniel Elia[1,2], *Trystan Nault*[3], *Hugh J. McMillan*[3], *Gail E. Graham*[4], *Lijia Huang*[4] and *Stephen C. Cannon*[1]*

[1] Department of Physiology, David Geffen School of Medicine at UCLA, Los Angeles, CA, United States, [2] Molecular, Cellular, and Integrative Physiology Program, UCLA, Los Angeles, CA, United States, [3] Division of Neurology, Children's Hospital of Eastern Ontario, University of Ottawa, Ottawa, ON, Canada, [4] Department of Genetics, Children's Hospital of Eastern Ontario, University of Ottawa, Ottawa, ON, Canada

The phenotypic spectrum associated with the skeletal muscle voltage-gated sodium channel gene (*SCN4A*) has expanded with advancements in genetic testing. Autosomal dominant *SCN4A* mutations were first linked to hyperkalemic periodic paralysis, then subsequently included paramyotonia congenita, several variants of myotonia, and finally hypokalemic periodic paralysis. Biallelic recessive mutations were later identified in myasthenic myopathy and in infants showing a severe congenital myopathy with hypotonia. We report a patient with a pathogenic *de novo SCN4A* variant, c.2386C>G p.L796V at a highly conserved leucine. The phenotype was manifest at birth with arthrogryposis multiplex congenita, severe episodes of bronchospasm that responded immediately to carbamazepine therapy, and electromyographic evidence of widespread myotonia. Another *de novo* case of p.L796V has been reported with hip dysplasia, scoliosis, myopathy, and later paramyotonia. Expression studies of L796V mutant channels showed predominantly gain-of-function changes, that included defects of slow inactivation. Computer simulations of muscle excitability reveal a strong predisposition to myotonia with exceptionally prolonged bursts of discharges, when the L796V defects are included. We propose L796V is a pathogenic variant, that along with other cases in the literature, defines a new dominant *SCN4A* disorder of myotonic myopathy with secondary congenital joint and skeletal involvement.

Keywords: skeletal muscle, channelopathy, sodium channel, $Na_V1.4$, myotonia, voltage-clamp

OPEN ACCESS

Edited by:
Emma Matthews, Institute of Neurology, University College London, United Kingdom

Reviewed by:
Elena Maria Pennisi, Ospedale San Filippo Neri, Italy
Gabriella Silvestri, Catholic University of the Sacred Heart, Italy

***Correspondence:**
Stephen C. Cannon
sccannon@mednet.ucla.edu

Specialty section:
This article was submitted to Neuromuscular Diseases, a section of the journal Frontiers in Neurology

Received: *05 December 2019*
Accepted: *22 January 2020*
Published: *13 February 2020*

Citation:
Elia N, Nault T, McMillan HJ, Graham GE, Huang L and Cannon SC (2020) Myotonic Myopathy With Secondary Joint and Skeletal Anomalies From the c.2386C>G, p.L796V Mutation in SCN4A. Front. Neurol. 11:77. doi: 10.3389/fneur.2020.00077

INTRODUCTION

Sodium channels are required for action potential generation and propagation. The sodium channel alpha-subunit gene (*SCN4A*) encodes the isoform $Na_V1.4$ which is the most abundant isoform in skeletal muscle.

Mutations affecting one *SCN4A* allele are often associated with a gain-of-function resulting in muscle stiffness (myotonia) that may worsen with repeated contraction (paramyotonia) as well as episodes of hyperkalemic periodic paralysis (1). Phenotypic variability has been reported among family members regarding the age of onset and clinical severity of myotonia (2). Another

class of heterozygous *SCN4A* mutations allow an anomalous leakage of ions through the voltage sensor of the channel, distinct from the sodium-conducting pore, and cause hypokalemic periodic paralysis (3).

With increased accessibility to genetic testing, the phenotypic spectrum of *SCN4A* mutations has been expanding. We now recognize *SCN4A* mutations to cause isolated exercise- or cold-induced myalgia (4). *De novo* heterozygous *SCN4A* mutations, often at p.Gly1306Glu, have been linked to a severe neonatal phenotype with episodic laryngospasm (5–8), stridor (9), or in other cases with apneic episodes (10).

More recently, biallelic mutations in *SCN4A* have been reported in congenital myasthenic syndromes (11–13), at times with myopathy (14), and in severe congenital myopathy with fetal hypokinesia (15). All these syndromes have recessive inheritance, with a single loss-of-function allele being asymptomatic, including even a functional null from a premature stop. Moderate loss-of-function mutations from enhanced inactivation are associated with congenital myasthenia (11), whereas biallelic mutations that include a single null cause congenital myopathy with fetal hypokinesia and biallelic null mutations are embryonic or neonatal lethal (15).

We report a patient who presented with arthrogryposis multiplex congenita, congenital myopathy, and episodes of bronchospasm who has the c.2386C>G, p.L796V variant in *SCN4A*. Expression studies of L796V channels revealed a two forms of gain-of-function, enhanced activation and impaired slow inactivation, and which in model simulations led to prolonged bursts of myotonic discharges. We propose L796V is a pathogenic mutation and that the clinical features shared with previously described cases defines a new *SCN4A* syndrome of myotonic myopathy with secondary deformities of joints and bone.

METHODS AND MATERIALS

Sodium Channel Currents

Sodium currents were measured from fibroblasts (HEK cells) transiently transfected with plasmids encoding the wild type (WT) or mutant L796V human $Na_V1.4$ α subunit and the β1 accessory subunit as previously described (16). Currents were recorded in whole-cell mode with a patch electrode that contained in mM: 100 CsF, 35 NaCl, 5 EGTA, 10 HEPES, pH to 7.3 with CsOH. The extracellular bath contained in mM: 140 NaCl, 4 KCl, 2 $CaCl_2$, 1 $MgCl_2$, 2.5 glucose, 10 HEPES, pH to 7.3 with NaOH. Cells with maximal peak Na^+ currents <1 nA were excluded to minimize the contribution from endogenous Na^+ currents (typically < 0.1 nA), and cells with peak Na^+ currents >5 nA were excluded to avoid series resistance errors.

The voltage-dependent activation of sodium currents was quantified by fitting the peak amplitude (I_{peak}) to a linear conductance ($G_{\max}$) with a reversal potential (E_{rev}) that was scaled with a Boltzmann function: $I_{peak} = G_{\max}(V - E_{rev})/(1 + e^{-(V - V_{1/2})/K})$. The voltage-dependence for activation of the channel is reflected by $V_{1/2}$, the voltage at which half the channels are activated, and K a steepness factor. The voltage dependence of the relative conductance (see **Figure 1D**) was calculated as I_{peak} divided by $G_{\max}(V - E_{rev})$. The time constant, τ, for entry to inactivation was estimated from a single exponential fit of the current decay (fast inactivation) or of the change in peak current after progressively longer conditioning pulses (slow inactivation). The voltage dependence of steady-state fast inactivation was quantified by fitting the relative peak current after a 300 ms conditioning pulse at a voltage of V_{cond} by a Boltzmann function $I_{peak}(V_{cond})/I_{peak\,\max} = 1/(1 + e^{(V - V_{1/2})/K})$. For the steady-state voltage dependence of slow inactivation, a plateau term (S_0) was included because slow inactivation does not reduce channel availability to 0 at strongly depolarized potentials (**Figure 3D**). Estimated values for parameters are presented as mean ± SEM.

Simulated Muscle Action Potentials

The functional consequences of altered sodium currents observed for the L796V mutant channels on muscle excitability were explored using computer simulation. The two-compartment model of a muscle fiber [modified from (17)] consisted of the plasma membrane (sarcolemma) and the transverse tubular membrane, each of which contained voltage-dependent conductances to simulate sodium channels, chloride channels, inward-rectifying potassium channels, and delayed-rectifier potassium channels. Mutant L796V channels were simulated by modifying the parameter values so that the currents predicted by a Hodgkin-Huxley model matched the currents we measured in the HEK cell expression system (see **Supplementary Material** for details).

RESULTS

Clinical Presentation and Genetic Analysis

A 7 year old boy of Morrocan descent was the first child to healthy, non-consanguineous parents. Routine antenatal ultrasounds at 13, 21, and 30 weeks gestation revealed normal fetal anatomy and amniotic fluid levels. Good fetal movements were reported throughout gestation. Repeat ultrasound at 41 weeks showed decreased amniotic fluid levels prompting a planned Caesarian section. Apgar scores were 1 at 1 min, 5 at 5 min, and 7 at 10 min. Although no chest compressions were required, he was intubated at birth and empiric surfactant was administered. His birth weight was 2,995 g (3–10%ile) and head circumference 36.0 cm (50%ile). He was noted to have facial weakness and arthrogryposis multiplex congenita with extensive bilateral contractures at the elbows, wrists, fingers, hips, knees and ankles. He did demonstrate antigravity movements of his arms and legs. Nerve conduction studies at 2 weeks of age revealed normal median and medial plantar nerve sensory responses. Median and tibial motor responses revealed abnormally low compound motor action potential (CMAP) amplitude. Needle EMG of his biceps, vastus lateralis, gastrocnemius and abductor hallicus revealed increased insertional activity (**Supplementary Video 1**).

Beginning at 2 weeks old, he began having episodes of bronchospasm associated with cessation of chest movement and desaturation. Episodes lasted for 30 s to 2 min and showed minimal response to supplemental oxygen and positive pressure

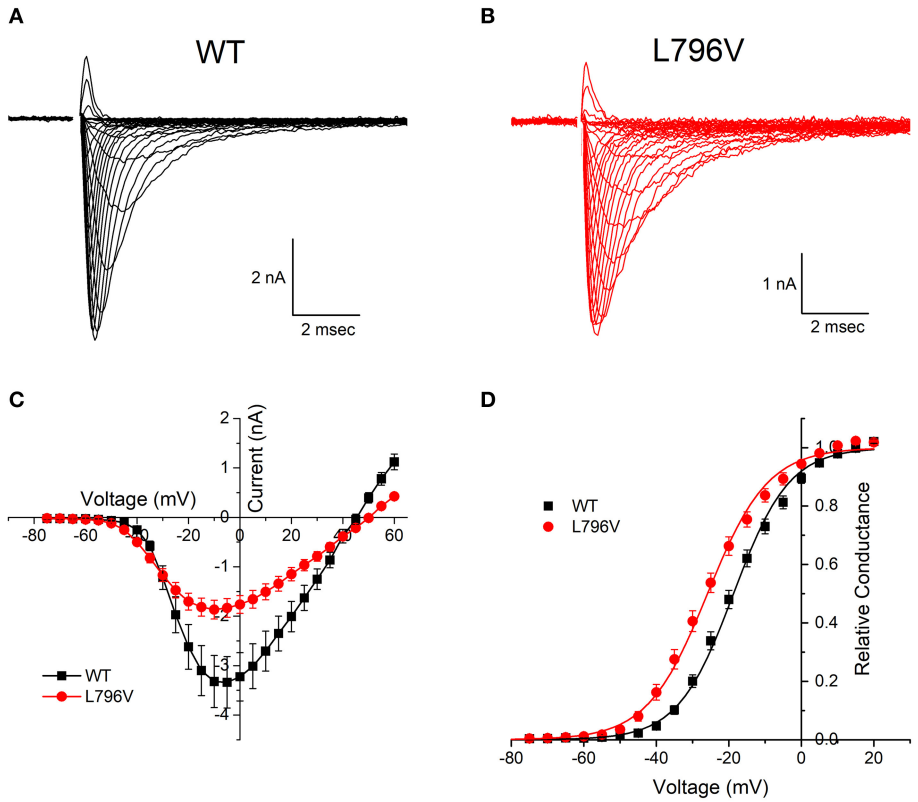

FIGURE 1 | Activation of L796V channels is shifted toward more negative potentials. Sodium currents were recorded from HEK cells expressing WT **(A)** and L796V **(B)** channels. Superimposed traces show currents elicited by depolarization to test potentials of −75 to +60 mV from a holding potential of −120 mV. **(C)** Peak sodium current is shown as a function of test potential and reveals a reduced amplitude for L796V compared to WT. **(D)** Transforming the peak current to relative conductance (see Methods and Materials) shows a 7.2 mV hyperpolarized shift for L796V channels. Symbols show means from $n = 16$ (WT) or $n = 10$ (L796V) cells.

ventilation. Video EEG was unremarkable with no epileptiform activity noted at the time of clinical events.

MRI brain, echocardiogram, serum creatine kinase, and quadriceps muscle biopsy were unremarkable. Repeat EMG of the deltoid, first dorsal interosseous and tibialis anterior at 6 weeks of age again revealed increased insertional activity; however, there were long runs of myotonic discharges with typical waxing and waning variation in frequency and amplitude (**Supplementary Video 2**) that were not seen on the earlier study.

Although the bronchospasm did not show any appreciable response to phenobarbital, it abruptly stopped with empiric carbamazepine 20 mg/kg/day. He remains on carbamazepine. At 5 years of age he has reported some cold-induced episodes of eyelid and facial muscle paramyotonia but no episodes of periodic paralysis.

The patient's medical history was also relevant for severe gastroesophageal reflux due to a sliding hiatus hernia. He required a fundoplication and gastro-jejunostomy (GJ) tube placement (removed at 4 years old). He had strabismus which required surgical correction at 16 months of age. He had bilateral cryptorchidism requiring orchidopexy. He required multiple orthopedic surgeries including bilateral ankle casting and eventual contracture release (at 15 months); treatment of the developmental dysplasia of the left hip with open reduction (at 3 years).

His language development has progressed normally. He is fluent in three languages and requires no modification to his academic curriculum. Gross motor development was significantly delayed; he rolled independently at 6 months and sat independently at 18 months. At 2–1/2 years he was able to walk using a walker. At 3–1/2 years he was able to rise and walk independently.

Array CGH and molecular testing for myotonic dystrophy type 1 were normal. HSPG2 gene sequencing revealed that the patient was heterozygous for a G>A transition in a highly conserved residue (nucleotide 4877, exon 39) (seen in 0.8% of the population) that had not been reported as either a mutation or a polymorphism. MLPA testing revealed no deletion or duplication affecting the other allele and immunohistochemical staining for perlecan on frozen muscle from prior biopsy was normal. LIFR sequencing and deletion-duplication analysis was normal. Collectively, these genetic and histochemical findings do not support a diagnosis of Schwartz-Jampel syndrome. Exome sequencing, performed as part of the Canada-wide Care4Rare research consortium identified a likely pathogenic variant in one *SCN4A* allele that was confirmed with Sanger sequencing:

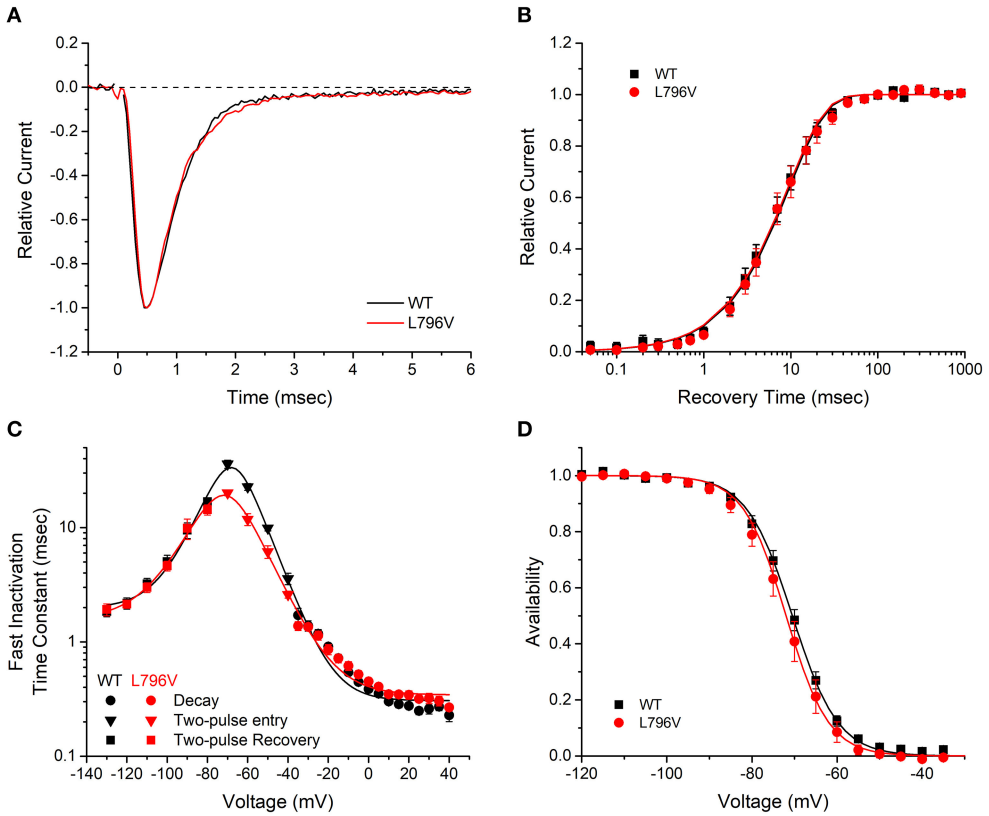

FIGURE 2 | Fast inactivation is not affected by the L796V mutation. **(A)** Sodium current decay kinetics are indistinguishable for WT and L796V channels. Representative current traces elicited at −10 mV have been normalized by peak amplitude. **(B)** Recovery from fast inactivation is identical for WT and L796V channels. Data show the time course for the recovery of peak current amplitude at a holding potential of −90 mV, after channels were inactivated with a conditioning pulse of 30 ms at −10 mV. Symbols show means for WT ($n = 8$) and L796V ($n = 5$). **(C)** Summary plot of the time constants for entry or recovery from fast inactivation shows identical kinetics for WT and L796V channels. Three separate protocols were used to measure inactivation kinetics, depending on the voltage range, as described in section Methods and Materials. Symbols show means from WT ($n = 16$) and L796V ($n = 10$). **(D)** The steady-state voltage dependence of fast inactivation was indistinguishable for WT ($n = 15$) and L796V ($n = 10$) channels. Plot shows relative amplitude for the peak sodium current elicited by a depolarization to −10 mV after a 300 ms conditioning pulse at the indicated voltage (abscissa).

SCN4A: NM_000334: c.2386C>G, p.Leu796Val. It was not present in either parent.

Functional Characterization of L796V Mutant Sodium Channels

Activation of L796V Channels Was Shifted to More Negative Potentials

Both wild type (WT) and L796V mutant sodium channels were expressed in the plasma membrane of transiently transfected fibroblasts (HEK cells), as shown in **Figure 1** by the sodium currents recorded in whole-cell voltage clamp. A plot of the peak sodium current as a function of membrane voltage (**Figure 1C**) shows the current amplitude was lower for cells expressing L796V compared to WT (−2.07 ± 0.19 and −3.32 ± 0.53 nA, respectively). A more accurate comparison of expression level is obtained from the maximum conductance, G_{max}, which is reflected by the slope of the current-voltage relation at voltages > 20 mV. On average, the G_{max} was 50% lower for cells expressing L796V than WT channels (37.4 ± 3.5 and 76.4 ± 10 nS, respectively, $p < 0.05$).

The voltage-dependence of activation is illustrated more clearly by transforming the peak current amplitude to relative conductance as a function of test potential (see section Methods and Materials), as shown in **Figure 1D**. The midpoint of the relative conductance curve, $V_{1/2}$, was shifted toward more negative potentials by −7.2 mV L796V channels (−25.9 ± 1.3 mV, $n = 10$) compared to WT channels (−18.7 ± 1.1 mV, $n = 16$; $p < 0.001$). The voltage dependence was slightly less steep for L796V channels (8.32 ± 0.20 mV) compared to WT (7.31 ± 0.22), but these values were not statistically different at the 0.05 level.

Fast Inactivation Was Not Altered by the L706V Mutation

Several voltage-pulse protocols were used to characterize the kinetics and steady-state voltage dependence of sodium channel fast inactivation. The time constant of the sodium current decay after the early peak provides a quantitative measure of channel fast inactivation from the open state. Superposition

of amplitude-normalized current traces (**Figure 2A**) shows the fast inactivation time course was indistinguishable between WT and L796V channels, and the values of the time constants over the measurable range from −35 to + 40 mV were overlapping (**Figure 2C**, circles). Recovery from fast inactivation was measured in a two-pulse protocol. First, channels were fast inactivated by a 30 ms conditioning pulse to −10 mV, then after a variable recovery interval at a hyperpolarized potential, the amount of recovery was measured as the relative current elicited by a test pulse to −10 mV. The time course of recovery at −90 mV was indistinguishable for WT and L796V channels (**Figure 2B**), and the time constant for recovery was identical over the measured range from −130 to −80 mV (**Figure 2C**, squares). The kinetics of entry to fast inactivation from closed states was measured in a two-pulse protocol for which a variable duration conditioning pulse was applied to partially inactivate channels (without opening), and then a test pulse to −10 mV was applied to measure the relative current. The time constant for the onset of close-state fast inactivation was modestly smaller for L796V over the voltage range from −70 to −50 mV (**Figure 2C**, inverted triangles). This difference is not predicted to be biologically significant, because the more rapid kinetics of entry to inactivation at the peak of the action potential (0–20 mV) and the rapid recovery at the resting potential (−80 to −95 mV) will dominate the kinetics of fast inactivation in muscle fibers. The voltage dependence of steady-state fast inactivation was measured as the relative peak current elicited at −10 mV, after a 300 ms conditioning pulse to potentials over a range from −120 to −40 mV. The data were indistinguishable for WT and L796V channels (**Figure 2D**), as confirmed by the parameter estimates from fits to a Boltzmann function ($V_{1/2}$ −70.5 ± 0.91 mV $n = 15$, −72.0 ± 1.5 mV $n = 10$ for WT and L796V, respectively; K 5.37 ± 0.56 mV, 5.02 ± 0.40 mV for WT and L796V, respectively).

Slow Inactivation Was Impaired by L796V

Slow inactivation of sodium channels occurs on a time scale of seconds, compared to the millisecond range for fast inactivation. Depolarization promotes both forms of inactivation, and the slow inactivated component is experimentally resolved by measuring the proportion of current that fails to recover during a brief hyperpolarization (−120 mV for 20 ms). The time course for the onset of slow inactivation is shown in **Figure 3A**, in which repeated trials with a progressively longer duration conditioning pulse to −50 mV have been applied and the relative current decreased as a greater proportion of channels became slow inactivated. The time constant of this exponential decay is shown for various test potentials from −50 to −10 mV in **Figure 3C** (inverted triangles). The time constant decreases (faster entry rate) at more positive potentials for WT channels, whereas the time constant is voltage independent and small for L796V channels.

The time course for recovery from slow inactivation at hyperpolarized potentials was measured by monitoring the recovery of peak sodium current after a 30 s conditioning pulse to −10 mV to maximally slow inactivate channels. Recovery at −80 mV is shown in **Figure 3B**. Fewer L796V channels are slow inactivated at the beginning of the recovery period (25% current already recovered at 0.020 s compared to 10% for WT) and the time course of recovery of L796V is more rapid than for WT (left shift of recovery curve). The recovery time constant measured over a voltage range from −80 to −120 mV was independent of voltage for L796V channels (**Figure 3C**, upright red triangles), whereas for WT channels the time constant decreased (faster recovery) with hyperpolarization (**Figure 3C**, upright black triangles).

The voltage dependence of steady-state slow inactivation was measured as the loss of current availability (i.e., decreased peak current amplitude) measured after a 30 s conditioning pulse (**Figure 3D**). The maximal extent of slow inactivation was reduced for L796V channels, as shown by the higher amplitude plateau in the availability curve at voltages more positive than −20 mV. The fitted parameter estimates for the plateau were S_0 0.11 ± 0.07, $n = 5$; 0.23 ± 0.02, $n = 5$ for WT and L796V, respectively ($p = 0.01$). In addition, the steepness of the voltage dependence was reduced for L796V channels (K 10.7 ± 1.0 mV, $n = 5$ for WT; 13.9 ± 0.4 mV, $n = 5$ for L796V, $p < 0.01$). There was a trend for a hyperpolarized shift in the midpoint for the voltage dependence of slow inactivation for L796V, but this difference was not distinguishable statistically ($V_{1/2}$ −59.1 ± 1.9 mV, $n = 5$ for WT; −67.0 ± 3.4 mV, $n = 5$ for L796V, $p = 0.11$).

At first glance, the changes in slow inactivation properties for L796V channels appear to be a mixture of gain and loss of function effects. Enhancement of slow inactivation is expected at the resting potential of −80 mV because of the reduced slope of the voltage dependence and the tendency for a left shift (**Figure 3D**, reduced availability at −80 mV), as well as for a faster rate of entry over the voltage range of −50 to −30 mV (**Figure 3C**, smaller time constants). On the other hand, impairment of slow inactivation is expected at depolarized potentials because inactivation of L796V is less complete than WT (**Figure 3D**, higher plateau −20 to 20 mV), and the recovery from slow inactivation is faster for L796V at the resting potential (**Figure 3C**, smaller time constant at −80 mV). We propose the overall effect will be impaired slow inactivation for L796V channels, in the context of the slow inactivation that occurs during sustained bursts of action potentials (e.g., myotonia). The basis for this prediction is that entry to slow inactivation occurs primarily at voltages near the peak depolarization of the action potential (where the predominant change is less complete slow inaction for L796V) and trapping of channels in the slow inactivated state is primarily dependent on the rate of recovery at the resting potential of −80 mV (which is faster for L796V channels). This prediction is supported by experimental evidence showing the use-dependent reduction of sodium current is more pronounced for WT than L796V channels during repetitive stimulation at 50 Hz. **Figure 4A** shows a superposition of sodium currents recorded in response to the first 10 pulses to +10 mV from a holding potential of −80 mV. The initial decline in peak amplitude from the first to the second pulse is predominantly caused by incomplete recovery from fast inactivation, whereas the subsequent decline for additional pulses is due to progressive loss of channel availability from slow inactivation. The slow inactivation effect is illustrated in **Figure 4B** for the entire 40 second train of 3 ms depolarizations at 50 Hz (2,000 pulses). The

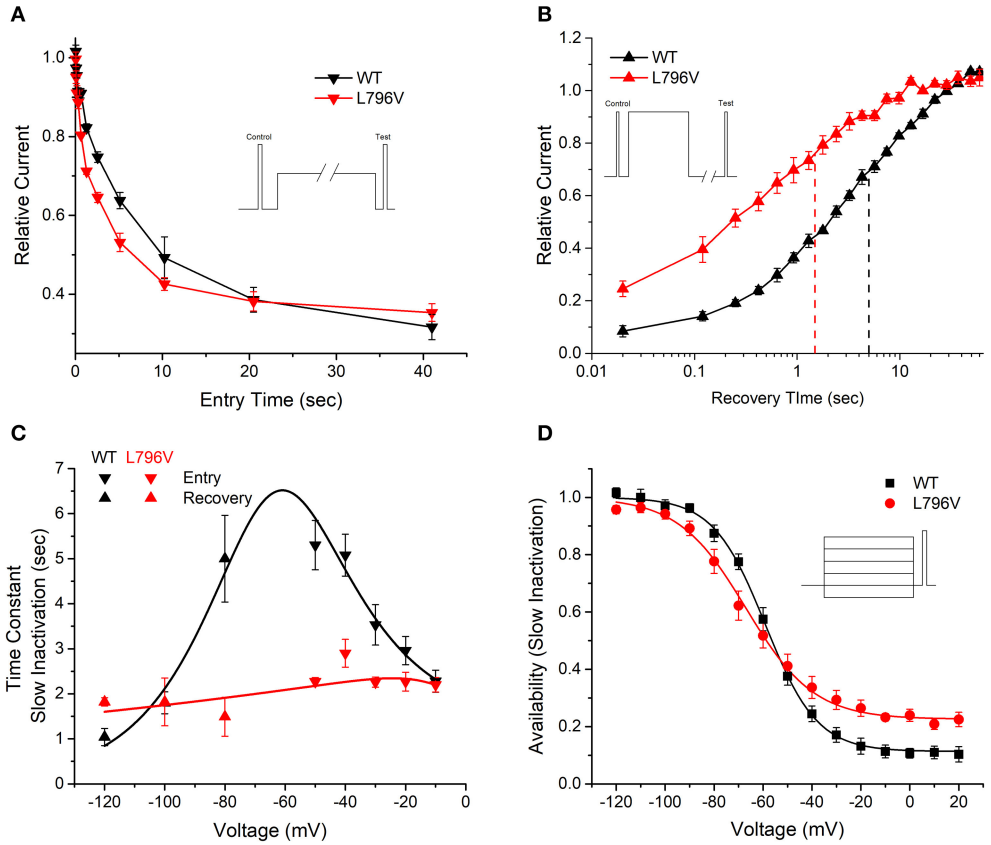

FIGURE 3 | Slow inactivation is altered by the L796V mutation. **(A)** A two-pulse protocol with a variable duration condition pulse to −50 mV (inset) shows accelerated onset of slow inactivation for L796V channels. Symbols show means for WT ($n = 5$) and L796V ($n = 3$) channels. **(B)** Recovery from slow inactivation at −80 mV is accelerated four-fold for L796V compared to WT channels. Channels were slow inactivated with a 30 s conditioning pulse to −10 mV (inset), and then recovery from slow inactivation was measured as the relative peak current elicited by a brief pulse to −10 mV, after variable period of recovery at −80 mV. Symbols show means for WT ($n = 5$) and L796V ($n = 4$). **(C)** Summary plot for the kinetics of slow inactivation entry and recovery shows a nearly voltage-independent time constant for L796V mutant channels. Symbols show means for WT ($n = 5$) and L796V ($n = 4$) channels. **(D)** Steady-state voltage dependence of slow inactivation shows a decreased slope (−100 to −40 mV range) and less complete slow inactivation (higher plateau at **–**20 to +20 mV) for L796V ($n = 5$) compared to WT ($n = 5$) channels.

peak amplitude for each pulse is normalized by the amplitude of the second pulse (**Figure 4A**, blue trace) to isolate the effect of slow inactivation, which under these conditions is about 10% less for L796V channels compared to WT.

Functional Defects of L796V Mutant Channels Cause Myotonia in a Simulated Muscle Fiber

The functional consequences of the defects in activation and in slow inactivation for L796V mutant channels were explored in a computational model of a muscle fiber (see **Supplementary Material** for details). For a simulated fiber with WT sodium channels, the resting potential was −90.3 mV and the voltage threshold to elicit an action potential was −66 mV. Susceptibility to myotonic discharges was tested by simulated injection of a 100 ms depolarizing current pulse (20 $\mu A/cm^2$). A single action potential was elicited in a simulated WT fiber (**Figure 5A**), followed by a small depolarization to about −80 mV that decayed back to the normal resting potential at the end of the current injection.

The model for the patient's muscle contained 50% WT sodium channels and 50% with L796V properties to emulate the heterozygous state. The derangements in the L796V channels were simulated as shown by the fitted curves in **Figures 2–4** (see **Supplementary Material** for details). The predominant changes for L796V mutant channels were reduced conductance, −7.2 mV left shift of activation, and altered slow inactivation (faster kinetics, reduced voltage dependence, and less complete). The resting potential was modestly depolarized in the simulated patient muscle (−86.0 mV), and more importantly the voltage threshold for an action potential was markedly hyperpolarized at a value of −79 mV. These effects are caused by the left shift in the voltage dependence of activation for L796V channels. The same 100 ms depolarizing current injection now elicited repetitive discharges that persisted beyond the duration of the stimulus (**Figure 5B**). The "after-discharges" are triggered by the small depolarization produced from the use-dependent accumulation of K^+ in the T-tubules. Each action potential produces an efflux of K^+ into the T-tubules, and the restricted diffusion of

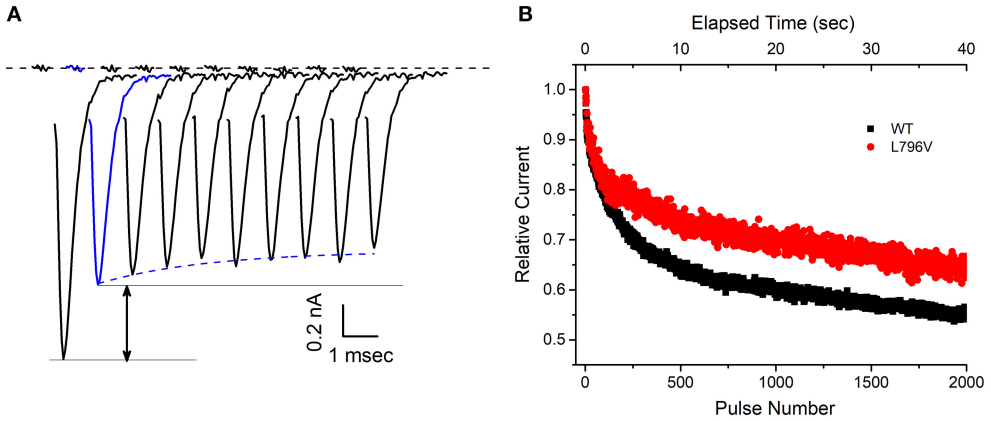

FIGURE 4 | The decline of sodium current peak amplitudes during a 50 Hz train of pulses is less pronounced for L796V channels, thereby showing a gain-of-function change caused by altered slow inactivation. **(A)** Exemplary WT sodium currents elicited by the first 10 pulses in a 50 Hz train of 3 ms depolarizations to −10 mV are shifted in time and superimposed to illustrate the decline in peak amplitude. The holding potential between pulses was −80 mV. The large decline between the first and second pulse (black arrow) reflects trapping of channels in the fast-inactivated state. The subsequent decline starting from the second pulse (blue) is caused by loss of channels successively trapped in the slow-inactivated state. **(B)** The decline in peak sodium current during a prolonged 50 Hz train of 3 ms pulses is attenuated for L796V channels. Points show mean relative current for WT ($n = 7$) and L796V ($n = 3$) channels, as defined by normalization to the peak amplitude of the sodium current elicited by the second pulse (blue).

these long narrow tubules results in an increase in extracellular $[K^+]$ and membrane depolarization. Normally, this small depolarization of only a few mV is insufficient to elicit action potentials, but with the left-shifted activation of L796V channels, the threshold is lower and self-sustained bursts of myotonic discharges occur.

Amongst the sodium channel gain-of-function defects known to cause myotonia, a left shift of activation is especially potent (e.g., compared to the more common cause from a slower rate of inactivation) because of the effect on action potential threshold (18, 19). Consequently, the trains of discharges tend to be very prolonged, lasting more than 10 s (**Figure 5C**). The mechanism by which a myotonic burst ends is not completely understood, and likely depends on several events. One proposal is that use-dependent reduction of sodium channel availability, caused by the normal trapping of channels in the slow inactivated state, reduces fiber excitability and thereby terminates the myotonic burst (20). This mechanism is impaired for L796V mutant channels because the recovery from slow inactivation is accelerated at the resting potential (**Figure 4B**), and the prediction is that myotonic bursts may be exceptionally prolonged. We demonstrate this effect by modifying the simulated L796V channels to include all the anomalies detected in the voltage-clamp experiments, except the kinetics of slow inactivation retained WT behavior (i.e., 3 times slower at the resting potential). Simulated muscle with this hypothetical mutant sodium channel still exhibited myotonic discharges (**Figure 5D**), because of the left shift of activation, but the duration of the myotonic burst was shortened. This simulation demonstrates how the addition of a slow inactivation defect can exacerbate the severity of myotonia, which heretofore has been attributed gain-of-function defects in fast gating mechanisms alone (activation and fast inactivation).

DISCUSSION

We report a patient with a *de novo* heterozygous *SCN4A* variant c.2386C>G; p.L796V who had congenital anomalies and early-onset myotonia. This same variant was recently been reported in a patient with multiple congenital anomalies including hip dysplasia, scoliosis, and myopathic features who developed myotonia and episodic weakness in adolescence (21). Several criteria support the assignment of pathogenic mutation to L796V. From a genetic perspective, this *de novo* heterozygous *SCN4A* allele arose independently in two families with the probands having severe myotonic syndromes with overlapping features, and the variant was not in unaffected family members or in public databases (gnomAD_v2.1.1 or ExAC, although the Moroccan population may be under represented). The L796V missense mutation is located in a functionally important transmembrane segment (S6 of domain I) that contributes to the inner vestibule of the ion-conducting pore (22). Residue L796 is highly conserved amongst human $Na_V1.x$ isoforms and across species. Moreover, a site three residues downstream, and therefore on the same face of the S6 helix, is an established mutation (A799S) with gain-of-function changes (23) that causes a severe myotonic phenotype with episodic laryngospasm (5). Finally, our expression studies revealed gain-of-function defects for L796V with enhanced activation and impaired slow inactivation.

The congenital onset, with secondary joint and skeletal anomalies, was notable in both L796V patients. Our patient had arthrogryposis multiplex, with the other reported L796V case having hip dysplasia and scoliosis (21). The etiology of these skeletal deformities remains to be established. In our patient, sonographic evidence of oligohydramnios was present just prior to delivery, but three prior ultrasounds (as late

as 30 weeks gestation) revealed normal amniotic fluid levels. One possibility is a contribution from reduced mobility *in utero* caused by myotonia. Both L796V patients had early-onset severe myotonia, and our patient required pharmacologic intervention with sodium channel blockers to alleviate neonatal breathing difficulties. The propensity for exceptionally long-duration myotonic discharges in our model simulation with the L796V functional defects (**Figure 5**) may predispose to secondary joint defects. A monoallelic variant of HSPG2 was identified in our patient, and while we cannot exclude the possibility of a modifier effect that exacerbates myotonia from the sodium channel L796V defect, we think this is unlikely for several reasons. First, perlecan staining was normal. Second, the needle EMG at 6 weeks of age (**Supplementary Video 2**) showed classical myotonic runs that waxed and waned in frequency and amplitude. Conversely, in the Schwartz-Jampel syndrome (SJS) with proven biallelic mutations of HSPG2 the needle EMG shows complex repetitive discharges of constant amplitude and frequency, with abrupt discontinuation of the burst (24). These discharges in SJS are attributed to peripheral nerve hyperexcitability, rather than myotonia from altered sarcolemmal excitability. Third, our model simulations show

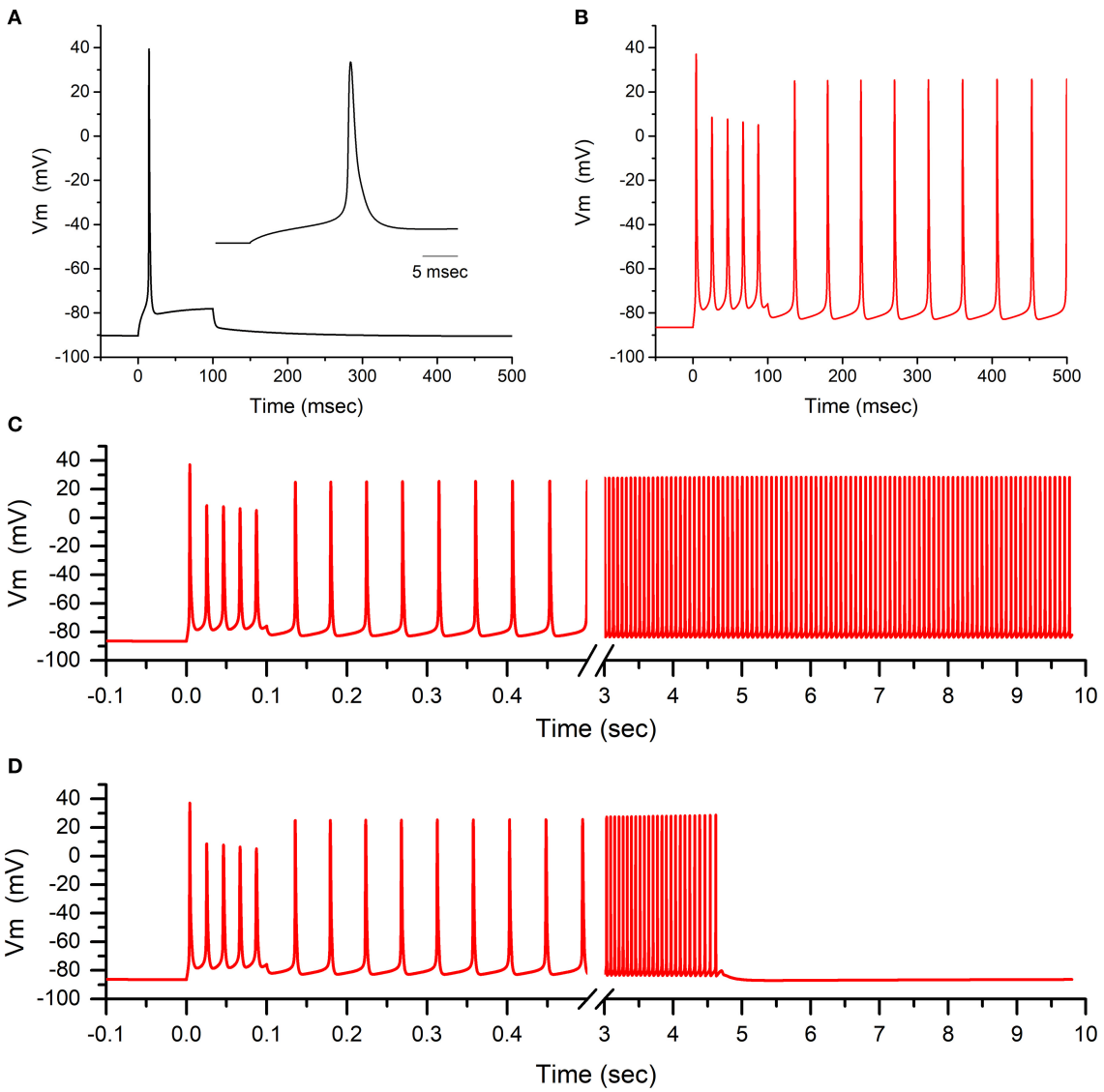

FIGURE 5 | Model simulation predicts sustained busts of myotonia from the L796V channel defects. **(A)** The action potential elicited by a 20 μA/cm^2 current pulse applied for 100 ms is shown for a simulated muscle fiber with normal values for voltage-activated ion channels. Inset shows the initial 25 ms of the model simulation. **(B)** When 50% of the simulated sodium channels are modeled using parameters to emulate the altered behavior of L796V channels, then the same 100 ms current stimulus triggers a burst of myotonic discharges that persist beyond the 100 ms duration of the stimulus. **(C)** Extended simulation over time shows stable self-sustained repetitive myotonic discharges that do not cease. **(D)** When the simulated mutant channels are modified to have the slow inactivation kinetics for WT channels, then use-dependent reduction of the sodium current is enhanced (see this figure) and the myotonic burst ends after 4.5 s.

the functional defect of L796V alone is sufficient to cause exceptionally prolonged myotonic bursts. Congenital joint and bone deformities are not a frequent accompaniment of congenital myotonia, but have been reported. Club foot with peripheral contractures, hip dislocation, and facial dysmorphism were reported for a newborn with diffuse muscle stiffness and widespread myotonic discharges who later developed muscle hypertrophy and was found to be heterozygous for *SCN4A* c.3539A>T; p.N1180I (25). Severe scoliosis with peripheral contractures in childhood was described for siblings with myotonic stiffness, profuse myotonic discharges, and the *SCN4A* p.P1158A mutation (26), but no details were provided about the clinical presentation at birth.

Congenital myopathy was a feature of the prior report for L796V, as manifest by polyhydramnios, fetal hypokinesia, hip dysplasia, and later progression to include high arched palate and elongated face (21). A muscle biopsy at age 27 had myopathic features with type I fiber predominance and hypertrophy. The other case of congenital myotonia with joint abnormalities (*SCN4A* p.N1180I) also had signs of neonatal myopathic weakness with polyhydramnios, high arched palate, and downslanting palpebral fissures (25). These cases are distinctly different, however, from the recently described syndrome of congenital myopathy with severe fetal hypokinesia caused by biallelic mutations for *SCN4A* (15, 27). In this latter syndrome, the core phenotype includes neonatal hypotonia, moderate to severe myopathic weakness that may be fatal, and *SCN4A* loss-of-function mutations that are asymptomatic in heterozygous parents. In contrast, the heterozygous p.L796V patients and the p.N1108I case had neonatal myotonic stiffness, only mild myopathic weakness that subsequently improved and in some progressed to muscle hypertrophy, and for p.L796V, experimentally established gain-of-function defects. Electromyographic evidence of myotonia in early infancy, as we observed at 6 weeks, is unusual and differentiates the weakness in our patient from the syndrome of congenital myopathy with hypotonia associated with recessive loss-of-function mutations of *SCN4A* (15). Myopathic features may be a component of the dominantly inherited *SCN4A* myotonic syndromes (sodium-channel myotonia, myotonia permanens, severe neonatal episodic laryngospasm, SNEL) or the late permanent muscle weakness of periodic paralysis. In our view, however, neither a single allelic variant of *SCN4A* nor a dominant inheritance pattern has been associated with a syndrome for which congenital myopathy is the predominant feature.

We propose a new *SCN4A* syndrome, myotonic myopathy with secondary joint and bone anomalies, should be applied to the phenotype for p.L796V and p.N1108I. The core elements are congenital joint and bone anomalies with neonatal or infantile myotonic stiffness and widespread myotonic discharges. Breathing difficulties may be present, as in our patient, but stridor and respiratory compromise are not the predominant presentation. The relation of myotonic myopathy with joint and bone anomalies to the other sodium channelopathies of skeletal muscle is illustrated in **Figure 6**. This new syndrome is envisioned to be positioned between SNEL and paramyotonia congenita (PMC). Overlap with SNEL may be manifest as breathing difficulties and with PMC as episodic weakness [reported for p.L796V (21)]. We have previously shown that impairment of slow inactivation predisposes to episodes of periodic paralysis, and the slow inactivation defect

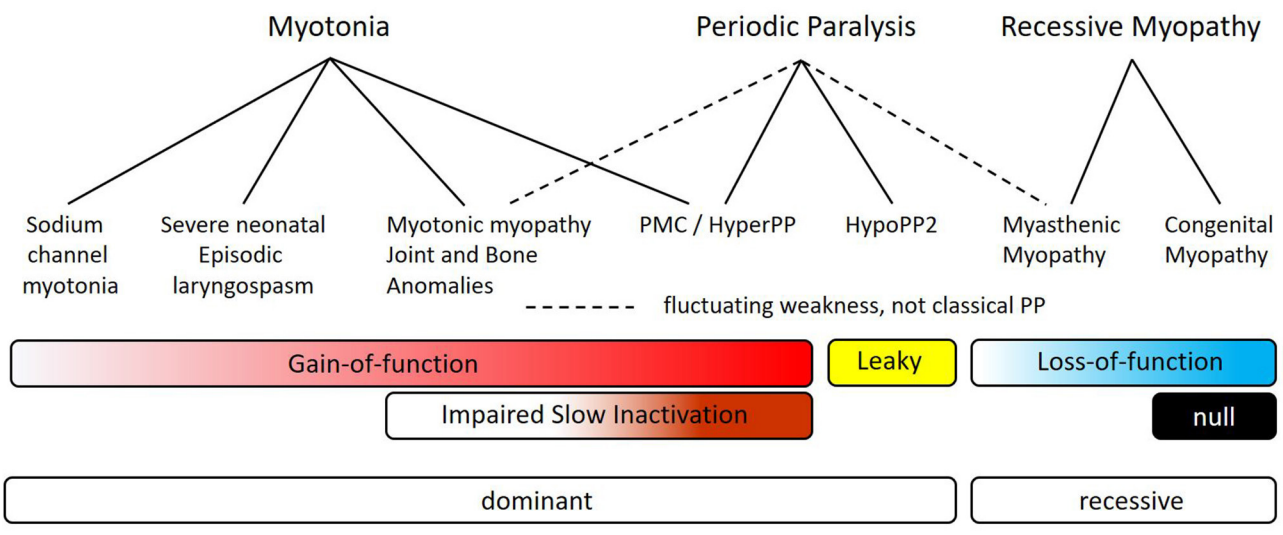

FIGURE 6 | Myotonic myopathy with secondary joint and bone anomalies is a dominantly expressed allelic disorder on the spectrum of *SCN4A* sodium channelopathies of skeletal muscle. The top row depicts the primary clinical manifestations, which may be overlapping in specific disorders (second row). Dashed lines are used to indicate fluctuating muscle weakness for myotonic myopathy and for myasthenic myopathy, as distinct from the more clearly demarcated attacks of classical periodic paralysis that usually have well-defined trigger factors (solid lines). The bars show the overlap of different functional defects of mutant sodium channels, with the more intense color indicating more severe changes. The final row indicates the inheritance pattern for expression of symptoms.

observed herein for L796V may account for susceptibility to episodic weakness.

DATA AVAILABILITY STATEMENT

The datasets generated for this study can be found in the National Center for Biotechnology Information. ClinVar; [VCV000383923.3], https://www.ncbi.nlm.nih.gov/clinvar/variation/VCV000383923.3 (accessed December 5, 2019).

ETHICS STATEMENT

The research protocol was approved by the Children's Hospital of Eastern Ontario Research Ethics Board, and clinical data were obtained in a manner conforming with research ethics board and funding agency guidelines. Written informed consent to participate in this study was provided by the participants' legal guardian/next of kin.

AUTHOR CONTRIBUTIONS

NE, SC, GG, and HM designed the study. HM performed the clinical assessment. TN, LH, and GG performed the genetic analysis. NE measured sodium currents and analyzed them with SC. Computer simulations were performed by SC. SC, GG, and HM wrote the paper.

FUNDING

This work was supported by a training grant in Molecular, Cellular and Integrative Physiology T32-GM065823 (NE) and Grant AR-42703 (SC) from NIAMS of the National Institutes of Health. The diagnostic testing was supported by the Care4Rare Canada Consortium (Enhanced Care for Rare Genetic Diseases in Canada) funded by Genome Canada, the Canadian Institutes of Health Research, the Ontario Genomics Institute, Ontario Research Fund, Genome Quebec, and Children's Hospital of Eastern Ontario Foundation (GG, LH).

ACKNOWLEDGMENTS

We thank Dr. Fenfen Wu and Marbella Quinonez at UCLA for assistance with the mutagenesis.

SUPPLEMENTARY MATERIAL

The Supplementary Material for this article can be found online at: https://www.frontiersin.org/articles/10.3389/fneur.2020.00077/full#supplementary-material

Supplementary Video 1 | EMG at 2 weeks of age shows increased insertional activity.

Supplementary Video 2 | EMG at 6 weeks of age shows myotonia.

REFERENCES

1. Cannon SC. Channelopathies of skeletal muscle excitability. *Compr Physiol.* (2015) 5:761–90. doi: 10.1002/cphy.c140062
2. Yoshinaga H, Sakoda S, Shibata T, Akiyama T, Oka M, Yuan JH, et al. Phenotypic variability in childhood of skeletal muscle sodium channelopathies. *Pediatr Neurol.* (2015) 52:504–8. doi: 10.1016/j.pediatrneurol.2015.01.014
3. Cannon SC. Sodium channelopathies of skeletal muscle. *Handb Exp Pharmacol.* (2018) 246:309–30. doi: 10.1007/164_2017_52
4. Palmio J, Sandell S, Hanna MG, Mannikko R, Penttila S, Udd B. Predominantly myalgic phenotype caused by the c.3466G>A p.A1156T mutation in SCN4A gene. *Neurology.* (2017) 88:1520–7. doi: 10.1212/WNL.0000000000003846
5. Lion-Francois L, Mignot C, Vicart S, Manel V, Sternberg D, Landrieu P, et al. Severe neonatal episodic laryngospasm due to *de novo* SCN4A mutations: a new treatable disorder. *Neurology.* (2010) 75:641–5. doi: 10.1212/WNL.0b013e3181ed9e96
6. Caietta E, Milh M, Sternberg D, Lepine A, Boulay C, McGonigal A, et al. Diagnosis and outcome of SCN4A-related severe neonatal episodic laryngospasm (SNEL): 2 new cases. *Pediatrics.* (2013) 132:e784–7. doi: 10.1542/peds.2012-3065
7. Singh RR, Tan SV, Hanna MG, Robb SA, Clarke A, Jungbluth H. Mutations in SCN4A: a rare but treatable cause of recurrent life-threatening laryngospasm. *Pediatrics.* (2014) 134:e1447–50. doi: 10.1542/peds.2013-3727
8. Portaro S, Rodolico C, Sinicropi S, Musumeci O, Valenzise M, Toscano A. Flecainide-responsive myotonia permanens with SNEL onset: a new case and literature review. *Pediatrics.* (2016) 137:e20153289. doi: 10.1542/peds.2015-3289
9. Matthews E, Manzur AY, Sud R, Muntoni F, Hanna MG. Stridor as a neonatal presentation of skeletal muscle sodium channelopathy. *Arch Neurol.* (2011) 68:127–9. doi: 10.1001/archneurol.2010.347
10. Gay S, Dupuis D, Faivre L, Masurel-Paulet A, Labenne M, Colombani M, et al. Severe neonatal non-dystrophic myotonia secondary to a novel mutation of the voltage-gated sodium channel (SCN4A) gene. *Am J Med Genet A.* (2008) 146:380–3. doi: 10.1002/ajmg.a.32141
11. Tsujino A, Maertens C, Ohno K, Shen XM, Fukuda T, Harper CM, et al. Myasthenic syndrome caused by mutation of the SCN4A sodium channel. *Proc Natl Acad Sci USA.* (2003) 100:7377–82. doi: 10.1073/pnas.1230273100
12. Arnold WD, Feldman DH, Ramirez S, He L, Kassar D, Quick A, et al. Defective fast inactivation recovery of Nav 1.4 in congenital myasthenic syndrome. *Ann Neurol.* (2015) 77:840–50. doi: 10.1002/ana.24389
13. Habbout K, Poulin H, Rivier F, Giuliano S, Sternberg D, Fontaine B, et al. A recessive Nav1.4 mutation underlies congenital myasthenic syndrome with periodic paralysis. *Neurology.* (2016) 86:161–9. doi: 10.1212/WNL.0000000000002264
14. Elia N, Palmio J, Castaneda MS, Shieh PB, Quinonez M, Suominen T, et al. Myasthenic congenital myopathy from recessive mutations at a single residue in NaV1.4. *Neurology.* (2019) 92:e1405–15. doi: 10.1212/WNL.0000000000007185
15. Zaharieva IT, Thor MG, Oates EC, van Karnebeek C, Hendson G, Blom E, et al. Loss-of-function mutations in SCN4A cause severe foetal hypokinesia or 'classical' congenital myopathy. *Brain.* (2016) 139:674–91. doi: 10.1093/brain/awv352
16. Hayward LJ, Brown RH Jr, Cannon SC. Inactivation defects caused by myotonia-associated mutations in the sodium channel III-IV linker. *J Gen Physiol.* (1996) 107:559–76. doi: 10.1085/jgp.107.5.559
17. Cannon SC, Brown RH Jr, Corey DP. Theoretical reconstruction of myotonia and paralysis caused by incomplete inactivation of sodium channels. *Biophys J.* (1993) 65:270–88. doi: 10.1016/S0006-3495(93)81045-2
18. Yang N, Ji S, Zhou M, Ptacek LJ, Barchi RL, Horn R, et al. Sodium channel mutations in paramyotonia congenita exhibit similar biophysical

phenotypes *in vitro*. *Proc Natl Acad Sci USA*. (1994) 91:12785–9. doi: 10.1073/pnas.91.26.12785
19. Green D, George A, Cannon S. Human sodium channel gating defects caused by missense mutations in S6 segments associated with myotonia: S804F and V1293I. *J Physiol.* (1998) 510:685–94. doi: 10.1111/j.1469-7793.1998.685bj.x
20. Hawash AA, Voss AA, Rich MM. Inhibiting persistent inward sodium currents prevents myotonia. *Ann Neurol.* (2017) 82:385–95. doi: 10.1002/ana.25017
21. Waldrop M, Amornvit J, Pierson CR, Boue DR, Sahenk Z. A novel *de novo* heterozygous scn4a mutation causing congenital myopathy, myotonia and multiple congenital anomalies. *J Neuromuscul Dis.* (2019) 6:467–73. doi: 10.3233/JND-190425
22. Pan X, Li Z, Zhou Q, Shen H, Wu K, Huang X, et al. Structure of the human voltage-gated sodium channel Nav1.4 in complex with β1. *Science.* (2018) 362:eaau2486. doi: 10.1126/science.aau2486
23. Simkin D, Lena I, Landrieu P, Lion-Francois L, Sternberg D, Fontaine B, et al. Mechanisms underlying a life-threatening skeletal muscle Na+ channel disorder. *J Physiol.* (2011) 589:3115–24. doi: 10.1113/jphysiol.2011.207977
24. Bauche S, Boerio D, Davoine CS, Bernard V, Stum M, Bureau C, et al. Peripheral nerve hyperexcitability with preterminal nerve and neuromuscular junction remodeling is a hallmark of Schwartz-Jampel syndrome. *Neuromuscul Disord.* (2013) 23:998–1009. doi: 10.1016/j.nmd.2013.07.005
25. Fusco C, Frattini D, Salerno GG, Canali E, Bernasconi P, Maggi L. New phenotype and neonatal onset of sodium channel myotonia in a child with a novel mutation of SCN4A gene. *Brain Dev.* (2015) 37:891–3. doi: 10.1016/j.braindev.2015.02.004
26. Xu YQ, Liu XL, Huang XJ, Tian WT, Tang HD, Cao L. Novel mutations in SCN4A gene cause myotonia congenita with scoliosis. *Chin Med J.* (2018) 131:477–9. doi: 10.4103/0366-6999.225061
27. Gonorazky HD, Marshall CR, Al-Murshed M, Hazrati LN, Thor MG, Hanna MG, et al. Congenital myopathy with "corona" fibres, selective muscle atrophy, and craniosynostosis associated with novel recessive mutations in SCN4A. *Neuromuscul Disord.* (2017) 27:574–80. doi: 10.1016/j.nmd.2017.02.001

Conflict of Interest: The authors declare that the research was conducted in the absence of any commercial or financial relationships that could be construed as a potential conflict of interest.

Copyright © 2020 Elia, Nault, McMillan, Graham, Huang and Cannon. This is an open-access article distributed under the terms of the Creative Commons Attribution License (CC BY). The use, distribution or reproduction in other forums is permitted, provided the original author(s) and the copyright owner(s) are credited and that the original publication in this journal is cited, in accordance with accepted academic practice. No use, distribution or reproduction is permitted which does not comply with these terms.

frontiers in Neurology

CORRECTION
published: 20 March 2020
doi: 10.3389/fneur.2020.00181

Corrigendum: Myotonic Myopathy With Secondary Joint and Skeletal Anomalies From the c.2386C>G, p.L796V Mutation in *SCN4A*

Nathaniel Elia[1,2], *Trystan Nault*[3], *Hugh J. McMillan*[3], *Gail E. Graham*[4], *Lijia Huang*[4] *and Stephen C. Cannon*[1]*

[1] Department of Physiology, David Geffen School of Medicine at UCLA, Los Angeles, CA, United States, [2] Molecular, Cellular, and Integrative Physiology Program, UCLA, Los Angeles, CA, United States, [3] Division of Neurology, Children's Hospital of Eastern Ontario, University of Ottawa, Ottawa, ON, Canada, [4] Department of Genetics, Children's Hospital of Eastern Ontario, University of Ottawa, Ottawa, ON, Canada

Keywords: skeletal muscle, channelopathy, sodium channel, $Na_V1.4$, myotonia, voltage-clamp

OPEN ACCESS

Approved by:
Frontiers Editorial Office, Frontiers Media SA, Switzerland

***Correspondence:**
Stephen C. Cannon
sccannon@mednet.ucla.edu

Specialty section:
This article was submitted to Neuromuscular Diseases, a section of the journal Frontiers in Neurology

Received: *21 February 2020*
Accepted: *24 February 2020*
Published: *20 March 2020*

Citation:
Elia N, Nault T, McMillan HJ, Graham GE, Huang L and Cannon SC (2020) Corrigendum: Myotonic Myopathy With Secondary Joint and Skeletal Anomalies From the c.2386C>G, p.L796V Mutation in SCN4A. Front. Neurol. 11:181. doi: 10.3389/fneur.2020.00181

A Corrigendum on

Myotonic Myopathy With Secondary Joint and Skeletal Anomalies from the c.2386C>G, p.L796V Mutation in *SCN4A*

by Elia, N., Nault, T., McMillan, H. J., Graham, G. E., Huang, L., and Cannon, S. C. (2020). Front. Neurol. 11:77. doi: 10.3389/fneur.2020.00077

In the original article there was a typographical error in the number for the amino acid missense mutation in *SCN4A*. The correct designation is L796V, which was erroneously transposed as L769V. Corrections have been made in several sections of the paper.

The title, which now reads:

"Myotonic Myopathy With Secondary Joint and Skeletal Anomalies From the c.2386C>G, p.L796V Mutation in *SCN4A*."

The Abstract:

"The phenotypic spectrum associated with the skeletal muscle voltage-gated sodium channel gene (*SCN4A*) has expanded with advancements in genetic testing. Autosomal dominant *SCN4A* mutations were first linked to hyperkalemic periodic paralysis, then subsequently included paramyotonia congenita, several variants of myotonia, and finally hypokalemic periodic paralysis. Biallelic recessive mutations were later identified in myasthenic myopathy and in infants showing a severe congenital myopathy with hypotonia. We report a patient with a pathogenic *de novo* *SCN4A* variant, c.2386C>G p.L796V at a highly conserved leucine. The phenotype was manifest at birth with arthrogryposis multiplex congenita, severe episodes of bronchospasm that responded immediately to carbamazepine therapy, and electromyographic evidence of widespread myotonia. Another *de novo* case of p.L796V has been reported with hip dysplasia, scoliosis, myopathy, and later paramyotonia. Expression studies of L796V mutant channels showed predominantly gain-of-function changes, that included defects of slow inactivation. Computer simulations of muscle excitability reveal a strong predisposition to myotonia with exceptionally prolonged bursts of

discharges, when the L796V defects are included. We propose L796V is a pathogenic variant, that along with other cases in the literature, defines a new dominant *SCN4A* disorder of myotonic myopathy with secondary congenital joint and skeletal involvement."

The final paragraph of the Introduction:

"We report a patient who presented with arthrogryposis multiplex congenita, congenital myopathy, and episodes of bronchospasm who has the c.2386C>G, p.L796V variant in *SCN4A*. Expression studies of L796V channels revealed a two forms of gain-of-function, enhanced activation and impaired slow inactivation, and which in model simulations led to prolonged bursts of myotonic discharges. We propose L796V is a pathogenic mutation and that the clinical features shared with previously described cases defines a new *SCN4A* syndrome of myotonic myopathy with secondary deformities of joints and bone."

The Results section, subsection Functional Characterization of L796V Mutant Sodium Channels, sub-subsection Slow Inactivation Was Impaired by L796V, final paragraph:

"At first glance, the changes in slow inactivation properties for L796V channels appear to be a mixture of gain and loss of function effects. Enhancement of slow inactivation is expected at the resting potential of −80 mV because of the reduced slope of the voltage dependence and the tendency for a left shift (Figure 3D, reduced availability at −80 mV), as well as for a faster rate of entry over the voltage range of −50 to −30 mV (Figure 3C, smaller time constants). On the other hand, impairment of slow inactivation is expected at depolarized potentials because inactivation of L796V is less complete than WT (Figure 3D, higher plateau −20 to 20 mV), and the recovery from slow inactivation is faster for L796V at the resting potential (Figure 3C, smaller time constant at −80 mV). We propose the overall effect will be impaired slow inactivation for L796V channels, in the context of the slow inactivation that occurs during sustained bursts of action potentials (e.g., myotonia). The basis for this prediction is that entry to slow inactivation occurs primarily at voltages near the peak depolarization of the action potential (where the predominant change is less complete slow inaction for L796V) and trapping of channels in the slow inactivated state is primarily dependent on the rate of recovery at the resting potential of −80 mV (which is faster for L796V channels). This prediction is supported by experimental evidence showing the use-dependent reduction of sodium current is more pronounced for WT than L796V channels during repetitive stimulation at 50 Hz. Figure 4A shows a superposition of sodium currents recorded in response to the first 10 pulses to +10 mV from a holding potential of −80 mV. The initial decline in peak amplitude from the first to the second pulse is predominantly caused by incomplete recovery from fast inactivation, whereas the subsequent decline for additional pulses is due to progressive loss of channel availability from slow inactivation. The slow inactivation effect is illustrated in Figure 4B for the entire 40 second train of 3 ms depolarizations at 50 Hz (2,000 pulses). The peak amplitude for each pulse is normalized by the amplitude of the second pulse (Figure 4A, blue trace) to isolate the effect of slow inactivation, which under these conditions is about 10% less for L796V channels compared to WT."

The legend to Figure 1:

"Figure 1. Activation of L796V channels is shifted toward more negative potentials. Sodium currents were recorded from HEK cells expressing WT **(A)** and L796V **(B)** channels. Superimposed traces show currents elicited by depolarization to test potentials of −75 to +60 mV from a holding potential of −120 mV. **(C)** Peak sodium current is shown as a function of test potential and reveals a reduced amplitude for L796V compared to WT. **(D)** Transforming the peak current to relative conductance (see Methods and Materials) shows a 7.2 mV hyperpolarized shift for L796V channels. Symbols show means from $n = 16$ (WT) or $n = 10$ (L796V) cells."

The legend to Figure 5:

"Figure 5. Model simulation predicts sustained busts of myotonia from the L796V channel defects. **(A)** The action potential elicited by a 20 $\mu A/cm^2$ current pulse applied for 100 ms is shown for a simulated muscle fiber with normal values for voltage-activated ion channels. Inset shows the initial 25 ms of the model simulation. **(B)** When 50% of the simulated sodium channels are modeled using parameters to emulate the altered behavior of L796V channels, then the same 100 ms current stimulus triggers a burst of myotonic discharges that persist beyond the 100 ms duration of the stimulus. **(C)** Extended simulation over time shows stable self-sustained repetitive myotonic discharges that do not cease. **(D)** When the simulated mutant channels are modified to have the slow inactivation kinetics for WT channels, then use-dependent reduction of the sodium current is enhanced (see this figure) and the myotonic burst ends after 4.5 s."

The authors apologize for this error and state that this does not change the scientific conclusions of the article in any way. The original article has been updated.

Copyright © 2020 Elia, Nault, McMillan, Graham, Huang and Cannon. This is an open-access article distributed under the terms of the Creative Commons Attribution License (CC BY). The use, distribution or reproduction in other forums is permitted, provided the original author(s) and the copyright owner(s) are credited and that the original publication in this journal is cited, in accordance with accepted academic practice. No use, distribution or reproduction is permitted which does not comply with these terms.

frontiers in Neurology

ORIGINAL RESEARCH
published: 29 April 2020
doi: 10.3389/fneur.2020.00255

Sodium Channel Myotonia Due to Novel Mutations in Domain I of $Na_V1.4$

Serena Pagliarani[1], Sabrina Lucchiari[1], Marina Scarlato[2], Elisa Redaelli[3], Anna Modoni[4], Francesca Magri[5], Barbara Fossati[6], Stefano C. Previtali[2], Valeria A. Sansone[7], Marzia Lecchi[8], Mauro Lo Monaco[4,9], Giovanni Meola[6] and Giacomo P. Comi[1,10]*

[1] Dino Ferrari Center, Department of Pathophysiology and Transplantation, University of Milan, Milan, Italy, [2] Department of Neurology and INSPE, IRCCS Ospedale San Raffaele, Milan, Italy, [3] Department of Biotechnology and Biosciences, University of Milano - Bicocca, Milan, Italy, [4] Institute of Neurology, Area of Neuroscience, Fondazione Policlinico Universitario A. Gemelli, IRCCS, Rome, Italy, [5] Fondazione IRCCS Ca' Granda Ospedale Maggiore Policlinico, Neurology Unit, Milan, Italy, [6] Department of Neurorehabilitation Sciences, casa di Cura del Policlinico, Milan, Italy, [7] Neurorehabilitation Unit, University of Milan; The NEMO (NEuroMuscular Omniservice) Clinical Center, Milan, Italy, [8] Department of Biotechnology and Biosciences and Milan Center for Neuroscience, University of Milano - Bicocca, Milan, Italy, [9] MIA (Myotonics in Association), Portici, Italy, [10] Fondazione IRCCS Ca' Granda Ospedale Maggiore Policlinico, Neuromuscular and Rare Diseases Unit, Milan, Italy

Sodium channel myotonia is a form of muscle channelopathy due to mutations that affect the $Na_V1.4$ channel. We describe seven families with a series of symptoms ranging from asymptomatic to clearly myotonic signs that have in common two novel mutations, p.Ile215Thr and p.Gly241Val, in the first domain of the $Na_V1.4$ channel. The families described have been clinically and genetically evaluated. p.Ile215Thr and p.Gly241Val lie, respectively, on extracellular and intracellular loops of the first domain of the $Na_V1.4$ channel. We assessed that the p.Ile215Thr mutation can be related to a founder effect in people from Southern Italy. Electrophysiological evaluation of the channel function showed that the voltage dependence of the activation for both the mutant channels was significantly shifted toward hyperpolarized potentials (Ile215Thr: -28.6 ± 1.5 mV and Gly241Val: -30.2 ± 1.3 mV vs. WT: -18.5 ± 1.3 mV). The slow inactivation was also significantly affected, whereas fast inactivation showed a different behavior in the two mutants. We characterized two novel mutations of the *SCN4A* gene expanding the knowledge about genetics of mild forms of myotonia, and we present, to our knowledge, the first homozygous patient with sodium channel myotonia.

Keywords: myotonia, sodium channel myotonia, founder effect, channelopathy, Na_v 1.4, mexiletine

OPEN ACCESS

Edited by:
Jean-François Desaphy, University of Bari Aldo Moro, Italy

Reviewed by:
Roope Mannikko, University College London, United Kingdom
Mohamed Chahine, Laval University, Canada

****Correspondence:***
Serena Pagliarani
serena.pagliarani@gmail.com

Specialty section:
This article was submitted to Neuromuscular Diseases, a section of the journal Frontiers in Neurology

Received: *23 December 2019*
Accepted: *17 March 2020*
Published: *29 April 2020*

Citation:
Pagliarani S, Lucchiari S, Scarlato M, Redaelli E, Modoni A, Magri F, Fossati B, Previtali SC, Sansone VA, Lecchi M, Lo Monaco M, Meola G and Comi GP (2020) Sodium Channel Myotonia Due to Novel Mutations in Domain I of $Na_v1.4$. Front. Neurol. 11:255. doi: 10.3389/fneur.2020.00255

INTRODUCTION

Myotonia is an impaired muscle relaxation after a voluntary muscle contraction and is the main feature of a group of heterogeneous skeletal muscle channelopathies named non-dystrophic myotonias (NDMs). NDMs are caused by mutations in *CLCN1* and *SCN4A* genes, coding, respectively, for the chloride (ClC-1) and sodium ($Na_V1.4$) muscle channels (1).

$Na_V1.4$, the α-subunit of the sodium channel complex, mainly expressed in skeletal muscle, is formed by 1836 amino acids and displays a tetrameric structure composed of 4 domains (DI-DIV), each including six transmembrane α-helices (S1–S6). The inner part of the channel contains a pore (S5–S6 from each domain) where sodium ions flow through thanks to four voltage sensors

(S1–S4 from each domain). After an action potential, the cell membrane enters a "refractory period" when it becomes inexcitable thanks to a double mechanism of $Na_v1.4$ inactivation, either related to a fast or a slow kinetic. Depending on their nature and localization, mutations in the *SCN4A* gene may enhance or decrease muscle excitability, and elicit different physiological reactions by the mutated channel which are related to different muscle diseases. These now include autosomal dominant sodium channel myotonia (SCM), paramyotonia congenita, hyperkalemic periodic paralysis, hypokalemic periodic paralysis, congenital recessive myasthenia, and the autosomal recessive congenital myopathy with hypotonia (2) and sudden infant death syndrome [SIDS; (3)].

SCMs are characterized by the absence of weakness and often by cold sensitivity and muscle pain (4). Clinical phenotype is highly variable, ranging from a severe neonatal presentation, which recently has been associated to SNEL (severe neonatal episodic laryngospasm) and stridor (5), passing through classical SCM with onset in the first or second decade, to mild, late-onset phenotypes (6).

To date, over 70 mutations inherited in autosomal dominant fashion have been reported in the *SCN4A* gene and related to SCM and periodic paralyzes. Some of these mutations are found in the first domain of the sodium channel and have been described to cause both SCM and paramyotonia congenita (7–11). Most of the mutant channels have been extensively investigated *in vitro*, indicating enhanced activation and/or impaired fast inactivation as the major mechanisms underlying the myotonia phenotype (1).

Here, we present the characterization of the novel mutations p.Ile215Thr and p.Gly241Val in the first domain of $Na_v1.4$. Ile215Thr is shared by six unrelated families from Southern Italy. Of note, one of the affected individuals is homozygous for this mutation but he does not share any of the features recently described for autosomal recessive congenital myopathy (12). Data from electrophysiological assays positively correlated with pathogenicity for both variants.

MATERIALS AND METHODS

Patients

This study was carried out in accordance with the recommendations of Fondazione IRCCS Ca' Granda Ospedale Maggiore Policlinico of Milan. All subjects gave written informed consent for genetic analysis in accordance with the Declaration of Helsinki. In families 2 and 4, we could analyze only the proband, while for family 5, we could analyze the proband and her father: the mother probably had the same symptomatology of her daughter but was not available for genetic testing. In family 6, we could analyze the proband and his mother (**Figure 1**).

Genetic Analysis

Genomic DNA was extracted from blood samples using FlexiGene DNA Kit (Qiagen, Hilden, Germany). DM1 and DM2 expansion and CLCN1 mutations were excluded in the probands of each family. PCR fragments containing all the 24 coding exons and intron–exon junctions of *SCN4A* were amplified (primer sequences and conditions are available upon request). The fragments were directly sequenced using the same PCR primers and Big Dye Terminator Cycle Sequencing Kit in an automated sequencer 3130 (Applied Biosystems, Foster City, USA). Sequences were aligned using SeqScape software (Applied Biosystems) and compared to sequences NG_011699 and NM_000334 from NCBI. To confirm the results obtained, amplification and sequencing were repeated and the novel variant was checked in 200 Italian controls.

Microsatellite markers analysis was performed in order to verify the hypothesis of a founder effect for the c.644T>C mutation. Families 1, 2, and 3 were genotyped using markers D17S787, D17S944, D17S949, and D17S785 from ABI PRISM Linkage Mapping Set v2.5 (panels 23 and 24; Applied Biosystems) and markers D17S1792, D17S113, D17S584, D17S789, and D17S1786 annotated in NCBI (amplification conditions are available upon request). The fragments were resolved in an automated sequencer 3130 and the results were analyzed with GeneMapper Software 5 (Applied Biosystems).

Cloning of $Na_v1.4$ and Electrophysiological Characterization in tsA Cells

Total RNA from a pulled skeletal muscle specimen (Human Total RNA Master Panel II, Clontech, Mountain View, USA) was reverse-transcribed with Ready-To-Go kit (GE Healthcare, Little Chalfont, UK). *SCN4A* cDNA was amplified with specific primers (primer sequences and conditions are available upon request) and cloned in mcs1 of pVITRO2-mcs vector (Invivogen, San Diego, USA); GFP cDNA was cloned in mcs2. Clones were checked by sequencing. Site-directed mutagenesis was performed using the Quick-change II kit (Stratagene, Santa Clara, USA) and specific primers for the mutation of interest. The mutant clones were verified again by direct sequencing.

The functional characterization of mutant channels was performed by transiently transfecting vectors containing mutated human cDNA in tsA human kidney epithelial cells, derived from HEK 293 cell line. The evoked sodium currents were recorded by the patch-clamp technique in the whole-cell configuration. Current recordings were performed 48–72 h after the transfection, using the MultiClamp 700A amplifier and pClamp 8.2 software (Axon Instruments, USA) for data acquisition. Pipette resistance was about 1.5–1.8 MΩ; capacitance and series resistance errors were compensated (85–90%) before each protocol run to reduce voltage errors to <5% of the protocol pulse. Recordings were performed at room temperature. During the experiments, cells were maintained in a physiological extracellular solution, containing (mM): NaCl 130, KCl 5, $CaCl_2$ 2, $MgCl_2$ 2, glucose 5, and Hepes 10. The solution for the patch electrodes was composed by (mM): CsF 105, CsCl 27, NaCl 5, $MgCl_2$ 2, Hepes 10, and EGTA 10.

Voltage dependence of activation was determined by the protocol represented in **Figure 2A**. Starting from a holding potential of −60 mV, cells were conditioned at −100 mV for 500 ms and successively tested by depolarizing potentials in 10-mV increments, from −80 to +40 mV. The properties of *fast* inactivation were studied using a double pulse protocol composed of 580-ms conditioning steps of varying voltages, from −110 to −20 mV, followed by a constant test pulse to −10 mV (**Figure 2B**). *Slow* inactivation was investigated by

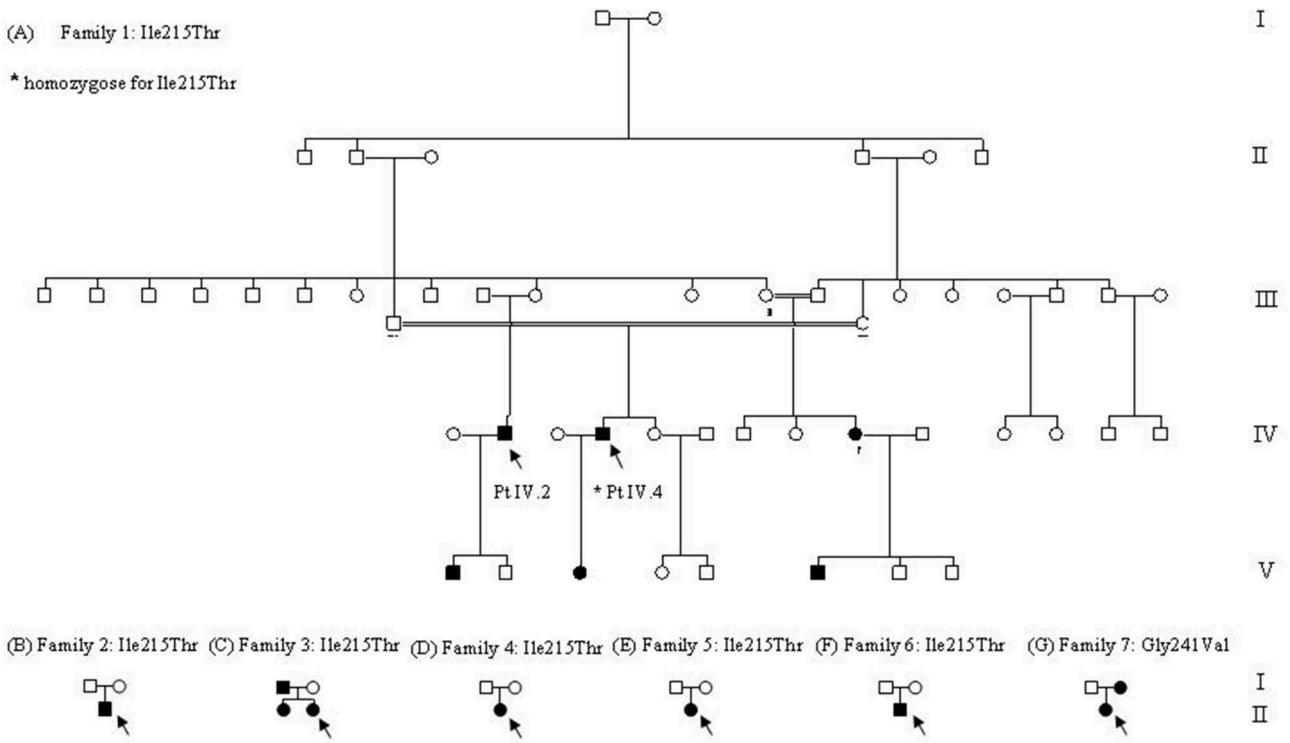

FIGURE 1 | Family trees. **(A–F)** Family trees of families that carried p.Ile215Thr. In the picture, we indicated by arrows the two probands, IV.2 heterozygote, and IV.4 homozygote for the target mutation. As depicted by the doubled lines, two marriages between relatives occurred in this family, and only one homozygote was generated (*). **(G)** Family tree of the only family carrying p.Gly241Val.

applying a conditioning 50-s pulse of increasing voltage (from −120 to 20 mV) to induce slow inactivation, followed by a 100-ms step to −130 mV for fast inactivation recovery and a test pulse to −20 mV (**Figure 2C**). Data were fitted with Boltzmann functions, $y = 1/(1 + \exp[(V-V_{1/2})/k])$ or $y = I_o + ([1-I_o]/[1 + \exp((V-V_{1/2})/k)])$ for the slow inactivation, where V is the membrane potential, $V_{1/2}$ is the half-maximal activation or inactivation voltage, k is the slope factor, and I_o is the non-zero current level.

All data are presented as mean ± SEM. Statistical evaluation was performed using one-way analysis of variance (ANOVA) with statistical significance set at $p < 0.05$.

RESULTS

Genetic Analysis

Direct sequencing of the *SCN4A* gene of the proband of each family revealed two novel variants in the first domain of $Na_v1.4$, not detected among healthy family members and among 200 Italian controls.

Patients from six unrelated families (families 1–6) shared the same variant in exon 5, c.644T>C, that causes an amino acid change at position 215 from isoleucine into threonine (p.Ile215Thr). Ile215 is located within the extracellular loop S3–S4 of the first domain (DI S3–S4 linker). Patient IV.4 from family 1 was born from consanguineous parents and carries the p.Ile215Thr mutation in homozygosis. Genetic analysis of family 7 revealed a c.722G>T variant in exon 6 leading to the amino acid change p.Gly241Val. Gly241 is located in the cytoplasmic loop S4–S5 (DI S4–S5 linker). Both amino acids, Gly241 and Ile215, are highly conserved through orthologs. Bioinformatic analysis of the variants was performed using free online tools. Polyphen 2, SIFT, and Mutation Taster predicted that both variants could affect protein function, while PMUT predicted a neutral effect. Both variants are not described either in gnomAD or in 1,000 G.

Clinical Examination of Patients Carrying p.Ile215Thr

The examined families showed a spectrum of clinical manifestations, ranging from asymptomatic, and subclinical subjects to patients with clear myotonic signs (**Table 1**). All the patients carrying p.Ile215Thr showed electrical myotonia at EMG examination.

Family 1 is a large Italian family originally from Sicily that could be traced through five generations, the last two showing family members with similar symptoms (**Figure 1A**). The first proband (Patient IV.2) was a 60-year-old man with no clinical symptoms and no muscle weakness that had just an incidental finding of high CK values (300–500 UI/l). At neurological examination, muscle hypertrophy, and mild eyelid myotonia were noticed without percussion myotonic phenomenon in other muscles. EMG showed high-frequency repetitive discharges

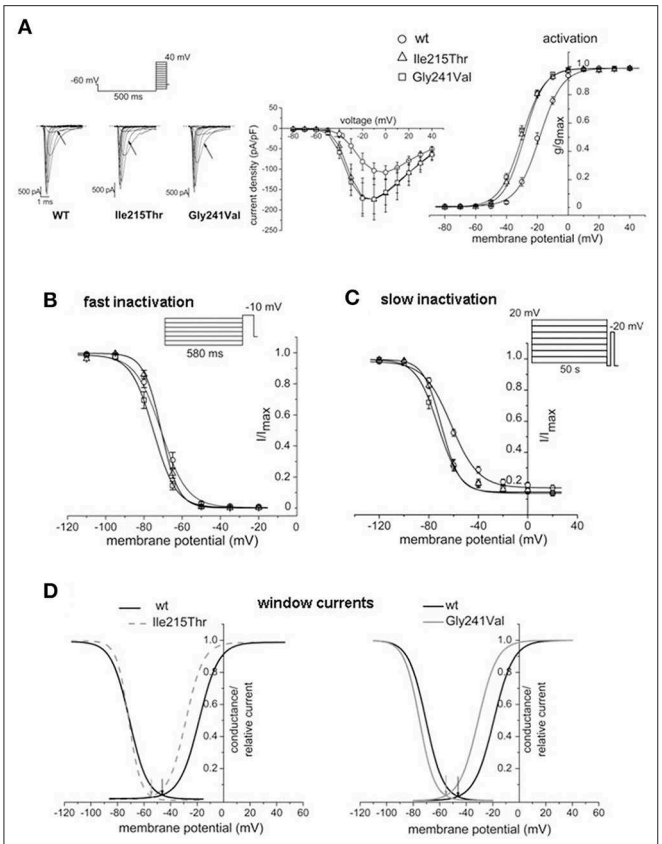

FIGURE 2 | Effects of p.Ile215Thr and p.Gly241Val mutations on $Na_v1.4$ functional properties. **(A)** Representative traces of whole-cell sodium currents; the arrows indicate the currents in response to the voltage step at −30 mV. Normalized current/voltage relationship was obtained by normalizing current by cell capacitance. Voltage dependence of activation was studied by applying the protocol represented and by fitting the normalized conductance by a Boltzmann curve. Comparison with WT indicates a shift of −10 and −12 mV for the curves of p.Ile215Thr and p.Gly241Val, respectively. **(B)** Voltage dependence of fast inactivation. A mild shift toward hyperpolarized potentials is observed only for p.Gly241Val. **(C)** Slow inactivation properties studied with long conditioning voltage pulses. Changes in the $V_{1/2}$ are observed for both p.Ile215Thr and p.Gly241Val. **(D)** Window currents obtained overlapping activation and inactivation curves; they identify the voltage range in which $Na_v1.4$ channels are available for opening. p.Ile215Thr and p.Gly241Val show to be available to open in a more hyperpolarized voltage range compared to WT.

without myopathic changes and muscle biopsy revealed mild myopathic abnormalities. Cold sensitivity was not reported. His elder son, who, at the first examination, was 23 years old, has a very similar phenotype with diffuse muscle hypertrophy, percussion myotonia, and a mild CK increase (223 U/L). One cousin (Patient IV.4, the second proband of this family) underwent neurological examination in another hospital when he was 60 years old for mild CK elevation (300 U/L) and stiffness occurred after statin administration and persisting despite therapy discontinuation. He was born from parents that were first cousins, without reported symptoms, and he was homozygote for p.Ile215Thr. Past medical history was positive for diabetes treated with oral antidiabetic drugs. Since childhood, he complained of mild difficulties in starting leg movements that did not interfere with activity of daily living. Neurological examination showed paramyotonia in the orbicularis oculi and grip myotonia. Muscle mass and strength were normal. Laboratory studies demonstrated normal thyroid hormone levels. EMG showed myotonic discharges in all the examined muscles. Muscle biopsy showed mild non-specific abnormalities such as increased fiber size variation, internal nuclei, and type 1 fiber atrophy. He was treated with mexiletine and he was a good responder. His 37-year-old daughter, which is an obligate heterozygous carrier for p.Ile215Thr, was asymptomatic, and during neurological examination, no clinical myotonia was noticed. She complained of a generalized stiffness only during pregnancy. The CK values were normal.

Patient II.2 from family 2 sought neurological attention at 35 years of age because of diffuse muscle pain and stiffness with symptoms worsening with cold exposure (**Figure 1B**). He had never experienced weakness or episodic paralysis. Neurological examination was normal except for very mild and fluctuating grip and percussion myotonia. CK was normal. Family history was negative for neuromuscular diseases. His family came from Sicily.

In family 3, which originates from Sicily, the proband is a 29-year-old woman (Patient II.2) who was seen because of muscle pain, worsening with cold exposure (**Figure 1C**). Symptoms had started in childhood with delayed relaxation of hand and leg muscles. She was also bothered by diffuse muscle hypertrophy despite the fact that she was not doing any intense physical activity. During the last decade, she experienced worsening of the symptoms with additional short episodes of lower limb episodic paralysis. Muscle biopsy showed mild unspecific features with type 2B fiber deficiency. Hypothyroidism was detected in the last 3 years. She was placed on replacement therapy and mexiletine 200 mg bid with improvement in the frequency, duration, and severity of the episodes of stiffness. Her 66-year-old father was asymptomatic and neurologic exam was normal except for lid-lag. CK were normal. Myotonic discharges were found on EMG. Her 33-year-old sister complained of mild grip myotonia. Neurologic exam was normal. CK were normal. She refused EMG studies.

In family 4, the proband is a 48-year-old woman (Patient II.1) who complained of a very mild myotonia that was aggravated by cold and stiffness at hands after exercise (**Figure 1D**). Clinical examination revealed only a tongue myotonia. She also complained of a diffuse muscle weakness but the strength was normal during manual testing. EMG showed myotonic discharges in all examined muscles. Her family came from Sicily.

Patient II.1 from family 5 underwent medical examination when she was 28 years old for muscle pain that started in childhood (**Figure 1E**). Symptoms worsened with fasting, rest, exercise, and emotional stress. Neurological examination did not reveal clinical myotonia. EMG showed myotonic discharges without myopathic changes and muscle biopsy was normal. She had a good response to mexiletine treatment while phenytoin was not effective and quinine was effective but was not tolerated. Her mother probably had the same symptomatology but was not available either for clinical or for genetic examination. Her father was negative at genetic testing.

TABLE 1 | Clinical signs and instrumental data.

							Ile215Thr							Gly241Val	
Family			**Family 1**				**Family 2**	**Family 3**			**Family 4**	**Family 5**	**Family 6**	**Family 7**	
Patients	**Patient IV.2**	**Patient V.1**	**Patient IV.9**	**Patient V.6**	**Patient IV.4**	**Patient V.3**	**Patient II.1**	**Patient II.2**	**Patient I.1**	**Patient II.1**	**Patient II.1**	**Patient II.1**	**Patient II.1**	**Patient II.1**	**Patient I2**
Age at last examination (years)	59	28	63	26	67	32		35	65	32	48	28	32	36	80
Onset	Subclinical	Asymptomatic	50 years		Childhood	32 years	35 years	Childhood	Asymptomatic	Asymptomatic	45 years	Childhood	Adolescence	early adulthood	adulthood
Clinical myotonia	Mild eye-lid myotonia	Percussion myotonia	Very mild grip myotonia	Very mild grip myotonia	Paramyotonia in the orbicularis oculi and grip myotonia	No myotonia	Fluctuating grip and percussion myotonia	Percussion myotonia	Lid-lag	Mild grip myotonia	Tongue	No	No	lid-lag, grip myotonia, spontaneous and percussion myotonia of the lower limbs	
Triggers for myotonia	Absent	Absent	Cold temperature	Cold temperature	Exercise	Pregnancy	Cold temperature	Cold temperature			Cold temperature	Fasting, exercise, rest, stress		cold temperature	
Paradoxical myotonia	Absent	Absent	Absent	Absent	Yes	No					No	Yes			
Stiffness	Absent	Absent	In the morning	In the morning	Yes	No	Yes	Severe			After exsercise at hands	Yes		lower limbs	mild
EMG	Myotonic discharges	Myotonic discharges	Myotonic discharges	Myotonic discharges	Myotonic discharges	No	Myotonic discharges	Myotonic discharges	Myotonic discharges	na	Myotonic discharges	Myotonic discharges	Myotonic discharges	myotonic discharges	na
Warm-up					No	No					No	No			
Muscle pain			Yes	Yes	Yes	No	Yes	Yes			Yes	Yes	No	yes, lower limbs	
Muscle weakness					No	No	no				Progressive and diffuse weakness	No			
Contractures			Muscle cramps	Muscle cramps	No	No					No		Contractures + muscle cramps		
Hypertrophy	Yes	Diffuse			No	No		Diffuse			no		Hypertrophy of calves	mild	
CK level (U/L)	300–500	223	na	200	300	Normal	Normal	na	Normal	Normal	na	Normal	Normal	normal	normal
Drugs					Mexiletine	No	No	Mexiletine and clonazepam				Phenytoin, quinine, mexiletine	No	mexiletine, acetazolamide, carbamazepine phenytoin	
Response to drugs					Good response to mexiletine—Worsening of myotonia after statin therapy			Improvement in the frequency, duration and severity of the episodes of stiffness				Phenytoin: not effective quinine: effective, but not tolerated mexiletine: good response		All drugs were not effective	
Biopsy	Mild myopathic abnormalities				Increased fiber size variation, type I fibers atrophy, internal nuclei			Mild myopathic abnormalities - type 2B deficiency				Normal. Increased acid fosfatase activity.	Normal		
Other diseases			Mild ptosis ogival cleft		Diabetes, hypercholesterolemia and hypertrigliceridia	Mutation of gene of MTHFR		Hypothyroidism			Low serum vitamin D				

In grey, the family that does not share the p.Ile215Thr.

TABLE 2 | Microsatellite analysis showing haplotypes for five families carrying the p.Ile215Thr.

Marker name	D17S787	D17S944	SCN4A	D17S1792	D17S113	D17S584	D17S789	D17S1786	D17S949	D17S785
Physical position (Mb)	53.28	61.4	62	63.06	63.9	65.12	66.63	67.5	68.5	75
			c.644 T>**C**							
Family 1 Patient IV.2	142	325	**C**	302	177	161	185	181	215	175
Family 1 Patient V.1	142	325	**C**	302	177	161	185	181	215	175
Family 1 Patient IV.9	142	325	**C**	302	177	161	185	181	215	175
Family 1 Patient V.6	142	325	**C**	302	177	161	185	181	215	175
Family 1 Patient IV.4	142	325	**C**	302	177	161	185	181	215	175
	142	325	**C**	302	177	153	183	177	221	173
Family 2 Patient II.1	144	325	**C**	302	177	161	185	181	215	169
Family 3 Patient II.2	154	323	**C**	302	179	161	187	177	217	169
Family 3 Patient II.1	154	323	**C**	302	179	161	187	177	217	169
Family 3 Patient I.1	154	323	**C**	302	179	161	187	177	217	169

In grey, markers in the minimal identity region. In bold, the allele in linkage on the disease gene.

TABLE 3 | Voltage dependence of activation, fast inactivation, and slow inactivation.

	Activation		Fast inactivation		Slow inactivation	
	$V_{1/2}$ (mV)	*k* (mV)	$V_{1/2}$ (mV)	*k* (mV)	$V_{1/2}$ (mV)	*k* (mV)
WT	−18.5 ± 1.3	7.4 ± 0.4	−71.2 ± 1.3	6.8 ± 0.5	−62.2 ± 1.1	11.3 ± 0.8
Ile215Thr	−28.6 ± 1.5***	6.6 ± 0.5	−71.0 ± 1.1	4.6 ± 0.4	−69.7 ± 0.9**	7.3 ± 0.4**
Gly241Val	−30.2 ± 1.3***	7.2 ± 0.5	−75.4 ± 1.4*	5.9 ± 0.5	−72.4 ± 1.1***	8.9 ± 0.5

*Values are expressed as means ± SEM. Asterisks represent significant differences between mutants and WT channels: *p < 0.05, **p < 0.01, ***p < 0.001.*

Patient II.1 from family 6 complained of contractures and muscle cramps not related to exercise or cold temperature from the age of 20 (**Figure 1F**). Clinical myotonia was not detected but EMG showed myotonic discharges. Muscle biopsy was normal. At the last examination when he was 32 years old, he complained of significant fatigue that let him work for only a few hours a day. His family came from Calabria.

Clinical Examination of Patients Carrying p.Gly241Val

This 36-year-old woman (family 7, patient II.1; **Figure 1G**) came to neurological attention because of muscle pain and stiffness predominantly in the lower limbs, which worsened with cold exposure. Symptoms had been present since her early adulthood. She never reported episodes of muscle weakness. Neurological examination was normal except for muscles of mildly increased bulk and myotonia: lid-lag, grip myotonia with warm-up phenomenon, and spontaneous and percussion myotonia in the proximal lower limb muscles were clearly evident. Treatment with the common anti-myotonic drugs (carbamazepine, phenytoin, acetazolamide, and mexiletine) was ineffective. There were, however, no major functional limitations in everyday activities. CK was normal. Needle EMG showed abundant myotonic discharges especially in proximal lower limb muscles. Her 80-year-old mother complained of mild muscle stiffness since adulthood (Patient I.2). She had never sought medical attention because she had never experienced functional limitations. CK was normal. EMG was not available.

Founder Effect

For five of the six independent Italian families that carried the p.Ile215Thr, we were able to verify the origin from Southern Italy; in particular, four families came from Sicily and one family came from Calabria. Therefore, we hypothesized that a founder effect could be responsible for the distribution of this mutation (**Table 2**). Microsatellite marker analysis in these families revealed that affected members from families 1 and 3 share the same allele spanning from 61.4 to 68.5 Mb in chromosome 17. Patient II.1 from family 2 share a smaller region of about 2,5 Mb with the other two families.

Functional Studies

Ile215Thr and Gly241Val mutants expressed in tsA cells were able to generate functional channels as demonstrated by the sodium currents they evoked. Measured current densities were 176 ± 50 and 172 ± 34 pA/pF, respectively, for Ile215Thr ($n = 10$) and Gly241Val ($n = 13$) and were not significantly different from that of WT currents (113 ± 11 pA/pF, $n = 13$). Analysis of channel properties was performed by the voltage protocols described in Methods and represented in **Figure 2**. The voltage dependence of the activation for both the mutants was significantly shifted toward hyperpolarized potentials; the corresponding values of $V_{1/2}$ were, respectively, −28.6 ± 1.5 mV for Ile215Thr and −30.2 ± 1.3 mV for p.Gly241Val vs. −18.5 ± 1.3 mV for WT channels (**Figure 2A**). The slow inactivation was also significantly affected; $V_{1/2}$ was translated of about −7.5 mV for p.Ile215Thr and of −10 mV for p.Gly241Val (**Figure 2C**). Moreover, for p.Ile215Thr,

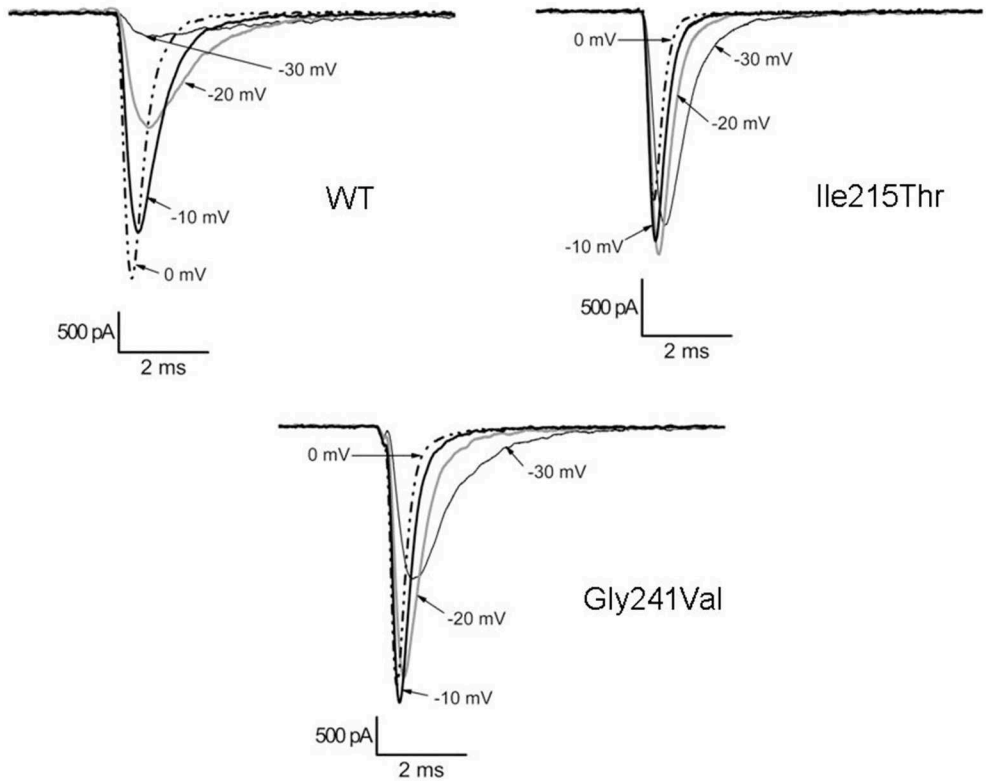

FIGURE 3 | Traces illustrating the current decay for WT and mutant channels.

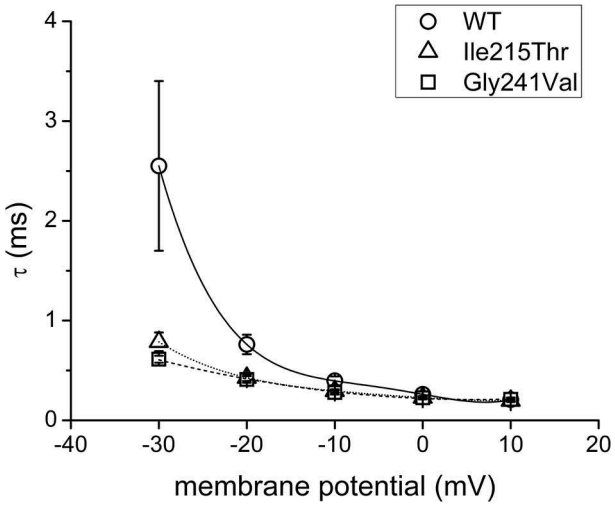

FIGURE 4 | Curves illustrating the time constants (τ) for WT and mutant channel current decay in the range of potentials from −30 to 10 mV.

the slope of the voltage dependence curve was also significantly changed (**Table 3**). Concerning the voltage dependence of fast inactivation, the two mutants manifested different behavior: no effects were recorded for p.Ile215Thr, whereas a modest but significant shift was evident for p.Gly241Val (**Figure 2B**; $V_{1/2}$ and k values listed in **Table 3**). By fitting the decay of the individual current traces (obtained by protocol in **Figure 2A**) using a monoexponential curve from 90% of peak (**Figure 3**), the time constants (τ) of inactivation onset at −20 mV for both mutants were significantly different from WT, and shifted ∼10 mV left (**Figure 4**; Ile215Thr vs. WT, $p = 0.01$; Gly241Val vs. WT, $p = 0.009$, ANOVA test, $n = 5$ cells for each condition).

DISCUSSION

In the present work, two additional novel dominant mutations, both sited in the first domain of the $Na_v1.4$ α-subunit, were extensively studied. The p.Ile215Thr and p.Gly241Val are, respectively, located within the S3–S4 extracellular linker and the S4–S5 intracellular loop. We consider both variants to be pathogenic because (i) these mutations segregate with affected family members and are absent in 400 Italian chromosomes; (ii) they involve highly conserved amino acids; and (iii) functional analysis show altered behaviors compared with wild-type channel.

Both the mutations caused two principal effects on channel behavior: an increase in the open probability and in the slow inactivation. The first one concurs in the enhancement of channel availability during depolarization and resulted in a shift of the window current of respectively −9 and −10 mV for Ile215Thr

and Gly241Val (**Figure 2D**). The second effect could prevent prolonged depolarization of the membrane, which is related to paralysis and episodes of weakness, as previously described by Petitprez et al. (10). These behaviors represent common traits of myotonic mutants and they have been shown for other mutations in sodium channel domain I (10). The alterations we observed in the activation properties are coherent with hyperexcitability phenomena and the myotonic symptoms referred by the patients. However, in both Ile215Thr and Gly241Val mutants, the shift in the voltage dependence of activation toward hyperpolarized potentials also accelerated the rate of the open-state inactivation, a mechanism consistent with a loss-of-function effect. This characteristic has already been observed by Petitprez et al. (10), but has not been described for other mutants (13, 14), which anyway showed a similar left shift for the voltage dependence of activation.

Moreover, the enhancement in the slow inactivation, which prevents prolonged membrane depolarization, is compatible with the observation that none of the patients present episodes of paralysis.

In fact, all probands and affected family members described in this report did not suffer from episodes of paralysis. The clinical presentation includes clinical myotonia and stiffness usually when initiating movement after rest, which worsens with cold exposure in some patients. Myotonia is described as diffuse in the patients with no specific skeletal district, being present in the face, in the hands, and in the lower limbs. Age at onset varies from childhood to adulthood. Muscle strength was normal in all. Some patients carrying p.Ile215Thr showed only electrical myotonia and came to medical attention for an incidental finding. Concomitant paradoxical myotonia may be present in the eyelids as in patient IV.4 from family 1. Only two patients reported weakness: patient II.2 from family 3 complained of mild and transient weakness in whom there was coexisting hypothyroidism so that interpretation of weakness is limited; patient II.1 from family 4 instead complained of progressive and diffuse weakness. Biopsies from Ile215Thr patients were normal or with mild myopathic abnormalities.

The p.Gly241Val patients showed a very different phenotype ranging from the almost asymptomatic mother to her daughter who showed clinical myotonia with muscle pain.

In our cohort of p.Ile215Thr patients, three patients were treated with mexiletine and all of them had good response. Instead, patient II.1 from family 7 that carried p.Gly241Val was treated with mexiletine, acetazolamide, carbamazepine, and phenytoin without success.

The p.Ile215Thr mutation is shared by patients belonging to five out of six unrelated families from Southern Italy. We postulated the existence of a founder effect for this mutation that was demonstrated by marker analysis in the chromosomal region around the *SCN4A* gene. The disease allele harbored by family 2 showed a relatively little region of homology compared to disease allele of families 1 and 3, which could be the result of two different events of chromosomal recombination that independently took place in the past. Another recombination event is shown in patient IV.4 from family 1, indicating that this region is prone to chromosomal recombination. To date, a single case of founder mutation in SCN4A gene has been reported in the French–Canadian population (15).

Recently, homozygous mutations in the *SCN4A* gene were described to cause severe congenital myopathy (12). Before this report, two cases of homozygous patients, one with paramyotonia congenita and one suffering from hypokalemic periodic paralysis, have been reported, leading to severe disability in both patients (16). We describe a new patient affected by SCM with a homozygous mutation in the *SCN4A* gene (patient IV.4, family 1). In our case, homozygosis does not seem to worsen the phenotype compared to heterozygous patients. To explain this counterintuitive phenotypic presentation, beyond an incomplete penetrance of this pathogenic variant that might result in a mild effect when present in a single copy, further modifier elements may be called into question, such as individual genetic background, epigenetic factors (17), and post-translational modifications by miRNA environment (16), each of them able to modulate the effect of the p.Ile215Thr on the phenotype (18). Moreover, the mutations that were described to cause congenital myopathy are loss-of-function mutations that lead to completely non-functional channels due to protein truncation or to the abolished channel function (12).

Given the variability of the myotonic symptoms described by patients carrying mutations in domain I of $Na_v1.4$, it is conceivable that the frequency of mutations at this site is underestimated: patients referring for symptoms of locking or stiffness although mild should be screened for SCM. In addition, the finding of a common ancestral disease allele in the Sicilian population is helpful for genetic diagnosis in mild myotonia patients from this region. Antimyotonic treatment may be beneficial and knowledge of a genetic disease will suggest caution when using drugs affecting channel function, i.e., anesthetics, as is recommended for other more severe skeletal channelopathies.

DATA AVAILABILITY STATEMENT

The raw data supporting the conclusions of this article will be made available by the authors, without undue reservation, to any qualified researcher.

ETHICS STATEMENT

The studies involving human participants were reviewed and approved by Comitato etico Fondazione IRCCS Ca Granda Ospedale Maggiore Policlinico. The patients/participants provided their written informed consent to participate in this study.

AUTHOR CONTRIBUTIONS

SPa and GC conceived the study and designed the research. SPa and SL collected the genetic data. ER and MLe collected the electrophysiological data. SPa, SL, ER, MS, MLe, GM, and GC analyzed the data. MS, FM, BF, SPr, VS, GM, AM, and MLo examined the patients. SPa wrote the paper. All authors reviewed and approved the paper.

FUNDING

This work was supported by Fondazione Malattie Miotoniche-FMM, Milan, Italy.

ACKNOWLEDGMENTS

The authors wish to acknowledge the Associazione Centro Dino Ferrari, Milan, Italy.

REFERENCES

1. Matthews E, Fialho D, Tan SV, Venance SL, Cannon SC, Sternberg D, et al. The non-dystrophic myotonias: molecular pathogenesis, diagnosis and treatment. *Brain*. (2010) 133(Pt 1):9–22. doi: 10.1093/brain/awp294
2. Cannon SC. Sodium channelopathies of skeletal muscle. In: Chahine M. editor. *Voltage-gated Sodium Channels: Structure, Function and Channelopathies. Handbook of Experimental Pharmacology*. Cham: Springer (2017). p. 309–330. doi: 10.1007/164_2017_52
3. Männikkö R, Wong L, Tester DJ, Thor MG, Sud R, Kullmann DM, et al. Dysfunction of NaV1.4, a skeletal muscle voltage-gated sodium channel, in sudden infant death syndrome: a case-control study. *Lancet*. (2018) 391:1483–92. doi: 10.1016/S0140-6736(18)30021-7
4. Suetterlin K, Männikkö R, Hanna MG. Muscle channelopathies: recent advances in genetics, pathophysiology and therapy. *Curr Opin Neurol*. (2014) 27:583–90. doi: 10.1097/WCO.0000000000000127
5. Lion-François L, Mignot C, Vicart S, Manel V, Sternberg D, Landrieu P, et al. Severe neonatal episodic laryngospasm due to *de novo* SCN4A mutations. *Neurology*. (2010) 75:641–5. doi: 10.1212/WNL.0b013e3181ed9e96
6. Raja Rayan DL, Hanna MG. Skeletal muscle channelopathies: nondystrophic myotonias and periodic paralysis. *Curr Opin Neurol*. (2010) 23:466–76. doi: 10.1097/WCO.0b013e32833cc97e
7. Rosenfeld J, Sloan-Brown K, George AL Jr. A novel muscle sodium channel mutation causes painful congenital myotonia. *Ann Neurol*. (1997) 42:811–4. doi: 10.1002/ana.410420520
8. Wu FF, Takahashi MP, Pegoraro E, Angelini C, Colleselli P, Cannon SC, et al. A new mutation in a family with cold-aggravated myotonia disrupts Na(+) channel inactivation. *Neurology*. (2001) 56:878–84. doi: 10.1212/WNL.56.7.878
9. Fournier E, Viala K, Gervais H, Sternberg D, Arzel-Hézode M, Laforêt P, et al. Cold extends electromyography distinction between ion channel mutations causing myotonia. *Ann Neurol*. (2006) 60:356–65. doi: 10.1002/ana.20905
10. Petitprez S, Tiab L, Chen L, Kappeler L, Rösler KM, Schorderet D, et al. A novel dominant mutation of the Nav1.4 subunit domain I leading to sodium channel myotonia. *Neurology*. (2008) 7:1669–75. doi: 10.1212/01.wnl.0000335168.86248.55
11. Trip J, Drost G, Verbove DJ, van der Kooi AJ, Kuks JB, Notermans NC, et al. In tandem analysis of CLCN1 and SCN4A greatly enhances mutation detection in families with non-dystrophic myotonia. *Eur J Hum Genet*. (2008) 16:921–9. doi: 10.1038/ejhg.2008.39
12. Zaharieva IT, Thor MG, Oates EC, van Karnebeek C, Hendson G, Blom E, et al. Loss-of-function mutations in SCN4A cause severe foetal hypokinesia or 'classical' congenital myopathy. *Brain*. (2016) 139(Pt 3):674–91. doi: 10.1093/brain/awv352
13. Yang N, Ji S, Zhou M, Barchi RL, Horn R, George AL Jr. Sodium channel mutations in paramyotonia congenita exhibit similar biophysical phenotypes *in vitro*. *Proc Natl Acad Sci USA*. (1994) 91:12785–9. doi: 10.1073/pnas.91.26.12785
14. Thor MG, Vivekanandam V, Sampedro-Castañeda M, Veronica TS, Suetterlin K, Sud R, et al. Myotonia in a patient with a mutation in an S4 arginine residue associated with hypokalaemic periodic paralysis and a concomitant synonymous CLCN1 mutation. *Sci Rep*. (2019) 9:17560. doi: 10.1038/s41598-019-54041-0
15. Rossignol E, Mathieu J, Thiffault I, Tétreault M, Dicaire MJ, Chrestian N, et al. A novel founder SCN4A mutation causes painful cold-induced myotonia in French-Canadians. *Neurology*. (2007) 69:1937–41. doi: 10.1212/01.wnl.0000290831.08585.2c
16. Vicart S, Sternberg D, Fontaine B, Meola G. Human skeletal muscle sodium channelopathies. *Neurol Sci*. (2005) 26:194–202. doi: 10.1007/s10072-005-0461-x
17. Wang Z. miRNA in the regulation of ion channel/transporter expression. *Compr Physiol*. (2013) 3:599–653. doi: 10.1002/cphy.c110002
18. Arzel-Hézode M, Sternberg D, Tabti N, Vicart S, Goizet C, Eymard B, et al. Homozygosity for dominant mutations increases severity of muscle channelopathies. *Muscle Nerve*. (2010) 41:470–7. doi: 10.1002/mus.21520

Conflict of Interest: The authors declare that the research was conducted in the absence of any commercial or financial relationships that could be construed as a potential conflict of interest.

The handling editor declared a past co-authorship with one of the authors with several of the author MS.

Copyright © 2020 Pagliarani, Lucchiari, Scarlato, Redaelli, Modoni, Magri, Fossati, Previtali, Sansone, Lecchi, Lo Monaco, Meola and Comi. This is an open-access article distributed under the terms of the Creative Commons Attribution License (CC BY). The use, distribution or reproduction in other forums is permitted, provided the original author(s) and the copyright owner(s) are credited and that the original publication in this journal is cited, in accordance with accepted academic practice. No use, distribution or reproduction is permitted which does not comply with these terms.

frontiers in Neurology

ORIGINAL RESEARCH
published: 20 May 2020
doi: 10.3389/fneur.2020.00300

Long-Term Safety and Usefulness of Mexiletine in a Large Cohort of Patients Affected by Non-dystrophic Myotonias

Anna Modoni[1]*, *Adele D'Amico*[2], *Guido Primiano*[1], *Fiorentino Capozzoli*[3], *Jean-François Desaphy*[4] and *Mauro Lo Monaco*[1,5]

[1] Department of Geriatric, Neurologic, Orthopedics and Head-Neck Science, Area of Neuroscience, Institute of Neurology, Fondazione Policlinico Universitario A. Gemelli, IRCCS, Rome, Italy, [2] Unit of Neuromuscular and Neurodegenerative Diseases, Laboratory of Molecular Medicine, Department of Neurosciences, Bambino Gesú Children's Hospital, Rome, Italy, [3] Department of Neurosciences, Italian National Institute of Health, Rome, Italy, [4] Department of Biomedical Sciences and Human Oncology, University of Bari Aldo Moro, Polyclinic, Bari, Italy, [5] MiA Onlus ("Miotonici in Associazione"), Portici, Italy

Objective: The aim of our study was to evaluate the long-term efficacy and safety of mexiletine in 112 patients affected by genetically confirmed non-dystrophic myotonias. The study was performed at the Neurophysiologic Division of Fondazione Policlinico Universitario A. Gemelli Istituto di Ricerca e Cura a Carattere Scientifico (IRCCS), Rome and the Children's Hospital Bambino Gesù, Rome.

Methods: The treatment was accepted by 59 patients according to clinical severity, individual needs, and concerns about a chronic medication. Forty-three patients were affected by recessive congenita myotonia, 11 by sodium channel myotonia, and five by dominant congenital myotonia. They underwent clinical examination before and after starting therapy, and Electromyography (EMG). A number of recessive myotonia patients underwent a protocol of repetitive nerve stimulations, for detecting and quantifying the transitory weakness, and a modified version of the Timed Up and Go test, to document and quantify the gait impairment.

Results: Treatment duration ranged from 1 month to 20 years and the daily dosages in adults ranged between 200 and 600 mg. No patient developed cardiac arrhythmias causing drug discontinuation. Mexiletine was suspended in 13 cases (22%); in three patients, affected by Sodium Channel myotonia, because flecainide showed better efficacy; in one patient because of a gastric cancer antecedent treatment; in four patients because of untreatable dyspepsia; and five patients considered the treatment not necessary.

Conclusions: In our experience, mexiletine is very useful and not expensive. We did not observe any hazarding cardiac arrhythmias. Dyspepsia was the most frequent dose-limiting side effect.

Keywords: mexiletine, non-dyspophyc myotonias, treatment tolerability, adverse effects, genotype-phenotype correlations

OPEN ACCESS

Edited by:
Rosanna Cardani,
IRCCS Policlinico San Donato, Italy

Reviewed by:
Giovanni Meola,
University of Milan, Italy
Carmelo Rodolico,
University of Messina, Italy

***Correspondence:**
Anna Modoni
anna.modoni@policlinicogemelli.it

Specialty section:
This article was submitted to Neuromuscular Diseases, a section of the journal Frontiers in Neurology

Received: *20 November 2019*
Accepted: *30 March 2020*
Published: *20 May 2020*

Citation:
Modoni A, D'Amico A, Primiano G, Capozzoli F, Desaphy J-F and Lo Monaco M (2020) Long-Term Safety and Usefulness of Mexiletine in a Large Cohort of Patients Affected by Non-dystrophic Myotonias. Front. Neurol. 11:300. doi: 10.3389/fneur.2020.00300

INTRODUCTION

Non-dystrophic myotonias are due to loss-of-function mutations in the voltage-gated chloride ClC-1 channel, encoded by the *CLCN1* gene, or gain-of-function mutations in the voltage-gated sodium Nav1.4 channel, encoded by the *SCN4A* gene (1–3). These are rare disorders, with a prevalence of < 1:100,000, characterized by clinical and electrophysiological myotonia, which is lifelong and impact quality of life. Today the drug of choice for treating myotonia is mexiletine, whatever the culprit gene (4–6). Mexiletine is a non-selective voltage-gated sodium channel blocker that belongs to the Class IB anti-arrhythmic drugs (6, 7).

In Italy, as in many other European countries, mexiletine was no longer available on the market, but since 2010 it can be obtained from the Military Chemical Pharmaceutical Plant of Florence (Stabilimento Chimico Farmaceutico Militare di Firenze) as a "named-patient" drug. Costs are entirely covered by the Italian National Health System.

Because of its activity on the heart, patients usually consider mexiletine a risky drug with potential cardiac side effects, a consideration that is often shared by primary care physicians despite literature data showing the absence of any significant change in Electrocardiogram (ECG) parameter or serious adverse cardiac event during long-term follow-up (6). On the other hand, some common non-cardiac side effects such as dyspepsia, nausea, heartburn, lightheadedness, and others are often dose-limiting (7).

The aims of this study were to evaluate the long-term efficacy and safety of mexiletine in 59 patients affected by non-dystrophic myotonias. The patients underwent clinical and neurophysiologic examination before and after treatment.

METHODS

Between 1999 and 2019, 112 patients affected by non-dystrophic myotonias have been followed at the Neurophysiologic Division of Fondazione Policlinico Universitario A. Gemelli IRCCS, Rome, and the Children's Hospital Bambino Gesù, Rome. Among these patients, 59 (33 males and 26 females) have accepted the suggestion of a symptomatic treatment and have been treated with mexiletine. Follow-up visits of treated patients have been scheduled every 6 months during the first year after starting treatment and then every year. Daily dosage and any side effects have been reported in each medical record.

Clinical Examination

All the patients have undergone an in-depth clinical assessment. Clinical examination included searching for action myotonia wrist, eyelid, and tongue muscles, as well as percussion myotonia in the upper limbs (*extensor digitorum communis*) and lower limbs (*rectus femori*). In particular, the presence and duration of the myotonic phenomenon at wrist and eyelid was evaluated after a three-second forced closure. This maneuver was repeated five times subsequently in order to detect any paradoxical myotonia. Before looking for eyelid myotonia, the presence of lid-lag phenomenon was verified in patients lying in a supine position. The presence of transitory weakness was verified by asking the patient to exert a maximal voluntary contraction of *biceps brachii*: as soon as the muscle reached its peak force, a quick exhaustion developed, lasting until the muscle was allowed to relax and contract for four or five times. The muscle could fully recover only after such a warming up maneuver.

In addition, we examined the lower limbs motor difficulties that may occur due to either myotonia or transitory weakness by using a modified version of the Timed Up and Go test (8, 9). Specifically, patients were asked to run around a chair three times, first after rest (i.e., 5 min of sitting on the chair in a complete relaxed position, with extended legs) and then after warming up. We calculated the percentage difference between the time spent to perform the test at rest and after warming up as follows: (time at rest – time after warm-up) × 100/time at rest (chair test normal values: mean: 4.7%; SD: 8.0; $n = 22$; cut-off: 21%).

We also paid attention to muscle hypertrophy (grading 1–4), especially in neck and shoulders for NaM patients and lower limbs for MC patients.

Neurophysiological Examination

All the patients were examined by needle EMG on *extensor digitorum communis* in order to detect myotonic discharges.

Clinical assessment oriented neurophysiologic evaluations, since different electromyographic patterns correlate with different pathogenic mechanism of muscle channelopathies (10–12). In particular, in our cohort of patients we performed the low-rate prolonged repetitive nerve stimulations (3Hz-RNS) to detect and quantify the transitory weakness of the intrinsic muscles of the hand (12). This test showed good tolerability and reproducibility, being performed before and after treatment. In short, the wrist ulnar nerve was stimulated at 3 Hz and the compound muscle action potential (CMAP) recorded from the *aductor digiti quinti* muscle. In some individuals, a transient depression of the CMAP amplitude developed during stimulation, reaching the nadir within about 30 s and recovering within 1 min of stimulation (12, 13). This transitory CMAP depression is considered the neurophysiological counterpart of the transitory weakness (14, 15).

Genetic Analysis

Genetic analyses were performed based on clinical and electrophysiological findings. In presence of a prevalent neck or shoulder muscle hypertrophy together with eyelid myotonia, especially when paradoxical, strabismus, transitory diplopia, and/or referred adynamia, the mutational analysis was first on *SCN4A*. When the clinical features were mainly characterized by muscle hypertrophy of lower limbs, a more severe myotonia in the upper limbs compared to facial muscles, or in cases of transitory weakness, presence of mutations was first verified in *CLCN1*.

Cardiac Evaluation

Before starting treatment with mexiletine, the patients performed a cardiac evaluation including a 12-derivations EKG and, if necessary, a 24 h-EKG monitoring. A cardiac follow-up was performed every year.

TABLE 1 | Demographics of the cohort of patients affected by non-dystrophic myotonias.

	All the patients	RCM	DCM	NaM
	112	60	26	26
Not treated	53 (47%)	17 (28%)	21 (81%)	15 (58%)
Treated with mexiletine	59 (53%)	43 (72%)	5 (19%)	11 (42%)
Situation on 2019-01-01				
Still on mexiletine	46 (78%)			
Drop-out	13 (22%)			
Duration of treatment				
<1 year	1 (7 drop-out)			
1–4 years (mean range: 2.5 years)	14 (2 drop-out)			
4–7 years (mean range: 5.5 years)	15 (1 drop-out)			
>7 (until 20) years (mean range: 13.5 years)	16 (3 drop-out)			

RCM, Recessive Congenital Myotonia; DMC, Dominant Congenital Myotonia; NaM, Myotonia due to Sodium Channel (SCN4A) Mutation.

TABLE 2 | Main adverse effects during mexiletine treatment.

Number of treated patients (59)	Mexiletine side effects	
29 (49%)	No side effects	
25	Dyspepsia	Mild Dyspepsia (no symptomatic drugs): 17
		Moderate Dyspepsia (dose limiting): 4
		Severe Dyspepsia (drop-out): 4
3	Insomnia	
1	Headache	
1	Dizziness	
1	Diarrhea	
1	Drowsiness	
3	"Intolerable" bitter taste	

Statistics

Average values are reported as mean ± SE. Statistical analysis was performed by using the paired Student's *t*-test.

Among patients affected by recessive congenital myotonia (RCM), we found several patients carrying the same mutation. Therefore, in each specific group of patients, we compared data obtained by 3Hz-RNS as well as Chair Test, also considering the different dosage of mexiletine in the three groups.

RESULTS

Cohort Demographics

From the 112 patients affected by non-dystrophic myotonia with confirmed genetic diagnostic (55 males and 57 females, aged 2–78 years), two came from Albania, two from Romania, one from Egypt, one from Morocco, one from Guatemala, and all the others from Italy (26 from Southern, 68 from Central, and 11 from Northern Italy). The mutations in *CLCN1* gene encoding the ClC-1 chloride channel were the most frequent (77%), especially the recessive ones (54%).

All the patients were offered treatment and only 52% accepted.

Mexiletine Dosage

Fifty-nine patients (33 males and 26 females) are or have been treated with mexiletine (**Table 1**). Until now, six of them are under 18 years and two of them are under 12. Patients under 12 are taking mexiletine at a dosage of 8 mg/Kg b.w. In adults and teenagers, the daily dosage range was between 200 and 600 mg according to clinical severity and individual needs.

Considering all the 59 treated patients, 43 (73%) were affected by recessive chloride channel myotonia (RCM), 11 (19%) had sodium channel myotonia (NaM), and five (8%) showed dominant chloride channel myotonia (DCM). Thus, 72% of all RCM patients, 19% of DCM, and 42% of NaM patients required treatment. Mexiletine treatment duration is reported in **Table 1**.

Adverse Effects

Mexiletine has been discontinued in 13 cases (22%), in most cases within the first months of treatment (five patients during the first month and two within the sixth month of treatment).

Within the first year of treatment, 2 patients suspended treatment because of intolerable side effects, especially dyspepsia, while one patient decided to test another drug. Within 1 and 7 years of treatment, drug suspension was observed in three other patients due to side effects or personal motivations. Regarding the treatment period of 7–20 years, three patients affected by Na channel myotonia discontinued mexiletine to test flecainide. They experienced a dramatic clinical improvement with flecainide, as hypothesized by *in vitro* pharmacological studies (16–19). In three pediatric cases, a galenic formulation of mexiletine using sweetening drops was necessary because of bitter taste, when dosages lower than 200 mg were requested, or in presence of difficulty in swallowing capsules.

No cardiac arrhythmias have been detected. All the reported side effects of mexiletine are summarized in **Table 2**.

Thus, four patients (7%) stopped mexiletine because of side effects, especially dyspepsia. Three patients (5%) shifted treatment to flecainide because of better efficacy. Five patients (8%) suspended the drug for personal motivations, while they were assuming mexiletine 200 mg/day (all these patients were affected by mild forms of myotonia and preferred not to establish a drug "addiction"), and one patient because of a gastric cancer pre-existent the treatment. In addition, four patients had to reduce daily drug doses from 600 to 400 mg/day because of the occurrence of dyspepsia.

Genotype-Phenotype Correlations

In the RCM group, the most frequent *CLCN1* mutations were p.F167L ($n = 15$), the intronic c.180+3A>T ($n = 9$), and p.G190S ($n = 6$). Only eight patients (53%) carrying p.F167L took an anti-myotonic treatment, while all the patients carrying c.180+3A>T or p.G190S required treatment.

TABLE 3 | Characterization of patients affected by recessive congenital myotonia carrying different *CLCN1* mutations.

Genotype	F167L	G190S or 180+3A>T	F167L; G190S; 180+3A>T treated vs. untreated pts
Number of patients	15	15	8 vs. 8
Mean mexiletine dosage (mg/die) (mean standard error)	160 (48)	460 (40), $p < 0.001$	
TD (mean standard error)	−4.5 (1.6)	−58 (5.9), $p < 0.001$	−18.4 (7.3) vs. −49.6 (12.5), $p < 0.01$
Chair test (mean standard error)	22.43 (4.3), $n = 7$	34.3 (3.2), $n = 12$, $p < 0.05$	22.8 (3.9) vs. 33.6 (6.2), $p < 0.05$

In the last column comparison between treated and untreated patients (n = 8).
TD, Nadir percent value of transitory CMAP depression during 3 Hz repetitive nerve stimulation. Chair test, three turns around a chair; percent amelioration after warm-up. Statistical analysis was performed with paired Student's t-test.

Before starting the drug, all these patients were examined using the 3Hz-RNS test. The Chair Test was performed in seven patients carrying p.F167L and in 12 patients carrying c.180+3A>T or p.G190S.

Table 3 shows the mean daily mexiletine dosage, the mean percent CMAP depression induced by 3Hz-RNS, and the mean percent time reduction measured by the Chair Test before and after warming up in all three groups of patients. We used a cut-off of −10% for 3Hz-RNS and +21% for the Chair Test (unpublished data). In the p.F167L group, only one patient resulted positive at both 3Hz-RNS and Chair Test, and only three out of 15 were positive to either 3Hz-RNS or Chair Test. In contrast, all the patients carrying p.G190S resulted positive to both tests. Likewise, all the patients carrying c.180+3A>T were positive to at least one of the two tests (8/9 positive to 3Hz-RNS and 4/6 to Chair test).

Importantly, we performed 3Hz-RNS and Chair Test in eight patients (two carrying p.F167L and six carrying p.G190S or c.180+3A>T) both before and during treatment: both tests showed a significant improvement during mexiletine treatment (**Table 3**).

DISCUSSION

It is worth noting that this study presents the limitations of a retrospective study and does not compare the treatment group to the non-treated patients. In addition, the population was not homogeneous due the different genes involved as well as their different mutations. Finally, the impact of myotonia on the limitation of the daily life activities is quite difficult to evaluate.

Notwithstanding, the study provides useful information on long-term mexiletine effects in a quite large cohort of myotonic patients followed up in a single center, taking also in account the rarity of these disorders. A multicenter study would allow examining a larger cohort but might also increase the risk of bias due to patients' evaluation in different centers by different physicians.

Mexiletine was a safe drug in most of the patients, as reported in other cohorts (4, 6). None of the treated patients developed cardiac arrhythmias or other severe side effects requiring drug discontinuation. Even in a pediatric patient aged three and affected by Wolf-Parkinson-White syndrome (WPW), mexiletine proved to be safe and the girl, now aged eight, is still on therapy. Although the treated population showed a predominance of patients with chloride channel mutations on those carrying sodium channel mutations, it is unlikely that safety was influenced by the genotype. Thus, we can assume a good profile of tolerance also in patients affected by NaM.

Considering the seven patients (12%) who discontinued mexiletine within the sixth month of treatment, five cases did not report any side effect and only one patient asked for another treatment. Thus, in our experience, the most important factor affecting the use of a symptomatic therapy is the patient's concern of taking medications "forever." For instance, some patients adjusted the doses of mexiletine according to their physical activity. The five patients who decided to suspend any form of symptomatic treatment within the first month can be added to the 53 patients who refused to try any treatment from the very beginning, raising the number of "skeptical or not interested to any treatment" individuals to 58 (52%) and lowering the number of "motivated to treatment" patients to 54 (48%). All the "skepticals" were mildly affected, whereas severely affected myotonic patient never refused treatment.

Not tolerated side effects were responsible for drug discontinuation in four cases (7%) and dose reduction in other four patients (7%). In particular, dyspepsia was the most frequent dose-limiting side effect, as previously reported (4, 6, 7).

We observed that patients affected by RCM requested an anti-myotonic therapy more than patients affected by NaM. This observation seems to be in contrast with literature data regarding the greater intensity of myotonia in NaM (6). However, quantification of myotonia is very difficult and no data are available about correlations between daily doses of mexiletine and the entity of myotonic phenomenon.

It could be very difficult to merge non-dystrophic myotonias in a single group of disorders, considering the variability in severity and distribution of myotonia, which primarily affects the head-neck muscles in NaM and the limb muscles in RCM/DCM. Moreover, the possible association with other signs or symptoms such as paradoxical myotonia, transitory weakness, cold sensitivity, myalgia, or episodes of paralysis, and the warm-up phenomenon, contribute to make the clinical and neurophysiologic diagnosis, as well as the quantification of myotonia severity, very challenging. For instance, there is no single neurophysiologic test available to give an objective rating to the severity of the different clinical manifestations in different patients. Similarly, the rating scales, such as SF-36 (20) and INQoL (21), giving a global evaluation of self-reported health status and impact of disease on quality of life in myotonia (4, 22–25), do not always show comparable data, possibly because of different social and cultural background (22).

Considering all these limitations, we focused our attention on a selected group of patients affected by RCM carrying the most common *CLCN1* mutations (p.F167L, c.180+3A>T, p.G190S) with the aim of evaluating the sensitivity and specificity of our clinical and neurophysiologic tests, either in the assessment of clinical severity or in monitoring the efficacy of a treatment. Thus, we compared between these patient subgroups the results of 3Hz-RNS, which indirectly evaluates transitory weakness, and the Chair Test, which estimates the motor impairment due to myotonia alone or together with transitory weakness.

In experimental functional studies, the p.F167L mutation showed little effects on chloride channel function (26–28), while p.G190S causes a severe channel dysfunction "*in vitro*" (28–30). Likewise, we observed that both "*in vivo*" tests showed better results in patients carrying p.F167L compared with those carrying p.G190S or c.180+3A>T. Accordingly, only eight patients (53%) carrying p.F167L took an anti-myotonic treatment, while all the patients carrying c.180+3A>T or p.G190S required treatment (**Table 3**). In addition, the treated p.F167L patients showed much better results at both neurophysiological and clinical tests.

Last but not least, mexiletine is not only safe but, in Italy, is reasonably priced and easily available for adult treatment. Some difficulties can be experienced in the pediatric setting due to the unavailability of specific formulations for this age group, requiring the use of a galenic formulation of mexiletine sweetened drops. Thus, a formulation of mexiletine alternative to the capsule as syrup or drops would be very useful, especially for pediatric patients, considering the importance of an early treatment for a correct psychomotor development. Indeed, it has been recently highlighted that *SCN4A* variants may determine relevant symptoms in neonates, compromising respiratory and laryngeal function, and might be associated with Sudden Infant Death Syndrome (31, 32).

DATA AVAILABILITY STATEMENT

The datasets generated for this study are available on request to the corresponding author.

ETHICS STATEMENT

The study was carried out in compliance with Helsinky Declaration, approved by the Ethic Committee-Fondazione Policlinico Universitario A. Gemelli, Rome, Italy (ethical approved ID 3075), and all patients gave a written informed consent authorizing storage and use of clinical data and DNA samples for any clinical research purpose about their data.

AUTHOR CONTRIBUTIONS

AM drafted the manuscript for intellectual content. AD'A analyzed data concerning pediatric patients. GP analyzed data with particular attention to adult patients. FC revised the text. JD critically revised the manuscript. ML conceptualized and designed the study.

ACKNOWLEDGMENTS

We thank all patients participating to the study and the parents' association MiA Onlus (Miotonici in Associazione), Portici, Italy. Publication fees were covered by MiA Onlus association.

REFERENCES

1. Suetterlin K, Männikkö R, Hanna MG. Muscle channelopathies: recent advances in genetics, pathophysiology and therapy. *Curr Opin Neurol.* (2014) 27:583–90. doi: 10.1097/WCO.0000000000000127
2. Cannon SC. Channelopathies of skeletal muscle excitability. *Compr Physiol.* (2015) 5:761–90. doi: 10.1002/cphy.c140062
3. Phillips L, Trivedi JR. Skeletal muscle channelopathies. *Neurotherapeutics.* (2018) 15:954–65. doi: 10.1007/s13311-018-00678-0
4. Statland JM, Bundy BN, Wang Y, Rayan DR, Trivedi JR, Sansone VA, et al. Mexiletine for symptoms and signs of myotonia in nondystrophic myotonia: a randomized controlled trial. *JAMA.* (2012) 308:1357–65. doi: 10.1001/jama.2012.12607
5. Imbrici P, Liantonio A, Camerino GM, De Bellis M, Camerino C, Mele A, et al. Therapeutic approaches to genetic ion channelopathies and perspectives in drug discovery. *Front Pharmacol.* (2016) 7:121. doi: 10.3389/fphar.2016.00121
6. Suetterlin KJ, Bugiardini E, Kaski JP, Morrow JM, Matthews E, Hanna MG, et al. Long-term safety and efficacy of mexiletine for patients with skeletal muscle channelopathies. *JAMA Neurol.* (2015) 72:1531–3. doi: 10.1001/jamaneurol.2015.2338
7. Singh S, Zeltser R. Mexiletine. *StatPearls [Internet]*. Treasure Island, FL: StatPearls Publishing (2018).
8. Podsiadlo D, Richardson S. The timed "Up & Go": a test of basic functional mobility for frail elderly persons. *J Am Geriatr Soc.* (1991) 39:142–8. doi: 10.1111/j.1532-5415.1991.tb01616.x
9. Hammaren E, Kjellby-Wendt G, Lindberg C. Quantification of mobility impairment and self-assessment of stiffness in patients with myotonia congenita by the physiotherapist. *Neuromuscul Disord.* (2005) 15:610–7. doi: 10.1016/j.nmd.2005.07.002
10. Fournier E, Arzel M, Sternberg D, Vicart S, Laforet P, Eymard B, et al. Electromyography guides toward subgroups of mutations in muscle channelopathies. *Ann Neurol.* (2004) 56:650–61. doi: 10.1002/ana.20241
11. Tan SV, Z'Graggen WJ, Boërio D, Rayan DR, Norwood F, Ruddy D, et al. Chloride channels in myotonia congenita assessed by velocity recovery cycles. *Muscle Nerve.* (2014) 49:845–57. doi: 10.1002/mus.24069
12. Modoni A, D'Amico A, Dallapiccola B, Mereu ML, Merlini L, Pagliarani S, et al. Low-rate repetitive nerve stimulation protocol in an Italian cohort of patients affected by recessive myotonia congenita. *J Clin Neurophysiol.* (2011) 28:39–44. doi: 10.1097/WNP.0b013e31820510d7
13. Lo Monaco M, D'Amico A, Luigetti M, Desaphy JF, Modoni A. Effect of mexiletine on transitory depression of compound motor action potential in recessive myotonia congenita. *Clin Neurophysiol.* (2015) 126:399–403. doi: 10.1016/j.clinph.2014.06.008
14. Aminoff MJ, Layzer RB, Satya-Murti S, Faden AI. The declining electrical response of muscle to repetitive nerve stimulation in myotonia. *Neurology.* (1977) 27:812–6. doi: 10.1212/WNL.27.9.812
15. Brown CB. Muscle weakness after rest in myotonic disorders: an electrophysiological study. *J Neurol Neurosurg Psychiatry.* (1974) 37:1336–42. doi: 10.1136/jnnp.37.12.1336

16. Desaphy JF, De Luca A, Didonna MP, George AL Jr, Camerino Conte D. Different flecainide sensitivity of hNav1.4 channels and myotonic mutants explained by state-dependent block. *J Physiol.* (2004) 554:321–34. doi: 10.1113/jphysiol.2003.046995
17. Desaphy JF, Modoni A, Lomonaco M, Camerino DC. Dramatic improvement of myotonia permanens with flecainide: a two-case report of a possible bench-to-bedside pharmacogenetics strategy. *Eur J Clin Pharmacol.* (2013) 69:1037–9. doi: 10.1007/s00228-012-1414-3
18. Desaphy J-F, Carbonara R, D'Amico A, Modoni A, Roussel J, Imbrici P, et al. Translational approach to address therapy in myotonia permanens due to a new SCN4A mutation. *Neurology.* (2016) 86:2100–8. doi: 10.1212/WNL.0000000000002721
19. Lehmann-Horn F, D'Amico A, Bertini E, LoMonaco M, Merlini L, Nelson KR, et al. Myotonia permanens with Nav1.4-G1306E displays varied phenotypes during course of life. *Acta Myol.* (2017) 36:125–34.
20. Ware JE, Sherbourne CD. The MOS 36-item short-form health survey (SF-36). I. Conceptual framework and item selection. *Med Care.* (1992) 30:473–83. doi: 10.1097/00005650-199206000-00002
21. Vincent KA, Carr AJ, Walburn J, Scott DL, Rose MR. Construction and validation of a quality of life questionnaire for neuromuscular disease (INQoL). *Neurology.* (2007) 68:1051–7. doi: 10.1212/01.wnl.0000257819.47628.41
22. Trivedi JR, Bundy B, Statland J, Salajegheh M, Rayan DR, Venance SL, et al. Non-dystrophic myotonia: prospective study of objective and patient reported outcomes. *Brain.* (2013) 136:2189–200. doi: 10.1093/brain/awt133
23. Sansone VA, Ricci C, Montanari M, Apolone G, Rose M, Meola G, INQoL Group. Measuring quality of life impairment in skeletal muscle channelopathies. *Eur J Neurol.* (2012) 19:1470–6. doi: 10.1111/j.1468-1331.2012.03751.x
24. Matthews E, Fialho D, Tan SV, Venance SL, Cannon SC, Sternberg D, et al. The non-dystrophic myotonias: molecular pathogenesis, diagnosis and treatment. *Brain.* (2010) 133:9–22. doi: 10.1093/brain/awp294
25. Andersen G, Hedermann G, Witting N, Duno M, Andersen H, Vissing J. The antimyotonic effect of lamotrigine in non-dystrophic myotonias: a double-blind randomized study. *Brain.* (2017) 140:2295–305. doi: 10.1093/brain/awx192
26. Zhang J, Bendahhou S, Sanguinetti MC, Ptácek LJ. Functional consequences of chloride channel gene (CLCN1) mutations causing myotonia congenita. *Neurology.* (2000) 54:937–42. doi: 10.1212/WNL.54.4.937
27. Lucchiari S, Ulzi G, Magri F, Bucchia M, Corbetta F, Servida M, et al. Clinical evaluation and cellular electrophysiology of a recessive CLCN1 patient. *J Physiol Pharmacol.* (2013) 64:669–78.
28. Desaphy J-F, Gramegna G, Altamura C, Dinardo MM, Imbrici P, George AL Jr, et al. Functional characterization of ClC-1 mutations from patients affected by recessive myotonia congenita presenting with different clinical phenotypes. *Exp Neurol.* (2013) 248:530–40. doi: 10.1016/j.expneurol.2013.07.018
29. Portaro S, Altamura C, Licata N, Camerino GM, Imbrici P, Musumeci O, et al. Clinical, molecular, and functional characterization of CLCN1 mutations in three families with recessive myotonia congenita. *Neuromolecular Med.* (2015) 17:285–96. doi: 10.1007/s12017-015-8356-8
30. Altamura C, Lucchiari S, Sahbani D, Ulzi G, Comi GP, D'Ambrosio P, et al. The analysis of myotonia congenita mutations discloses functional clusters of amino acids within the CBS2 domain and the C-terminal peptide of the ClC-1 channel. *Hum Mutat.* (2018) 39:1273–83. doi: 10.1002/humu.23581
31. Matthews E, Silwal A, Sud R, Hanna MG, Manzur AY, Muntoni F, et al. Skeletal muscle channelopathies: rare disorders with common pediatric symptoms. *J Pediatr.* (2017) 188:181–5. doi: 10.1016/j.jpeds.2017.05.081
32. Männikkö R, Wong L, Tester DJ, Thor MG, Sud R, Kullmann DM, et al. Dysfunction of NaV1.4, a skeletal muscle voltage-gated sodium channel, in sudden infant death syndrome: a case-control study. *Lancet.* (2018) 391:1483–92. doi: 10.1016/S0140-6736(18)30021-7

Conflict of Interest: The authors declare that the research was conducted in the absence of any commercial or financial relationships that could be construed as a potential conflict of interest.

Copyright © 2020 Modoni, D'Amico, Primiano, Capozzoli, Desaphy and Lo Monaco. This is an open-access article distributed under the terms of the Creative Commons Attribution License (CC BY). The use, distribution or reproduction in other forums is permitted, provided the original author(s) and the copyright owner(s) are credited and that the original publication in this journal is cited, in accordance with accepted academic practice. No use, distribution or reproduction is permitted which does not comply with these terms.

frontiers in Neurology

ORIGINAL RESEARCH
published: 19 June 2020
doi: 10.3389/fneur.2020.00541

Depletion of ATP Limits Membrane Excitability of Skeletal Muscle by Increasing Both ClC1-Open Probability and Membrane Conductance

Pieter Arnold Leermakers[1], Kamilla Løhde Tordrup Dybdahl[1], Kristian Søborg Husted[1], Anders Riisager[1], Frank Vincenzo de Paoli[1], Tomàs Pinós[2,3], John Vissing[4], Thomas Oliver Brøgger Krag[4] and Thomas Holm Pedersen[1]*

[1] Department of Biomedicine, Aarhus University, Aarhus, Denmark, [2] Mitochondrial and Neuromuscular Disorders Unit, Vall d'Hebron Institut de Recerca, Universitat Autònoma de Barcelona, Barcelona, Spain, [3] Centro de Investigación Biomédica en Red de Enfermedades Raras (CIBERER), Madrid, Spain, [4] Department of Neurology, Rigshospitalet, Copenhagen Neuromuscular Center, University of Copenhagen, Copenhagen, Denmark

Activation of skeletal muscle contractions require that action potentials can be excited and propagated along the muscle fibers. Recent studies have revealed that muscle fiber excitability is regulated during repeated firing of action potentials by cellular signaling systems that control the function of ion channel that determine the resting membrane conductance (G_m). In fast-twitch muscle, prolonged firing of action potentials triggers a marked increase in G_m, reducing muscle fiber excitability and causing action potential failure. Both ClC-1 and K_{ATP} ion channels contribute to this G_m rise, but the exact molecular regulation underlying their activation remains unclear. Studies in expression systems have revealed that ClC-1 is able to bind adenosine nucleotides, and that low adenosine nucleotide levels result in ClC-1 activation. In three series of experiments, this study aimed to explore whether ClC-1 is also regulated by adenosine nucleotides in native skeletal muscle fibers, and whether the adenosine nucleotide sensitivity of ClC-1 could explain the rise in G_m muscle fibers during prolonged action potential firing. First, whole cell patch clamping of mouse muscle fibers demonstrated that ClC-1 activation shifted in the hyperpolarized direction when clamping pipette solution contained 0 mM ATP compared with 5 mM ATP. Second, three-electrode G_m measurement during muscle fiber stimulation showed that glycolysis inhibition, with 2-deoxy-glucose or iodoacetate, resulted in an accelerated and rapid >400% G_m rise during short periods of repeated action potential firing in both fast-twitch and slow-twitch rat, and in human muscle fibers. Moreover, ClC-1 inhibition with 9-anthracenecarboxylic acid resulted in either an absence or blunted G_m rise during action potential firing in human muscle fibers. Third, G_m measurement during repeated action potential firing in muscle fibers from a murine McArdle disease model suggest that the rise in G_m was accelerated in a subset of fibers. Together, these results are compatible with ClC-1 function being regulated by the level of adenosine nucleotides in native tissue, and that the channel operates as a sensor of skeletal muscle metabolic state, limiting muscle excitability when energy status is low.

Keywords: skeletal muscle, ATP, membrane excitability, fatigue, membrane conductance, ClC-1, McArdle disease

OPEN ACCESS

Edited by:
Jean-François Desaphy, University of Bari Aldo Moro, Italy

Reviewed by:
Christoph Fahlke, Helmholtz-Verband Deutscher Forschungszentren (HZ), Germany
Bruno Allard, Université Claude Bernard Lyon 1, France

****Correspondence:***
Pieter Arnold Leermakers
pal@biomed.au.dk

Specialty section:
This article was submitted to Neuromuscular Diseases, a section of the journal Frontiers in Neurology

Received: *28 February 2020*
Accepted: *14 May 2020*
Published: *19 June 2020*

Citation:
Leermakers PA, Dybdahl KLT, Husted KS, Riisager A, de Paoli FV, Pinós T, Vissing J, Krag TOB and Pedersen TH (2020) Depletion of ATP Limits Membrane Excitability of Skeletal Muscle by Increasing Both ClC1-Open Probability and Membrane Conductance. Front. Neurol. 11:541. doi: 10.3389/fneur.2020.00541

INTRODUCTION

Skeletal muscle contractions support human overall health, underlying both body movement and posture, and ventilation. The ability to sustain contractile function over time, which enables prolonged physical activity during exercise, is both highly variable between different muscles and individuals, and determines the onset of muscle-fatigue (i.e., a state in which this contractile function becomes impaired and the muscular power output gradually declines). Multiple cellular mechanisms are likely to contribute to fatigue during exercise, depending on the type of exercise and type of muscle fibers being recruited by the nervous system (1).

The energy consumption of skeletal muscle increases dramatically when contracting during exercise, and a correlation between the metabolic state and performance of the muscle is well-known (2). Exhaustion of the muscular metabolic state may introduce fatigue, and excessive muscle fatigue is a well-recognized symptom in patients suffering from in-born metabolic myopathies involved in glycogen breakdown such as myophosphorylase deficiency (McArdle disease) (3). Mechanistically, several steps in the excitation-contraction coupling that link neuronal command to muscle force production are known to be sensitive to fluctuations in metabolites during exercise (2, 4).

Action potential excitation and propagation are essential steps in the normal activation of skeletal muscle fibers to generate muscle contractions, and surface membrane ion channels and ion transport proteins are key factors determining the electrophysiological properties and excitability of muscle fibers. The ClC-1 chloride (Cl^-) ion channel is a voltage-gated chloride channel (5), that is exclusively expressed in skeletal muscle to physiological relevant levels (5–7). This ion channel, which only has a single channel conductance of about 1 pS (8), accounts for 80% of the total ion permeability of the surface membrane of resting muscle fibers, a feature that is highly conserved among muscle fiber types and species (9–13).

The equilibrium potential for Cl^- is close to the resting membrane potential (V_m) in muscle fibers, because Cl^- is predominantly passively distributed across the muscle fiber surface membrane. Together, these properties of Cl^- (i.e., high Cl^- membrane conductance (G_{Cl}), passive Cl^- distribution, and the equilibrium potential that is close to resting V_m) enforce ClC-1-mediated Cl^- currents to stabilize the resting membrane potential. Therefore, G_{Cl} and muscle excitability are inversely related, with reduction in G_{Cl} enhancing muscle fiber excitability while a rise in G_{Cl} dampening excitability. A significant rise in G_{Cl} may even compromise muscle excitability and prevent muscle fiber activation, indicating that ClC-1 has the capability to serve as a physiological gatekeeper of the first step in the excitation-contraction coupling that underlies muscle activation (14–16).

During the last decade, the understanding of the biophysical properties of ClC-1, and the cellular signaling systems that regulate ClC-1 expression and function, has been greatly expanded. Interestingly, studies from expression systems suggest that adenosine nucleotides (i.e., ATP, ADP, and AMP) regulate the voltage dependency of the ClC-1 channel by binding to the large C-terminal part of the channel, between two cystathionine-β-synthase *(CBS)* domains (17–19). These studies show that adenosine nucleotide binding shifts the activation voltage of ClC-1 in the depolarizing direction, which implies that a loss of cellular adenosine levels could inversely cause the activation voltage of ClC-1 to shift in the hyperpolarizing direction, leading to an increased open probability at the resting membrane potential with consequent loss of muscle excitability. As ATP, ADP, and AMP had similar effects on ClC-1, the combined adenosine nucleotide levels would have to decrease for the channel to shift toward an increased opening probability. However, it is currently not clear whether ClC-1 is also regulated by adenosine nucleotides in native tissue.

Support for ClC-1 as a metabolic sensor in native tissue came from observations in action potential firing muscle fibers, where it was reported that prolonged action potential firing resulted in substantial ClC-1 activation in rodent fast-twitch muscle, leading to reduced muscle fiber excitability in combination with action potential excitation- and propagation failure. As this ClC-1 activation was rapidly reversible, this activation likely reflects physiological relevant ClC-1 regulation during skeletal muscle activity (20). Although ClC-1 is present in, and regulates the membrane conductance of, both fast- and slow-twitch fiber-types, this substantial action potential firing-induced ClC-1 activation was only observed in fast-twitch muscle fibers. As fast-twitch muscle fibers have been shown to undergo larger ATP-depletion during exercise than slow-twitch fibers (21), these results are compatible with a possible role of ClC-1 as a metabolic sensor linking metabolic state to muscle fiber excitability.

The cellular signaling that underlies ClC-1 activation during prolonged action potential firing remains incompletely understood, and there is no data available describing the relationship between adenosine nucleotides and ClC-1 activation in native skeletal muscle tissue. The present study aimed to explore if depletion of adenosine nucleotides results in increased ClC-1 opening in native tissue of muscle fibers. Such a mechanism of ClC-1 regulation may underlie the ClC-1 activation during prolonged action potential firing that has been observed in fast-twitch muscle fibers of rat and mice (20, 22, 23). Given that this ClC-1 activation has been observed in muscles with a fast-twitch fiber-type only, the present study also explored whether similar rises in membrane conductance can be triggered in both rat muscle with a slow-twitch fiber-type and in human abdominal muscle with a mixed fiber-type under conditions of compromised glycolysis. Moreover, as a proof-of-principle, this study explored whether skeletal muscle fibers of McArdle mice were prone to an accelerated increase in membrane conductance during repetitive action potential firing.

MATERIALS AND METHODS

Animals and Ethical Approval

C57BL/6 mice (3–4 week old, male/female), Wistar rats (12–14 week old, females), and McArdle mice (12 months old, male/female) were housed under 12 h light/dark conditions at 21°C and fed *ad libitum*. Wistar rats and C57BL/6 mice were euthanized by CO_2 exposure/inhalation, and McArdle mice

were anesthetized with s.c. injection of Hypnorm/Midazolam (0.01 ml/g, 25% Hypnorm, 25% Midazolam, 50% H_2O) and subsequently euthanized by cervical dislocation. Extensor digitorum longus (EDL), flexor digitorum brevis (FDB), or soleus (SOL) muscles were freshly harvested for experimental procedures. Both EDL and FDB contain predominantly fast-twitch fibers, while SOL contains predominantly slow-twitch fibers (24–26).

McArdle ($PYGM^{R50X/R50X}$) and representative wild-type ($PYGM^{wt/wt}$) mice were generated on a C57BL/6 background and extensively characterized as previously described (27, 28).

All handling and use of animals complied with Danish Animal Welfare regulations and was conducted in accordance with the European Convention for the Protection of Vertebrate Animals used for Experimental and Other Scientific Purposes (ETS 123). Experimental procedures were approved by the animal welfare officer at Aarhus University or Copenhagen University, and the complied with Danish Animal Experiments Inspectorate (permit no 2014-15-0201-00041).

Human Muscle Fibers and Ethical Approval

Human rectus abdominis muscle (HAM) biopsies were isolated as described elsewhere (29). In short, bundles of well-defined muscle fibers with tendinous insertions at both ends, measuring approx. 8 cm × 2 cm × 1, cm were isolated from human subjects undergoing for abdominal surgery. Subjects had no known neuromuscular diseases. HAM contains an almost equal contribution of fast- and slow-twitch fibers (30). The isolation and use of human skeletal muscle was approved by the Danish Ethics Committee, Region Midtjylland, Comité I (reference number 1-10-72-20-13), and experiments were performed in accordance with the Declaration of Helsinki. Informed consent was obtained from test subjects.

Whole Cell Patch Clamping

Muscle Preparation

C57BL/6 FDB muscles were incubated in HEPES-Ringer solution [122 mM NaCl, 15 mM Na-HEPES, 9 mM HCl, 2.8 mM KCl, 1.27 mM $CaCl_2$, 1.2 mM $MgSO_4$, 1.2 mM KH_2PO_4, 5 mM D-glucose and collagenase type 1 (2 mg/ml)] for 45 min at 37°C. Collagenase was removed by a serial removal of supernatant followed by washing in solution without collagenase. To dissociate the individual fibers, the muscles were triturated with Pasteur pipettes of decreasing pore size, and only fibers with maximal length of 400 μm and clear striation were used for experiments. Fibers were stored in HEPES-Ringer solution at 5°C, and all electrophysiological recordings were performed within 10 h after dissection.

Experimental Setup

The dissociated FDB fibers were mounted in an organ bath with a constant perfusion of extracellular (EC) solution [72.5 mM TEA-Cl, 1.2 mM $CaCl_2$, 6 mM $MgSO_4$, 120 mM HEPES, 20 μM nifedepine, pH 7.3 by CsOH (around 40 mM)], and they were allowed to adhere to the glass surface for 5 at least minutes before perfusion of chamber was started. Glass patch pipettes, with a maximum resistance of 2.5 MΩ, were pulled using a micropipette puller model P-97 (Sutter Instruments, California, US), and were back-filled with either an intracellular (IC) solution containing 0 mM ATP [10 mM BAPTA, 180 mM HEPES, 1.3 mM $MgSO_4$, 5 mM Na_2SO_4, 15 mM CsCl, pH 7.2 by CsOH (around 95 mM)] or 5 mM ATP [10 mM BAPTA, 174.5 mM HEPES, 5 mM Na_2ATP, 5.85 mM $MgSO_4$, 15 mM CsCl, pH 7.2 by CsOH (around 90 mM)].

To achieve similar free Mg^{2+} content in both solutions, the required amount of $MgSO_4$ was calculated with Maxchelator (Chris Patton, Stanford University, US). Muscle contractions were prevented by BAPTA (a highly selective Ca^{2+} chelator) ensuring a proper seal during recordings. Moreover, the composition of the IC and EC solutions prevented any K^+ (0 mM K^+, TEA-Cl and Cs^+) and Ca^{2+} (nifedepine) currents and allowed only negligible Na^+ currents (10 mM Na^+ in the IC solution).

Electrophysiology

ClC-1 current amplitude was determined in individual muscle fibers using the whole-cell voltage clamp technique controlled by a MultiClamp 700B Amplifier (Molecular Devices, California, US) and sampled using an analog-to-digital Micro1401-3 converter (Cambridge Electronic Design, UK). The voltage protocol and data acquisition were controlled using Signal 6.03 software (Cambridge Electronic Design, UK) with a sampling frequency of 40 kHz.

The glass pipettes were inserted in the experimental bath under a slight positive pressure. At first contact between the pipette and the fiber membrane, the positive pressure was released, and a negative pressure was generated to establish a tight seal between the glass pipette and the membrane. A minimum resistance of 1.5 GΩ was obtained before going whole-cell. To secure proper equilibration of the IC solution, no recordings were made for the first 8 min after establishing whole cell voltage control. Experiments were only possible in fibers where contractions were abolished by the BAPTA that was diffused into the muscle fibers. Hence only fibers where dialysis of the intracellular space had taken place could be used. During the recordings, the serial resistance was compensated to at least 90%. The voltage protocol started at −40 mV (holding potential), and consisted of multiple cycles that each contained a 200-ms depolarization step (+60 mV), a 250-ms variable "test" voltage step (between +60 to −140 mV), and a 200-ms constant step (−100 mV) (**Figure 1A**) from which the instantaneous current or tail current was obtained. This is a similar procedure to what has been used elsewhere (31). The holding potential of −40 mV corresponds to the calculated equilibrium potential for Cl^- under the experimental conditions and this meant that ClC-1 current would be minimal at the holding potential. Some leak current did develop over the course of the experiments that at least in part could reflect incomplete ClC-1 deactivation between sweeps. This was corrected for in the data analysis. The extracellular Cl^- concentration, which is lower relative to more physiological levels (74.9 vs. ∼140 mM), was chosen to minimize ClC-1 current to improve voltage control during the voltage steps. The variable "test" voltage started at −140 mV in the first cycle and increased with 10 mV with each cycle. Three

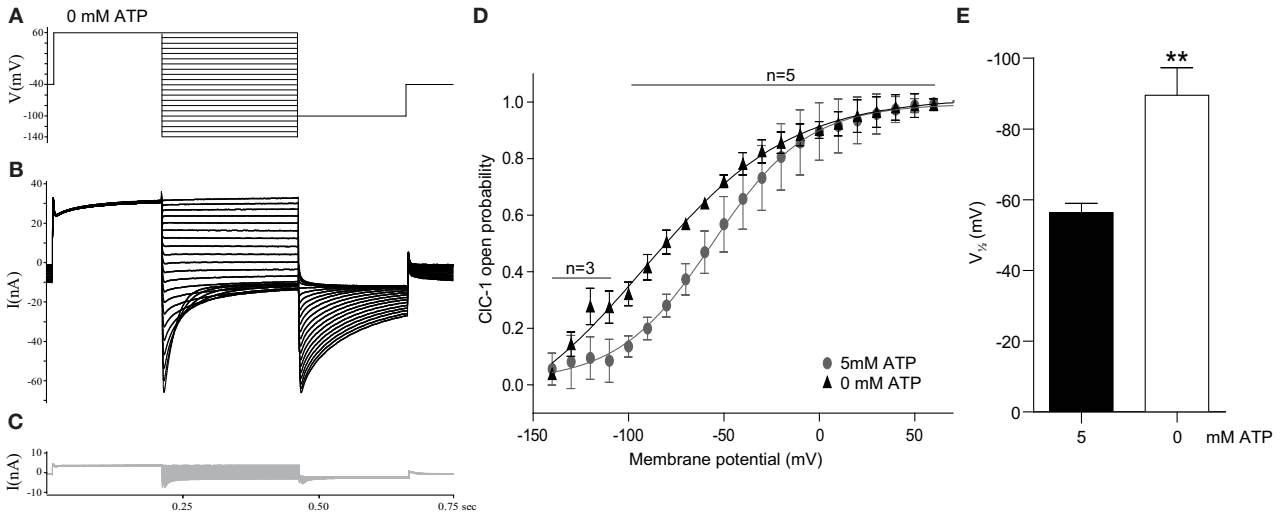

FIGURE 1 | ATP depletion results in an increased ClC-1 open probability. Isolated murine fast-twitch FDB muscle fibers were subjected to whole-cell patch clamping. **(A)** The protocol used to evoke currents through ClC-1 in fibers exposed to pipette solution with 0 or 5 mM ATP. **(B,C)** Examples of whole-cell current traces from a fiber before **(B)** and after **(C)** incubation with 400 μM 9-AC. **(D)** The average open probability of ClC-1 with either 0 or 5 mM ATP in the pipette. Data are depicted as average ± SD and the solid line represents a sigmoidal fit to the data. **(E)** The average $V_{½}$ for fibers exposed to pipette solution with 0 or 5 mM ATP. A *T*-test was performed to test significance of observed differences between 0 mM ATP ($n = 5$) and 5 mM ATP ($n = 5$) and $p < 0.01^{**}$ is depicted.

repeats were performed at each test voltage. In a few fibers, the test voltage started at −100 mV but this did not appear to affect the average data and it was judged acceptable to include all data. Measurements were performed first in absence and subsequent in presence of 400 μM 9-anthracenecarboxylic acid (9-AC). Leak current was subtracted in all recordings, and having recordings from the same fibers before and after 9-AC meant that residual leak-current and capacitive artifact could be eliminated by subtracting the measurement with 9-AC from the measurement without 9-AC. The 9-AC sensitive current was taken to represent ClC-1 current.

The open probability (P_o) of ClC-1 at the different clamping voltages was estimated from the peak tail currents at the −100 mV constant voltage step that followed the variable test voltage steps (**Figures 1A–C**). By comparing the peak tail currents that followed each test voltage step to the tail current obtained when the test pulse was +60 mV, the open probability (P_o) could be calculated and plotted against the clamping voltage step. Based on these calculations, the data from each fiber was fitted to the 4-parameter sigmoidal function (Equation 1):

$$P_{o(V)} = P_{o(r)} + \frac{a}{1 + \exp(\frac{V_{½} - V}{b})} \quad (1)$$

Where $P_{o(V)}$ is the channel open probability at the voltage V, $P_{o(r)}$ is a constant that represents the residual channel opening at infinitely hyperpolarized conditions, a represents the amplitude from the residual current to the maximal ClC-1 current at +60 mV (maximal P_o), b represents the slope, and $V_{½}$ represents the midpoint potential at which 50 % of a is achieved.

Two- and Three-Electrode Membrane Conductance Measurements in Action Potential Firing Muscle Fibers

Experimental Setup

Freshly excised skeletal muscles from Wistar rat (EDL or SOL), mice (McArdle mouse EDL), or human (HAM) were used in these experiments. In all cases, the muscles were mounted under slight tension in an organ bath containing Krebs-Ringer solution (122 mM NaCl, 25 mM $NaHCO_3$, 2.8 mM KCl, 1.2 mM KH_2PO_4, 1.2 mM $MgSO_4$, 1.3 mM $CaCl_2$). The solution was supplemented with 5.0 mM D-glucose (Sigma Aldrich, Denmark) (CTRL), 5.0 mM 2-deoxy-D-glucose (2DG, Sigma Aldrich, Denmark)/100 IU insulin (Humulin R, Lilly, USA), or 5.0 mM D-glucose + 100 μM iodoacetate (IAA, Sigma Aldrich, Denmark) as indicated. For experiments with 2DG, muscles were exposed to 2DG/insulin for at least 3 h before experiments were initiated. This was done to enable the proper loading of 2DG as facilitated by insulin into the muscle fibers to impose the metabolic challenge of compromise glycolytic flux. Other muscles were incubated in the organ bath for at least 20 min prior to initiating experiments. Pharmacological inhibition of ClC-1 was achieved by supplementing HAM muscle with 100 μM 9-Anthracenecarboxylic acid (9-AC, Sigma Aldrich, Denmark). 10 nM tetrodotoxin (TTX, Tocris, UK) was used to prevent spontaneous action potential firing in the presence of 9-AC. The buffer was continuously gassed with a mixture of 95% O_2/5% CO_2 (pH ≈ 7.4) and kept at 30°C. Glass pipettes (8–12 MΩ) were pulled using a micropipette puller model P-97 and back-filled with 2 M potassium-citrate.

To enable electrodes to remain inserted in the muscle fibers while repeatedly firing action potentials, the contractile activity

of the muscles was reduced by 50 μM N-benzyl-p-toluene sulphonamide (BTS, Toronto Research Chemicals, Canada) for EDL (32), and 25 μM blebbistatin (Sigma Aldrich, Denmark) for SOL or HAM. Previous studies have shown that these compounds have minimal effect on muscle excitability (20) and BTS was shown to reduce energy consummation during activity only by 20% (33). BTS and blebbistatin were dissolved in DMSO, which resulted in a maximal DMSO concentration of 0.15%, which did not affect resting conditions in muscles. BTS and blebbistatin were added to the solution that perfused the experimental chamber at least 30 min prior to start of measurements, and reduction in contractile activity was visually verified.

Individual muscle fibers and the electrodes were visualized using a Nikon DS-Vi1/Nikon Eclipse FN1 microscope. Electrodes were connected to TEC-05X clamp amplifier systems (NPI, Germany), and to a Power1401 converter (Cambridge Electronic Design, UK). The voltage protocol and data acquisition were controlled using Signal software (Cambridge Electronic Design, UK) with a sampling frequency of >30 kHz.

Electrophysiology

Electrophysiology was performed using the two-electrode technique for McArdle mice and three-electrode technique for Wistar rats and human muscle biopsy material as described previously (23).

G_m determination using three electrodes

Three electrodes (E_1-E_3) were placed into the same fiber, where the inter-electrode distance between E_2-E_3 (X_1) was twice the inter-electrode distance between E_1-E_2 (X_2, **Figure 2A**). Current *(I)* was first, injected by E_1 while the steady membrane potential response (ΔV) was measured with E_2 and E_3, and subsequently, current was injected by E_3 while ΔV was measured with E_1 and E_2. This resulted in the measurement of ΔV at three different distances on the fiber (X_1-X_3). The transfer resistances at the different inter-electrode distances were calculated by dividing ΔV by I, and they were plotted against the respective inter-electrode distances and, finally fitted to the cable equation (Equation 2) that applies to cells of infinite length with a membrane represented by a parallel RC circuit (34). R_{in} and λ refer to the fiber input resistance and length constant of the fiber that were obtained from the cable equation fit (Equation 2):

$$\Delta V(x) = \Delta V_{x=0} \exp(-x\lambda^{-1}) = IR_{in} \exp(-x\lambda^{-1}) \quad (2)$$

$\Delta V(x)$ represents the steady state change in membrane potential at position x relative to where the current was injected at $x = 0$. From R_{in} and λ the membrane resistance per unit length of fiber (r_m), the intracellular resistance per length of muscle fiber (r_i), and the membrane conductance per unit length of fiber (g_m) were calculated:

$$r_m = 2R_{in}\lambda = (g_m)^{-1} \quad (3)$$

$$r_i = \frac{2R_{in}}{\lambda} \quad (4)$$

G_m, the surface membrane specific conductance, was then calculated by dividing g_m with the surface area per unit length of fiber (*FSA*). In resting muscle fibers a common approach for estimating *FSA* is to first determine the cross sectional area of the fiber (*CSA*) from r_i assuming a constant value for the specific sarcoplasmic resistivity (R_i), here taken to be 180 Ω cm as determined in resting fibers (35), using Equation 5:

$$r_i = \frac{R_i}{CSA} \quad (5)$$

Next, by assuming the muscle fiber to be a perfect cylinder, *FSA* can be calculated from *CSA* as:

$$FSA = \sqrt{4\pi CSA} \quad (6)$$

and G_m can be then be calculated as:

$$G_m = \frac{g_m}{FSA} = \frac{g_m}{\sqrt{4\pi CSA}} \quad (7)$$

Stimulation protocol mimicking muscle activity using three-electrode technique

Repeated firing of action potentials with interspaced G_m determinations was performed in muscle fibers from Wistar rat (SOL and EDL) and human (HAM) muscles with the three-electrode technique. Three electrodes were inserted in these muscle fibers, as described above under *G_m determination*, and current was injected according to a current-injection protocol with a pre-defined number of cycles. Each cycle of the protocol started with two square negative currents (−30 nA, 50 ms) which were injected through E_1 and E_3, respectively (used for the *G_m determination* as described above), followed by either a train of action-potential generating positive currents injected through E_1 (i.e., stimulation protocol) or a rest period for the remainder of the cycle (i.e., recovery protocol). All three electrodes recorded the membrane potential at their respective locations.

For Wistar rat SOL/EDL fibers, the stimulation protocol [1000 ms, 9 pulses (500 nA, 15 Hz, 1 ms)] was repeated 500x to trigger 4500 action potentials in control fibers, or 200x to trigger 1800 action potentials in 2DG-exposed fibers. Subsequently, the recovery protocol [1000 ms, 0 pulses] was repeated 120x during which no action potentials were triggered and only G_m was monitored, which was followed by a re-stimulation period in which the stimulation protocol was again repeated 120x to trigger 1080 action potentials. The stimulation duration used in rat muscle fibers was based on a previous publication, which describes the presence and absence of a rise in G_m in EDL and SOL in this time-frame, respectively (20).

For HAM fibers, the stimulation protocol [1400 ms, 10 pulses (300 nA, 30 Hz, 1 ms)] was repeated 143x to trigger 1430 action potentials in all conditions. The protocol was ceased before it reached 1430 action potentials when failure in action potential excitation/propagation was observed. The stimulation duration used in HAM fibers was based on the development of the rise in G_m under glycolysis inhibition and the protocol is similar to a previous publication (15).

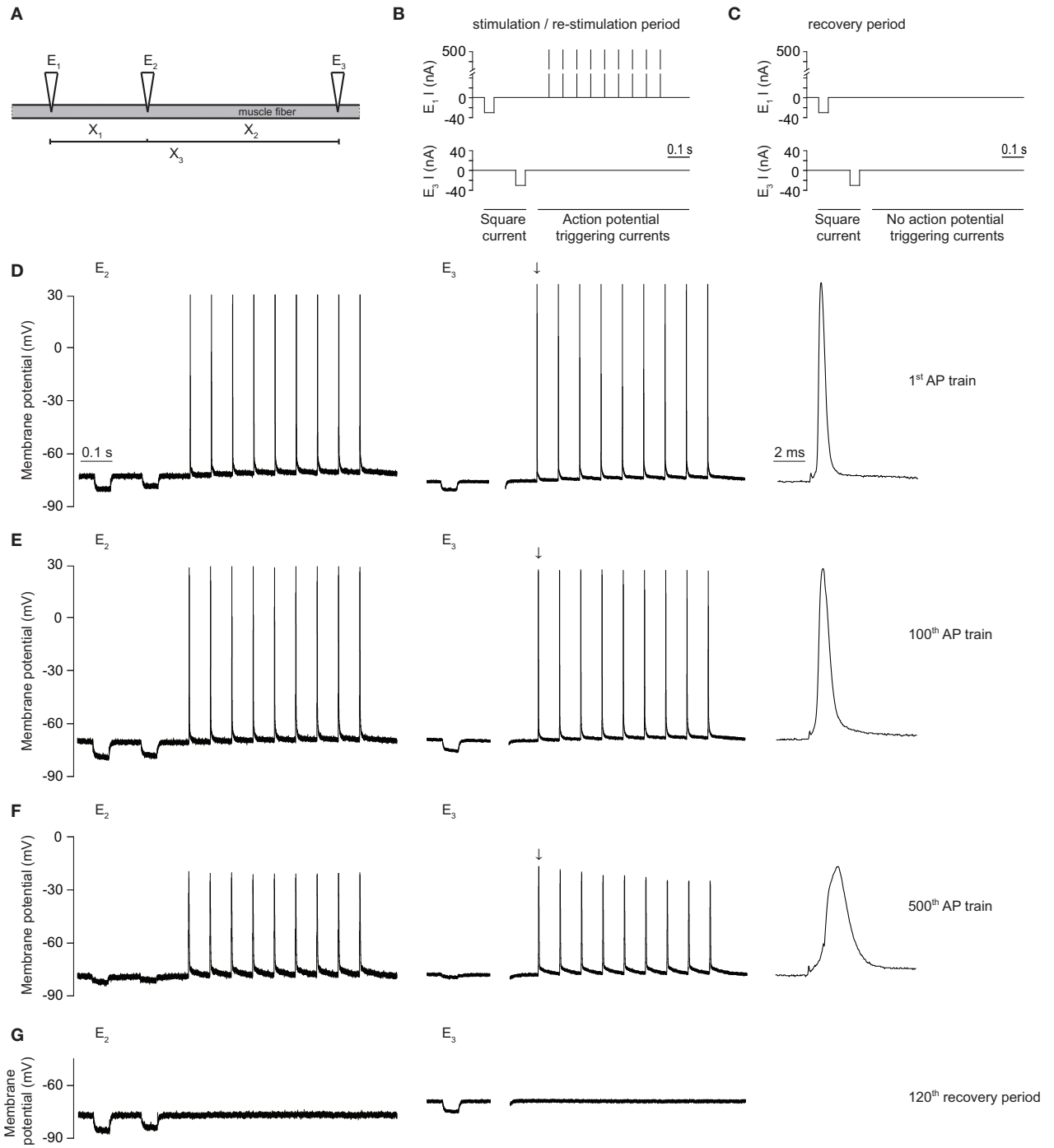

FIGURE 2 | Voltage protocol and representative traces of a rat EDL-muscle control fiber using the three-electrode technique. **(A)** Schematic depiction of the placement of three electrodes (E_1, E_2, E_3) in a muscle fiber, in order to obtain three inter-electrode distances (X_1, X_2, X_3). **(B)** Schematic depiction of the current injections through E_1 and E_3 during the G_m determination and action potential stimulation protocol. The used protocol, with a total duration of 1000 ms, consisted of two square hyperpolarizing currents used for determination of G_m (−30 nA, 50 ms duration) and a train of large amplitude depolarizing current pulses to trigger a short train of action potentials [9 pulses (500 nA, 15 Hz, 1 ms)]. **(C)** The recovery protocol was similar to **(B)** except that the action potential firing pulses were not included. **(D–G)** Representative traces of the membrane potential recorded with E_2 and E_3 in a rat EDL muscle fiber during a CTRL experiment, with the first action potential measured with E_3 (black downward arrow) depicted at higher time resolution on the right side. **(D)** Traces obtained during injection of the first action potential (AP) train of the protocol, **(E)** during the 100th action potential train of the protocol, and **(F)** during the 500th action potential train of the protocol. **(G)** The last (120th) trace of the recovery protocol.

Stimulation protocol mimicking muscle activity using two-electrode technique

The two-electrode technique was chosen for experiments with EDL muscles from McArdle mice as this approach has a higher success rate, and these animals were in very short supply. Likewise, the stimulation protocol was chosen to maximize the success rate of the experiments. Two electrodes (E_1-E_2) were placed in close proximity (≈0 μm) within one fiber, of which E_1 injected current according to a current-injection protocol with a pre-defined number of cycles, and E_2 measured the membrane potential at $x = 0$. Each cycle of the protocol started with a square negative current (−30 nA, 50 ms), which was used to measure the fiber R_{in}. This was followed either by a train of action-potential generating positive currents (i.e. stimulation protocol) or a rest period for the remainder of the cycle (i.e., recovery protocol).

The stimulation protocol [1500 ms, 15 pulses (300 nA, 30 Hz, 1 ms)] was repeated 200x to trigger 3000 action potentials. Subsequently, the recovery protocol [1500 ms, 0 pulses] was repeated 100x during which no action potentials were triggered and only R_{in} was monitored, which was followed by a re-stimulation period in which the stimulation protocol was again repeated 100x to trigger 1500 action potentials. The stimulation was continued until the R_{in} started to decline drastically reflecting the development of the rise in G_m.

These experiments thus measured R_{in} and to convert this into G_m during activity, the three electrode techniques described above in 2.4.2.2. was used to determine G_m in inactive fibers of the same muscle. G_m during muscle activity could then be estimated using equation 8 as described previously (22).

$$G_{m(t=x)} = G_{m(t=0)} \frac{{R_{in(t=0)}}^2}{{R_{in(t=x)}}^2} \quad (8)$$

Fitting properties to determine the timing and size of the rise in G_m

Based on observations of G_m during muscle activity the data from each fiber was fitted to the following 4-parameter sigmoidal function as previously described, to determine the timing and maximal size of the rise in G_m (22) (Equation 9):

$$G_m = G_{m_{(\min)}} + \frac{\Delta G_{m_{(\max)}}}{1 + \exp(\frac{t_x - t}{b})} \quad (9)$$

Where G_m represents the G_m at the time t, $G_{m(min)}$ represents the minimal G_m, $\Delta G_{m(max)}$ represents the difference between the minimal and maximal G_m, b represents the slope, and t_x represents the time at which G_m is 50% of $\Delta G_{m(max)}$.

Statistics and Data Handling

All fibers in which the resting membrane potential recorded by one of the electrodes depolarized beyond −60 mV during the experimental procedure were excluded from analyses. The number of analyzed fibers (n) is depicted for each group in the graph legends, and originated from at least 3 different animals per group for all experiments performed on C57BL/6 mice and Wistar rats. Data from McArdle mice and representative controls were shown per individual mouse, and human biopsy data originated from one HAM muscle. Data was presented as mean ± SEM unless otherwise indicated. Differences between data depicted in two groups were tested with Student's *t*-test, and differences between data depicted in multiple groups were tested with ANOVA and Bonferroni's *post-hoc* test (parametric distributions) or Kruskal-Wallis and Dunn's *post-hoc* test (non-parametric distributions) where appropriate. Differences between binary data depicted in multiple groups were tested using the Fisher's exact test, and corrected for multiple comparisons. $p<0.05$ was considered significant, and $p<0.05^*$, $p<0.01^{**}$, $p<0.001^{***}$ are depicted in the figures.

RESULTS

ATP-Dependent ClC-1 Open Probability in Native Skeletal Muscle Fibers

To study whether ClC-1 opening is sensitive to differences in intracellular ATP levels ([ATP]) in native skeletal muscle fibers, whole cell patch clamping was performed on isolated fast-twitch muscle fibers from mice with either 0 or 5 mM ATP in the pipette solution. The protocol for determining ClC-1 current in the muscle fibers and the calculation of the voltage dependent open probability (P_o) of ClC-1 was as performed as previously described elsewhere (31) (**Figure 1A**). Ionic currents were measured before (**Figure 1B**) and after addition of 400 μM 9-AC (**Figure 1C**) in the same muscle fiber, and the ClC-1-specific ionic current was calculated by subtracting the ionic current obtained with 9-AC from the current obtained without 9-AC. In general, the membrane current in the presence of 9-AC was markedly reduced, showing that ClC-1 facilitated the majority of the current flow under these experiment conditions (compare black and gray traces in **Figures 1B,C**). There was no significant difference in peak ClC-1 current at +60 mV between groups exposed to 5 and 0 mM ATP pipette solutions (5 mM ATP: −40 ±13 nA, 0 mM ATP: −34 ±16 nA, $p = 0.553$). Also, there was no difference in currents between the groups after 9-AC exposure.

The calculated P_o at each specific membrane potential was plotted against that membrane potential, and subsequently fitted to the sigmoidal function in Equation 1 (**Figure 1D**). The parameters from the fits of individual fibers were obtained and comparison of parameters was performed between groups. The slope (5 mM ATP: 33 ±23 mV, 0 mM ATP: 33 ±8 mV, $p = 0.944$) and residual opening probability at the most hyperpolarized potentials (5 mM ATP: −0.074 ± 0.232, 0 mM ATP: −0.181 ± 0.319, $p = 0.563$) were not different between the groups. The membrane voltage that resulted in 50% of the voltage dependent ClC-1 current to be activated, $V_{½}$, was shifted significantly in the hyperpolarizing direction in fibers subjected to a pipette solution with 0 mM ATP (**Figures 1D,E**).

A Repetitive Action Potential Firing-Induced Rise in G_m Occurs Only in Fast- and Not in Slow-Twitch Fibers Under Conditions With Functional Glycolysis

The initial series of experiments in muscle fibers was conducted to verify previous findings that repetitive action potential firing

resulted in large increases in G_m with subsequent loss of muscle excitability in fast-twitch (EDL) but not in slow-twitch (SOL) muscle fibers from rat. Experimentally, the three-electrode technique (**Figure 2A**) was used and a 1000 ms stimulation protocol was repeated 500 times in each fiber. During each run of the protocol, G_m was first determined with two square currents, and, subsequently, 9 action potentials were triggered in the fiber (**Figure 2B**). After 500 runs of the protocol, the action potential firing was ceased, and the recovery of G_m was monitored during 120 runs of the protocol without triggering action potentials (**Figure 2C**). Finally, action potential triggering was re-started and 120 runs of the action potential triggering protocol (**Figure 2B**) were performed.

In line with previous work from our group, G_m showed a biphasic response during repetitive action potential stimulation in EDL but not in SOL muscle fibers (15, 20, 22). Thus, G_m decreased during the first 1500 action potentials (phase 1) of repetitive action potential firing in both EDL and SOL muscle fibers (**Figures 2E**, **3A**). This has previously been shown to primarily reflect protein kinase C-mediated inhibition of ClC-1 ion channels in both muscle fiber types (15, 20), and was not the aim of the current manuscript. In EDL fibers only, G_m rapidly increased after around 1500–2000 action potentials (phase 2) (**Figures 2F**, **3A**). G_m returned to baseline values during the recovery period, and subsequently increased quickly upon re-stimulation (**Figures 2G**, **3A**). During prolonged action potential firing, the action potential amplitude, and depolarization and repolarization speed decreased gradually over time (**Figures 2D–F**).

The Repetitive Action Potential Firing-Induced Rise in G_m Occurs in Both Fast- and Slow-Twitch Fibers Under Conditions of Compromised Glycolysis

To test if the regulation of G_m is dependent on a functional ATP supply, pharmacological inhibition of glycolysis (i.e., by replacing 5.0 mM D-glucose with 5.0 mM 2DG + 100 IU insulin) was performed in the above-described experiments, but with a shorter action potential stimulation period (200 s, 1800 action potentials). The stimulation period was shorter in these experiments because less action potentials were needed to trigger the activity-induced rise in G_m. Glycolysis-inhibited EDL muscle fibers showed an accelerated phase 2-like increase in G_m directly after the onset of action potential-firing (**Figures 3B,E**). Moreover, this rise in G_m was steeper and reached a higher maximal G_m before becoming stable compared to muscle with fully functional glycolysis (**Figures 3B,D**). Consequently, an initial phase 1-like decrease in G_m was not observed in glycolysis-inhibited EDL muscle fibers. Similar to control conditions, G_m returned to baseline values in the recovery period, and subsequently increased quickly upon re-stimulation (**Figure 3B**).

Similar to the results from glycolysis-inhibited EDL muscle fibers, inhibition of glycolysis resulted in a rapid phase 2-like increase in G_m in SOL muscle fibers (**Figures 3C,E**). Moreover, the increase in G_m in glycolysis-inhibited SOL muscle fibers was also steep but plateaued earlier (±450 action potentials), and at a much lower maximal G_m compared with the maximal G_m of glycolysis-inhibited EDL muscle fibers (**Figures 3B–D**). Like in glycolysis-inhibited EDL muscle fibers, the G_m of glycolysis-inhibited SOL muscle fibers returned to baseline values in the recovery period, and subsequently increased quickly upon re-stimulation (**Figure 3C**).

Inhibition of Glycolysis Triggers an Action Potential Firing-Induced ClC-1-Dependent Rise in G_m in Human Muscle Fibers

Previous experiments, using a similar approach to determine G_m changes during repetitive action potential firing, have shown that although ClC-1 inhibition during the first phase of activity is also present in human muscle, a prolonged activity-induced rise in G_m has not been observed in the first 2000 action potentials (15). To determine whether this rise in G_m can, similar to SOL muscles from rat, be brought out with inhibition of glycolysis, a series of experiments with the three-electrode technique was conducted in HAM muscle in the absence and presence of iodoacetate (IAA). Indeed, no repetitive action potential firing-induced rise in G_m was observed in control conditions in human muscle fibers during the 200 s of running the stimulation protocol (**Figures 4A,D,G**). Similar to the results from glycolysis-inhibited rat SOL muscle fibers, however, inhibition of glycolysis resulted in the appearance of a phase 2-like increase in G_m in all tested human muscle fibers (**Figures 4B,E,G**). This increase in $G_m$correlated strongly with action potential-excitation failure, as can been clearly seen in the action potential train from the representative trace depicted in the third panel of **Figure 4B**. To study the relative contribution of ClC-1 to the observed increase in G_m, the above described glycolysis-inhibition experiments were repeated in presence of the ClC-1 inhibitor 9-AC. ClC-1 inhibition prevented the rise in G_m in 75% of the measured glycolysis-inhibited human muscle fibers (**Figures 4C,F,G**). As ClC-1 inhibition resulted in a binary effect on the rise of G_m, measured fibers were depicted individually and not as mean values (**Figures 4D–F**), and the percentage of fibers that showed an increase in G_m during the first 200 s of the stimulation protocol were depicted (**Figure 4G**). During prolonged action potential firing, the action potential amplitude, and depolarization and repolarization speed decreased gradually over time. Moreover, 9-AC-mediated inhibition of ClC-1 currents resulted in a decreased repolarization speed at baseline (**Figures 4A–C**). Since the access to human muscle was limited, IAA was used to inhibit glycolysis, as this approach was much faster and allowed paired measurements to be performed in the same preparations. This was not possible with 2DG that required substantial pre-incubation.

Action Potential Firing-Induced Rise in G_m Is Accelerated in Murine McArdle EDL Muscle Fibers

The above-described experiments in rat and human muscles showed that G_m rise can be markedly accelerated by pharmacological inhibition of glycolysis. This is compatible with ClC-1 being a metabolic sensor that can switch open

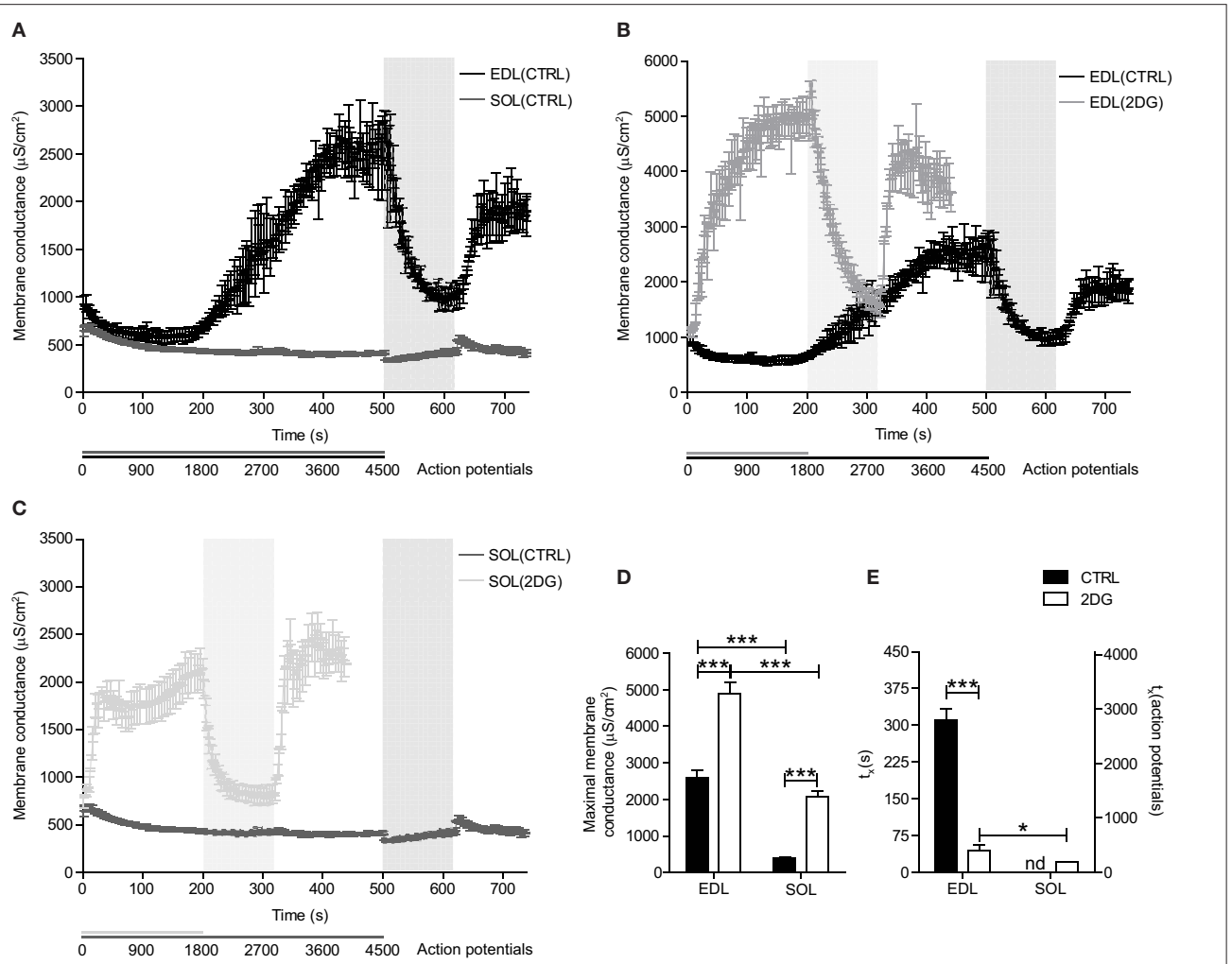

FIGURE 3 | Changes in G_m during repetitive action potential firing in fast- and slow-twitch fibers under control conditions and with inhibition of glycolysis. **(A)** G_m of EDL (black line) and SOL (gray line) muscle fibers in buffer with 5.0 mM D-glucose is depicted over time. G_m of EDL **(B)** and SOL **(C)** muscle fibers in solution with 5.0 mM D-glucose (dark line) or 5.0 mM 2DG + 100 IU insulin (light-gray line) is depicted over time. $G_{m(max)}$ **(D)** and time until 50% of $G_{m(max)}$ is reached (t_x) **(E)** were extracted from sigmoid-fitted data and depicted. CTRL fibers were subjected to 500x the stimulation protocol [1000 ms, 9 pulses (500 nA, 15 Hz, 1 ms)], 120x the recovery protocol [1000 ms, 0 pulses], and to a re-stimulation period that consisted of 120x the stimulation protocol. 2DG fibers were subjected to 200x the stimulation protocol, 120x the recovery protocol, and to a re-stimulation period that consisted of 120x the stimulation protocol. Data from EDL-CTRL and SOL-CTRL fibers depicted in panel **(A)** is also depicted as CTRL data in panel **(B,C)**, respectively. Gray vertical bars represent the recovery period during the stimulation protocol. ANOVA with Bonferroni's *post-hoc* tests were performed to test significance of observed differences between EDL-CTRL ($n = 4$), EDL-2DG ($n = 12$), SOL-CTRL ($n = 18$), and SOL-2DG ($n = 32$), and $p < 0.05$* or $p < 0.001$*** are depicted.

and compromise muscle excitability if the metabolic state of muscle fibers becomes critical. To further explore for a link between membrane conductance and glycolysis, a genetic model for impaired muscle glucose and energy homeostasis (i.e., McArdle mouse model) was used. Interestingly, the observations from the two analyzed McArdle mice showed marked differences regarding the onset of the repetitive action potential firing-induced rise in G_m (**Figure 5A**). Experimentally, the two-electrode technique was used and a 1500 ms stimulation protocol was repeated 200 times (300 sec, 3000 action potentials), followed by a recovery period (150 s, 0 action potentials), and a re-stimulation period in which the same stimulation protocol was repeated 100 times (150 s, 1,500 action potentials) in each fiber. The muscle fibers from the first McArdle mice showed a consistently accelerated increase in G_m compared with wild-type muscle fibers. However, the muscle fibers from the second McArdle mouse did not show an accelerated increase in G_m compared with wild-type (**Figures 5A,B**). Both McArdle and wild-type muscle fibers showed a similar return of G_m to baseline during the recovery period as well as a similar rapid increase in G_m upon re-stimulation (**Figure 5A**). Taken together, the combined observations are compatible with malfunctional glycolysis (pharmacologically or genetically induced) being able to introduce an accelerated rise in G_m during muscle activity. Given the limited amount of data available from these McArdle mice, this data must be considered with appropriate

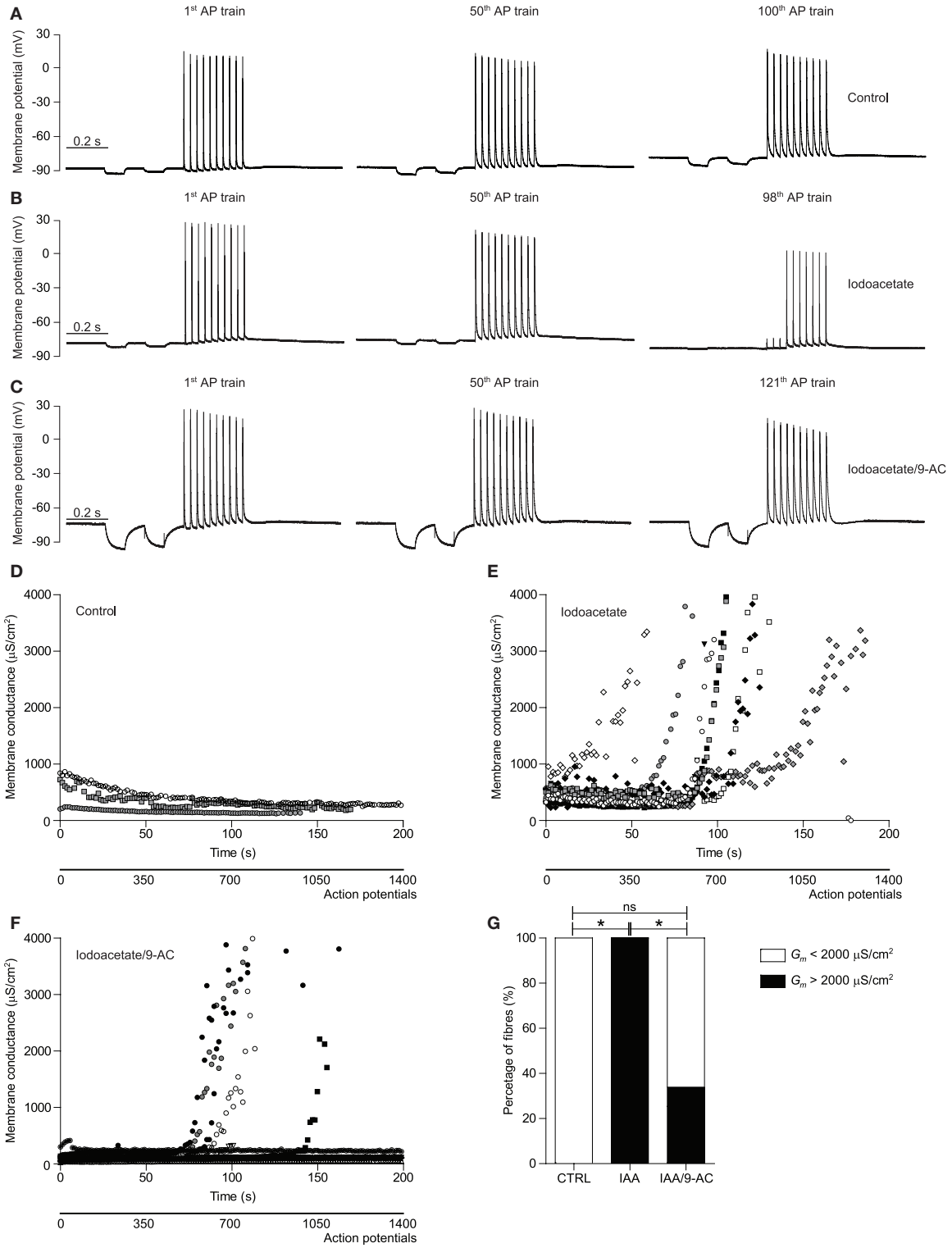

FIGURE 4 | Glycolysis-inhibition resulted in a repetitive action potential firing-induced ClC-1-dependent rise in G_m in human muscle fibers. **(A–C)** Representative traces of the membrane potential recorded with E_2 (for schematic depiction of electrodes see **Figure 2A**) of a control (CTRL) **(A)**, 100 μM iodoacetate (IAA) subjected **(B)**, and 100 μM IAA + 100 μM 9-AC + 10 nM Tetrodotoxin subjected **(C)** human HAM muscle fiber during the 1st, 50th, and ∼100th action potential (AP) train of the stimulation protocol have been depicted. The protocol, with a total duration of 1400 ms, consisted of two square hyperpolarizing currents used for determination of G_m (−30 nA, 50 ms duration) and a train of large amplitude depolarizing current pulses to trigger a short train of action potentials [10 pulses (300 nA, 30 Hz, 1 ms)]. **(D–F)** G_m of CTRL **(D)**, IAA subjected **(E)**, and IAA/9-AC subjected **(F)** individual HAM muscle fiber are depicted over time. **(G)** The percentage of HAM muscle fibers that showed an increase in G_m that was >2000 μS/cm^2 during the first 200 s of action potential stimulation. Fisher's exact tests corrected for multiple comparisons were performed to test significance of observed differences between CTRL ($n = 3$), IAA ($n = 9$), and IAA/9-AC ($n = 12$), and $p < 0.05$* is depicted.

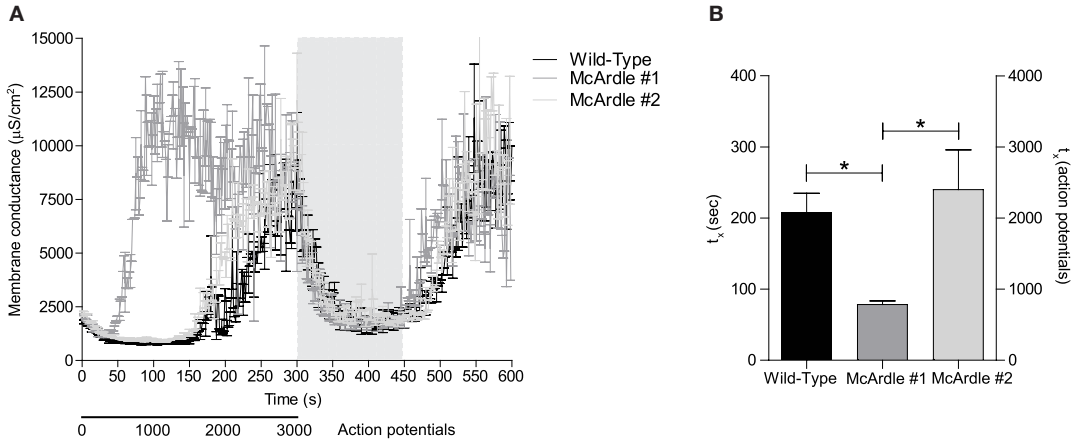

FIGURE 5 | Rise in G_m is accelerated in murine McArdle EDL muscle fibers compared with wild-type EDL muscle fibers. **(A)** Murine EDL muscle fibers of McArdle (gray lines) and genetic wild-type (black line) mice were subjected repetitive action potential stimulation and G_m of is depicted over time. **(B)** Time until 50% of $G_{m(max)}$ is reached was extracted from sigmoid-fitted data and depicted. Fibers were subjected to 200x the stimulation protocol [1500 ms, 15 pulses (300 nA, 30 Hz, 1 ms)], 100x the recovery protocol [1500 ms, 0 pulses], and to a re-stimulation period that consisted out of 100x the stimulation protocol. Gray vertical bars represent the recovery period during the stimulation protocol. Kruskal-Wallis and Dunn's *post-hoc* test was performed to test significance of observed differences between wild-type ($n = 9$), McArdle #1 ($n = 9$), and McArdle #2 ($n = 13$), and $p < 0.05^*$ is depicted.

reservations, and more experiments are required to explore this in further detail.

DISCUSSION

The metabolic requirement of skeletal muscle fibers increases many-fold during physical activity. Although the muscular ATP replenishing capacity is extensive, a fiber type-specific exhaustion of the metabolic state occurs during intense exercise. Indeed, [ATP] was reported to decline by 80% in fast-twitch and 25% in slow-twitch human muscle fibers after 25 s of maximal exercise. These changes in [ATP] were generally accompanied by corresponding increases in inositol monophosphate (IMP) levels, showing that the exercise led marked decline in the adenosine nucleotides pool in the active muscle fibers (21). The amplitude of this decrease suggest that severe energy depletion is a physiologically relevant event during high-intensity activity, especially for fast-twitch muscle fibers.

The physiological importance of a decline in adenosine nucleotides and altered metabolic profile for muscle function has been studied extensively and several cellular mechanisms involved in the excitation-contraction coupling are sensitive to the specific metabolites. A correlation between metabolic state of muscle fibers and their performance is evident, suggesting that metabolically driven fatigue mechanisms exist in skeletal muscle. The current study shows that depletion of adenosine nucleotides results in an increased ClC-1 open probability in skeletal muscle, and that the inhibition of glycolysis results in an accelerated increase in membrane conductance during repetitive action potential firing in both slow- and fast-twitch muscle fiber types. Interestingly, this accelerated increase of membrane conductance was present in both rodent and human muscle fibers, and it was found to be ClC-1 dependent. Moreover, as a proof-of-principle, this study indicates that fast-twitch muscle fibers from McArdle mice, that have an impaired intra-muscular glucose homeostasis, exhibit accelerated increase of membrane conductance during repetitive action potential firing. Together, these results suggest that ClC-1 function is regulated by the level of adenosine nucleotides, and that the channel operates as a sensor of the metabolic state in skeletal muscle fibers. ClC-1 thereby represents a mechanistic link between metabolism and muscle fiber excitability that can be envisioned to have a role in muscle fatigue during exercise and, possibly, neuromuscular disease including McArdle disease.

Whole Cell Patch Clamp of Muscle Fibers Show Increased ClC-1 Opening Probability Under Conditions of Low Intracellular ATP Levels

Previous patch clamp studies using heterologous expressed ClC-1 reported that adenosine nucleotides cause a pH dependent inhibition of ClC-1 (17, 36, 37). Others were, however, unable to reproduce these findings (38). This apparent discrepancy between studies was later explained by the high sensitivity of the ATP-ClC-1 binding to the redox state of the cell (39). Although voltage clamping of mammalian muscle fibers has already been used to measure chloride currents for over 25 years (40), the adenosine nucleotide sensitivity of ClC-1 in native mammalian muscle fibers has not been explored. We now show that ATP-depletion results in a hyperpolarizing shift of the ClC-1 open probability in native skeletal muscle fibers, confirming the expression system-obtained data from previous studies in a more physiological relevant setting (17, 36).

The whole cell patch clamping used in the current study does have some experimental limitations that must be considered. As muscle fibers have a complex cellular geometry (size and composition), complete voltage control during the experiments may have been compromised. At least it must be assumed that

the T-tubular membrane was not fully under voltage control due to the T-tubular lumen imposing substantial resistance to current flow (16). Furthermore, it is unlikely that the level of ATP was fully controlled by the pipette solution due to the large fiber volume (41). The change in the ClC-1 activation with 0 mM ATP in the pipette was nevertheless of a clear magnitude, and the limitations considered here indicate that our results may be an underestimation of the effect of ATP on ClC-1.

The ATP depletion-induced shift in activation of ClC-1 results in a higher ClC-1 opening at resting membrane potential in native muscle fibers and, predictably, would cause an increase in the resting membrane conductance of resting skeletal muscle fibers. Adenosine nucleotide mediated regulation of ClC-1 could therefore provide a mechanistic link between metabolic state of muscle fibers and their excitability. This was next explored in muscle fibers during repetitive firing of action potentials.

Effect of Pharmacological Inhibition of Glycolysis on Regulation of Resting Membrane Conductance During Repetitive Action Potential Firing in Muscle Fibers of Rat and Human

Previous studies showed that repetitive firing of action potentials results in the activation of both ClC-1 and K_{ATP} ion channels, which markedly increase the resting membrane conductance leading to compromised muscle fiber excitability (22). This increase in membrane conductance has thus far only been observed in fast-twitch muscle fibers and not in slow-twitch fibers. This fiber-type specific activation of ClC-1 and K_{ATP} ion channels is compatible with fast-twitch fibers undergoing the largest depression in adenosine nucleotides during intense muscle activity. To further explore the role of the metabolic state for the activity-induced rise in membrane conductance, two series of experiments were conducted using both rat and human muscles to confirm translatability from rodent to man.

First, the effect of pharmacological inhibition of glycolysis with 2DG on the regulation of the resting membrane conductance during repeated firing of action potentials was explored in rat fast- and slow-twitch muscle fibers. With glycolysis inhibition, the rise in membrane conductance happened rapidly after onset of action potential firing in both fast- and slow-twitch muscle fibers. This rise in membrane conductance was observed significantly later in untreated fast-twitch fibers, and it was not observed at all in untreated slow-twitch fibers. This shows that the ion channels that trigger the increased membrane conductance during prolonged action potential firing have the capacity to be activated in both types of muscle fibers. The absence of the increase in membrane conductance in slow-twitch fibers under control conditions is likely due to the relatively stable metabolic state in active slow-twitch fibers, where adenosine nucleotide levels might not decrease to a level that triggers ClC-1 activation.

Second, when similar experiments were conducted in untreated abdominal rectus muscle fibers from human, the onset of muscle activity caused a reduction in the membrane conductance as has been reported previously (15). This state of low membrane conductance during onset of action potential was previously shown to be caused by protein kinase C-mediated ClC-1 inhibition, and has been associated with well-preserved muscle fiber excitability (15). In our experiments, the low membrane conductance and well-preserved excitability was maintained for the complete protocol of action potential firing in the untreated human muscle fibers. When similar experiments were conducted in the presence of iodoacetate, a marked and consistent rise in membrane conductance was observed during the repeated action potential firing in the human muscle fibers. This rise in membrane conductance led to complete loss of muscle fiber excitability in many fibers and, importantly, this activity-induced rise in membrane conductance was significantly abolished in the presence of a ClC-1 inhibitor. Although these findings show that ClC-1 has the capacity to activate during metabolic compromised conditions in human muscle fibers, it remains to be established if ClC-1 also activates under control conditions if stimulations are either intensified or extended beyond 2000 action potentials in these fibers. It is possible that such ClC-1 activation during prolonged muscle activity would occur in a subset of human fibers most closely comparable to the EDL muscle fibers of the rat.

Taken together, the findings from these two series of experiments show that the rise in membrane conductance during repeated firing of action potentials is a conserved capacity between different muscle fibers and species. In the currently explored rat slow-twitch and human muscle fibers, the rise in conductance was only observed with glycolytic inhibition. Although this is an indication that these muscle fibers were not metabolically challenged by the imposed activity, and that the adenosine nucleotide levels were well-preserved in these muscle fibers during the activity, especially for human abdominal muscle fibers longer stimulation periods are needed to verify this. Although we did not study intra-muscular adenosine nucleotide concentrations in the current study, it is known from literature that 2DG and iodoacetate both result in depletion of adenosine nucleotides in challenged cardiac muscle (42). Nevertheless, it would be interesting to study if the rise in membrane conductance starts at similar intra-muscular adenosine nucleotide concentrations in glycolysis-inhibited and control fibers and possibly make inter-species comparisons.

Role of ClC-1 in the Rise in Membrane Conductance During Repeated Action Potential Firing

Collectively, the patch clamping data and the observations in human muscle during repeated firing of action potentials suggest that the ClC-1-mediated chloride conductance is largely responsible for the accelerated rise in membrane conductance during prolonged muscle activity. The primary data implicating ClC-1 channels in the rise in membrane conductance during muscle activity stems, in the present experiments, from the observation from human muscle fibers where pharmacological blockage of ClC-1 resulted in the abolishment of the rise in membrane conductance. This data is in line with previous data, showing that the rise in membrane conductance during repetitive

action potential firing in rat fast-twitch muscle was to a large extend mediated by ClC-1 activation (22). Although we clearly show an important role for ClC-1 for the rise in membrane conductance during prolonged action potential firing, a possible role for K_{ATP} should not be disregarded. Since both ClC-1 and K_{ATP} channels are sensitive to the metabolic state of muscle fibers, these channels may be speculated to introduce some degree of redundancy in the capacity of muscle fibers to shut down muscle excitability in the case of challenged metabolic state (22).

Although the membrane conductance is extremely important for functional excitation-contraction coupling, multiple cellular mechanisms that regulate down-stream sarcoplasmic reticulum Ca^{2+} release are sensitive to the metabolic state of muscle fibers. Indeed, previous studies not only showed that the sarcoplasmic reticulum Ca^{2+} release was greatly impaired by both low [ATP] and by the inhibition of glycolysis with 2DG or IAA, but they also showed that the opening of the skeletal muscle Ca^{2+} release channel Ryanodine-receptor 1 (RyR1) itself is dependent on ATP-binding (43, 44). Interestingly, both ClC-1 and RyR1 seem to have similar sensitivities to [ATP], where a decline below 1 mM ATP causes activation or inhibition, respectively. Therefore, it is possible that adenosine nucleotides have a universal role as regulators of the excitation contraction coupling and that coordinated shutdown of muscle activation by several cellular mechanisms can take place if [ATP] declines below 1 mM.

Effect of Genetically Compromised Glycolysis on Regulation of the Resting Membrane Conductance During Repetitive Firing of Action Potentials—Role in Neuromuscular Disease

Although the currently used McArdle mice were generated to model human McArdle disease (28), they were included in this manuscript as a, proof-of-concept, genetic model for impaired muscle glucose and energy homeostasis. These mice were characterized by complete absence of the glycogen phosphorylase (a.k.a. myophosphorylase), and in a previous study they were shown to have a dramatically decreased time to fatigue (28). Moreover, the currently included EDL muscle of McArdle mice showed clear signs of structural damage, and displayed impaired twitch and tetanic force production (45). The currently presented data, that shows that the membrane conductance rises after around 1500 action potentials in McArdle wild-type (i.e., C57BL/6 $PYGM^{wt/wt}$) muscle fibers, corresponds exactly to reliable membrane conductance data from an extensive previous characterization of C57BL/6 EDL fiber cable parameters (23). From the two different McArdle knock-in mice ($PYGM^{R50X/R50X}$) tested here, only one showed a clear accelerated rise in membrane conductance. Although it is unclear why this response was observed in only one of the mice, it is possible that not all animals were affected equally by the mutation. As all the reported data was obtained in fibers that remained polarized throughout the experimental protocol, and the membrane conductance of all fibers returned quickly to baseline during the recovery period, all fibers were considered healthy and viable and, thus, the data to be reliable. The currently presented McArdle data only served as proof-of-concept, to verify the pharmacological glycolysis inhibition data in a non-pharmacological genetic system. Together with the data from pharmacological glycolysis inhibition, these data converge to a conclusion that the observed acceleration of the rise in membrane conductance is physiologically relevant and a conserved response to low energy status. Due to the limited amount of observations that we gathered from McArdle mice, substantial precautions must be taken when extrapolating and interpreting the current data the McArdle disease *per se*.

Combined, our data clearly indicates the importance of a functional energy homeostasis for proper membrane conductance physiology and the data shows that ClC-1 acts as a metabolic sensor that increases membrane conductance and limits muscle excitability when energy status is low.

DATA AVAILABILITY STATEMENT

The datasets generated for this study are available on request to the corresponding author.

ETHICS STATEMENT

The animal study was reviewed and approved by Danish Animal Experiments Inspectorate. The studies involving human participants were reviewed and approved by Danish Ethics Committee, Region Midtjylland, Comité I. The patients/participants provided their written informed consent to participate in this study.

AUTHOR CONTRIBUTIONS

PL, FP, TP, JV, TK, and THP contributed conception and design of the study. PL, KD, KH, and AR contributed to acquisition of data. PL, KH, AR, TK, and THP contributed to analysis or interpretation of data. PL and THP contributed to writing the first draft of the manuscript. KH and AR wrote sections of the manuscript. All authors contributed to manuscript revision, read and approved the submitted version.

FUNDING

This work was kindly funded by Aarhus University Research Foundation (AUFF) NOVA.

ACKNOWLEDGMENTS

We would like to thank Vibeke Uhre and Dorte Olsson from Aarhus university for the scientific and technical support in the presented work.

REFERENCES

1. Westerblad H, Bruton JD, Katz A. Skeletal muscle: energy metabolism, fiber types, fatigue and adaptability. *Exp Cell Res*. (2010) 316:3093–9. doi: 10.1016/j.yexcr.2010.05.019
2. Allen DG, Lamb GD, Westerblad H. Skeletal muscle fatigue: cellular mechanisms. *Physiol Rev*. (2008) 88:287–332. doi: 10.1152/physrev.00015.2007
3. Mc AB. Myopathy due to a defect in muscle glycogen breakdown. *Clin Sci*. (1951) 10:13–35.
4. Wan JJ, Qin Z, Wang PY, Sun Y, Liu X. Muscle fatigue: general understanding and treatment. *Exp Mol Med*. (2017) 49:e384. doi: 10.1038/emm.2017.194
5. Fahlke C, Rosenbohm A, Mitrovic N, George AL Jr, Rudel R. Mechanism of voltage-dependent gating in skeletal muscle chloride channels. *Biophys J*. (1996) 71:695–706. doi: 10.1016/S0006-3495(96)79269-X
6. Jentsch TJ, Steinmeyer K, Schwarz G. Primary structure of torpedo marmorata chloride channel isolated by expression cloning in xenopus oocytes. *Nature*. (1990) 348:510–4. doi: 10.1038/348510a0
7. Koch MC, Steinmeyer K, Lorenz C, Ricker K, Wolf F, Otto M, et al. The skeletal muscle chloride channel in dominant and recessive human myotonia. *Science*. (1992) 257:797–800. doi: 10.1126/science.1379744
8. Pusch M, Steinmeyer K, Jentsch TJ. Low single channel conductance of the major skeletal muscle chloride channel, ClC-1. *Biophys J*. (1994) 66:149–52. doi: 10.1016/S0006-3495(94)80753-2
9. Palade PT, Barchi RL. Characteristics of the chloride conductance in muscle fibers of the rat diaphragm. *J Gen Physiol*. (1977) 69:325–42. doi: 10.1085/jgp.69.3.325
10. Kwiecinski H, Lehmann-Horn F, Rudel R. The resting membrane parameters of human intercostal muscle at low, normal, and high extracellular potassium. *Muscle Nerve*. (1984) 7:60–5. doi: 10.1002/mus.880070110
11. Bryant SH, Morales-Aguilera A. Chloride conductance in normal and myotonic muscle fibres and the action of monocarboxylic aromatic acids. *J Physiol*. (1971) 219:367–83. doi: 10.1113/jphysiol.1971.sp009667
12. Rudel R, Senges J. Mammalian skeletal muscle: reduced chloride conductance in drug-induced myotonia and induction of myotonia by low-chloride solution. *N-S Arch Pharmacol*. (1972) 274:337–47. doi: 10.1007/BF00501271
13. Hutter OF, Noble D. The chloride conductance of frog skeletal muscle. *J physiol*. (1960) 151:89–102.
14. de Paoli FV, Broch-Lips M, Pedersen TH, Nielsen OB. Relationship between membrane Cl- conductance and contractile endurance in isolated rat muscles. *J Physiol*. (2013) 591:531–45. doi: 10.1113/jphysiol.2012.243246
15. Riisager A, de Paoli FV, Yu WP, Pedersen TH, Chen TY, Nielsen OB. Protein kinase C-dependent regulation of ClC-1 channels in active human muscle and its effect on fast and slow gating. *J Physiol*. (2016) 594:3391–406. doi: 10.1113/JP271556
16. Pedersen TH, Huang LH, Fraser JA. An analysis of the relationships between subthreshold electrical properties and excitability in skeletal muscle. *J Gen Physiol*. (2011) 138:73–93. doi: 10.1085/jgp.201010510
17. Bennetts B, Rychkov GY, Ng HL, Morton CJ, Stapleton D, Parker MW, et al. Cytoplasmic ATP-sensing domains regulate gating of skeletal muscle ClC-1 chloride channels. *J Biol Chem*. (2005) 280:32452–8. doi: 10.1074/jbc.M502890200
18. Tseng PY, Yu WP, Liu HY, Zhang XD, Zou X, Chen TY. Binding of ATP to the CBS domains in the C-terminal region of CLC-1. *J Gen Physiol*. (2011) 137:357–68. doi: 10.1085/jgp.201010495
19. Meyer S, Savaresi S, Forster IC, Dutzler R. Nucleotide recognition by the cytoplasmic domain of the human chloride transporter ClC-5. *Nat Struct Mol Biol*. (2007) 14:60–7. doi: 10.1038/nsmb1188
20. Pedersen TH, Macdonald WA, de Paoli FV, Gurung IS, Nielsen OB. Comparison of regulated passive membrane conductance in action potential-firing fast- and slow-twitch muscle. *J Gen Physiol*. (2009) 134:323–37. doi: 10.1085/jgp.200910291
21. Karatzaferi C, de Haan A, Ferguson RA, van Mechelen W, Sargeant AJ. Phosphocreatine and ATP content in human single muscle fibres before and after maximum dynamic exercise. *Pflugers Arch*. (2001) 442:467–74. doi: 10.1007/s004240100552
22. Pedersen TH, de Paoli FV, Flatman JA, Nielsen OB. Regulation of ClC-1 and KATP channels in action potential-firing fast-twitch muscle fibers. *J Gen Physiol*. (2009) 134:309–22. doi: 10.1085/jgp.200910290
23. Riisager A, Duehmke R, Nielsen OB, Huang CL, Pedersen TH. Determination of cable parameters in skeletal muscle fibres during repetitive firing of action potentials. *J Physiol*. (2014) 592:4417–29. doi: 10.1113/jphysiol.2014.280529
24. Smith IC, Gittings W, Huang J, McMillan EM, Quadrilatero J, Tupling AR, et al. Potentiation in mouse lumbrical muscle without myosin light chain phosphorylation: is resting calcium responsible? *J Gen Physiol*. (2013) 141:297–308. doi: 10.1085/jgp.201210918
25. Edstrom L, Hultman E, Sahlin K, Sjoholm H. The contents of high-energy phosphates in different fibre types in skeletal muscles from rat, guinea-pig and man. *J Physiol*. (1982) 332:47–58. doi: 10.1113/jphysiol.1982.sp014399
26. Banas K, Clow C, Jasmin BJ, Renaud JM. The KATP channel Kir6.2 subunit content is higher in glycolytic than oxidative skeletal muscle fibers. *Am J Physiol Regul Integr Comp Physiol*. (2011) 301:R916–25. doi: 10.1152/ajpregu.00663.2010
27. Real-Martinez A, Brull A, Huerta J, Tarraso G, Lucia A, Martin MA, et al. Low survival rate and muscle fiber-dependent aging effects in the McArdle disease mouse model. *Sci Rep*. (2019) 9:5116. doi: 10.1038/s41598-019-41414-8
28. Nogales-Gadea G, Pinos T, Lucia A, Arenas J, Camara Y, Brull A, et al. Knock-in mice for the R50X mutation in the PYGM gene present with McArdle disease. *Brain*. (2012) 135(Pt 7):2048–57. doi: 10.1093/brain/aws141
29. Skov M, De Paoli FV, Lausten J, Nielsen OB, Pedersen TH. Extracellular magnesium and calcium reduce myotonia in isolated ClC-1 chloride channel-inhibited human muscle. *Muscle Nerve*. (2015) 51:65–71. doi: 10.1002/mus.24260
30. Haggmark T, Thorstensson A. Fibre types in human abdominal muscles. *Acta Physiol Scand*. (1979) 107:319–25. doi: 10.1111/j.1748-1716.1979.tb06482.x
31. Lueck JD, Mankodi A, Swanson MS, Thornton CA, Dirksen RT. Muscle chloride channel dysfunction in two mouse models of myotonic dystrophy. *J Gen Physiol*. (2007) 129:79–94. doi: 10.1085/jgp.200609635
32. Cheung A, Dantzig JA, Hollingworth S, Baylor SM, Goldman YE, Mitchison TJ, et al. A small-molecule inhibitor of skeletal muscle myosin II. *Nat Cell Biol*. (2002) 4:83–8. doi: 10.1038/ncb734
33. Zhang SJ, Andersson DC, Sandstrom ME, Westerblad H, Katz A. Cross bridges account for only 20% of total ATP consumption during submaximal isometric contraction in mouse fast-twitch skeletal muscle. *Am J Physiol Cell Physiol*. (2006) 291:C147–54. doi: 10.1152/ajpcell.00578.2005
34. Hodgkin AL, Rushton WA. The electrical constants of a crustacean nerve fibre. *Proc R Soc Med*. (1946) 134:444–79. doi: 10.1098/rspb.1946.0024
35. Albuquerque EX, Thesleff S. A comparative study of membrane properties of innervated and chronically denervated fast and slow skeletal muscles of the rat. *Acta Physiol Scand*. (1968) 73:471–80. doi: 10.1111/j.1365-201X.1968.tb10886.x
36. Bennetts B, Parker MW, Cromer BA. Inhibition of skeletal muscle ClC-1 chloride channels by low intracellular pH and ATP. *J Biol Chem*. (2007) 282:32780–91. doi: 10.1074/jbc.M703259200
37. Tseng PY, Bennetts B, Chen TY. Cytoplasmic ATP inhibition of CLC-1 is enhanced by low pH. *J Gen Physiol*. (2007) 130:217–21. doi: 10.1085/jgp.200709817
38. Zifarelli G, Pusch M. The muscle chloride channel ClC-1 is not directly regulated by intracellular ATP. *J Gen Physiol*. (2008) 131:109–16. doi: 10.1085/jgp.200709899
39. Zhang XD, Tseng PY, Chen TY. ATP inhibition of CLC-1 is controlled by oxidation and reduction. *J Gen Physiol*. (2008) 132:421–8. doi: 10.1085/jgp.200810023
40. Fahlke C, Rudel R. Chloride currents across the membrane of mammalian skeletal muscle fibres. *J Physiol*. (1995) 484(Pt 2):355–68. doi: 10.1113/jphysiol.1995.sp020670
41. Pusch M, Neher E. Rates of diffusional exchange between small cells and a measuring patch pipette. *Pflugers Arch*. (1988) 411:204–11. doi: 10.1007/BF00582316

42. Pirolo JS, Allen DG. Assessment of techniques for preventing glycolysis in cardiac muscle. *Cardiovasc Res*. (1986) 20:837–44. doi: 10.1093/cvr/20.11.837
43. Kockskamper J, Zima AV, Blatter LA. Modulation of sarcoplasmic reticulum Ca2+ release by glycolysis in cat atrial myocytes. *J Physiol*. (2005) 564(Pt 3):697–714. doi: 10.1113/jphysiol.2004.078782
44. Dutka TL, Lamb GD. Effect of low cytoplasmic [ATP] on excitation-contraction coupling in fast-twitch muscle fibres of the rat. *J Physiol*. (2004) 560(Pt 2):451–68. doi: 10.1113/jphysiol.2004.069112
45. Krag TO, Pinos T, Nielsen TL, Brull A, Andreu AL, Vissing J. Differential muscle involvement in mice and humans affected by McArdle disease. *J Neuropathol Exp Neurol*. (2016) 75:441–54. doi: 10.1093/jnen/nlw018

Conflict of Interest: The authors declare that the research was conducted in the absence of any commercial or financial relationships that could be construed as a potential conflict of interest.

Copyright © 2020 Leermakers, Dybdahl, Husted, Riisager, de Paoli, Pinós, Vissing, Krag and Pedersen. This is an open-access article distributed under the terms of the Creative Commons Attribution License (CC BY). The use, distribution or reproduction in other forums is permitted, provided the original author(s) and the copyright owner(s) are credited and that the original publication in this journal is cited, in accordance with accepted academic practice. No use, distribution or reproduction is permitted which does not comply with these terms.

frontiers in Neurology

ORIGINAL RESEARCH
published: 26 June 2020
doi: 10.3389/fneur.2020.00593

Genotype-Phenotype Correlations and Characterization of Medication Use in Inherited Myotonic Disorders

Alayne P. Meyer[1], Jennifer Roggenbuck[1], Samantha LoRusso[2], John Kissel[2], Rachel M. Smith[3], David Kline[3] and W. David Arnold[2]*

[1] Division of Human Genetics, The Ohio State University, Columbus, OH, United States, [2] Department of Neurology, The Ohio State University, Columbus, OH, United States, [3] Department of Biomedical Informatics, Center for Biostatistics, The Ohio State University, Columbus, OH, United States

Introduction: Inherited myotonic disorders are genetically heterogeneous and associated with overlapping clinical features of muscle stiffness, weakness, and pain. Data on genotype-phenotype correlations are limited. In this study, clinical features and treatment patterns in genetically characterized myotonic disorders were compared.

Methods: A retrospective chart review was completed in patients with genetic variants in *CLCN1, SCN4A, DMPK,* and *CNBP* to document clinical signs and symptoms, clinical testing, and antimyotonia medication use.

Results: A total of 142 patients (27 *CLCN1*, 15 *SCN4A*, 89 *DMPK*, and 11 *CNBP*) were reviewed. The frequency of reported symptoms (stiffness, weakness, and pain) and electromyographic spontaneous activity were remarkably similar across genotypes. Most patients were not treated with antimyotonia agents, but those with non-dystrophic disorders were more likely to be on a treatment.

Discussion: Among the features reviewed, we did not identify clinical or electrophysiological differences to distinguish *CLCN1*- and *SCN4A*-related myotonia. Weakness and pain were more prevalent in non-dystrophic disorders than previously identified. In addition, our results suggest that medical treatments in myotonic disorders may be under-utilized.

Keywords: myotonia, channelopathies, inherited, treatment, genotype-phenotype, myotonic dystrophy, myotonia congenita, paramyotonia congenital

OPEN ACCESS

Edited by:
Emma Matthews, University College London, United Kingdom

Reviewed by:
Karen Joan Suetterlin, University College London, United Kingdom
Lorenzo Maggi, Fondazione IRCCS Istituto Neurologico Carlo Besta, Milan, Italy
Masanori P. Takahashi, Osaka University, Japan

****Correspondence:***
Alayne P. Meyer
alayne.meyer@nationwidechildrens.org

Specialty section:
This article was submitted to Neuromuscular Diseases, a section of the journal Frontiers in Neurology

Received: *05 December 2019*
Accepted: *22 May 2020*
Published: *26 June 2020*

Citation:
Meyer AP, Roggenbuck J, LoRusso S, Kissel J, Smith RM, Kline D and Arnold WD (2020) Genotype-Phenotype Correlations and Characterization of Medication Use in Inherited Myotonic Disorders. Front. Neurol. 11:593. doi: 10.3389/fneur.2020.00593

INTRODUCTION

Myotonia is a phenomenon of skeletal muscle hyperexcitability that impairs muscle relaxation following contraction or percussion (1–4). Myotonia can be clinically evident with visually appreciable delays in muscle relaxation, but can also be subclinical with myotonic discharges noted on electromyography (EMG) in the absence of overt clinical signs. Etiologies of myotonia include monogenic inherited causes as well as acquired causes such as hypothyroidism, denervation, inflammatory myopathies, or toxic myopathies (5). Inherited myotonic disorders are generally divided into two major categories, dystrophic and non-dystrophic, with the major differentiating factor being the presence of progressive muscle degeneration in patients with dystrophic forms of myotonia (1, 3, 6, 7). Dystrophic myotonic disorders include myotonic dystrophy type I

(DM1), characterized by prominent distal limb weakness and multisystem disease, and myotonic dystrophy type II (DM2, also known as proximal myopathic myotonia or PROMM), characterized by proximal limb weakness with less prevalent multisystem disease (3).

DM1 is caused by a pathogenic CTG expansion in *DMPK* (>50 repeats) which results in altered splicing of *CLCN1,* as well as other genes, leading to reduced chloride conductance and myotonia (8–10). Intergenerational expansion of repeat size may be observed, with an increased repeat size correlating with earlier age of onset and increased severity of symptoms, a phenomenon known as anticipation (9–11). The most severe form of DM1 is seen in individuals with congenital symptoms, typically caused by a repeat size of >1000 (10, 11). DM2 is caused by a pathogenic CCTG expansion in *CNBP* and also affects splicing of *CLCN1*. Genetic anticipation and congenital onset of disease are not observed in DM2 (9–13). Typically, DM2 is milder and has a later age of onset than DM1. Additionally, repeat length is not correlated with severity of symptoms or age of onset (9–12). Pain is a more prominent feature in many individuals with DM2 and may be the presenting symptom, often leading to misdiagnoses (13). Patients with DM1 and DM2 also experience systemic complications including progressive cardiac conduction defects, respiratory insufficiency, premature cataracts, daytime hypersomnolence, gastrointestinal and endocrine dysfunction, cognitive and behavioral deficits, and increased malignancy rates (9–11).

The non-dystrophic myotonias are caused by mutations of specific skeletal muscle ion channels and are usually categorized on the basis of the ion channel affected, inheritance pattern, and clinical features. The two skeletal muscle ion channels that are associated with non-dystrophic disorders include chloride (*CLCN1)* and sodium (*SCN4A)* channels. The non-dystrophic myotonias are known to be highly variable in expression, leading to missed or delayed diagnosis in many cases (1, 14).

Dominant and recessive pathogenic variants in *CLCN1* cause myotonia congenita (MC), the most common inherited muscle channelopathy (6, 7). Variants lead to loss-of-function and dominant negative effects in the CLC-1 channel causing reduced chloride conductance and membrane hyperexcitability (2–4). Both forms are typically characterized by childhood onset muscle stiffness (1, 3). Stiffness can be triggered by emotional surprise and aggravated by cold temperatures and pregnancy. Repetitive motion or "warm up" can alleviate these symptoms (1, 2, 6, 7, 14). Recessively inherited MC often causes more severe symptoms and may cause a slowly progressive muscle weakness that may be identified on clinical examination, as well as transient weakness (1, 3, 14).

Paramyotonia congenita (PMC), sodium channel myotonia (SCM), and hyperkalemic periodic paralysis (HyperPP) are all caused by dominant gain-of-function variants in *SCN4A* (15). These variants lead to an excessive inward sodium ion current which causes muscle hyperexcitability, leading to myotonia, or transient loss of excitability, causing periodic paralysis (16). Symptoms of PMC typically begin in the first decade of life and include myotonia that is induced by cold or repeated muscle activity (paradoxical myotonia or paramyotonia), as well as episodic weakness triggered by exercise, cold, potassium ingestion, or fasting (6, 7, 12, 15, 16). On clinical examination patients with variants in *SCN4A* often display eyelid myotonia that worsens with repetitive eyelid closure (1). SCM is characterized by pure, often painful, myotonia without episodic weakness and typically not triggered by cold temperatures (1, 6, 7, 15). HyperPP is characterized by recurrent episodes of weakness triggered by exercise, potassium ingestion, or emotional stress that can last hours to days. Over time, a slowly progressive permanent weakness may occur in HyperPP (16). Hypokalemic periodic paralysis (HypoPP) is also caused by mutations in *SCN4A* and is usually not associated with myotonia, although rarely is has been described in patients with homozygous loss-of-function variants (17).

Treatment of myotonic disorders is generally influenced by symptom severity and ability to control symptoms through avoidance of triggers (6). Pharmacological treatment may not be necessary in all patients, but patients who accept medical treatment may experience significant improvement in myotonia symptoms, including pain (5). There are currently no FDA approved medications for the treatment of myotonia; however, mexiletine has been approved in the EU as an antimyotonia agent. A multinational study has found that only 40% of patients received treatment for this symptom (14). Off-label antimyotonia treatments include anti-arrhythmic, anti-epileptic, and anti-depressant medications, which have shown clinical benefit, usually in small case series or single case reports. Mexiletine has demonstrated efficacy in multiple controlled studies in non-dystrophic myotonia and in DM1 (18, 19). In addition, a recent n-of-1 aggregate study also showed efficacy in a study cohort of 27 patients with non-dystrophic myotonia (20). Similarly, lamotrigine has been demonstrated to be effective in non-dystrophic myotonia (21). There is a lack of published data detailing usage and efficacy of antimyotonia agents in clinical practice.

In this study, we retrospectively reviewed patient-reported symptoms and clinical data of patients with genetically defined myotonic disorders seen at a large tertiary center. We aimed to characterize the phenotypic profiles of each disorder by comparing symptom profiles between the disorders as well as the usage of commonly prescribed antimyotonia agents.

MATERIALS AND METHODS

A retrospective chart review was performed of patients with inherited myotonic disorders seen at The Ohio State University Wexner Medical Center from March 2009 to December 2018. This study and waiver of consent was approved by the Ohio State University institutional review board.

Subjects

Initial patient search was conducted to identify all patients with myotonia-related diagnostic codes. A complete list of codes utilized are found in **Table 1**. Patients were included in the review if they or a family member had a documented variant in *CLCN1* or *SCN4A* or a pathogenic expansion in *DMPK* or *CNBP*. Patients were excluded if they had absence of myotonia both clinically and

TABLE 1 | List of diagnostic codes utilized in the search for candidates meeting inclusion criteria.

ICD-9/ICD-10	Diagnosis
359.39/G71.19	Myotonia fluctuans
359.21/G71.11	Myotonia atrophica
359.23/G71.13	Myotonia chondrodystrophica
359.22/G71.12	Myotonia congenita
728.85, 319, 756.50/M62.89, F79, Q78.9	Myotonia with intellectual disability and skeletal anomaly
359.24, E980.5/G71.14	Myotonia, drug-induced
359.3/G72.3	Periodic myotonia
794.17/R94.131	Myotonic changes present on EMG
V83.89/Z14.8	Carrier of myotonic dystrophy
271/E74.02	Pompe disease
796.4/R89.0	Low acid maltase in muscle determined by biopsy
792.9/R89.0	Low acid maltase levels in fibroblasts
359.0, V84.89/G71.2, Z15.89	Autosomal dominant centronuclear myopathy associated with mutation in DMN2 gene
359.89, 359.0/G72.89, G71.2	Myofibrillar myopathy

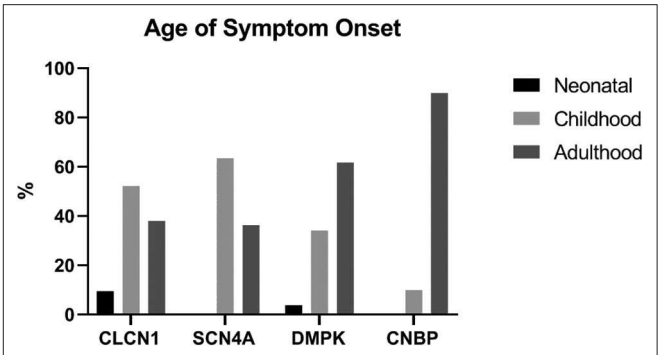

FIGURE 1 | Age range at time of symptom onset by genotype. Neonatal < 1 year old, childhood 1–18 years old, adulthood >18 years old.

electrically or if they had a pathogenic or likely pathogenic variant identified in a second gene related to neuromuscular disease.

Chart Review

Data were collected on patient demographics, patient-reported symptoms (including stiffness, weakness, pain, cramping, and exacerbating factors), family history, and medication history. Physical examination data were documented, including presence of clinical myotonia and weakness, creatine kinase levels, and EMG data. Presence of periodic paralysis and paradoxical myotonia were not ascertained. Genetic testing results, including genetic tests completed and complete variant data, including pathogenic classification (pathogenic, likely pathogenic, or uncertain), were ascertained via review of laboratory reports. For patient-reported symptoms and clinical examination data, each symptom was recorded as present only if the chart note specifically stated that the patient had that symptom. To avoid ascertainment bias, if a symptom was not recorded as present or absent in the chart note, it was listed as "unknown" and data on that symptom in that patient was not utilized in the statistical analysis. Exacerbating factors were recorded as present if documented in the patient's chart, and recorded as absent if it was not documented or if specifically noted as not being present. Muscle weakness was considered present on clinical examination if a patient scored a "4" or less in any muscle group at any clinical visit during manual muscle testing by a neuromuscular specialist. If multiple creatine kinase levels were available, the highest value was recorded. Reference ranges used were 30-220 U/L for men and 30-184 U/L for women. Values recorded from electromyography (EMG) studies included number of muscles tested and number of muscles with abnormal spontaneous activity, including myotonia, positive sharp waves, and fibrillation potentials. If multiple EMG studies were performed, the number of muscles tested and the number of muscles with abnormal spontaneous activity were summed across all studies for each patient in each of these categories. Usage of the following medications was recorded: Acetazolamide, Clomipramine, Diazapam, Dichlorphenamide, Dispyramide, Imipramine, Lamotrigine, Mexiletine, Nifedipine, Phenytoin, Procainamide, Quinine, Ranolazine, Taurine, Thiazides, and Tocainide.

Statistical Analysis

Descriptive statistics were utilized to create the phenotypic profile for each genotype. Mean values were utilized for participant age and age of symptom onset. For the remaining chart review data, percentages were utilized to depict the incidence of a given phenotypic characteristic by genotype. Any characteristic that was not explicitly recorded as present or absent was not utilized in the statistical analysis for that characteristic. Comparison of symptoms across genotype groups and dystrophic versus non-dystrophic groups were made utilizing a Fisher's exact test. Descriptive statistics were utilized to determine the proportion of each genotype group who had trialed and were currently taking an antimyotonia agent. Patients currently taking a medication at the time of review were divided by genotype and type of medication utilized.

RESULTS

Demographics

A total of 142 patients were included in this study: 27 had one or more variants in *CLCN1,* 15 had a variant in *SCN4A*, 89 had an expansion in *DMPK,* and 11 had an expansion in *CNBP*. The average age of symptom onset for individuals with *CLCN1*, *SCN4A, DMPK,* and *CNBP* variants was 16.5 years [standard deviation (*SD*) 12.1], 23.6 years (*SD* 21.0), 28.0 years (*SD* 15.9), and 40.7 (*SD* 12.0), respectively. **Figure 1** depicts symptom onset by age category (neonatal being defined as <1 year of age, childhood as 1–18 years old, and adulthood being greater than 18 years old) and genotype. Most participants were Caucasian (83.8%) and female (81.5% *CLCN1*, 73.3% *SCN4A*, 60.7% *DMPK*,

45.5% *CNBP*). A total of 13 individuals included in the study were deceased at the time of chart review. Eleven of these individuals had *DMPK* expansions, with the average age of death among these individuals being 54.3 years (*SD* 10.4). The other two deaths both occurred at the age of 68, one in an individual with an expansion in *CNBP* and the other in an individual with a variant in *CLCN1*.

Genetic Variants

Of the 27 individuals with at least one variant in *CLCN1*, 23 individuals had one variant identified and 4 had two variants with apparent autosomal recessive inheritance of disease. A total of 13 different variants were identified in the *CLCN1* cohort with eight being classified as pathogenic, two as likely pathogenic, and three as variants of uncertain significance (VUS). No individuals with an *SCN4A* variant were identified to have more than one variant in this gene on their genetic lab report. In the *SCN4A* cohort, 9 different variants were identified with eight being classified as pathogenic and one as a VUS. A full list of genotypes identified and corresponding myotonia phenotypes are summarized in **Tables 2–4**. Additional details on the genetic testing performed for patients with unclear results (including those with single variants previously associated with recessive disease, those with variants of uncertain significance and those possessing variants with conflicting interpretations) are summarized in **Supplementary Table 1**. Expansion length in *DMPK* ranged from 74 repeats to 2,450 repeats. Among individuals in this cohort, 5.6% ($n = 5$) were identified as having <100 repeats, 67.4% ($n = 60$) were identified as having between 100 and 1000 repeats, and 27% ($n = 24$) were identified as having greater than 1,000 repeats in at least part of the sample (in the case of mosaicism). Due to the retrospective nature of this study, we were unable to ascertain the subtype of DM1 for each patient; however, only two patients had onset of symptoms in infancy, while the remaining had childhood or adult onset symptoms.

Patient Reported Symptoms

Stiffness was reported by all individuals in our *CLCN1* cohort and was reported in ∼80% of the remaining three groups. Weakness was reported in a similar proportion of individuals with non-dystrophic myotonias, 65.2% ($n = 15$) of individuals with *CLCN1* variants, and 69.2% ($n = 9$) *SCN4A* variants. Weakness was more often reported in individuals with dystrophic myotonia than non-dystrophic myotonia, with 90.8% ($n = 79$) of individuals

TABLE 2 | List of patients with one variant identified in *CLCN1*.

c.	p.	Lab reported classification	ClinVar classification	Apparent inheritance pattern	Clinical myotonia	Spontaneous activity on EMG
c.469delC	p.Leu157Phefs*13	Pathogenic	Pathogenic	Negative family Hx	No	Yes (8/11)
c.501C>G	p.Phe167Leu	VUS	Conflicting	Negative family Hx	Yes	Yes (4/10)
c.592C>G	p.Leu198Val	VUS	Conflicting	AD	Yes	Yes (3/5)
c.689G>A	p.Gly230Glu	Pathogenic	Pathogenic	AD	Yes	Yes (3/3)
c.689G>A	p.Gly230Glu	Pathogenic	Pathogenic	AD	Yes	Unknown
c.689G>A	p.Gly230Glu	Pathogenic	Pathogenic	AD	Unknown	Yes (3/9)
c.689G>A	p.Gly230Glu	Pathogenic	Pathogenic	AD	Yes	Unknown
c.689G>A	p.Gly230Glu	Pathogenic	Pathogenic	AD	No	Unknown
c.689G>A	p.Gly230Glu	Pathogenic	Pathogenic	AD	Yes	Yes (3/3)
c.689G>A	p.Gly230Glu	Pathogenic	Pathogenic	AD	Yes	Unknown
c.689G>A	p.Gly230Glu	Pathogenic	Pathogenic	Unknown	Unknown	Unknown
c.689G>A	p.Gly230Glu	Pathogenic	Pathogenic	Unclear	Yes	Unknown
c.929C>T	p.Thr310Met	Pathogenic	Pathogenic	AD	No	Unknown
c.929C>T	p.Thr310Met	Pathogenic	Pathogenic	AD	Unknown	Unknown
c.937G>A	p.Ala313Thr	Pathogenic	Pathogenic	AD	Unknown	Yes (8/17)
c.937G>A	p.Ala313Thr	Pathogenic	Pathogenic	AD	Yes	Yes
c.1167-10 T>C	Intronic	Likely pathogenic	Likely pathogenic	Unclear	Yes	Yes (8/8)
c.1444G>C	p.Gly482Arg	Likely pathogenic	Likely pathogenic	AD	No	Yes (10/10)
c.1655A>G	p.Gln552Arg	Pathogenic	Conflicting (LP/P)	AD	Yes	Yes
c.2680C>T	p.Arg894Ter	Pathogenic	Conflicting (LP/P)	Unknown	No	Unknown
c.2680C>T	p.Arg894Ter	Pathogenic	Conflicting (LP/P)	Unknown	Yes	Unknown
c.2848G>A	p.Glu950Lys	VUS	N/a	AD	Yes	Yes (3/5)

For each patient, the classification of the variant as listed on the original laboratory report as well as the classification in the ClinVar database are included. Apparent inheritance is based on family history information identified in the chart. Patients with family members with a diagnosis of myotonia congenita (with or without genetic confirmation), EMG positive for myotonia or reported symptoms of myotonia or stiffness were categorized as autosomal dominant inheritance ("AD"). Patients with family history information available which was negative for any of these symptoms were categorized as "negative family hx." Patients with no family history information listed in the chart were categorized as "unknown" and patients with family history of symptoms of unclear diagnostic significance (pain, cramping or weakness) were categorized as "unclear." Presence of clinical myotonia is listed as positive, negative or unknown for each patient. Spontaneous activity on EMG is listed as positive, negative or unknown. In parentheses, the number of muscles affected with spontaneous activity divided by the total muscles tested on EMG for that individual is recorded (if known).

TABLE 3 | List of patients with two variants identified in *CLCN1*.

c.	p.	Lab reported classification	ClinVar classification	Apparent inheritance pattern	Clinical myotonia	Spontaneous activity on EMG
c.689G>A	p.Gly230Glu	Pathogenic;	Pathogenic;	AD	Yes	Unknown
c.1444G>C	p.Gly482Arg	Likely pathogenic	Likely pathogenic			
c.568G>A	p.Gly190Arg	VUS;	Conflicting;	Negative family Hx	Unknown	Yes
c.1238T>G	p.Phe413Cys	Pathogenic	Pathogenic			
c.979G>A	p.Val327Ile	Pathogenic;	Pathogenic;	Negative family Hx	Yes	Unknown
c.1262G>T	p.Arg421Leu	VUS	Likely pathogenic			
c.1238T>G	p.Phe413Cys	Pathogenic;	Pathogenic;	Negative family Hx	Yes	Yes (3/5)
c.2680C>T	p.Arg894Ter	Pathogenic	Conflicting (LP/P)			
c.409T>G	p.Tyr137Asp	Likely pathogenic;	Likely pathogenic;	Negative family Hx	Yes	Yes (18/18)
c.1238T>G	p.Phe413Cys	Pathogenic	Pathogenic			

For each patient, the classification of the variant as listed on the original laboratory report as well as the classification in the ClinVar database are included. Apparent inheritance is based on family history information identified in the chart. Patients with family members with a diagnosis of myotonia congenita (with or without genetic confirmation), EMG positive for myotonia or reported symptoms of myotonia or stiffness were categorized as autosomal dominant inheritance ("AD"). Patients with family history information available which was negative for any of these symptoms were categorized as "negative family hx." Patients with no family history information listed in the chart were categorized as "unknown" and patients with family history of symptoms of unclear diagnostic significance (pain, cramping or weakness) were categorized as "unclear." Presence of clinical myotonia is listed as positive, negative or unknown for each patient. Spontaneous activity on EMG is listed as positive, negative or unknown. In parentheses, the number of muscles affected with spontaneous activity divided by the total muscles tested on EMG for that individual is recorded (if known).

TABLE 4 | List of patients with variants in *SCN4A*.

c.	p.	Lab reported classification	ClinVar classification	Apparent inheritance pattern	Clinical myotonia	Spontaneous activity on EMG
c.1333G>A	p.Val445Met	Pathogenic	Pathogenic	AD	Yes	Yes (6/6)
c.1333G>A	p.Val445Met	Pathogenic	Pathogenic	AD	Yes	Yes (2/2)
c.1333G>A	p.Val445Met	Pathogenic	Pathogenic	AD	No	Yes (3/3)
c.2078T>C	p.Ile693Thr	Pathogenic	Pathogenic	AD	Yes	Unknown
c.3917G>C	p.Gly1306Ala	Pathogenic	Pathogenic	Unclear	No	Unknown
c.3917G>C	p.Gly1306Ala	Pathogenic	Pathogenic	Unknown	Yes	Unknown
c.3917G>C	p.Gly1306Ala	Pathogenic	Pathogenic	AD	Yes	Unknown
c.3938C>T	p.Thr1313Met	Pathogenic	Pathogenic	Negative Family Hx	Yes	Yes (7/7)
c.4343G>A	p.Arg1448His	Pathogenic	Pathogenic	AD	Yes	Yes (5/5)
c.4343G>A	p.Arg1448His	Pathogenic	Pathogenic	Unknown	No	Unknown
c.4343G>A	p.Arg1448His	Pathogenic	Pathogenic	AD	Yes	Yes (2/2)
c.4372G>T	p.Val1458Phe	Likely Pathogenic	VUS	Negative Family Hx	Unknown	Yes (16/22)
c.4386C>G	p.Ile1462Met	Pathogenic	VUS	Unknown	Unknown	Yes
c.4765G>A	p.Val1589Met	Pathogenic	Pathogenic	AD	Yes	Yes (2/2)
c.5126A>G	p.Asn1709Ser	VUS	VUS	Unclear	Unknown	Yes (2/4)

For each patient, the classification of the variant as listed on the original laboratory report as well as the classification in the ClinVar database are included. Apparent inheritance is based on family history information identified in the chart. Patients with family members with a diagnosis of paramyotonia congenita or sodium channel myotonia (with or without genetic confirmation), EMG positive for myotonia or reported symptoms of myotonia or stiffness were categorized as autosomal dominant inheritance ("AD"). Patients with family history information available which was negative for any of these symptoms were categorized as "negative family hx." Patients with no family history information listed in the chart were categorized as "unknown" and patients with family history of symptoms of unclear diagnostic significance (pain, cramping or weakness) were categorized as "unclear." Presence of clinical myotonia is listed as positive, negative or unknown for each patient. Spontaneous activity on EMG is listed as positive, negative or unknown. In parentheses, the number of muscles affected with spontaneous activity divided by the total muscles tested on EMG for that individual is recorded (if known).

with *DMPK* expansions and 90% ($n = 9$) with *CNBP* expansions reporting this as a symptom. History of pain was reported by all individuals with *CNBP* expansions ($n = 11$), while it was found in 50–70% of the remaining three groups. Presence of muscle cramping was similar across all groups with 50% ($n = 6$) of individuals with *SCN4A* variants and 30–40% of the remaining three groups reporting this. Cold as an exacerbating factor for symptoms was most commonly reported in individuals with non-dystrophic myotonias, with 40.7% ($n = 11$) of individuals with *CLCN1* variants and 46.7% ($n = 7$) of individuals with *SCN4A* variants reporting this compared to 36.4% ($n = 4$) of individuals with *CNBP* expansions and in 7.9% ($n = 7$) of individuals with *DMPK* expansions. A summary of patient reported symptom data is in **Table 5**.

Clinical Examination

Most individuals in the overall cohort had at least one form of clinical myotonia with 69–94% of each group having this

TABLE 5 | Summary of patient reported symptoms by genotype.

Symptom		Non-dystrophic		Dystrophic		Total	*p*-value
		CLCN1	SCN4A	DMPK	CNBP		
Stiffness	Yes	24 (100.0%)	11 (78.6%)	62 (78.5%)	8 (80.0%)	105 (82.7%)	0.0371
	Unknown	3	1	10	1	15	
Weakness	Yes	15 (65.2%)	9 (69.2%)	79 (90.8%)	9 (90.0%)	112 (84.2%)	0.0072
	Unknown	4	2	2	1	9	
Pain	Yes	18 (69.2%)	8 (53.3%)	50 (59.5%)	10 (100.0%)	86 (63.7%)	0.0417
	Unknown	1	0	5	1	7	
Cramping	Yes	8 (34.8%)	6 (50.0%)	30 (37.5%)	3 (30.0%)	47 (37.6%)	0.8021
	Unknown	4	3	9	1	17	
Cold exacerbation	Yes	11 (40.7%)	7 (46.7%)	7 (7.9%)	4 (36.4%)	29 (20.4%)	<0.0001

P-values were obtained using Fisher's exact test.

TABLE 6 | Summary of clinical examination findings by genotype.

Symptom		Non-dystrophic		Dystrophic		Total	*p*-value
		CLCN1	SCN4A	DMPK	CNBP		
Clinical myotonia	Yes	17 (73.9%)	9 (69.2%)	75 (93.8%)	7 (77.8%)	108 (86.4%)	0.0067
	Unknown	4	2	9	2	17	
Hand grip myotonia	Yes	14 (70.0%)	9 (75.0%)	63 (85.1%)	1 (16.7%)	87 (77.7%)	0.0022
	Unknown	7	3	15	5	30	
Percussion myotonia	Yes	12 (70.6%)	4 (57.1%)	70 (94.6%)	5 (62.5%)	91 (85.8%)	0.0006
	Unknown	10	8	15	3	36	
Muscle weakness (on MMT)	Yes	4 (16.0%)	4 (26.7%)	78 (91.8%)	6 (54.5%)	92 (67.6%)	<0.0001
	Unknown	2	0	4	0	6	

P-values were obtained using Fisher's exact test.

present on physical examination. Hand grip myotonia was least common in individuals with expansions in *CNBP* at 16.7% ($n = 1$) while both hand grip and percussion myotonia were most commonly identified in individuals with *DMPK* expansions at 85.1% ($n = 63$) and 94.6% ($n = 70$), respectively. Muscle weakness was most common in the individuals with *DMPK* expansions at 91.8% ($n = 78$) followed by individuals with *CNBP* expansions at 54.5% ($n = 6$). However, 16% ($n = 4$) of individuals with *CLCN1* variants and 26.7% ($n = 4$) of individuals with *SCN4A* variants were also found to have weakness in at least one muscle group. Distribution of weakness on MMT was most commonly identified as proximal only in *SCN4A* patients, was evenly split between proximal only and both proximal and distal in *CLCN1* and *CNBP* patients and was most commonly identified as both proximal and distal in patients with expansions in *DMPK*. A summary of clinical examination data is in **Table 6**.

EMG Results

In this cohort, individuals with *DMPK* expansions were least likely to have had an EMG performed at 43.8% of the group compared to 70–100% of the remaining three groups. The proportion of muscles with spontaneous activity was similar among the four groups ranging from 71 to 88%. Proportion of muscles with spontaneous activity by genotype is depicted in **Figure 2**.

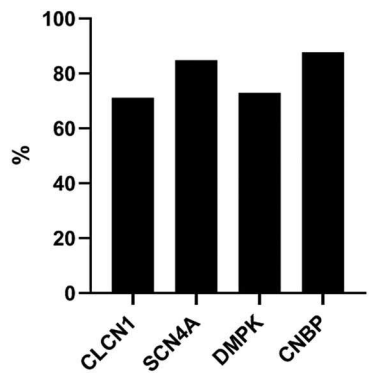

FIGURE 2 | Proportion of muscles on EMG with abnormal spontaneous activity by genotype.

Creatine Kinase Levels

CK levels were available for 81 participants. Values were similar for the non-dystrophic groups, with the average being 157.8 U/L (*SD* 153.6) for individuals with *CLCN1* variants and 168.6 U/L (*SD* 137.8) for individuals with *SCN4A* variants. Values were

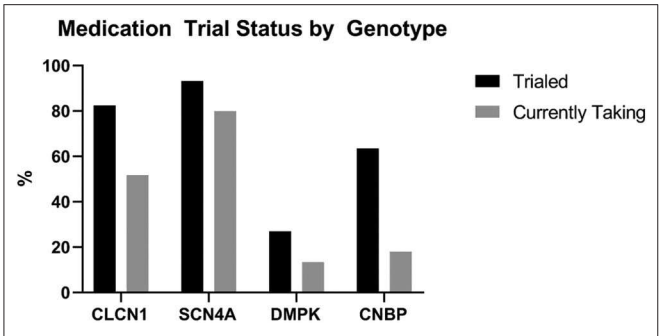

FIGURE 3 | Proportion of individuals, by genotype, who had ever trialed an antimyotonia medication and who were currently taking one at the time of chart review.

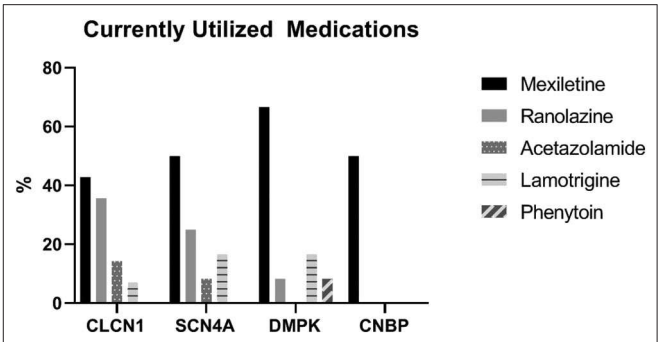

FIGURE 4 | Proportion (of those currently taking a medication) of individuals taking each type of antimyotonia agent.

higher for the individuals with *DMPK* and *CNBP* expansions with the averages being 243.4 and 345.6 U/L, respectively. The proportion of individuals with an abnormal CK level was 23.1% ($n = 3$) of individuals with *CLCN1* variants, 37.5% ($n = 3$) of individuals with *SCN4A* variants, 54% ($n = 27$) of individuals with *DMPK* expansions, and 40% ($n = 4$) of individuals with *CNBP* expansions.

Medication Usage

Patients with *DMPK* expansions were the least likely to have trialed an antimyotonia medication at 27% ($n = 24$). Medications had been trialed in 85.2% of individuals with *CLCN1* variants ($n = 23$), 93.3% of individuals with *SCN4A* variants ($n = 14$), and 63.6% of individuals with *CNBP* expansions ($n = 7$). Genotype specific medication trialing data is summarized in **Figure 3**. Of those who trialed medications, 56.5% ($n = 13$) of *CLCN1* patients, 66.7% ($n = 10$) of *SCN4A* patients, and 8.3% ($n = 2$) of *DMPK* patients had tried more than one medication for myotonia. No patients with *CNBP* expansion had trialed multiple medications. The most commonly trialed medication across all four groups was mexiletine at 40.4% of individuals who trialed any medication ($n = 42$). Currently utilized medications by genotype are depicted by **Figure 4**. More individuals with non-dystrophic myotonias were currently taking at least one medication for myotonia with 51.9% ($n = 14$) of individuals with *CLCN1* variants and 80.0% ($n = 12$) of individuals with *SCN4A* variants compared to 13.5% ($n = 12$) of individuals with *DMPK* expansions, and 18.2% ($n = 2$) of individuals with *CNBP* expansions. Out of the patients trialing at least one medication, none with *SCN4A* variants had discontinued all medication use for myotonia. Patients with dystrophic myotonias more commonly had discontinued all antimyotonia agents with 50.0% ($n = 12$) patients with *DMPK* expansions and 71.4% ($n = 5$) patients with *CNBP* expansions having done so compared to 17.4% ($n = 4$) of individuals with *CLCN1* variants. Reason for discontinuation was given for 30 (60%) of the medications stopped. The frequency that each medication was stopped due to cost, drug interactions, efficacy, or side effects is presented recorded in **Table 7**. The most common reasons for discontinuation overall were lack of efficacy (32%, $n = 16$) and side effects (20%, $n = 10$). For mexiletine, reason for discontinuation was known in nine of cases with 21.2% ($n = 4$) being due to lack of efficacy and 26.3% ($n = 5$) due to side effects.

Dystrophic (D) vs. Non-dystrophic (ND)

Many clinical features differentiated the *D* and *ND* cohorts. The average age of onset of symptoms was significantly younger in the *ND* cohort compared to the *D* cohort at 18.6 years (*SD* 15.1) and 29.9 years (*SD* 16.0), respectively ($p = 0.0037$). Cold exacerbation of symptoms was less commonly reported in the *D* cohort (11 vs. 42.9%, $p < 0.0001$) and muscle weakness was more commonly reported (90.7 vs. 66.7%, $p = 0.0022$). On examination, clinical myotonia (92.1 vs. 72.2%, $p = 0.0073$), percussion myotonia (91.5 vs. 66.7%, $p = 0.0051$), and muscle weakness (87.5 vs. 20%, $p < 0.0001$) were more common in the *D* cohort. Average CK levels among the two cohorts (161.9 U/L in *ND* vs. 261.1 U/L in *D*, $p = 0.0708$) and proportion of individuals with an abnormal CK level (28.6% *ND* vs. 51.7% *D*, $p = 0.0797$) appeared to differ but were not statistically significant. Patient reported symptoms and clinical examination findings between these groups are summarized in **Figure 5**. From a treatment standpoint, ND patients were significantly more likely to have trialed (88.1% *ND* vs. 31% *D*, $p < 0.001$) and to be currently taking an antimyotonia agent than were the individuals with dystrophic myotonia (61.9% *ND* vs. 14% *D*, $p < 0.0001$). Furthermore, *ND* patients were more likely to remain on a medication after trialing than *D* patients (70.3% *ND* vs. 45.2% *D*, $p < 0.0001$).

CLCN1 vs. SCN4A

The only significant difference identified between these two cohorts was a greater proportion of individuals reporting stiffness in the *CLCN1* cohort. In our cohort, 100% ($n = 24$) of individuals with *CLCN1* variants reported stiffness compared to 78.6% ($n = 11$) of individuals with *SCN4A* variants ($p = 0.0431$). Surprisingly, weakness (65.2% *CLCN1* vs. 69.2% *SCN4A*, $p = 1.0000$) and pain (69.2% *CLCN1* vs. 53.3% *SCN4A*, $p = 0.3357$) were not significantly different between these cohorts. Patient reported symptoms and clinical examination findings between these groups are summarized in **Figure 6**.

TABLE 7 | Summary of reasons patients discontinued commonly utilized antimyotonia agents.

Reason	Procainamide	Phenytoin	Quinine	Mexiletine	Acetazolamide	Ranolazine	Lamotrigine	Total
Cost	–	–	1 (33.3%)	–	–	2 (16.7%)	–	3 (6.0%)
Drug interactions	–	–	–	–	–	1 (8.3%)	–	1 (2.0%)
Efficacy	1 (100.0%)	3 (42.9%)	–	4 (21.1%)	4 (80.0%)	4 (33.4%)	–	16 (32.0%)
Side effects	–	1 (14.3%)	–	5 (26.3%)	1 (20.0%)	2 (16.7%)	1 (50.0%)	10 (20.0%)

**No patients discontinued medications due to allergic reaction.*

***Not all fields will add to 100% as not all individuals discontinuing a medication had a reason in their chart.*

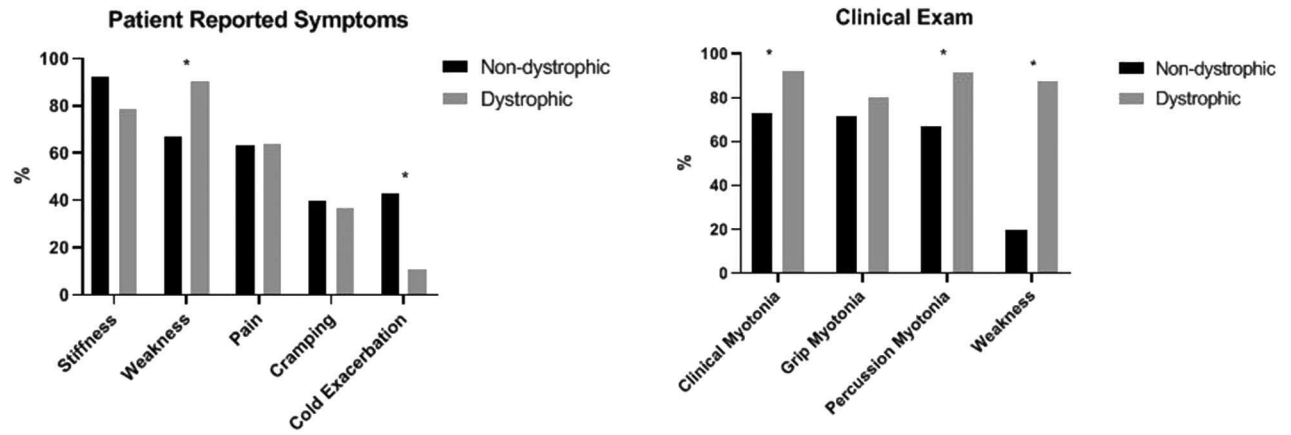

FIGURE 5 | Comparison of patient reported symptoms and clinical examination between patients with non-dystrophic myotonia and dystrophic myotonia. Asterisks indicate areas with statistically significant differences. Clinical myotonia ($p = 0.0073$), percussion myotonia ($p = 0.0051$), and muscle weakness ($p < 0.0001$) were more common in the *D* cohort. Muscle weakness was more commonly reported by the *D* cohort ($P = 0.0022$) and cold exacerbation was more commonly reported by the *ND* cohort ($P < 0.0001$).

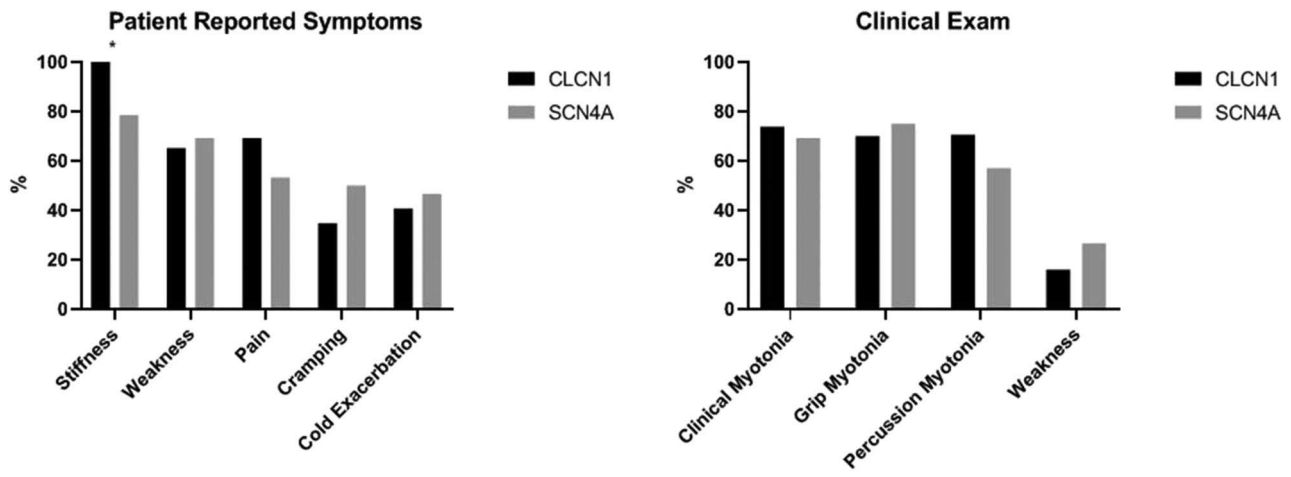

FIGURE 6 | Comparison of patient reported symptoms and clinical examination between patients with variants in *CLCN1* and *SCN4A*. Asterisks indicate areas with statistically significant differences. Patients with *CLCN1* variants were more likely to report stiffness than those with *SCN4A* variants ($p = 0.0431$).

DISCUSSION

In this retrospective study, we performed a comprehensive review of medical record data from a large group of patients with genetically confirmed dystrophic and non-dystrophic myotonic disorders. Our goals included an improved understanding of the phenotypic presentation of hereditary myotonic disorders, as well as characterization of medication use in affected persons. Utilizing this data, we are able to summarize symptom profiles and compare phenotypic features between genotypes.

Additionally, we reviewed antimyotonia treatment usage, which has been understudied for this group of disorders.

Muscle stiffness is the primary clinical symptom attributed to myotonia (3). Interestingly, the prevalence of stiffness was the only feature that differed significantly among patients with non-dystrophic myotonias, with more individuals with *CLCN1* variants reporting this symptom than individuals with *SCN4A* variants. In contrast, Trivedi et al., found that 100% of both *CLCN1* and *SCN4A* patients reported stiffness (23). Although eyelid myotonia has been previously identified as a hallmark of *SCN4A*-related myotonia, we were unable to characterize its prevalence in this cohort, as it was not commonly commented on in the charts reviewed (1, 6, 7).

We found that the majority of patients with non-dystrophic myotonic disorders reported weakness and that there was no significant difference in the occurrence of these symptoms with respect to genotype. The high prevalence of reported weakness is particularly notable given that the majority (85%) of our *CLCN1* cohort had a single variant identified, and dominant CLCN1-related myotonia has not been classically associated with weakness. Patient-reported weakness in non-dystrophic myotonia has also been identified in two prospective studies; however, the proportion of individuals manifesting weakness differed by genotype. Trip et al. found that patient-reported weakness was almost twice as common in individuals with *CLCN1* variants (75%) compared to *SCN4A* variants (36.7%) while Trivedi et al. found episodic weakness to be approximately twice as common in individuals with *SCN4A* variants (76.5%) compared to individuals with *CLCN1* variants (37.5%) (22, 23). These disparate findings may reflect the different proportion of individuals with dominant versus recessive inheritance in the *CLCN1* cohorts. The majority of the Trip et al. cohort had recessive *CLCN1* variants (previously reported to be associated with a higher incidence of muscle weakness), while the cohort in the Trivedi et al. study had approximately equivalent proportions of dominant and recessive variants (22, 23). Alternatively, these variable findings could be due to differences in symptom ascertainment. Trip et al. documented the presence of "muscle weakness," while Trivedi et al. documented "episodic weakness." In future studies, it may be helpful to ascertain patient-reported weakness in several different ways to better characterize the spectrum of weakness and its functional impact for affected persons.

MMT data revealed that 20% of our non-dystrophic cohort had weakness that was identified via clinical examination. In a *SCN4A* cohort reported by Matthews et al., four out of seventeen (23.5%) had weakness, none with strength of <4/5 (24). Similarly, we identified clinical weakness in 26.7% of our *SCN4A* cohort. Data correlating weakness identified on MMT with *CLCN1* variants has not been published, but within our cohort was present in 16% ($n = 4$). The presence of muscle weakness on MMT is considered uncommon in individuals with non-dystrophic myotonia, despite the fact that a large proportion of these patients report weakness as a symptom (5, 6, 22, 23). Additionally, weakness that is episodic or associated with a specific trigger may be missed during standard strength testing, which could account for some of the discrepancy between patient report and clinical examination.

Pain was reported in a high proportion of all cohorts, affecting 63.7% overall. Furthermore, we found that similar proportions of patients with *CLCN1* variants and *SCN4A* variants experience pain, at 69.2 and 53.3%, respectively. Although painful myotonia is an accepted clinical feature of *SCN4A*-related myotonia, *CLCN1*-related myotonia was originally described as being painless (1). Prior studies have reported pain in 57–82% of individuals with *SCN4A* variants and in 28–53% of individuals with *CLCN1* variants (22, 23). We found that pain was reported in all DM2 patients and 59.5% of patients with DM1. Presence of pain is often considered more common in individuals with DM2, which our data supports (25, 26). Identification of pain and weakness in a high proportion of patients, particularly in those with disease not historically associated with these symptoms, is important in understanding phenotype, disease burden, and potential treatment opportunities.

Another aim of our study was to understand the treatment approaches in patients with inherited myotonic disorders. Currently, there are no medications that are approved for the treatment of myotonia, but a number of medications are used off label. In our study cohort, 47.9% of patients trialed at least one medication for myotonia and 28.2% were taking an antimyotonia medication at the time of chart review. Trivedi et al. similarly found that 60.6% of their cohort (*CLCN1, SCN4A, CNBP)* was currently taking an antimyotonia agent, but did not specify medication usage by genotype; and DM1 patients were not studied (19). In our cohort, 83% of all patients reported stiffness and 64% reported pain. This suggests that some symptomatic individuals are not being treated, and lack of medication utilization cannot be explained by lack of symptoms. Individuals with non-dystrophic myotonia were significantly more likely to have trialed and remained on an antimyotonia agent. Of those who tried an antimyotonia medication, non-dystrophic patients were also more likely to have trialed two or more medications than the dystrophic patients. Given that clinical myotonia was more common in the dystrophic cohort, and that patient-reported myotonia was similar in the dystrophic and non-dystrophic cohorts, the different rates of medication usage are evidently not due to differences in symptom prevalence. Although it is possible that the non-dystrophic cohort experienced less symptoms due higher medication use, charts were reviewed at multiple time points, including the initial patient visit, to reduce the effect of medication on these data points. Other possible explanations for this discrepancy include: non-dystrophic patients may have better therapeutic response to currently available medications, non-dystrophic patients may be more compliant in taking medications or due to the lack of systemic symptoms in non-dystrophic patients, the focus for therapy may be on their myotonia symptoms rather than symptoms in other body systems. None the less, this data suggests that there could be a gap between patients who may benefit from use of antimyotonia agents and those who are actually treated. Ideally, treatable symptoms should be ascertained and medication offered for patients who may benefit. Further study of medical treatment of myotonia, including

genotype-specific treatment, dose, duration, side effects, reasons for discontinuation, and non-compliance is necessary to optimize symptom management for patients affected with these disorders.

This study has limitations associated with retrospective chart review and single center bias. These include limitations in type of data that is charted and available to review, lack of consistency in the type and depth of information recorded in the medical record, variability in number of appointments and time between appointments for patients included and the possibility that patients may be not reporting all symptoms to a physician or falsely reporting presence or absence of symptoms and/or treatment response. Consistency of type of data recorded, and format in which it was recorded, was controlled by utilization of a standardized database which aided in consistency during the data entry process.

Inherited myotonic disorders present diagnostic and treatment challenges in the clinical setting. Different types of myotonic disorders may be difficult to distinguish clinically, emphasizing the importance of comprehensive genetic testing. In patients suspected of having a non-dystrophic myotonia, the most expeditious, and cost-effective approach is panel testing including *CLCN1* and *SCN4A* sequencing. We found that the majority of patients with myotonic disorders had symptoms of pain, weakness, and stiffness. This includes individuals with non-dystrophic myotonia, a group where pain and weakness have not always been considered common symptoms. Despite this, only about half of the patients in this study were treated with antimyotonia agents. Advances in pharmacologic treatments for myotonia are needed, as there are no medications specifically approved for the indication of myotonia. Future studies should be designed to investigate relationships between specific genetic variants, clinical phenotypes, and symptom profiles, as well as response to different potential antimyotonia treatments.

DATA AVAILABILITY STATEMENT

All datasets generated for this study are included in the article/**Supplementary Material**.

ETHICS STATEMENT

This project was approved by the Ohio State Biomedical Sciences IRB.

AUTHOR CONTRIBUTIONS

AM performed chart reviews and data entry. RS and AM created the database. RS and DK performed statistical analysis. AM, JR, SL, and WA wrote the manuscript. All authors were involved in the design of this study.

FUNDING

This study was funded in part by The Ohio State University Center for Clinical and Translational Sciences (CCTS) and The Ohio State Neuroscience Research Institute.

SUPPLEMENTARY MATERIAL

The Supplementary Material for this article can be found online at: https://www.frontiersin.org/articles/10.3389/fneur.2020.00593/full#supplementary-material

REFERENCES

1. Heatwole CR, Moxley RT. The non-dystrophic myotonias. *Neurotherapeutics.* (2007) 4:238–51. doi: 10.1016/j.nurt.2007.01.012
2. Tang C-Y, Chen T-Y. Physiology and pathophysiology of CLC-1: mechanisms of a chloride channel disease, myotonia. *J Biomed Biotechnol.* (2011) 2011:685328. doi: 10.1155/2011/685328
3. Timothy M. Differential diagnosis of myotonic disorders. *Muscle Nerve.* (2008) 37:293–9. doi: 10.1002/mus.20923
4. Trip J, Drost G, Verbove DJ, van der Kooi AJ, Kuks JB, Notermans NC, et al. In tandem analysis of CLCN1 and SCN4A greatly enhances mutation detection in families with non-dystrophic myotonia. *Eur J Hum Gene.* (2008) 16:921–9. doi: 10.1038/ejhg.2008.39
5. Heatwole CR, Statland JM, Logigian EL. The diagnosis and treatment of myotonic disorders. *Muscle Nerve.* (2013) 47:632–48. doi: 10.1002/mus.23683
6. Matthews E, Fialho D, Tan SV, Venance SL, Cannon SC, Sternberg D, et al. The non-dystrophic myotonias: molecular pathogenesis, diagnosis and treatment. *Brain.* (2010) 133:9–22. doi: 10.1093/brain/awp294
7. Horga A, Raja Rayan DL, Matthews E, Sud R, Fialho D, Durran SC, et al. Prevalence study of genetically defined skeletal muscle channelopathies in England. *Neurology.* (2013) 80:1472–5. doi: 10.1212/WNL.0b013e31828cf8d0
8. Mankodi A, Takahashi MP, Jiang H, Beck CL, Bowers WJ, Moxley RT, et al. Expanded CUG repeats trigger aberrant splicing of ClC-1 chloride channel pre-mRNA and hyperexcitability of skeletal muscle in myotonic dystrophy. *Mol Cell.* (2002) 10:35–44. doi: 10.1016/S1097-2765(02)00563-4
9. Meola G. Meola G. Clinical and genetic heterogeneity in myotonic dystrophies. *Muscle Nerve.* (2000) 23:1789–99. doi: 10.1002/1097-4598(200012)23:12<1789::AID-MUS2>3.0.CO;2-4
10. Thornton CA. Myotonic Dystrophy. *Neurologic Clinics.* (2014) 32:705–19. doi: 10.1016/j.ncl.2014.04.011
11. Turner C, Hilton-Jones D. Myotonic dystrophy: diagnosis, management and new therapies. *Curr Opin Neurol.* (2014) 27:599–606. doi: 10.1097/WCO.0000000000000128
12. Lehmann-Horn F, Rüdel R. Hereditary nondystrophic myotonias and periodic paralyses. *Curr Opin Neurol.* (1995) 8:402–10. doi: 10.1097/00019052-199510000-00014
13. Meola G, Cardani R. Myotonic dystrophy type 2 and modifier genes: an update on clinical and pathomolecular aspects. *Neurol Sci.* (2017) 38:535–46. doi: 10.1007/s10072-016-2805-5
14. Trivedi JR, Cannon SC, Griggs RC. Nondystrophic myotonia: challenges and future directions. *Exp Neurol.* (2014) 253:28–30. doi: 10.1016/j.expneurol.2013.12.005
15. Loussouarn G, Sternberg D, Nicole S, Marionneau C, Le Bouffant F, Toumaniantz G, et al. Physiological and Pathophysiological Insights of Nav1.4 and Nav1.5 Comparison. *Front Pharmacol.* (2016) 6:314. doi: 10.3389/fphar.2015.00314
16. Cannon SC. Sodium channelopathies of skeletal muscle. In Chahine M, ed. *Voltage-Gated Sodium Channels: Structure, Function and Channelopathies. Vol. 246.* Cham: Springer International Publishing (2017). 309–330. doi: 10.1007/164_2017_52
17. Luo S, Sampedro Castañeda M, Matthews E, Sud R, Hanna MG, Sun J, et al. Hypokalaemic periodic paralysis and myotonia in a

patient with homozygous mutation p.R1451L in NaV1.4. *Sci Rep*. (2018) 8:27822. doi: 10.1038/s41598-018-27822-2
18. Logigian EL, Martens WB, Moxley RT 4th, McDermott MP, Dilek N, Wiegner AW, et al. Mexiletine is an effective antimyotonia treatment in myotonic dystrophy type 1(LOE Classification). *Neurology*. (2010) 74:1441–8. doi: 10.1212/WNL.0b013e3181dc1a3a
19. Statland JM, Bundy BN, Wang Y, Rayan DR, Trivedi JR, Sansone VA, et al. Mexiletine for symptoms and signs of myotonia in non-dystrophic myotonia: a randomized controlled trial. *JAMA*. (2012) 308:1357–65. doi: 10.1001/jama.2012.12607
20. Stunnenberg BC, Raaphorst J, Groenewoud HM, Statland JM, Griggs RC, Woertman W, et al. Effect of mexiletine on muscle stiffness in patients with nondystrophic myotonia evaluated using aggregated N-of-1 trials. *JAMA*. (2018) 320:2344–53. doi: 10.1001/jama.2018.18020
21. Andersen G, Hedermann G, Witting N, Duno M, Andersen H, Vissing J. The antimyotonic effect of lamotrigine in non-dystrophic myotonias: a double-blind randomized study. *Brain*. (2017) 140:2295–305. doi: 10.1093/brain/awx192
22. Trip J, Drost G, Ginjaar HB, Nieman FH, van der Kooi AJ, de Visser M, et al. Redefining the clinical phenotypes of non-dystrophic myotonic syndromes. *J Neurol Neurosurg Psychiatry*. (2009) 80:647–52. doi: 10.1136/jnnp.2008.162396
23. Trivedi JR, Bundy B, Statland J, Salajegheh M, Rayan DR, Venance SL, et al. Non-dystrophic myotonia: prospective study of objective and patient reported outcomes. *Brain*. (2013) 136:2189–200. doi: 10.1093/brain/awt133
24. Matthews E, Tan SV, Fialho D, Sweeney MG, Sud R, Haworth A, et al. What causes paramyotonia in the United Kingdom? Common and new SCN4A mutations revealed. *Neurology*. (2008) 70:50–3. doi: 10.1212/01.wnl.0000287069.21162.94
25. Parmova O. The character and frequency of muscular pain in myotonic dystrophy and their relationship to myotonia. *Int J Neurol Neurother*. (2014) 1:9. doi: 10.23937/2378-3001/1/1/1009
26. Peric M, Peric S, Rapajic N, Dobricic V, Savic-Pavicevic D, Nesic I, et al. Multidimensional aspects of pain in myotonic dystrophies. *Acta Myol*. (2015) 34:126–32.

Conflict of Interest: WA received funding from Gilead Sciences, the Neuroscience Research Institute at The Ohio State University, and has served as a paid consultant to Genentech and La Hoffmann Roche.

The remaining authors declare that the research was conducted in the absence of any commercial or financial relationships that could be construed as a potential conflict of interest.

Copyright © 2020 Meyer, Roggenbuck, LoRusso, Kissel, Smith, Kline and Arnold. This is an open-access article distributed under the terms of the Creative Commons Attribution License (CC BY). The use, distribution or reproduction in other forums is permitted, provided the original author(s) and the copyright owner(s) are credited and that the original publication in this journal is cited, in accordance with accepted academic practice. No use, distribution or reproduction is permitted which does not comply with these terms.

frontiers in Neurology

ORIGINAL RESEARCH
published: 29 July 2020
doi: 10.3389/fneur.2020.00646

Clinical and Molecular Spectrum of Myotonia and Periodic Paralyses Associated With Mutations in *SCN4A* in a Large Cohort of Italian Patients

Lorenzo Maggi[1†], Raffaella Brugnoni[1†], Eleonora Canioni[1], Paola Tonin[2], Veronica Saletti[3], Patrizia Sola[4], Stefano Cotti Piccinelli[5], Lara Colleoni[1], Paola Ferrigno[6], Antonella Pini[7], Riccardo Masson[3], Fiore Manganelli[8], Daniele Lietti[9], Liliana Vercelli[10], Giulia Ricci[11], Claudio Bruno[12], Giorgio Tasca[13], Antonio Pizzuti[14,15], Alessandro Padovani[5], Carlo Fusco[16], Elena Pegoraro[17], Lucia Ruggiero[8], Sabrina Ravaglia[18], Gabriele Siciliano[11], Lucia Morandi[1], Raffaele Dubbioso[8], Tiziana Mongini[10], Massimiliano Filosto[5], Irene Tramacere[19], Renato Mantegazza[1] and Pia Bernasconi[1]*

[1] Neuroimmunology and Neuromuscular Diseases, Fondazione IRCCS Istituto Neurologico Carlo Besta, Milan, Italy, [2] Section of Clinical Neurology, Department of Neurosciences, Biomedicine and Movement Sciences, University of Verona, Verona, Italy, [3] Developmental Neurology Unit, Fondazione IRCCS Istituto Neurologico Carlo Besta, Milan, Italy, [4] Clinica Neurologica, Azienda Ospedaliero Universitaria di Modena, Modena, Italy, [5] Unit of Neurology, Center for Neuromuscular Diseases, ASST Spedali Civili and University of Brescia, Brescia, Italy, [6] SC Neurologia e Stroke Unit, Azienda Ospedaliera Brotzu, Cagliari, Italy, [7] Child Neurology and Psychiatry Unit, IRCCS Istituto delle Scienze Neurologiche di Bologna, Bologna, Italy, [8] Department of Neurosciences, Reproductive Sciences and Odontostomatology, University of Naples "Federico II," Naples, Italy, [9] Pediatric Unit, Ospedale Valduce, Como, Italy, [10] Department of Neurosciences Rita Levi Montalcini, University of Turin, Turin, Italy, [11] Department of Clinical and Experimental Medicine, University of Pisa, Pisa, Italy, [12] Center of Translational and Experimental Myology, Istituto Giannina Gaslini, Genova, Italy, [13] Unità Operativa Complessa di Neurologia, Dipartimento di Scienze Dell'Invecchiamento, Neurologiche, Ortopediche e della Testa-Collo, Fondazione Policlinico Universitario A. Gemelli IRCCS, Rome, Italy, [14] Fondazione IRCCS Casa Sollievo della Sofferenza, Laboratory of Medical Genetics, San Giovanni Rotondo, Italy, [15] Department of Experimental Medicine, Sapienza University of Rome, Rome, Italy, [16] Dipartimento Materno-Infantile, S.C. Neuropsichiatria Infantile, Presidio Ospedaliero Provinciale Santa Maria Nuova, IRCCS di Reggio Emilia, Reggio Emilia, Italy, [17] Department of Neurosciences, University of Padova, Padova, Italy, [18] Emergency Neurology, IRCCS Mondino Foundation, Pavia, Italy, [19] Research and Clinical Development Department, Scientific Directorate, Fondazione IRCCS Istituto Neurologico Carlo Besta, Milan, Italy

Background: Four main clinical phenotypes have been traditionally described in patients mutated in SCN4A, including sodium-channel myotonia (SCM), paramyotonia congenita (PMC), Hypokaliemic type II (HypoPP2), and Hyperkaliemic/Normokaliemic periodic paralysis (HyperPP/NormoPP); in addition, rare phenotypes associated with mutations in SCN4A are congenital myasthenic syndrome and congenital myopathy. However, only scarce data have been reported in literature on large patient cohorts including phenotypes characterized by myotonia and episodes of paralysis.

Methods: We retrospectively investigated clinical and molecular features of 80 patients fulfilling the following criteria: (1) clinical and neurophysiological diagnosis of myotonia, or clinical diagnosis of PP, and (2) presence of a pathogenic SCN4A gene variant. Patients presenting at birth with episodic laryngospasm or congenital myopathy-like phenotype with later onset of myotonia were considered as neonatal SCN4A.

OPEN ACCESS

Edited by:
Irene Litvan, University of California, San Diego, United States

Reviewed by:
Giovanni Meola, University of Milan, Italy
Angelo Schenone, University of Genoa, Italy

***Correspondence:**
Lorenzo Maggi
lorenzo.maggi@istituto-besta.it

†These authors have contributed equally to this work and share first authorship

Specialty section:
This article was submitted to Neuromuscular Diseases, a section of the journal Frontiers in Neurology

Received: *23 December 2019*
Accepted: *29 May 2020*
Published: *29 July 2020*

Citation:
Maggi L, Brugnoni R, Canioni E, Tonin P, Saletti V, Sola P, Piccinelli SC, Colleoni L, Ferrigno P, Pini A, Masson R, Manganelli F, Lietti D, Vercelli L, Ricci G, Bruno C, Tasca G, Pizzuti A, Padovani A, Fusco C, Pegoraro E, Ruggiero L, Ravaglia S, Siciliano G, Morandi L, Dubbioso R, Mongini T, Filosto M, Tramacere I, Mantegazza R and Bernasconi P (2020) Clinical and Molecular Spectrum of Myotonia and Periodic Paralyses Associated With Mutations in SCN4A in a Large Cohort of Italian Patients. Front. Neurol. 11:646. doi: 10.3389/fneur.2020.00646

Results: PMC was observed in 36 (45%) patients, SCM in 30 (37.5%), Hyper/NormoPP in 7 (8.7%), HypoPP2 in 3 (3.7%), and neonatal SCN4A in 4 (5%). The median age at onset was significantly earlier in PMC than in SCM ($p < 0.01$) and in Hyper/NormoPP than in HypoPP2 ($p = 0.02$). Cold-induced myotonia was more frequently observed in PMC ($n = 34$) than in SCM ($n = 23$) ($p = 0.04$). No significant difference was found in age at onset of episodes of paralysis among PMC and PP or in frequency of permanent weakness between PP ($n = 4$), SCM ($n = 5$), and PMC ($n = 10$). PP was more frequently associated with mutations in the S4 region of the NaV1.4 channel protein compared to SCM and PMC ($p < 0.01$); mutations causing PMC were concentrated in the C-terminal region of the protein, while SCM-associated mutations were detected in all the protein domains.

Conclusions: Our data suggest that skeletal muscle channelopathies associated with mutations in SCN4A represent a continuum in the clinical spectrum.

Keywords: myotonia, periodic paralysis, SNEL, channelopathies, voltage-gated sodium channel $Na_V1.4$, *SCN4A* gene mutation

INTRODUCTION

The *SCN4A* gene on chromosome 17q23 encodes the α-subunit of the voltage-gated sodium channel $Na_V1.4$, responsible for the generation of action potentials and excitation of skeletal muscle fibers. The sodium channel is constituted by α subunits associated with β subunits (1). The α subunit is a single polypeptide chain that folds to four homologous but non-identical repeats (repeats I to IV). Each repeat contains six transmembrane segments (S1–S6). When inserted in the membrane, the four repeats form a central pore with segments five and six lining its wall, while the segment S4 is the channel voltage sensor due to positively charged amino acids. The loop (*P* loop) between S5 and S6 forming the extracellular domain is responsible for ion selectivity (1). The activation of the channel generates an action potential (AP) and the fast inactivation after AP can prevent repetitive discharge, which assures the physiological excitability changes of sarcolemma and the normal skeletal muscle contraction. Mutations in *SCN4A* lead to changes in skeletal muscle excitability, which is connected with the activation or inactivation speed of muscle ion channels (1). These mutations are responsible for a wide spectrum of clinical manifestations, ranging from myotonia to periodic paralysis (PP) and recently discovered phenotypes such as severe neonatal episodic laryngospasms, severe fetal hypokinesia or classical congenital myopathy, myalgia, and exercise intolerance, congenital myasthenic syndrome, and sudden infant death syndrome (2–4). However, four main clinical phenotypes have been traditionally described in patients mutated in *SCN4A* based on myotonia and paralysis features, including sodium-channel myotonia (SCM) and paramyotonia congenita (PMC) considered as non-dystrophic myotonias (NDM) and characterized by increased skeletal muscle excitability, and Hypokalemic type II (HypoPP2) and Hyperkalemic/Normokalemic PP (HyperPP/NormoPP), instead associated with reduced excitability. All three phenotypes represent a continuum in the clinical spectrum and their combined prevalence has been estimated in 0.5 per 100,000 in UK (5). However, only scarce data have been reported in literature on large cohorts of patients including all the aforementioned phenotypes, most of the studies being focused on single clinical subgroups (6, 7). Here, we describe the clinical, neurophysiological, and molecular features of a large cohort of Italian patients affected by skeletal muscle channelopathies associated with *SCN4A* mutations.

MATERIALS AND METHODS

Patients

In this retrospective study, 80 patients genetically diagnosed in our laboratory at Fondazione IRCCS Istituto Neurologico Carlo Besta since 2004 were included fulfilling the following criteria: (1) clinical and neurophysiological diagnosis of myotonia, or clinical diagnosis of PP, and (2) presence of a pathogenic *SCN4A* gene variant. We also included two familial asymptomatic cases mutated in *SCN4A*. Clinical phenotypes were defined on the basis of predominant symptom (myotonia vs. periodic paralysis); in the myotonia subgroup, we identified PMC or SCM according to the presence of paradoxical myotonia or warm-up phenomenon, respectively. PP were classified as HyperPP/NormoPP and Hypo PP2 according to the potassium levels during paralytic attacks. Furthermore, patients presenting at birth with severe neonatal episodic laryngospasm (SNEL) or congenital myopathy-like phenotype and later onset of myotonia were considered as neonatal *SCN4A*. Pattern of muscle weakness was defined according to neurological examination at the end of the follow-up period.

The local ethics committees approved the study. All patients, parents/guardians provided written informed consent for genetic

TABLE 1 | Clinical features according to phenotype.

	Whole cohort	NDM	PMC	SCM	PP	Hyper/ NormoPP	HypoPP2	Neonatal	*p*-value
N° (%)	80	66 (82.5)	36 (45)	30 (37.5)	10 (12.5)	7 (8.7)	3 (3.7)	4 (5)	
M/F	1.36/1	1.36/1	1.25/1	1.5/1	2.33/1	1.33/1	3/0	1/1	0.96
Median age at onset (y, range)	6 (0–48)	8 (0.3–48)	5.2 (0.3–48)	14.2 (1.5–48)	7.75 (1–33)	5.5 (1–10)	15.5 (15–33)	Birth	**<0.01**[a]
Cold-induced myotonia (%)	58 (72.5)	57 (86.4)	34 (94.4)	23 (76.7)	1 (10)	1 (14.3)	0	3 (75)	
Painful myotonia (%)	18 (22.5)	14 (21.2)	4 (11.1)	10 (33.3)	0	0	0	0	
Lower limb myotonia (%)	39 (48.7)	37 (56.1)	16 (44.4)	21 (70)	1 (10)	1 (14.3)	0	1 (25)	0.07
Handgrip myotonia (%)	53 (66.2)	49 (74.2)	28 (77.8)	21 (70)	3 (30)	3 (42.9)	0	1 (25)	0.13
Cranial myotonia (%)	56 (70)	51 (77.3)	30 (83.3)	21 (70)	2 (20)	2 (28.6)	0	3 (75)	0.17
Episodes of paralyses (%)	33 (41.2)	23 (34.8)	23 (63.9)	0	10 (100)	7 (100)	3 (100)	0	
Permament weakness (%)	21 (26.2)	15 (22.7)	10 (27.8)	5 (16.7)	4 (40)	4 (57.1)	0	2 (50)	0.24
Muscle hypertrophy (%)	37 (46.2)	29 (43.9)	13 (36.1)	17 (56.7)	5 (50)	5 (71.4)	0	3 (75)	0.20
Mexiletine benefit (n° treated pts)[b]	27 (43)	24 (40)[c]	10 (19)	14 (21)	0	0	0	3 (3)	
Acetazolamide benefit (n° treated pts)[b]	11 (20)	6 (12)	6 (12)	0	5 (8)	3 (6)	2 (2)	0	

[a]*Neonatal cases were excluded from this analysis.*
[b]*Data on treatment were available only for 53 patients.*
[c]*Mexiletine was stopped in 1st days of treatment in four patients due to side effects.*
NDM, non-dystrophic myotonias; PMC, paramyotonia congenita; SCM, sodium channel myotonia; PP, periodic paralysis; HyperPP/NormoPP, hyperkaliemic/normokaliemic periodic paralysis; HypoPP2, hypokaliemic periodic paralysis type II; M, male; F, female; y, years; pts, patients.
Bold values resulted significant.

analysis and use of their anonymized clinical data at the time of their first visit at the individual centers.

Genetic Analyses

Direct Sanger sequencing of the *SCN4A* 24 exons was performed for 62 patients on genomic DNA extracted from peripheral blood as previously reported (8).

For 20 patients a targeted next generation sequencing panel covering the *SCN4A* gene was used. The panel was designed by Sure Design (https://earray.chem.agilent.com/suredesign/) (Agilent Technologies). DNA libraries were prepared using the HaloPlex Target Enrichment System (Agilent Technologies), following the manufacturer's instructions, and sequenced on the MiSeq Illumina (Illumina, San Diego, CA, USA). Alignment to human genome assembly hg19 (GRCh37) was carried out and Binary alignment/map (BAM file) and variant call format (VCF file) was generated. The variants were annotated with the free web server wANNOVAR (http://wannovar.usc.edu/) to generate the VCF files. To identify pathogenic variants and to exclude variants with allele frequency more than 1% public database (i.e., dbSNP, 1000 Genome project, ExAC, ClinVar, and HGMD) were used. To predict the functional effect of a novel variant Mutation Taster (http://www.mutationtaster.org/), PolyPhen-2 (http://genetics.bwh.harvard.edu/pph2/), Proven (http://provean.jcvi.org/genome_submit_2.php), and Human Splicing Finder (http://www.umd.be/HSF3/) were consulted.

All the NGS-discovered pathogenic variants were validated by Sanger sequencing on an ABI3500Dx DNA Analyzer (Thermo Fisher Scientific) in the DNA of the patient and, if any, the parents.

Statistics

Continuous variables were expressed as means with standard deviations and medians with value ranges, while categorical variables were expressed as numbers and percentages. Associations between variables were assessed by the Mann-Whitney test or Fisher exact test, as appropriate. $P < 0.05$ were considered statistically significant and all tests were two-sided. STATA statistical software, version 15 (StataCorp. 2017. Stata Statistical Software: Release 15. College Station, TX: StataCorp LLC) was used for the statistical analysis.

RESULTS

We observed a PMC phenotype in 36/80 (45%) patients, SCM in 30 (37.5%), PP in 10 (12.5%), and neonatal *SCN4A* in 4 (5%), with a male/female ratio of 1.36. The median age at onset was 6 years (range 0–48) and the median disease duration was 22.5 years (range 2–61). Clinical features according to phenotypes are shown in **Table 1**. In addition, two familial asymptomatic patients were included, carrying the p.F1298C and p.A1156S mutations, respectively; the two mutations were associated with SCM in the probands. Despite not having symptoms or signs related to myotonia, both the subjects, aged 65 and 89 years at the end of the follow-up, showed myotonic discharges on electromyography. Fifty-six out of 82 (68.3%) patients were familial cases belonging to 20 different pedigrees. Phenotype concordance was observed in all families, except for the two aforementioned families including an asymptomatic subject, one family with the proband showing a neonatal SCN4A, and the mother displaying a mild SCM and two siblings carrying the p.M1592V mutation affected by Hyper/NormoPP and SCM, respectively. Electromyography response to short and long exercise test and cooling of muscle (9, 10) was performed in 26/80 (32.5%) patients, resulting in agreement with clinical phenotype in almost all the patients; in particular 15 PMC showed a pattern I, 8 SCM a pattern III, and 2 Hyper/NormoPP a pattern IV. The

only exception was a patient displaying a neonatal *SCN4A and* showing a pattern III, suggestive of SCM, but with clear clinical paradoxical myotonia; a similar discrepancy has already been reported (11).

Non-dystrophic Myotonias

PMC ($n = 36$) was slightly more frequent than SCM ($n = 30$). Median age at onset was significantly ($p < 0.01$) earlier in PMC (5.2 years; range 0.3–48) than in SCM (14.2 years; range 1.5–48). Myotonia in NDM involved more frequently cranial muscles ($n = 51$), followed by hand ($n = 49$), and lower limb muscles ($n = 37$), especially at thigh level. Lower limb muscles were more frequently involved in SCM ($n = 21$) than in PMC ($n = 16$) ($p = 0.05$); although not significant, cranial muscle ($p = 0.09$) and handgrip myotonia ($p = 0.59$) were slightly more frequent in PMC than in SCM (see **Table 1** for details). Cold-induced myotonia was more frequently observed in PMC ($n = 34$) than in SCM ($n = 23$) ($p = 0.04$). Painful myotonia tended to be more frequent in SCM ($n = 10$) than in PMC ($n = 4$), although not statistically significant. Permanent weakness was detected in 10/36 (27.8%) PMC and 5/30 (16.7%) SCM ($p = 0.41$), mainly in cranial ($n = 8$), thigh ($n = 8$), neck flexor ($n = 6$), and distal upper limb ($n = 5$) muscles. Of note, distal upper limb weakness was detected only in PMC. Muscle weakness was mild to moderate in most of the cases (Medical Research Council muscle power scale: MRC 3-4/5) in both NMD and PP. Muscle hypertrophy was evident in 13 (36.1%) PMC and 17 (56.7%) SCM ($p = 0.15$), mainly at calves ($n = 18$), and thigh ($n = 12$), while generalized hypertrophy with Hercules-like appearance was observed in 5 (16.7%) SCM and 3 (8.3%) PMC. Twenty-three out of 36 (63.9%) PMC patients had PP presenting at a median age of 5.5 years (range 1–20) and a median time from myotonia to PP onset of 0 years (range 0–15), without any case with PP preceding myotonia presentation. Of note, 1 SCM carrying the p.A699T mutation had stridor presenting in adult age. Triggering factors for episodes of paralysis in PMC were mainly cold temperature ($n = 17$), prolonged exercise ($n = 14$), and rest after exercise ($n = 9$). Data on treatment were available for 53 (66.2%) NDM patients; mexiletine was administered in 21/30 (70%) SCM and 19/36 (52.8%) PMC patients with benefit in 14 (66.7%) and 10 (71.4%), respectively; four out of 40 NDM patients stopped mexiletine due to side effects in 1st days of treatment. Acetazolamide was given to 12/36 (33.3%) PMC patients, with benefit in 6 (50%). Further seven patients had benefit from lamotrigine ($n = 3$), carbamazepine ($n = 2$), buprenorphine ($n = 1$), and propafenone ($n = 1$); all of them had PMC, except for the three patients taking lamotrigine, who displayed a SCM phenotype.

Periodic Paralyses

The median age at onset of PP was 7.75 years (range 1–33), not significantly different from age at onset of episodes of paralysis in PMC ($p = 0.72$). Hyper/NormoPP was observed in 7 (70%) patients and HypoPP2 in 3 (30%). Median age at onset was significantly ($p = 0.02$) earlier in Hyper/NormoPP (5.5 years; range 1–10) than in HypoPP2 (15.5 years; range 15–33). Five (50%) patients, all with Hyper/NormoPP, also had myotonia, with warm-up phenomenon, worsened by cold in only one case and never reported as painful. No significant difference was found in muscle distribution and age at onset of myotonia in PP and in NDM. Median time from PP and myotonia onset was 5 years (range 0–21); of note, PP onset always preceded myotonia presentation. Triggering factors for Hyper/Normo were mainly post-exercise period ($n = 5$) and cold temperature ($n = 4$), for HypoPP2 post-exercise period ($n = 2$). Episodes of paralysis were usually generalized in 3/7 (42.9%) Hyper/NormoPP and in all HypoPP2 or limited to lower limbs in 4/7 (57.1%) Hyper/NormoPP. Duration of PP was usually more than 24 h in all HypoPP2 patients and in 2/7 (28.6%) Hyper/NormoPP and <24 h in remaining 5 (71.4%) Hyper/NormoPP, in most of the cases lasting 1–4 h.

Permanent weakness was found in 4/10 (40%) patients, all affected by Hyper/NormoPP, and its occurrence was not statistically different from that in NDM; weakness was limited to thigh muscles in all patients, except for one with also involvement of distal upper limb muscles. Muscle hypertrophy was found in 5/7 (71.4%) Hyper/NormoPP patients and its frequency was not significantly different among PP and NDM.

Data on treatment were available for 8/10 (80%) PP patients; acetazolamide was administered in 6/7 (85.7%) Hyper/NormoPP and 2/3 (66.7%) HypoPP2, with benefit in 3 (50%) and 2 (100%), respectively.

Neonatal SCN4A

Three out of 4 (75%) patients with neonatal phenotype had typical SNEL and one had congenital myopathy-like presentation with bilateral clubfoot, hip dislocation, facial dysmorphism in association with myotonia characterized by warm-up phenomenon, and absence of stridor, previously reported in literature (12). This patient had an affected mother, carrying the same mutation p.N1180I and showing a SCM, with onset of hand and facial myotonia at the age of 12 years; mother's neurological examination revealed mild handgrip myotonia, diffuse muscle hypertrophy, pes cavus, hyporeflexia, and nasal speech. Notably, two SNEL patients were mother and son, respectively, carrying the p.I693T mutation and presenting with laryngeal stridor and hypotonia at birth, followed by paradoxical myotonia of facial and bulbar muscles at the age of 6 months followed by muscle hypertrophy. Stridor was triggered by cold temperature or cold food or beverages and spontaneously disappeared in adolescence in both patients. The sporadic patient carrying the p.G1306E mutation presented at birth with inguinal and hiatal hernia, hypotonia, myotonia with warm-up phenomenon, and laryngeal stridor, which disappeared after 1-year treatment with mexiletine. Permanent weakness was found in the patient with congenital myopathy-like presentation and limited to axial muscles and in the mother with paradoxical myotonia displaying weakness of neck flexor and tongue and facial muscles. Only the three patients with SNEL had cold-induced myotonia, and none of the neonatal *SCN4A* showed painful myotonia.

Molecular Genetics

Genetic analysis of *SCN4A* gene in our patient cohort revealed 28 potential disease-causing variants in the 80 patients and

TABLE 2 | Panel of the 28 mutations of the SCN4A gene found in our 80 patients.

Nucleotide change	Amino acid change	Exon	Position on $Na_V1.4$ channel	Phenotype	References	N. pt
c.644T>C	p.I215T	5	loop S3DI-S4DI	SCM	Novel	1
c.716T>G	p.I239S	5	loop S4DI-S5DI	SCM	Novel	5
c.825C>A	p.N275K	5	loop S5DI-S6DI	SCM	Novel	1
c.968C>T	p.T323M	6	loop S5DI-S6DI	SCM	SCN4A_000113	1
c.1333G>T	p.V445L	9	loop DI-DII	SCM	Novel	2
c.1333G>A	p.V445M	9	loop DI-DII	SCM	SCN4A_000015	1
c.2006G>A	p.R669H	13	S4DII	HypoPP2	SCN4A_00019	2
c.2023C>G	p.R675G	13	S4DII	Hyper/NormoPP	rs121908556	1
c.2076C>G	p.I692M	13	loop S4DII-S5DII	Hyper/NormoPP	Novel	2
c.2078T>C	p.I693T	13	loop S4DII-S5DII	PMC/Neonatal	SCN4A_00031	3
c.2095G>A	p.A699T	13	S5DII	PMC	rs1057518865	3
c.2111C>T	p.T704M	13	S5DII	Hyper/NormoPP	SCN4A_00033	2
c.3395G>A	p.R1132Q	18	S4DIII	HypoPP2	SCN4A_00043	1
c.3466G>T	p.A1156S	19	loop S4DIII-S5DIII	SCM/asym	Novel	2
c.3491TC	p.L1164P	19	S5DIII	SCM	rs749033669	3
c.3539A>T	p.N1180I	19	loop S5DIII-S6DIII	SCM/Neonatal	(13)	2
c.3877G>A	p.V1293I	21	loop DIII-DIV	SCM	SCN4A_00048	7
c.3890A>G	p.N1297S	21	loop DIII-DIV	SCM	(14)	2
c.3893T>G	p.F1298C	21	loop DIII-DIV	SCM/asym	(14)	2
c.3917G>A	p.G1306E	22	loop DIII-DIV	Neonatal	SCN4A_00050	1
c.3917G>C	p.G1306A	22	loop DIII-DIV	SCM	SCN4A_00051	1
c.3917G>T	p.G1306V	22	loop DIII-DIV	PMC	SCN4A_00052	1
c.3938C>T	p.T1313M	22	loop DIII-DIV	PMC	VAR_001570	18
c.4342C>T	p.R1448C	24	S4DIV	PMC	VAR_001572	6
c.4342C>G	p.R1448G	24	S4DIV	PMC	SCN4A_00070	3
c.4343G>A	p.R1448H	24	S4DIV	PMC	VAR_001573	4
c.4690G>A	p.V1564I	24	loop S5DIV-S6DIV	PMC	rs202106192	2
c.4774A>G	p.M1592V	24	S6DIV	SCM/Hyper/NormoPP	VAR_001575	3

S, transmembrane segment; D, domain (or repeat); loop, region intra/extra-cellular between 2 segments and 2 domain; SCM, sodium-channel myotonia; PMC, paramyotonia congenita; HypoPP2, hypokalemic periodic paralysis; Hyper/NormoPP, hyperkalemic/normokalemic periodic paralysis; Neonatal, Neonatal SCN4A; asym, asymptomatic; pt, patients.
The position of all mutations have been established using NextProt (https://www.nextprot.org/entry/NX_P35499/sequence).

two asymptomatic familial cases. These variants involved nine different exons and the most mutated were exons 22, 24, 21, and 13 (**Table 2**). The most frequent mutations were p.T1313M, p.R1448C/G/H, and p.V1293I found in 18, 13, and 7 patients, respectively (**Table 2**).

Six mutations in the *SCN4A* gene have not been previously reported in the molecular databases (Leiden Open Variation Database, NextProt, The Human Gene Mutation Database, Exome Variant Server and UniProtKB): p.I215T, p.I239S, p.N275K, p.V445L, p.I692M, p.A1156S, p.N1180I, p.N1297S, and p.F1298C (**Table 2**). Some of these variants were located in the same position or immediately nearby the amino acid of a codon already known to be mutated and associated with disease, or showing pathogenic score, or segregating with disease in familial genetic studies, strongly suggesting that our nine unknown variants are potential disease-causing mutations.

The p.I215T variant present in one SCM patient was placed in the extracellular loop between the transmembrane segments S3 and S4 of the first repeat (loop S3DI-S4DI) (**Figure 1**). In the same codon the known variant p.I215M (rs373289931) had been previously reported with a pathogenic score (score = 0.98).

The p.I239S mutation detected in 5 SCM patients was located in the extracellular loop between the transmembrane segments S4 and S5 of the first repeat (loop S4DI-S5DI) (**Figure 1**); in the same loop the variants p.T238K/M and p.V240M (rs201661188 and rs746216167, respectively) had already been reported.

One SCM patient harbored the unreported p.N275K variant localized in the extracellular loop between the transmembrane segments S5 and S6 of the first repeat (loop S5DI-S6DI) (**Figure 1**); in the previous codon the variant p.G274E had been described (COSM3890178) with a pathogenic score (score 0.99).

The p.V445L mutation found in 2 SCM patients was located in the adjacent N-terminal area of the loop connecting repeats I and II (**Figure 1**). The novel p.V445L mutation could be pathogenic since the known mutation p.V445M at the same position has been reported in multiple families and individuals affected by myotonia congenita and was associated with marked phenotypic variability. According to the prediction sites the p.V445L also had a pathogenic score (score = 0.82).

In two patients affected by Hyper/NormoPP the p.I692M mutation was placed in the intracellular loop between the

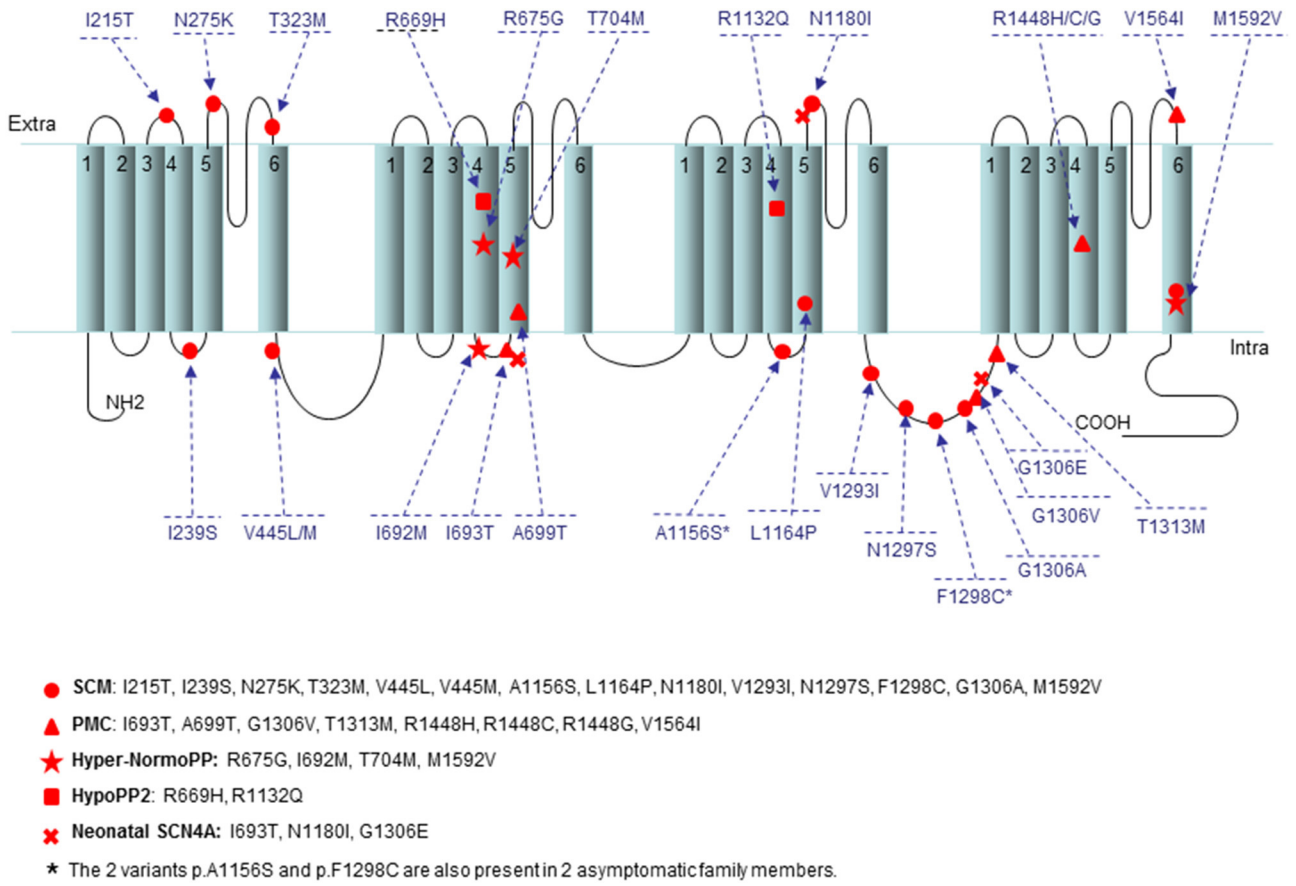

FIGURE 1 | Location of the 28 mutations present in this study onto a secondary structure of $Na_v1.4$ channel. The variants are indicated by small circle for SCM, triangle for PMC, star for Hyper/NormoPP, square for HypoPP2, and cross for SNEL. The two variants p.A1156S and p.F1298C are also present in two asymptomatic family members. The position of all variants has been established using NextProt (https://www.nextprot.org/entry/NX_P35499/sequence).

transmembrane segments S4 and S5 of the second repeat (loop S4DII-S5DII) (**Figure 1**), nearby the two known mutations p.I692T and p.I692F (rs757943588 and rs765779586).

The p.A1156S variant found in 1 SCM patient and the asymptomatic father (**Table 2**) affect the same codon of the p.A1156T mutation (LOVD: SCN4A_00044), which was reported to alter the function of Nav1.4 channel causing a channelopathy, interestingly associated with a mild phenotype without overt myotonia or periodic paralysis but with muscle pain (15).

Three mutations (p.N1180I, p.N1297S, and p.F1298C) found in six patients were already reported and associated to non-dystrophic myotonias (**Table 2**) (13, 14). Of note, p.N1297S was found in our cohort in two patients also carrying the p.F167L variant in *CLCN1* gene, which probably mitigated the severe effect of the mutation in the Nav1.4 channel, as already reported (8). In our cohort of patients PP was more frequently associated with mutations distributed in the S4 region compared to NDM ($p < 0.01$). No significant association was found between specific domains of Nav1.4 channel and the presence of episodes of paralyses in PMC ($p = 0.75$).

DISCUSSION

The present study includes a cohort of Italian patients mutated in *SCN4A*, displaying different phenotypes, spanning from SCM and PMC throughHyper/NormoPP and HypoPP2 to Neonatal SCN4A. To our knowledge, this is the first report on a large population of patients investigating clinical features of all these phenotypes together. Skeletal muscle channelopathies associated to *SCN4A* gene mutations indeed represent a continuum in the clinical spectrum, as also supported by the high frequency of episodes of paralysis in PMC and the relative high incidence (50%) of myotonia in Hyper/NormoPP. In addition, features of myotonia and episodes of paralysis did not differ between NDM and PP in terms of muscle distribution and age at onset. Phenotypes were consistent in the same family except for four out of 20 pedigrees, including two asymptomatic patients in late adult life, suggesting relative strong genotype-phenotype correlations in these diseases. On the other hand, clinical heterogeneity could also be a feature of sodium muscle channelopathies, as demonstrated by the p.G1306V/A/E mutations found in three patients displaying three different phenotypes (PMC, SCM, and SNEL), demonstrating how the

replacement of glycine at the same codon of the $Na_V1.4$ with three different amino acids (Valine/Alanine/Glutamic Acid) may lead to different phenotypes. Hence, other mechanisms, such as the coexistence of *SCN4A* and *CLCN1* gene mutations and non-genetic factors (epigenetic, environmental, and hormonal), should be considered to explain the clinical variability in these disorders (8, 16).

In our cohort PMC was the most frequent phenotype, accounting for almost a half of the whole population, followed by SCM and then by PP and Neonatal *SCN4A*, which represent a minority of the cases. Our data showing greater frequency of NDM than PP caused by *SCN4A* gene mutations are in agreement with previous studies on large cohorts of British and Dutch patients (5, 17), although in our cohort PP seems to be underrepresented, being only 12.5% of the population.

In our study, PMC appeared to be significantly associated to earlier onset and cold-sensitivity than SCM and tended to affect more frequently cranial and hand muscles; conversely, SCM tended to show more frequently lower limb and painful myotonia and muscle hypertrophy than PMC, in agreement with previous reports (2, 6, 7). Hyper/NormoPP had earlier onset than HypoPP2 and tended to be associated more frequently with focal and shorter episodes of paralysis; myotonia and muscle hypertrophy were found only in Hyper/NormoPP patients (6, 18, 19). On the other hand, HypoPP2 displayed more frequently generalized PP than Hyper/NormoPP. Permanent weakness still represents an issue in skeletal muscle channelopathies, mainly due to the poor and somehow conflicting data on its frequency, presentation, and progression over time; in addition, its pathomechanisms are still not completely elucidated (20, 21). In our cohort, permanent weakness was detected in about one quarter of the patients, without any significant difference between NDM and PP or SCM and PMC. Of note, permanent muscle weakness was observed with neurological examination in about half of Hyper/NormoPP patients and in none of HypoPP2 patients, as previously reported (6). Muscle weakness was limited to thigh muscle in Hyper/NormoPP and more diffuse in NDM, including also cranial, axial, and distal upper limb muscles, with the latter appearing to be specific for PMC. To date, no predictive factors for permanent weakness are known and this phenomenon seems to occur regardless of the mutation.

Neonatal-*SCN4A* represents 5% of the whole cohort. There is a partial overlap with congenital myopathies due to the presentation at birth with hypotonia in three out four patients and bilateral clubfoot, hip dislocation, facial dysmorphism, or inguinal and hiatal hernia in two out of four patients. Autosomal recessive mutations in *SCN4A* gene have been reported in association with severe congenital myopathy without myotonia (22), while patients with simple heterozygous mutations may represent a milder phenotype associated with myotonia presenting at birth or in 1st years of age (23–26). Notably, myotonia in neonatal SCN4A may be associated to warm-up phenomenon or paradoxical, depending on the causing mutations, mainly the p.G1306E and p.I693T, respectively (23–25). Although the SNEL cases reported in literature are usually sporadic, we report here two familial cases (mother and son) with autosomal dominant inheritance displaying this phenotype.

The alpha-subunit of the voltage-gated sodium channel $Na_V1.4$ is composed of four highly homologous domains (DI-DIV) each consisting of six transmembrane segments (S1–S6). When inserted in the membrane, the four repeats form a central pore with segments five and six lining its wall (**Figure 1**). The repeats are connected by intracellular loops; one of them is in the III–IV linker which contains the fast-inactivation particle and many mutations found in our population are located in this region, such as the frequent p.T1313M mutation found in 18 patients (**Table 2**). Notably, we found seven missense mutations (p.V1293I, p.N1297S, p.F1298C, p.G1306V/A/E, and p.T1313M) in this relevant portion of the $Na_V1.4$ in 32 patients affected by different myotonic phenotype (SCM, PMC, and SNEL) and with various degrees of severity (**Table 2**, **Figure 1**). A further important region for the functionality of the $Na_v1.4$ channel is the voltage sensor localized in the transmembrane segment S4. In this region we found six mutations: p.R669H and p.R675G in the second domain, p.R1132Q in the third domain, and p.R1448C/G/H in the fourth repeat (**Figure 1**).

Both the p.R669H and p.R1132Q mutations found in 3 HypoPP2 patients cause a change of an arginine in S4 segments of the second and third repeats, respectively; conversely, as also reported by Cannon (1). In addition, the p.R675G variant found in 1 patient affected by Hyper/NormoPP, and the mutations p.R1448C/G/H in 13 patients affected by PMC, further confirm that the S4 is an essential region for the function of the sodium channel and that changes in this transmembrane segment are associated with a large phenotypic variability. These mutations may increase the continuous current of the sodium channel, change the voltage-dependent activation process, lead to abnormal depolarization of resting potential, or slow down the inactivation process, affecting the normal function of sodium channel and leading to disease. However, mutations in the S4 segments appeared to be significantly more frequent in PP than NDM patients.

Based on the distribution of mutations along the *SCN4A* gene, we may conclude that the hot-spot regions for sodium channelopathies in our cohort patients involve the exons 13, 21, 22, 24, in agreement with the literature (27, 28). These exons encoding the S4–S5 segments of the second domain, the loop between the third and the fourth domain and the segments S4 and S6 of the fourth domain, as shown in **Figure 1** and **Table 2**.

Genetic analysis of *SCN4A* gene in our cohort patients revealed a greater prevalence of PMC-associated mutations in the C-terminal region of the $Na_V1.4$ channel protein than the more diffuse distribution of SCM-associated mutations, detected in all 4 domains of the protein (**Table 2**, **Figure 1**).

In conclusion, our data provide further insight in the field of skeletal muscle channelopathies due to mutations in *SCN4A*; however, prospective studies on large cohort of patients are needed to better clarify the natural history of these diseases and investigate possible genetic and non-genetic modifiers of the phenotype.

DATA AVAILABILITY STATEMENT

The datasets generated for this study can be found in the https://databases.lovd.nl/shared/individuals/SCN4A.

ETHICS STATEMENT

The studies involving human participants were reviewed and approved by Ethics Committee at Fondazione IRCCS Istituto Neurologico Carlo Besta. Written informed consent to participate in this study was provided by the participants' legal guardian/next of kin.

AUTHOR CONTRIBUTIONS

LM, RB, and PB conceived and designed the study. LM, RB, PB, RM, and IT drafted manuscript, figure, and tables. All the authors acquired and analyzed the data and gave the final approval to the current version of the manuscript.

REFERENCES

1. Cannon SC. Sodium channelopathies of skeletal muscle. *Handb Exp Pharmacol.* (2018) 246:309–30. doi: 10.1007/164_2017_52
2. Matthews E, Fialho D, Tan SV, Venance SL, Cannon SC, Sternberg D, et al. The non-dystrophic myotonias: molecular pathogenesis, diagnosis and treatment. *Brain.* (2010) 133:9–22. doi: 10.1093/brain/awp294
3. Arnold WD, Feldman DH, Ramirez S, He L, Kassar D, Quick A, et al. Defective fast inactivation recovery of Nav 1.4 in congenital myasthenic syndrome. *Ann Neurol.* (2015) 77:840–50. doi: 10.1002/ana.24389
4. Männikkö R, Wong L, Tester DJ, Thor MG, Sud R, Kullmann DM, et al. Dysfunction of NaV1.4, a skeletal muscle voltage-gated sodium channel, in sudden infant death syndrome: a case-control study. *Lancet.* (2018) 391:1483–92. doi: 10.1016/S0140-6736(18)30021-7
5. Horga A, Raja Rayan DL, Matthews E, Sud R, Fialho D, Durran SC, et al. Prevalence study of genetically defined skeletal muscle channelopathies in England. *Neurology.* (2013) 80:1472–5. doi: 10.1212/WNL.0b013e31828cf8d0
6. Miller TM, Dias da Silva MR, Miller HA, Kwiecinski H, Mendell JR, Tawil R, et al. Correlating phenotype and genotype in the periodic paralyses. *Neurology.* (2004) 63:1647–55. doi: 10.1212/01.WNL.0000143383.91137.00
7. Trip J, Drost G, Ginjaar HB, Nieman FH, van der Kooi AJ, de Visser M, et al. Redefining the clinical phenotypes of non-dystrophic myotonic syndromes. *J Neurol Neurosurg Psychiatry.* (2009) 80:647–52. doi: 10.1136/jnnp.2008.162396
8. Maggi L, Ravaglia S, Farinato A, Brugnoni R, Altamura C, Imbrici P, et al. Coexistence of CLCN1 and SCN4A mutations in one family suffering from myotonia. *Neurogenetics.* (2017) 18:219–25. doi: 10.1007/s10048-017-0525-5
9. Fournier E, Arzel M, Sternberg D, Vicart S, Laforet P, Eymard B, et al. Electromyography guides toward subgroups of mutations in muscle channelopathies. *Ann Neurol.* (2004) 56:650–61. doi: 10.1002/ana.20241
10. Fournier E, Viala K, Gervais H, Sternberg D, Arzel-Hézode M, Laforet P, et al. Cold extends electromyography distinction between ion channel mutations causing myotonia. *Ann Neurol.* (2006) 60:356–65. doi: 10.1002/ana.20905
11. Trivedi JR, Bundy B, Statland J, Salajegheh M, Rayan DR, Venance SL, et al. Non-dystrophic myotonia: prospective study of objective and patient reported outcomes. *Brain.* (2013) 136:2189–200. doi: 10.1093/brain/awt133
12. Matthews E, Manzur AY, Sud R, Muntoni F, Hanna MG. Stridor as a neonatal presentation of skeletal muscle sodium channelopathy. *Arch Neurol.* (2011) 68:127–9. doi: 10.1001/archneurol.2010.347
13. Fusco C, Frattini D, Salerno GG, Canali E, Bernasconi P, Maggi L. New phenotype and neonatal onset of sodium channel myotonia in a child with a novel mutation of SCN4A gene. *Brain Dev.* (2015) 37:891–3. doi: 10.1016/j.braindev.2015.02.004
14. Farinato A, Altamura C, Imbrici P, Maggi L, Bernasconi P, Mantegazza R, et al. Pharmacogenetics of myotonic hNav1.4 sodium channel variants situated near the fast inactivation gate. *Pharmacol Res.* (2019) 141:224–35. doi: 10.1016/j.phrs.2019.01.004
15. Suokas K, Palmio J, Sandell S, Udd B, Hietaharju A. Pain in SCN4A mutated P.A1156T muscle sodium channelopathy-a postal survey. *Muscle Nerve.* (2018) 57:1014–1017. doi: 10.1002/mus.26050
16. Suetterlin K, Männikkö R, Hanna MG. Muscle channelopathies: recent advances in genetics, pathophysiology and therapy. *Curr Opin Neurol.* (2014) 27:583–90. doi: 10.1097/WCO.0000000000000127
17. Stunnenberg BC, Raaphorst J, Deenen JCW, Links TP, Wilde AA, Verbove DJ, et al. Prevalence and mutation spectrum of skeletal muscle channelopathies in the Netherlands. *Neuromuscul Disord.* (2018) 28:402–7. doi: 10.1016/j.nmd.2018.03.006
18. Venance SL, Cannon SC, Fialho D, Fontaine B, Hanna MG, Ptacek LJ, et al. The primary periodic paralyses: diagnosis, pathogenesis and treatment. *Brain.* (2006) 129:8–17. doi: 10.1093/brain/awh639
19. Statland JM, Fontaine B, Hanna MG, Johnson NE, Kissel JT, Sansone VA, et al. Review of the diagnosis and treatment of periodic paralysis. *Muscle Nerve.* (2018) 57:522–30. doi: 10.1002/mus.26009
20. Amarteifio E, Nagel AM, Weber MA, Jurkat-Rott K, Lehmann-Horn F. Hyperkalemic periodic paralysis and permanent weakness: 3-T MR imaging depicts intracellular 23Na overload–initial results. *Radiology.* (2012) 264:154–63. doi: 10.1148/radiol.12110980
21. Charles G, Zheng C, Lehmann-Horn F, Jurkat-Rott K, Levitt J. Characterization of hyperkalemic periodic paralysis: a survey of genetically diagnosed individuals. *J Neurol.* (2013) 260:2606–13. doi: 10.1007/s00415-013-7025-9
22. Zaharieva IT, Thor MG, Oates EC, van Karnebeek C, Hendson G, Blom E, et al. Loss-of-function mutations in SCN4A cause severe foetal hypokinesia or 'classical' congenital myopathy. *Brain.* (2016) 139:674–91.
23. Gay S, Dupuis D, Faivre L, Masurel-Paulet A, Labenne M, Colombani M, et al. Severe neonatal non-dystrophic myotonia secondary to a novel mutation of the voltage-gated sodium channel (SCN4A) gene. *Am J Med Genet.* (2008) 146A:380–3. doi: 10.1002/ajmg.a.32141
24. Lion-Francois L, Mignot C, Vicart S, Manel V, Sternberg D, Landrieu P, et al. Severe neonatal episodic laryngospasm due to *de novo* SCN4A mutations: a new treatable disorder. *Neurology.* (2010) 75:641–5. doi: 10.1212/WNL.0b013e3181ed9e96
25. Caietta E, Milh M, Sternberg D, Lépine A, Boulay C, McGonigal A, et al. Diagnosis and outcome of SCN4A-related severe neonatal episodic laryngospasm (SNEL):2 new cases. *Pediatrics.* (2013) 132:784–7. doi: 10.1542/peds.2012-3065
26. Waldrop M, Amornvit J, Pierson CR, Boue DR, Sahenk Z. A novel de novo heterozygous SCN4A mutation causing congenital myopathy, myotonia and multiple congenital anomalies. *J Neuromuscul Dis.* (2019) 6:467–73. doi: 10.3233/JND-190425
27. Matthews E, Tan SV, Fialho D, Sweeney MG, Sud R Haworth A, Stanley E, et al. What causes paramyotonia in the United Kingdom? Common and new SCN4A mutations revealed. *Neurology.* (2008) 70:50–3. doi: 10.1212/01.wnl.0000287069.21162.94
28. Heidari MM, Khatami M, Nafissi S, Hesami-Zokai F, Khorrami A. Mutation analysis in exons 22 and 24 of SCN4A gene in Iranian patients with non-dystrophic myotonia. *Iran J Neurol.* (2015) 14:190–4.

Conflict of Interest: The authors declare that the research was conducted in the absence of any commercial or financial relationships that could be construed as a potential conflict of interest.

Copyright © 2020 Maggi, Brugnoni, Canioni, Tonin, Saletti, Sola, Piccinelli, Colleoni, Ferrigno, Pini, Masson, Manganelli, Lietti, Vercelli, Ricci, Bruno, Tasca, Pizzuti, Padovani, Fusco, Pegoraro, Ruggiero, Ravaglia, Siciliano, Morandi, Dubbioso, Mongini, Filosto, Tramacere, Mantegazza and Bernasconi. This is an open-access article distributed under the terms of the Creative Commons Attribution License (CC BY). The use, distribution or reproduction in other forums is permitted, provided the original author(s) and the copyright owner(s) are credited and that the original publication in this journal is cited, in accordance with accepted academic practice. No use, distribution or reproduction is permitted which does not comply with these terms.

frontiers in Neurology

ORIGINAL RESEARCH
published: 04 September 2020
doi: 10.3389/fneur.2020.01019

Pathomechanisms of a *CLCN1* Mutation Found in a Russian Family Suffering From Becker's Myotonia

*Concetta Altamura[1], Evgeniya A. Ivanova[2], Paola Imbrici[3], Elena Conte[3], Giulia Maria Camerino[3], Elena L. Dadali[2], Alexander V. Polyakov[2], Sergei Aleksandrovich Kurbatov[4], Francesco Girolamo[5], Maria Rosaria Carratù[1] and Jean-François Desaphy[1]**

[1] Section of Pharmacology, Department of Biomedical Sciences and Human Oncology, School of Medicine, University of Bari Aldo Moro, Bari, Italy, [2] N.P. Bochkov's Research Centre for Medical Genetics, Federal State Budgetary Scientific Institution, Moscow, Russia, [3] Section of Pharmacology, Department of Pharmacy-Drug Sciences, University of Bari Aldo Moro, Bari, Italy, [4] Voronezh Regional Clinical Consulting and Diagnostic Center, Voronezh, Russia, [5] Unit of Human Anatomy and Histology, Department of Basic Medical Sciences, Neuroscience, and Sense Organs, School of Medicine, University of Bari Aldo Moro, Bari, Italy

Objective: Myotonia congenita (MC) is a rare muscle disease characterized by sarcolemma over-excitability inducing skeletal muscle stiffness. It can be inherited either as an autosomal dominant (Thomsen's disease) or an autosomal recessive (Becker's disease) trait. Both types are caused by loss-of-function mutations in the *CLCN1* gene, encoding for ClC-1 chloride channel. We found a ClC-1 mutation, p.G411C, identified in Russian patients who suffered from a severe form of Becker's disease. The purpose of this study was to provide a solid correlation between G411C dysfunction and clinical symptoms in the affected patient.

Methods: We provide clinical and genetic information of the proband kindred. Functional studies include patch-clamp electrophysiology, biotinylation assay, western blot analysis, and confocal imaging of G411C and wild-type ClC-1 channels expressed in HEK293T cells.

Results: The G411C mutation dramatically abolished chloride currents in transfected HEK cells. Biochemical experiments revealed that the majority of G411C mutant channels did not reach the plasma membrane but remained trapped in the cytoplasm. Treatment with the proteasome inhibitor MG132 reduced the degradation rate of G411C mutant channels, leading to their expression at the plasma membrane. However, despite an increase in cell surface expression, no significant chloride current was recorded in the G411C-transfected cell treated with MG132, suggesting that this mutation produces non-functional ClC-1 chloride channels.

Conclusion: These results suggest that the molecular pathophysiology of G411C is linked to a reduced plasma membrane expression and biophysical dysfunction of mutant channels, likely due to a misfolding defect. Chloride current abolition confirms that the mutation is responsible for the clinical phenotype.

Keywords: myotonia congenita, ClC-1, chloride channel, patch-clamp, intracellular trafficking

OPEN ACCESS

Edited by:
Xin-Ming Shen,
Mayo Clinic, United States

Reviewed by:
Stephen Cannon,
UCLA David Geffen School of Medicine, United States
Chih-Yung Tang,
National Taiwan University, Taiwan

***Correspondence:**
Jean-François Desaphy
jeanfrancois.desaphy@uniba.it

Specialty section:
This article was submitted to Neuromuscular Diseases, a section of the journal Frontiers in Neurology

Received: *16 December 2019*
Accepted: *04 August 2020*
Published: *04 September 2020*

Citation:
Altamura C, Ivanova EA, Imbrici P, Conte E, Camerino GM, Dadali EL, Polyakov AV, Kurbatov SA, Girolamo F, Carratù MR and Desaphy J-F (2020) Pathomechanisms of a CLCN1 Mutation Found in a Russian Family Suffering From Becker's Myotonia. Front. Neurol. 11:1019. doi: 10.3389/fneur.2020.01019

INTRODUCTION

A difficulty in muscle relaxation after a voluntary contraction is the basis of the myotonic phenomenon, which is the main clinical feature of non-dystrophic myotonias (NDM). These disorders are caused by a dysfunction of skeletal muscle voltage-gated ion channels (1, 2). Thus, sodium channel myotonia and paramyotonia congenita are both linked to gain-of-function mutations of the *SCN4A* gene coding for Nav1.4 sodium channel, while myotonia congenita (MC) is related to loss-of-function mutations in the *CLCN1* gene, encoding the chloride channel ClC-1. MC can be inherited in a recessive mode (Becker's disease) or dominant manner (Thomsen's disease). Clinically, the two forms of MC differ by the age of onset, spreading of myotonia, and a typical transient muscular weakness present only in the recessive trait. Becker's disease is more common and generally more severe (3).

The ClC-1 chloride channel is expressed almost exclusively in skeletal muscle, where it accounts for ∼80% of plasma membrane ion conductance at rest. The chloride current stabilizes the resting membrane potential of skeletal muscle and contributes to the repolarization of action potentials (4, 5). Thus, the reduced chloride conductance resulting from MC mutations predisposes the sarcolemma to spontaneous action potential runs or abnormal after-discharges that hamper muscle relaxation after contraction, causing myotonia.

So far, more than 200 mutations in *CLCN1* have been identified (5, 6) in patients with MC and a number of these have been functionally studied to confirm the genotype-phenotype relationship and to better understand the relationship between ClC-1 channel structure and function.

In vitro functional studies have demonstrated that MC mutations cause various alterations of channel function, including shift of voltage dependence, reduced single channel conductance, altered ion selectivity, or a defect in protein trafficking (5, 6). All these alterations reduce the activity of ClC-1 channel mutants, leading to a reduced sarcolemmal chloride conductance.

In this study, we report a mutation, p.G411C, identified in a Russian family affected by recessive MC. We have investigated the molecular defect of G411C chloride channels by means of a combined biochemical and electrophysiological approach in transiently transfected mammalian cells, in order to define the molecular mechanisms causing MC and to correlate it with the clinical manifestations of the affected patients.

MATERIALS AND METHODS

Genetic Analysis

Written informed consent for DNA storage and use for genetic analysis and research purposes was obtained from all the patients and relatives, in accordance with the Declaration of Helsinki. Genomic DNA was extracted from peripheral blood cells according to the standard method with DLAtom™ DNA Prep100 kit. All the 23 exons of *CLCN1* were amplified by polymerase chain reaction (PCR) and were sequenced using intronic primers, as previously described (7).

Clinical Diagnosis

We examined a young Russian boy presenting with muscle stiffness and his relatives. Neurological examination was specifically conducted to search for myotonic signs as tongue, eyelid, lid-lag, jaw, handgrip, and percussion myotonia. EMG study was performed according to Fournier's guidelines (8).

Mutagenesis and Expression of WT and G411C Mutant hClC-1 Channels

The c.1231G>T mutation was introduced into the plasmid pRc/CMV containing the full-length WT hClC-1 cDNA using the QuickChange™ site-directed mutagenesis kit (Stratagene Cloning Systems), as previously described (9). For confocal imaging, point mutation was inserted into pRcCMV-YFP-hClC-1 vector, kindly provided by Dr. Christoph Fahlke (10).

The complete coding region of the cDNA was sequenced to exclude polymerase errors. Human embryonic kidney 293T (HEK293T) cells were transiently transfected with a mixture of wild-type or mutated hClC-1 (5 μg) and CD8 reporter plasmids (1 μg) using the calcium–phosphate precipitation method. The transfected cells were maintained at 37°C for 40–80 h before being used for electrophysiological or biochemical experiments. Where indicated, drugs (MG132, dithiothreitol) were diluted in the culture medium.

Electrophysiology and Data Analysis

Transfected HEK293T cells were examined between 40 and 80 h after transfection. Only cells decorated with anti-CD8 antibody-coated microbeads (Dynabeads M450; Invitrogen, Carlsbad, California, USA) were used for electrophysiological studies.

Standard whole-cell patch-clamp recordings were performed at room temperature (∼20°C) using an Axopatch 200B amplifier and pClamp suite software (Axon Instruments), as previously described (11, 12). The composition of the extracellular solution was (in mM): 140 NaCl, 4 KCl, 2 $CaCl_2$, 1 $MgCl_2$ and 5 Hepes, and the pH was adjusted to 7.4 with NaOH. The pipette solution contained (in mM): 130 CsCl, 2 $MgCl_2$, 5 EGTA and 10 Hepes, and the pH was adjusted to 7.4 with CsOH. In this condition, the equilibrium potential for chloride ions was about −2.8 mV and cells were clamped at the holding potential (HP) of 0 mV. Pipettes were pulled from borosilicate glass and had <3 MΩ resistance, when filled with the above pipette solutions. Currents were low-pass filtered at 2 kHz and digitized with sampling rates of 50 kHz using the Digidata 1440A AD/DA converter (Axon Instruments). Chloride currents were recorded ∼5 min after achieving the whole-cell configuration, to allow the pipette solution to diffuse into the cell. Patches with a series resistance voltage error >5 mV and those with non-negligible leak current were discarded.

We measured the I–V relationship and the overall apparent open probability in high-chloride (134 mM) intracellular solutions to enhance current amplitude. The holding potential (HP) was set at 0 mV. Voltage steps of 400 ms were applied from −150 to +150 mV in 10 mV intervals, each followed by a voltage step at −105 mV to record tail currents. Voltage steps were applied every 3 s to allow complete recovery of current amplitude at the HP between two pulses. Data were analyzed off-line by using pClamp 10.3 (Axon Instruments) and SigmaPlot

8.02 (Systat Software GmbH) software. The instantaneous and steady-state current amplitudes were measured at the beginning (∼1 ms) and end (∼390 ms) of each voltage step and normalized by cell capacitance to calculate current densities in pA/pF. Current densities are reported as means ± S.E.M from n cells and statistical analysis was performed using Student's *t*-test, with $P < 0.05$ considered as significant.

For pharmacological experiments, transfected HEK293T cells were incubated with the proteasome inhibitor MG132 (MG-132 Ready Made Solution, Sigma-Aldrich, M7449) at the final concentration of 20 μM for 16 h and then used for patch-clamp recordings. The reducing agent dithiothreitol (DTT, Pierce, Rockford, IL, USA) was added at the final concentration of 1 or 2 mM in the culture medium for cell incubation or in the extracellular patch-clamp solution for acute gravity-driven diffusion around the patched cell (13).

Biotinylation of Cell-Surface Proteins

Cell-surface biotinylation was carried out with the Pierce Cell Surface Protein Isolation Kit (Pierce, Rockford, IL, USA). Transfected HEK293 cells were incubated for 16 h at 37°C in the absence or presence of 20 μM MG132 and, subsequently, cell-surface proteins were labeled with sulfosuccinimidyl-2-(biotinamido) ethyl-1,3-dithiopropionate (Sulfo-NHS-SS-biotin). In brief, cells were washed twice with ice-cold PBS and incubated with Sulfo-NHS-SS-biotin in PBS for 30 min at 4°C, with gentle rocking on an orbital shaker. Excess biotin was quenched with quenching solution. Cells were treated with lysis buffer and centrifuged at 10,000 *g* for 2 min at 4°C. Clear supernatant was reacted with immobilized NeutrAvidin gel slurry in columns for 60 min at room temperature. After centrifugation, cytoplasmic proteins were recovered from the flow-through, whereas surface proteins were obtained after elution with a sample buffer containing DTT. Both samples were quantified by using Pierce™ BCA Protein Assay Kit—Reducing Agent Compatible (Thermo Scientific, USA) and then used for Western Blot experiments.

Western Blot Analysis

To measure total ClC-1 protein expression, HEK293 cells were transfected with pRcCMV-hClC-1 WT or G411C constructs (5 μg each) and then incubated for 16 h in the absence or presence of 20 μM MG132. After incubation, cells were harvested in 200 μl of cold RIPA buffer (20 mM Tris-HCl, 150 mM NaCl, 1,5% Non-idet P-40, 100 mM sodium orthovanadate, 10 mg/ml PMSF and a protease inhibitor cocktail) and placed for 10 min in ice. To complete cell lysis, suspensions were passed through a syringe with a needle for 10 times. After 15 min in ice, cell lysates were centrifuged at 14,000 rpm for 30 min at 4°C, and supernatant was collected. Total protein amounts were quantified by using a BCA protein assay kit (Bio-Rad, Hercules, CA, USA).

Total proteins or surface and cytoplasmic proteins from biotinylation assay (8 μg) were separated on a 10% SDS-PAGE and transferred onto nitrocellulose membrane for 1 h at 200 mA (SemiDry transferblot, Bio-Rad). Membrane was blocked for 2 h with 0.2 M Tris-HCl, 1.5 M NaCl, and pH 7.4 buffer (TBS) containing 5% non-fat dry milk and 0.5% Tween-20 and incubated overnight at 4°C with rabbit anti-ClC-1 antibody–C-terminal (ab189857, Abcam) diluted 1:500 and monoclonal mouse anti-Actin (Sc-47778, Santa Cruz Biotechnology) diluted 1:300 with TBS containing 5% non-fat dry milk. After three washes with TBS containing 0.5% Tween-20 (TTBS), membrane was incubated for 1 h with goat anti-rabbit IgG conjugated to horseradish peroxidase (Biorad). Membrane was then washed with TTBS, developed with a chemiluminescent substrate (Clarity Western ECL Substrate; Bio-Rad), and visualized on a Chemidoc imaging system (Bio-Rad). Western blots were quantified with Image Lab software (Bio-Rad), which allows the chemiluminescence detection of each experimental protein band to obtain the absolute signal intensity automatically adjusted by subtracting the local background. For total protein expression, density was standardized as the ratio of the ClC-1 signal to the cognate β-actin signal. For biotinylation assay, the distribution of ClC-1 was quantified by calculating the ratio of surface proteins to the sum of surface and cytoplasmic proteins. Quantitative analysis was performed from 3 to 4 independent experiments. Statistical analysis was performed using ANOVA followed by Sidak's multiple comparisons test (Prism 8.4.3, GraphPad Software Inc.).

Confocal Imaging

The HEK293T cells were seeded on 1X polylysine-treated culture dishes (CELLview™–Cell Culture Dish with Glass Bottom 627860, Greiner) and then transfected with cDNA encoding wild-type or G411C YFP-hClC-1 (1 μg) using the calcium-phosphate precipitation method.

Two days after transfection, cell plasma membrane was stained with wheat germ Agglutinin, Alexa Fluor™555 Conjugate (WGA-555W32464, Thermo Fisher Scientific, Waltham, MA, USA) in PBS for 10 min at 37°C at a final concentration of 3 μg/ml. Confocal images were obtained using a Leica TCS SP5 confocal laser scanning microscope (Leica Microsystems, Mannheim, Germany). The YFP-ClC-1 fluorescence was excited with a green argon laser (450–500 nm of excitation wavelength) and recorded at 490–550 nm. The WGA-555 fluorescence was excited using red HeNe 543 laser, selecting an excitation at 500–590 nm and emission at 550–650 nm. Single confocal optical planes, containing a cluster of one to five transfected cells, were collected with a 63x oil lenses, using a sequential scan procedure at 0.45 μm intervals through the z-axis of the section.

Quantitative evaluation of the colocalization of YFP-ClC-1 and WGA-555 fluorescence pixels was performed by two independent observers (AC and FG), blinded for group allocation, using ImageJ JACoP plugin (NIH, Bethesda, MD, USA), according to developer's instructions (14). Analysis was performed on 2–4 optical planes (2.25 μm intervals) of 64 WT and 34 GC different fields containing 1–5 cells. A total of 101 WT and 50 GC cells were thus analyzed. The selected fields were segmented using the automatic threshold calculated by JACoP for the two channels (red and green); the resulting pairs of binary images were then analyzed to obtain the Pearson's correlation coefficient (*P*) and the Mander's colocalization coefficients (M1 and M2). The pixel intensity scatter-plots were obtained by using

EzColocalization plugin for ImageJ according to developer's instructions (15). The results were expressed as mean value ± *SD*. Statistical analysis was performed using unpaired Student's *t*-test. Differences were considered significant with $P < 0.05$.

RESULTS

Clinical Report

The proband showed generalized muscle stiffness for the first time at the age of 1 year, when he begun to walk on his own. Clinical examination was carried out at the age of 5 years and revealed muscle hypertrophy and percussion myotonia with warm up phenomenon. Electromyography (EMG) study in proximal and distal muscles confirmed electrical myotonia and showed a 24.5% decrement of the amplitude of the compound muscle action potential at repetitive 10-Hz nerve stimulation (**Figure 1A**). The short exercise test revealed characteristic EMG pattern II generally associated with defects in the chloride channel (16). The tendon reflexes on hands and legs were decreased, whereas muscle force in proximal parts of hands and legs was normal without muscle weakness. Probands' father showed myotonic signs similar to his son and was treated with acetazolamide 500 mg/day with no improvement.

The c.1231G>T (p.Gly411Cys) recessive mutation in *CLCN1* was detected in the proband in compound heterozygosis with the already known c.2680C>T mutation (p.Arg894*) (17). Probands' father also carried p.Gly411Cys mutation, in association with the well-known c.568GG>TC transition (p.Gly190Ser) (9, 18, 19). Conversely, the relatives who carried G411C, R894X, or G190S mutation in heterozygosis with WT showed no sign of myotonia, confirming a recessive inheritance of the disease (**Figure 1B**).

Functional and Biochemical Characterization of G411C Mutant Channels

Using Clustal Omega, multiple amino acid sequence alignment showed that G411 residue is well-conserved among ClC-1 of mammals and various human CLC proteins (ClC-2 and ClC-K) (**Figure 1C**). Positioning of the mutation in the 3D structural model of hClC-1 channel modeled upon the structure of CmClC (PDB id: 3ORG) (20, 21) suggested that G411 is located in the transmembrane region, between the α-helix domains K and L (**Figure 1D**), far away from the conducting pore of the channel (22–24). Analysis using MutPred software scored G411C substitution with 0.8 probability to be deleterious.

To understand better the consequence of the mutation and its role in MC, we performed functional characterization of G411C ClC-1 channels using the patch-clamp technique.

For WT channels, instantaneous currents were observed at each voltage steps, which decreased over time between −150 and −60 mV (corresponding to current deactivation) or remained stable within 400 ms between −60 and +150 mV. Current amplitudes saturated at voltages > +50 mV. In contrast, transfected HEK293T with ClC-1 mutant did not generate any chloride current within the voltage range of −150/+150 mV (**Figure 2**).

To verify whether G411C channels were expressed or not, we constructed fluorescent plasmids containing cDNA encoding YFP-tagged WT or mutant ClC-1 proteins, and we examined transfected cells using confocal imaging (**Figure 3**). We used wheat germ agglutinin AlexaFluor^{TM}555 to stain cell plasma membrane and evaluated the co-localization with the YFP-ClC-1. Wild type ClC-1 (green) was mainly expressed at the plasma membrane level as shown by the high degree of co-localization with WGA-555 (**Figure 3**). Conversely, the G411C hClC-1-YFP protein was little present on the cell surface and green fluorescence was essentially cytoplasmic, suggesting that the mutation induced a defect in subcellular distribution.

We thus investigated total ClC-1 protein expression level and ClC-1 distribution within cell compartments using Western Blotting analysis and biotinylation assay. Quantitative analysis revealed no significant difference between WT and G411C in total protein expression level (**Figures 4A,B**). Noticeably, the distribution of G411C protein between plasma membrane and cytoplasmic compartments was inverted compared to WT (**Figures 4C,D**), with a dramatically reduced surface expression of the mutant (−51% compared to WT), in full agreement with confocal imaging analysis.

Effect of the Proteasome Inhibitor MG132 on WT and Mutant hClC-1

Several mechanisms might have been responsible for the dramatic reduction of G411C protein surface expression, including an increase in protein degradation. We explored the possibility that G411C mutation could induce a folding defect in ClC-1 protein, making it more sensitive to the ubiquitin-proteasome system. For these experiments, we exploited peptide aldehydes such as MG132, commonly used to examine the involvement of this mechanism.

Transfected HEK293T were incubated with 20 μM of MG132 for 16 h and then used for Western Blot analysis of total protein or surface and cytoplasmic proteins (biotinylation assay). MG132 treatment significantly increased the total protein level of WT and G411C mutant by more than 2-fold (**Figures 4A,B**). No significant difference was observed in wild-type ClC-1 protein distribution within plasma membrane and cytoplasm. However, MG132 treatment enhanced G411C protein expression at the plasma membrane, showing a subcellular distribution more similar to WT (**Figures 4C,D**).

We next verified if the MG132 treatment also restored chloride currents. **Figure 2** shows the effect of MG132 treatment on G411C mutant channel, after 16 h of incubation. Surprisingly, despite the increase of the surface protein level as evidenced by biotinylation assay, no significant chloride current was recorded from the G411C-transfected cell treated with MG132, suggesting that this mutation produced non-functional ClC-1 chloride channels.

Effect of the Reducing Agent DDT on G411C hClC-1

Because the mutation introduces a cysteine residue in ClC-1, we wondered whether the formation of unnatural disulfide bridge might account for channel defect. In a series of experiments, the

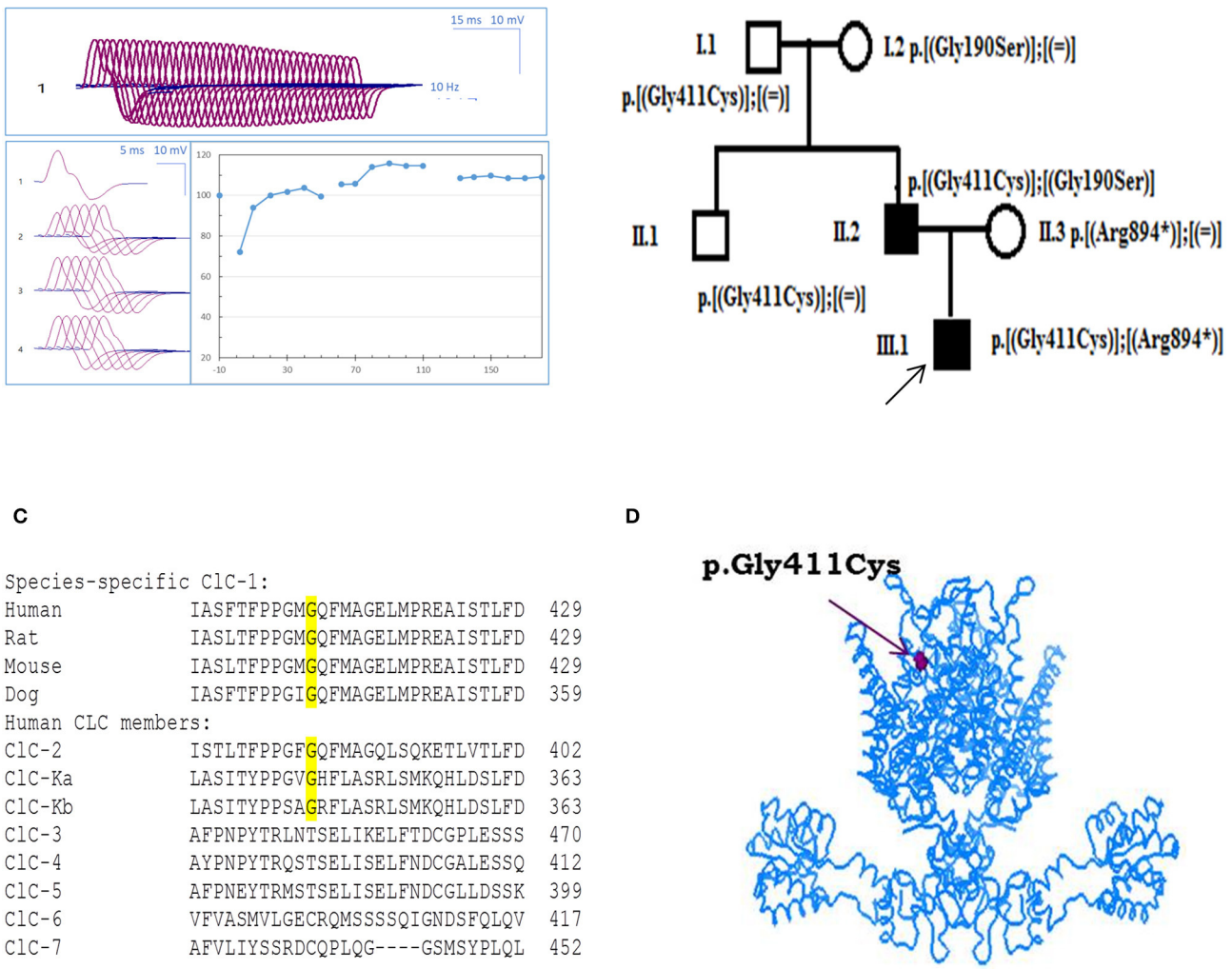

FIGURE 1 | Probands' EMG, pedigree, and ClC-1 mutation. **(A)** Repetitive nerve stimulation (RNS) on *abductor digiti minimi* muscle. **(B)** Pedigrees of the Russian family affected by Becker disease. Squared symbols indicate men and round symbols indicate women. Empty symbols denote healthy individuals and dark filled symbols denote affected individuals. The arrow indicates the proband in the family. **(C)** Amino acid alignment of the ClC-1 chloride channel among different species and human CLC members. **(D)** Three-dimensional representation of hClC-1 channel modeled upon the X-ray structure of a eukaryotic Cl^-/H^+ exchanger CmClC showing the localization of G411C mutation.

HEK cells transfected with G411C were exposed to the reducing agent DTT (1 or 2 mM) either acutely during patch-clamp recordings or through cell incubation for up to 2 h. According to the crystal structure, G411C is located close to the external surface of the protein and should be thus easily accessible to DTT. In no case, DTT was able to restore G411C chloride currents, suggesting that the cysteine impairs channel function without forming disulfide bond (not shown).

DISCUSSION

In the present manuscript, we reported a detailed study of a ClC-1 mutation, p.G411C, identified in a Russian family. This mutation was detected only recently in a large group of patients with skeletal muscle channelopathies from the Netherlands (25). The mutation was associated with the frameshift mutation Phe404Hisfs*16, suggesting a recessive trait, but was not functionally characterized. The Russian pedigree confirms such a recessive inheritance, as the probands' grandfather and uncle carrying G411C in heterozygosis with WT were asymptomatic. In the symptomatic proband and his father, the mutation was associated in compound heterozygosis with two well-known mutations, p.R894X (17) and p.G190S (9), respectively. Thus, the inheritance pattern and the clinical examination of both patients suggested a Becker's phenotype associated with severe myotonia.

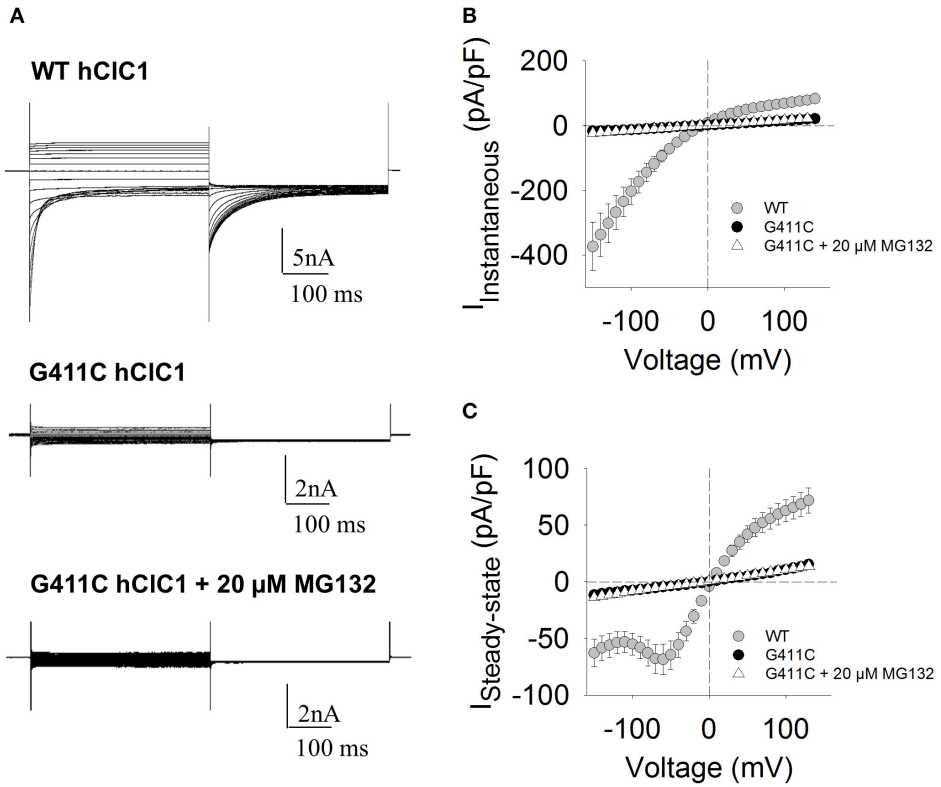

FIGURE 2 | Chloride currents of WT and G411C hClC-1 channels expressed in HEK293T cells. **(A)** Representative chloride currents recorded from HEK293T cells transfected with 5 μg WT or G411C hClC-1 cDNAs in high-chloride intracellular solution. The G411C currents were also measured after 16 h incubation with 20 μM MG132. The holding potential (HP) was set at 0 mV. Voltage steps of 400 ms were applied from −150 to +150 mV in 10 mV intervals, each followed by a voltage step at −105 mV to record tail currents. Voltage steps were applied every 3 s to allow complete recovery of current amplitude at the HP between two pulses. **(B)** Instantaneous currents were measured at the beginning (~1 ms) of voltage step and normalized with respect to cell capacitance (pA/pF) to calculate current density. **(C)** Steady-state current densities were measured at the end of voltage step (~390 ms). Each data point is the mean ± S.E.M. from 10 to 12 cells.

The pathogenicity of p.G411C was further confirmed by functional and biochemical studies. In transfected HEK293T cells, p.G411C mutant did not produce discernible chloride currents, which can account for muscle hyperexcitability and myotonic discharges. The associated p.R894X mutation deletes 94 amino acids of the C-terminus of the protein, leading to a large reduction of chloride conductance due to a decrease of surface protein expression (17, 26). The p.G190S mutation, identified in compound heterozygosis in the father, induces a dramatic shift of the open probability voltage dependence toward very positive voltages, resulting in nearly zero chloride current within the physiological range of sarcolemma voltage (9). The coexistence of p.G411C with these mutations may result in a huge reduction of the sarcolemma chloride conductance and is therefore likely responsible for the severe myotonic phenotype.

Biochemical studies suggest that p.G411C does not impair total protein expression, but rather reduces the fraction of the protein expressed at the surface membrane. Impaired subcellular distribution of G411C mutant channel was also confirmed by confocal imaging studies.

Because of the evident recessive inheritance mode of p.G411C, a dominant-negative effect on wild-type is unlikely. This suggests that either G411C does not significantly assemble with WT to form heterodimers or WT-G411C heterodimers can reach the membrane and WT protopore work normally. In both cases, WT channels would ensure at least 50% of the sarcolemma chloride conductance, which is sufficient to guarantee normal muscle function.

Interestingly, several myotonia-causing mutations are located near G411 residue, such as p.P408A (27), p.Q412P (28), p.F413C (26, 29, 30), p.A415V (31), pG416E (32), and p.E417G (33). Among these, p.Q412P was shown to induce a drastic reduction of ClC-1 chloride currents in *Xenopus* oocytes and HEK293 cells, as the consequence of a severe folding defect, rendering ClC-1 protein more susceptible to its degradation (28). Yet, the small proportion of mutated channels reaching the plasma membrane showed biophysical properties undistinguishable from wild-type. The F413C mutant was shown to impair channel trafficking in transfected myotubes (26) and to induce small changes in chloride current voltage–dependence and kinetics in transfected HEK293 cells (30). Similar to G411C, G416E did not produce any chloride current in transfected HEK293 cells (32). Thus, mutations located in the K-L loop may have different effects on chloride channel gating but all impair the ClC-1 channel

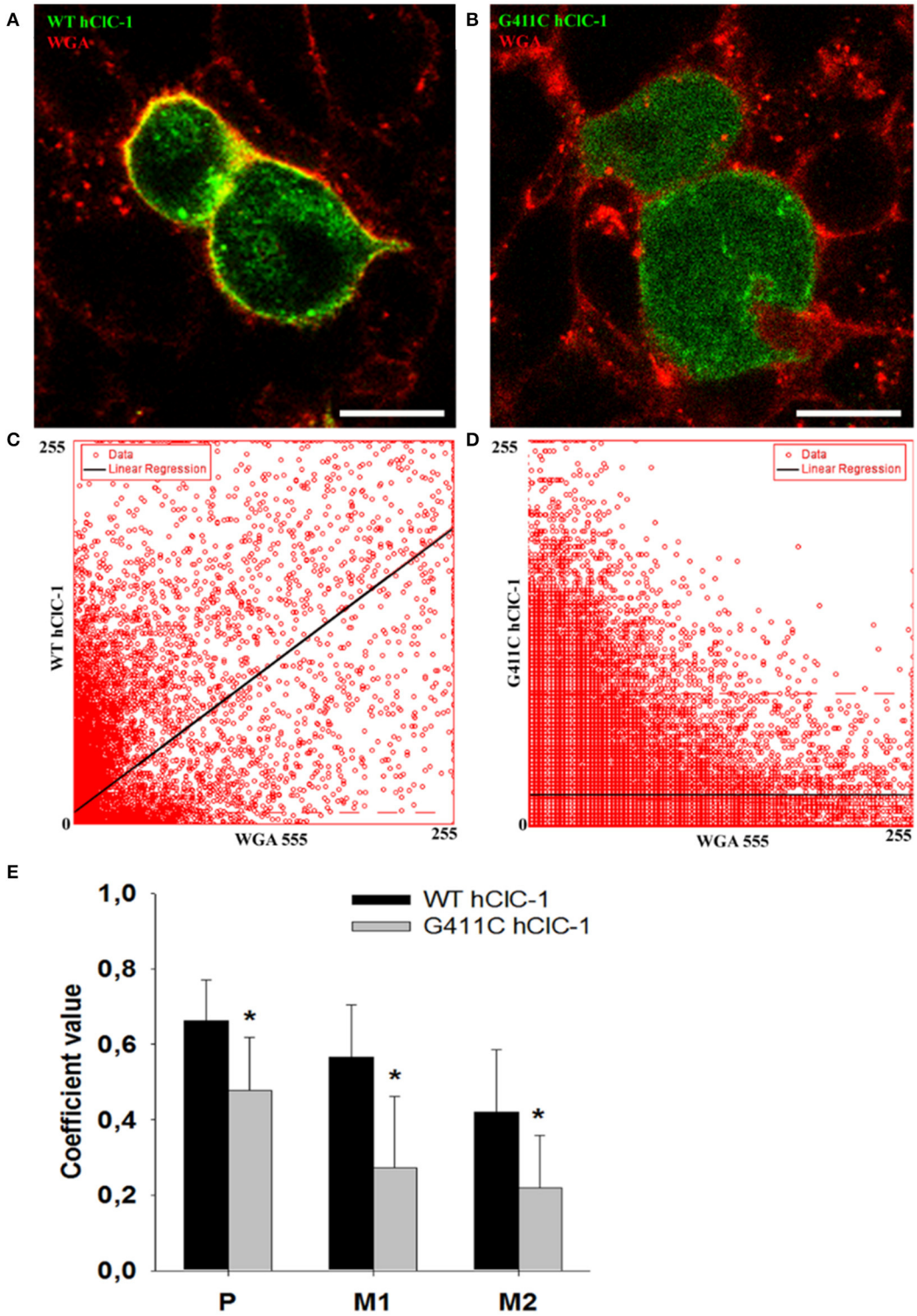

FIGURE 3 | Confocal microscopy images of HEK293T cells expressing wild-type YFP-ClC-1 channel and YFP-ClC-1 G411C mutant. **(A)** Representative confocal single optical plane image showing localization of wild-type YFP-ClC-1 (green signal), plasma membrane marker WGA-555 (red signal), and colocalization (yellow signal) in a dividing cell doublet. **(B)** Representative dividing cell doublet showing localization of YFP-G411C (green signal), plasmalemma WGA-555 (red signal), and colocalization (yellow signal). **(C,D)** Scatter-plots of pixel intensity in images **(A,B)**, showing the relationship between WT or G411C and WGA. Linear regressions

(Continued)

FIGURE 3 | (black lines) demonstrate significant colocalization of WT hClC-1 with WGA [Pearson's correlation coefficient (*P*) of 0.7] and anticolocalization of G411C with WGA ($P = 0.4$). **(E)** Histograms reporting the Pearson's coefficient (*P*) of pixel intensity scatter-plot linear regressions (as in **C,D**), and the Mander's overlap coefficients (M1 and M2) of the two markers (WGA-555 and YFP-ClC-1). M1 indicates summed intensities of red pixels overlapping with green to the total red intensity (proportion of WGA overlapping with ClC-1). M2 indicates summed intensities of green pixels overlapping with red to the total green intensity (proportion of ClC-1 overlapping with WGA). Each bar is the mean ± *SD* from 64 (WT) and 34 (G411C) cell clusters. *$p < 0.001$ between WT and G411C hClC-1 with unpaired Student's *t*-test.

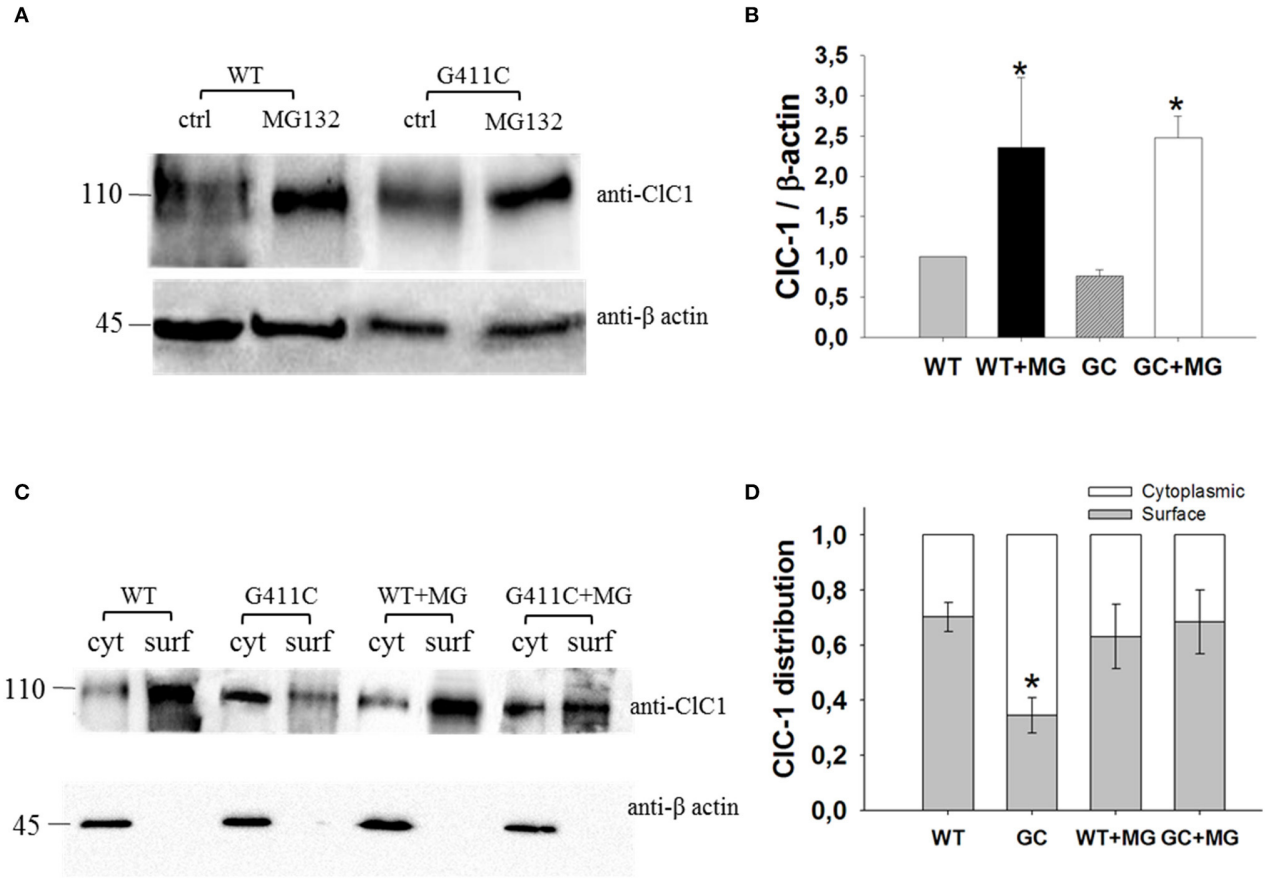

FIGURE 4 | ClC-1 protein expression in HEK293T cells transfected with WT or G411C ClC-1 channels and effects of MG132 incubation. **(A)** Representative western blot of total ClC-1 and β-actin proteins from transfected HEK293T incubated for 16 h in absence or presence of 20 μM MG132. **(B)** Quantification of ClC-1 total protein expression level. The ClC-1 signal of each column was standardized to β-actin signal and normalized to WT on the same blot. Each bar is the mean ± S.E.M. from three independent experiments. Asterisks denote significant difference ($p < 0.04$) between control condition and MG132 treatment using two-way ANOVA. **(C)** Representative western blot of surface and cytoplasmic ClC-1 and β-actin proteins obtained from biotinylation assay of transfected HEK293T cells incubated for 16 h in absence or presence of 20 μM MG132. **(D)** Quantification of surface and cytoplasmic ClC-1 protein distribution. Each bar is the mean ± S.E.M. from 3 to 4 independent experiments. Statistical analysis was performed using two-way ANOVA followed by Sidak's multiple comparison test (* at least $p < 0.05$ vs. WT and GC + MG132).

surface expression, suggesting an important role of the loop in channel trafficking. It is also worth noting that all these mutations are recessive.

Post-translational alteration of ion channel expression can occur at different levels: altered intracellular trafficking, increased turnover at the plasma membrane, or increased degradation rate (34, 35). Misfolded proteins may be retained into the ER and redirected through the ER-associated degradation (ERAD) pathway toward proteasomal degradation. Misfolded proteins reaching the plasma membrane may also be removed by the peripheral quality control system and degraded through the endosome/lysosome pathway. Such mechanisms are also valid for misfolded ClC-1 mutants causing myotonia congenita (7). In the case of G411C, we observed that the total protein expression level was similar to WT, suggesting that there was no enhancement of protein degradation. Rather, the altered distribution of G411C between surface and cytoplasm suggests a trafficking defect of the mutant toward the plasma membrane and/or an increased turnover at the plasma membrane. We incubated transfected HEK cells with MG132 in order to assess the role

of the proteasome in G411C distribution (36). As expected, MG132 treatment increased total G411C protein expression in a manner similar to WT, arguing for a normal degradation rate of the mutated protein. Importantly, the treatment with MG132 also restored the cellular distribution of the G411C mutant. A possible explanation might be that inhibition of the proteasome enables G411C mutant to leave the ER and reach the plasma membrane more efficiently, maybe through modulation of molecular chaperone activity. Dedicated experiments would be needed to confirm such hypothesis. Despite an increase of the surface protein level of G411C by the MG132 treatment, no significant increase in chloride current was observed in patches recorded from the G411C-transfected cells. Taken together, these results suggest that G411C mutation disrupts the folding of ClC-1 protein, making the chloride channels non-functional and trafficking-defective.

In conclusion, the present study expands the spectrum of *CLCN1* mutations responsible for MC and contributes to the understanding of genotype-phenotype correlation. The improved understanding of the molecular mechanisms underlying MC could help the discovery of new drugs targeting specific mutant channels defects. The ideal pharmacological approach would point to the development of molecules able to correct biophysical defects in case of gating-defective mutations, as for G190S mutation, or able to restore protein surface expression, as for R894X and G411C mutants. Pharmacological chaperones could represent the elective tools able to stabilize protein correct folding and stability and to limit ER retention, thus overcoming the membrane expression defect and allowing the development of a personalized treatment for MC patients. Recently, two small molecules inhibiting the ubiquitination of ClC-1 in the ER proved effective in correcting the impaired biogenesis of misfolded ClC-1 protein (37, 38). However, in the case of G411C, the drug should be able, not only to restore cell surface expression, but also to improve channel function.

DATA AVAILABILITY STATEMENT

The datasets generated for this study can be found in the Leiden Open variation database (#00269797).

ETHICS STATEMENT

The studies involving human participants were reviewed and approved by Ethics committee of the FSBI N.P. Bochkov's Research Centre for Medical Genetics, Moscow, Russia. Written informed consent to participate in this study was provided by the participants' legal guardian/next of kin.

AUTHOR CONTRIBUTIONS

CA: *in vitro* experiment data acquisition, analysis, interpretation, and manuscript writing. PI, EC, and GC: *in vitro* experiment data acquisition. FG: confocal imaging experiments and contribution to manuscript writing. EI: clinical, genetic data acquisition, and contribution to manuscript writing. ED, AP, and SK: clinical and genetic data acquisition. MC: critical revision of manuscript. J-FD: study concept, design, interpretation of data, study supervision, and critical revision of manuscript. All authors contributed to the article and approved the submitted version.

FUNDING

This work was supported by Telethon-Italy (grant number GGP14096) and Bari University Research Grant (2017–2018).

REFERENCES

1. Cannon SC. Channelopathies of skeletal muscle excitability. *Compr Physiol.* (2015) 5:761–90. doi: 10.1002/cphy.c140062
2. Phillips L, Trivedi JR. Skeletal muscle channelopathies. *Neurotherapeutics.* (2018) 15:954–65. doi: 10.1007/s13311-018-00678-0
3. Stunnenberg BC, LoRusso S, Arnold WD, Barohn RJ, Cannon SC, Fontaine B, et al. Guidelines on clinical presentation and management of non-dystrophic myotonias. *Muscle Nerve*. (2020). doi: 10.1002/mus.26887. [Epub ahead of print].
4. Jentsch TJ, Pusch M. CLC chloride channels and transporters: structure, function, physiology, and disease. *Physiol Rev.* (2018) 98:1493–590. doi: 10.1152/physrev.00047.2017
5. Altamura C, Desaphy JF, Conte D, De Luca A, Imbrici P. Skeletal muscle ClC-1 chloride channels in health and diseases. *Pflugers Arch.* (2020) 472:961–75. doi: 10.1007/s00424-020-02376-3
6. Jeng CJ, Fu SJ, You CY, Peng YJ, Hsiao CT, Chen TY, et al. Defective gating and proteostasis of human clC-1 chloride channel: molecular pathophysiology of myotonia congenita. *Front Neurol.* (2020) 11:76. doi: 10.3389/fneur.2020.00076
7. Ivanova EA, Dadali EL, Fedotov VP, Kurbatov SA, Rudenskaia GE, Proskokova TN, et al. The spectrum of CLCN1 gene mutations in patients with non-dystrophic Thomsen's and Becker's myotonias. *Genetika.* (2012) 48:1113–23. doi: 10.1134/S1022795412090049
8. Fournier E, Arzel M, Sternberg D, Vicart S, Laforet P, Eymard B, et al. Electromyography guides toward subgroups of mutations in muscle channelopathies. *Ann Neurol.* (2004) 56:650–61. doi: 10.1002/ana.20241
9. Desaphy JF, Gramegna G, Altamura C, Dinardo MM, Imbrici P, George AL, et al. Functional characterization of ClC-1 mutations from patients affected by recessive myotonia congenita presenting with different clinical phenotypes. *Exp Neurol.* (2013) 248:530–40. doi: 10.1016/j.expneurol.2013.07.018
10. Ronstedt K, Sternberg D, Detro-Dassen S, Gramkov T, Begemann B, Becher T, et al. Impaired surface membrane insertion of homo- and heterodimeric human muscle chloride channels carrying amino-terminal myotonia causing mutations. *Sci Rep.* (2015) 5:15382. doi: 10.1038/srep15382
11. Imbrici P, Altamura C, Camerino GM, Mangiatordi GF, Conte E, Maggi L, et al. Multidisciplinary study of a new ClC-1 mutation causing myotonia congenita: a paradigm to understand and treat ion channelopathies. *FASEB J.* (2016) 30:3285–95. doi: 10.1096/fj.201500079R
12. Altamura C, Lucchiari S, Sahbani D, Ulzi G, Comi GP, D'Ambrosio P, et al. The analysis of myotonia congenita mutations discloses functional clusters of amino acids within the CBS2 domain and the C-terminal peptide of the ClC-1 channel. *Hum Mutat.* (2018) 39:1273–83. doi: 10.1002/humu.23581
13. Altamura C, Mangiatordi GF, Nicolotti O, Sahbani D, Farinato A, Leonetti F, et al. Mapping ligand binding pockets in chloride ClC-1 channels through an integrated *in silico* and experimental approach using anthracene-9-carboxylic acid and niflumic acid. *Br J Pharmacol.* (2018) 175:1770–80. doi: 10.1111/bph.14192

14. Bolte S, Cordelières SP. A guided tour into subcellular colocalization analysis in light microscopy. *J Microsc.* (2006) 224:213–32. doi: 10.1111/j.1365-2818.2006.01706.x
15. Stauffer W, Sheng H, Lim HN. EzColocalization: an ImageJ plugin for visualizing and measuring colocalization in cells and organisms. *Sci Rep.* (2018) 8:15764. doi: 10.1038/s41598-018-33592-8
16. Fournier E, Tabti N. Clinical electrophysiology of muscle diseases and episodic muscle disorders. *Handb Clin Neurol.* (2019) 161:269–80. doi: 10.1016/B978-0-444-64142-7.00053-9
17. Meyer-Kleine C, Steinmeyer K, Ricker K, Jentsch TJ, Koch MC. Spectrum of mutations in the major human skeletal muscle chloride channel gene (CLCN1) leading to myotonia. *Am J Hum Genet.* (1995) 57:1325–34.
18. Shalata A, Furman H, Adir V, Adir N, Hujeirat Y, Shalev SA, et al. Myotonia congenita in a large consanguineous Arab family: insight into the clinical spectrum of carriers and double heterozygotes of a novel mutation in the chloride channel CLCN1gene. *Muscle Nerve.* (2010) 41:464–9. doi: 10.1002/mus.21525
19. Brugnoni R, Kapetis D, Imbrici P, Pessia M, Canioni E, Colleoni L, et al. A large cohort of myotonia congenita probands: novel mutations and a high-frequency mutation region in exons 4 and 5 of the cLCN1 gene. *J Hum Genet.* (2013) 58:581–7. doi: 10.1038/jhg.2013.58
20. Bennetts B, Parker MW. Molecular determinants of common gating of a ClC chloride channel. *Nat Commun.* (2013) 4:2507. doi: 10.1038/ncomms3507
21. Feng L, Campbell EB, Hsiung, Y, MacKinnon, R. Structure of a eukaryotic CLC transporter defines an intermediate state in the transport cycle. *Science.* (2010) 330:635–41. doi: 10.1126/science.1195230
22. Dutzler R, Campbell EB, Cadene M, Chait BT, MacKinnon R. X-ray structure of a ClC chloride channel at 3.0 å reveals the molecular basis of anion selectivity. *Nature.* (2002) 415:287–94. doi: 10.1038/415287a
23. Park E, MacKinnon R. Structure of the ClC-1 chloride channel from Homo sapiens. *Elife.* (2018) 7:e36629. doi: 10.7554/eLife.36629
24. Wang K, Preisler SS, Zhang L, Cui Y, Missel JW, Grønberg C, et al. Structure of the human ClC-1 chloride channel. *PLoS Biol.* (2019) 17:e3000218. doi: 10.1371/journal.pbio.3000218
25. Stunnenberg BC, Raaphorst J, Deenen JCW, Links TP, Wilde AA, Verbove DJ, et al. Prevalence and mutation spectrum of skeletal muscle channelopathies in the Netherlands. *Neuromuscul Disord.* (2018) 28:402–7. doi: 10.1016/j.nmd.2018.03.006
26. Papponen H, Nissinen M, Kaisto T, Myllylä VV, Myllylä R, Metsikkö K. F413C and A531V but not R894X myotonia congenita mutations cause defective endoplasmic reticulum export of the muscle-specific chloride channel ClC-1. *Muscle Nerve.* (2008) 37:317–25. doi: 10.1002/mus.20922
27. Fialho D, Schorge S, Pucovska U, Davies NP, Labrum R, Haworth A, et al. Chloride channel myotonia: exon 8 hot-spot for dominant-negative interactions. *Brain.* (2007) 130:3265–74. doi: 10.1093/brain/awm248
28. Vindas-Smith R, Fiore M, Vásquez M, Cuenca P, Del Valle G, Lagostena L, et al. Identification and functional characterization of CLCN1 mutations found in non-dystrophic myotonia patients. *Hum Mutat.* (2016) 37:74–83. doi: 10.1002/humu.22916
29. Koch MC, Steinmeyer K, Lorenz C, Ricker K, Wolf F, Otto M, et al. The skeletal muscle chloride channel in dominant and recessive human myotonia. *Science.* (1992) 257:797–800. doi: 10.1126/science.1379744
30. Zhang J, Bendahhou S, Sanguinetti MC, Ptacek LJ. Functional consequences of chloride channel gene (CLCN1) mutations causing myotonia congenita. *Neurology.* (2000) 54:937–42. doi: 10.1212/WNL.54.4.937
31. Mailänder V, Heine R, Deymeer F, Lehmann-Horn F. Novel muscle chloride channel mutations and their effects on heterozygous carriers. *Am J Hum Genet.* (1996) 58:317–24.
32. Mazon MJ, Barros F, De la Pena P, Quesada JF, Escudero A, Cobo AM, et al. Screening for mutations in Spanish families with myotonia. Functional analysis of novel mutations in CLCN1 gene. *Neuromuscul Disord.* (2012) 22:231–43. doi: 10.1016/j.nmd.2011.10.013
33. Trip J, Drost G, Verbove DJ, van der Kooi AJ, Kuks JB, Notermans NC, et al. In tandem analysis of CLCN1 and SCN4A greatly enhances mutation detection in families with non-dystrophic myotonia. *Eur J Hum Genet.* (2008) 16:921–9. doi: 10.1038/ejhg.2008.39
34. Curran J, Mohler PJ. Alternative paradigms for ion channelopathies: disorders of ion channel membrane trafficking and posttranslational modification. *Annu Rev Physiol.* (2015) 77:505–24. doi: 10.1146/annurev-physiol-021014-071838
35. Terragni B, Scalmani P, Franceschetti S, Cestèle S, Mantegazza M. Post-translational dysfunctions in channelopathies of the nervous system. *Neuropharmacology.* (2018) 132:31–42. doi: 10.1016/j.neuropharm.2017.05.028
36. Kisselev AF, Goldberg AL. Proteasome inhibitors: from research tools to drug candidates. *Chem Biol.* (2001) 8:739–58. doi: 10.1016/S1074-5521(01)00056-4
37. Chen YA, Peng YJ, Hu MC, Huang JJ, Chien YC, Wu JT, et al. The Cullin 4A/B-DDB1-Cereblon E3 ubiquitin ligase complex mediates the degradation of CLC-1 chloride channels. *Sci Rep.* (2015) 5:10667. doi: 10.1038/srep10667
38. Peng YJ, Huang JJ, Wu HH, Hsieh HY, Wu CY, Chen SC, et al. Regulation of CLC-1 chloride channel biosynthesis by FKBP8 and Hsp90b. *Sci Rep.* (2016) 6:32444. doi: 10.1038/srep32444

Conflict of Interest: The authors declare that the research was conducted in the absence of any commercial or financial relationships that could be construed as a potential conflict of interest.

Copyright © 2020 Altamura, Ivanova, Imbrici, Conte, Camerino, Dadali, Polyakov, Kurbatov, Girolamo, Carratù and Desaphy. This is an open-access article distributed under the terms of the Creative Commons Attribution License (CC BY). The use, distribution or reproduction in other forums is permitted, provided the original author(s) and the copyright owner(s) are credited and that the original publication in this journal is cited, in accordance with accepted academic practice. No use, distribution or reproduction is permitted which does not comply with these terms.

Advantages of publishing in Frontiers

OPEN ACCESS
Articles are free to read for greatest visibility and readership

FAST PUBLICATION
Around 90 days from submission to decision

HIGH QUALITY PEER-REVIEW
Rigorous, collaborative, and constructive peer-review

TRANSPARENT PEER-REVIEW
Editors and reviewers acknowledged by name on published articles

Frontiers
Avenue du Tribunal-Fédéral 34
1005 Lausanne | Switzerland

Visit us: www.frontiersin.org
Contact us: frontiersin.org/about/contact

REPRODUCIBILITY OF RESEARCH
Support open data and methods to enhance research reproducibility

DIGITAL PUBLISHING
Articles designed for optimal readership across devices

FOLLOW US
@frontiersin

IMPACT METRICS
Advanced article metrics track visibility across digital media

EXTENSIVE PROMOTION
Marketing and promotion of impactful research

LOOP RESEARCH NETWORK
Our network increases your article's readership